

# Static Pile Load Tests on Driven Piles into Intermediate-Geo Materials

---

James H. Long  
University of Illinois at Urbana/Champaign

WisDOT ID no. 0092-12-08

September 2016



RESEARCH & LIBRARY UNIT



WISCONSIN HIGHWAY RESEARCH PROGRAM

**WISCONSIN DOT**  
PUTTING RESEARCH TO WORK

## TECHNICAL REPORT DOCUMENTATION PAGE

1. Report No. WHRP 0092-12-08	2. Government Accession No No	3. Recipient's Catalog No	
4. Title and Subtitle Static Pile Load Tests on Driven Piles into Intermediate Geo Materials		5. Report Date Sept. 2016	
6. Performing Organization Code		8. Performing Organization Report No. 08-07	
7. Authors James H. Long		10. Work Unit No. (TRAIS)	
9. Performing Organization Name and Address Department of Civil Engineering University of Illinois 205 North Mathews/Urbana, IL 61801		11. Contract or Grant No. WisDOT SPR#0092-12-08	
12. Sponsoring Agency Name and Address Wisconsin Department of Transportation Research & Library Unit 4802 Sheboygan Ave. Rm 104 Madison, WI 53707		13. Type of Report and Period Covered Final Report 2010 -2015	
		14. Sponsoring Agency Code	
15. Supplementary Notes Research was funded by the Wisconsin DOT through the Wisconsin Highway Research Program. Wisconsin DOT contact: Jeffrey Horsfall (608) 243-5993			
16. Abstract The Wisconsin Department of Transportation (WisDOT) has concerns with both predicting pile lengths and pile capacities for H-piles driven into Intermediate-Geo Materials (IGM). The goal of the research was to perform 7 static axial load tests at 7 locations to compare results with capacities determined with the WisDOT driving formula, and with PDA and CAPWAP. An additional 208 dynamic load tests were added to the database using the results from production piling. In general, the methods for predicting capacities based on dynamic measurements taken at beginning of restrrike predicted static load test capacities of about 85 percent of the static load test value. Dynamic formulas, namely the FHWA modified Gates and the Washington State DOT method predicted about 85 and 95 percent of the static capacity as determined by static load tests. A common range of tip resistance in IGM soils was observed to be between 300 and 500 kips. The tip resistance was affected by the Penetration resistance (Nspt) exhibited by the IGM and therefore six test sites were revisited and modified standard penetration tests (MSPT) were conducted to get a more consistent record of IGM strength in the soil profiles. While there was considerable scatter, tip resistance increases as MSPT increase from 30 to 200 bpf. For values greater than 200 bpf, the scatter in the relationship revealed no trend. IGMs that were coarse grained exhibited higher resistance than IGM's that were fined grained. Results of the dynamic load tests were used to develop design recommendations for end bearing and side resistance for piles driven into IGMs. Design equations rely on results of the MSPT.			
17. Key Words Piles, driving piles, Intermediate Geomaterials, pile formula, pile capacity, predictive methods		18. Distribution Statement  No restriction. This document is available to the public through the National Technical Information Service 5285 Port Royal Road Springfield VA 22161	
18. Security Classif.(of this report) Unclassified	19. Security Classif. (of this page) Unclassified	20. No. of Pages 155	21. Price

## DISCLAIMER

This research was funded through the Wisconsin Highway Research Program by the Wisconsin Department of Transportation and the Federal Highway Administration under Project 0092-12-08. The contents of this report reflect the views of the authors who are responsible for the facts and accuracy of the data presented herein. The contents do not necessarily reflect the official views of the Wisconsin Department of Transportation or the Federal Highway Administration at the time of publication.

This document is disseminated under the sponsorship of the Department of Transportation in the interest of information exchange. The United States Government assumes no liability for its contents or use thereof. This report does not constitute a standard, specification or regulation.

The United States Government does not endorse products or manufacturers. Trade and manufacturers' names appear in this report only because they are considered essential to the object of the document.

## EXECUTIVE SUMMARY

The Wisconsin Department of Transportation (WisDOT) has concerns with both predicting pile lengths and pile capacities for H-piles driven into Intermediate-Geo Materials (IGM). IGM materials are the transition material from soil to hard bedrock. Materials could range from very dense sand and gravels to very hard tills to weak sandstones to weathered limestone and weathered granite. Typically, the SPT N values are greater than 50, uniaxial compressive strength in the range of 10 ksf to 100 ksf as defined by O'Neill and Reese (1999).

The goal of the research was to perform 7 static axial load tests at 7 locations to compare results with capacities determined with the WisDOT driving formula, and with PDA and CAPWAP. An additional 208 dynamic load tests were added to the database using production piling. Furthermore, driving stresses will be monitored using PDA measurements and CAPWAP interpretations. The test piles were 14 x 73 H-pile and driven to the required driving resistance as determined by the modified Gates dynamic formula.

Three axial load tests and dynamic tests on 33 piles were conducted in November and December of 2011 along the interchange of US 41 – STH 29 flyovers located in Brown County, Wisconsin. Results of the static pile load tests, and results of the dynamic monitoring are provided in this report.

An additional four static axial load tests and dynamic tests on 44 piles were conducted on H14x73 piles between September and November of 2012 along the interchange of US 41 – IH43 flyovers located in Brown County, Wisconsin.

An additional 208 dynamic tests were added to the database developed from dynamic monitoring of production piling.

Capacities as determined from static load tests for piles along the US41/STH29 corridor and the US41/IH43 corridor were compared with predictive methods. The CAPWAP BOR predicted capacities less than measured during the static load test. Median values of  $Q_p/Q_m$  were around 85 percent, meaning that CAPWAP (BOR) predicted about 85 percent of the capacity as determined from a static load test. Other studies have identified that 90 – 92 percent is typical, so these findings are slightly less than other studies. However, there were only 6 static load tests in this study, and the median value may change if more data were available.

The CAPWAP EOD and PDA EOD methods underestimated static pile capacity because the pile capacities increased with time. Typical delays of 3-7 days were used between EOD and BOR. However, the scatter for the two methods was low.

The dynamic formulas from FHWA modified Gates and Washington State DOT also under predicted capacities for the static load test, but not as much as CAPWAP EOD and PDA EOD; and there was less scatter associated with the predictions.

Capacities were compared for dynamic tests conducted on the piling from all three datasets. These results do not have static load test results, so the pile capacity is taken as the prediction made with CAPWAP

BOR. Furthermore, most of the dynamic load tests used a 24-hour restrrike to determine BOR, therefore, it is likely that the capacity for CAPWAP BOR for the dynamic test data is less than the true static piles capacity. The result is that ratios of  $Q_p/Q_m$  for the 208 pile database are higher than they would be if static pile capacity was used as the measure of  $Q_m$ .

The methods that exhibited the least scatter are the CAPWAP EOD and PDA EOD. This result is reasonable since they methods are based on measurements of energy delivered by the hammer and measured response of the pile. Values of  $\mu_{50}$  for CAPWAP EOD and PDA EOD were approximately 0.93, meaning that these two methods predicted, on the average, about 93 percent of the capacity of the pile as determined by CAPWAP BOR. The scatter associated with FHWA modified Gates and Washington State DOT were greater, and values of  $\mu_{50}$  were also greater: 1.16 and 1.31 for Gates and Washington, respectively. Although these ratios appear high, the ratios are based on CAPWAP BOR. If CAPWAP BOR predicts 85 percent of the static capacity (as determined from the static load tests), then the ratios are  $1.16 \cdot 0.85 = 0.98$  and  $1.31 \cdot 0.85 = 1.11$  which are more reasonable estimates. The presence of driving shoes did not appear to influence the ability of predictive methods to estimate capacity.

Tip capacity developed in IGMs was investigated by noting the soil type, the penetration resistance in the soil ( $N_{spt}$ ), and whether the pile had shoes. A plot of tip capacity versus  $N_{spt}$  for different soil types showed that there is significant scatter in the relationship, however, a general trend can be noted of increasing tip resistance with increasing  $N_{spt}$ . Piles with shoes developed a bit more tip capacity than piles without shoes. Tip capacities in the range of 300 to 500 kips were common. Tip capacities increased for  $N_{spt}$  values between 10 and 200; however, above 200 there is no discernable trend.

Design recommendations are developed to predict the capacity for piles driven into IGMs. Separate recommendations are given for IGMs that are primarily fine grained, and IGMs that are primarily coarse grained. Recommendations for end bearing pressure and side resistance are made for each IGM based on the penetration resistance exhibited by the layer using a Modified Standard Penetration Test (MSPT). Design recommendations for each component are given below:

The unit end bearing for piles driven into fine grained IGMs is specified as

$$q_{eb}(\text{ksf}) = 0.935 \cdot \text{MSPT} \quad (\text{not to exceed } 200\text{ksf})$$

and for piles driven into coarse grained IGMs

$$q_{eb}(\text{ksf}) = 65 \cdot \text{MSPT}^{0.3} \quad (\text{not to exceed } 300\text{ksf})$$

The unit side resistance for piles driven into fine grained IGMs is specified as a function of the MSPT value as follows:

$$f_s(\text{ksf}) = 0.021 \cdot \text{MSPT} \quad (\text{not to exceed } 2\text{ksf})$$

and the unit side resistance for piles driven into coarse grained IGMs is

$$f_s(\text{ksf}) = 0.9 \cdot \text{MSPT}^{0.25} \quad (\text{not to exceed } 3\text{ksf})$$

# TABLE OF CONTENTS

Disclaimer .....	i
Technical Report Documentation Page .....	ii
Executive Summary .....	iii
Chapter 1 Introduction and Literature Review.....	1
1.1 Organization of the Report.....	1
1.2 Background and Problem Statement .....	1
1.3 Literature Review.....	1
1.3.1 Mokwa and Brooks (2008) .....	2
1.3.2 Strength Properties from Standard Penetration Tests .....	3
1.3.3 Use of standard penetration test for determining strength.....	3
1.3.4 Use of a modified standard penetration test for determining strength.....	4
1.3.5 Penetration resistance related to pile end bearing pressure - cohesive.....	5
1.3.6 end bearing pressure for piles - cohesionless.....	6
1.3.7 Side resistance for piles - cohesive.....	7
1.3.8 Side resistance for piles - cohesionless.....	7
Chapter 2 Load Test Program .....	17
2.1 Introduction.....	17
2.2 Evaluation and Monitoring of Static Pile Load Tests.....	17
2.2 Special Provision for the Static load test .....	18
2.3 Special provision for dynamic pile monitoring.....	20
Chapter 3 Load Test Program at US41 and STH29.....	22
3.1 Introduction.....	22
3.1 Site 1 - Pier 6 of bridge structure B-05-658 .....	22
3.2 Site 2 - Pier 2 of bridge structure B-05-660 .....	23
3.3 Site 3 - Pier 12 of bridge structure B-05-660 .....	24
3.4 Summary.....	26
Chapter 4 Pile Load Tests - Intersection of US41 and IH43.....	47
4.1 Introduction.....	47
4.2 Site 1 - Pier 5 of bridge structure B-05-671 (11/06/2012 – 11/14/2012).....	48
4.3 Site 2 - Pier 16 of bridge structure B-05-678 (10/03/2012 – 10/11/2012).....	49
4.4 Site 3 - Pier 10 of bridge structure B-05-681 (9/18/2012 – 9/27/2012) .....	50

4.5 Site 4 - Pier 1 of bridge structure B-05-678 (10/24/2012 – 11/01/2012).....	51
4.6 Summary.....	52
Chapter 5 Dynamic Testing of Production Piling.....	89
5.1 Introduction.....	89
5.2 Bridge Structure B-5-671.....	89
5.3 Bridge Structure B-5-678.....	89
5.4 Bridge Structure B-5-679.....	89
5.5 Bridge Structure B-5-681.....	89
5.6 Discussion of Tables and Selection of Pile Tests .....	90
Chapter 6 Results of Static and Dynamic Testing.....	112
6.1 Introduction.....	112
6.1 Statistics used to quantify agreement between predicted and measured.....	112
6.2 Results for Static Load Tests.....	113
6.3 Results for dynamic load tests .....	113
6.4 End Bearing load as affected by soil type and Nspt .....	114
6.5 Use of MSPT to identify penetration resistance of IGMs at six sites .....	115
6.5.1 MSPT procedure.....	115
6.5.2 Results of MSPT conducted at pile load test sites in Green Bay, Wis .....	116
6.6 End Bearing load as affected by soil type and MSPT .....	116
6.6.1 End Bearing load for fine grained IGMs.....	117
6.6.2 End Bearing load for coarse grained IGMs .....	119
6.7 Unit side resistance .....	120
6.8 Design Recommendations for piles driven into IGMs.....	121
6.8.1 Unit end bearing in fine grained IGM .....	121
6.8.2 Unit end bearing in coarse grained IGM.....	122
6.8.3 Unit side resistance.....	122
Chapter 7 Summary and Conclusions .....	149
Chapter 8 References .....	152

# CHAPTER 1 INTRODUCTION AND LITERATURE REVIEW

## 1.1 ORGANIZATION OF THE REPORT

Background and general details of the static pile load test program are given in Ch. 2. Chapters 3 and 4 go into great detail about the static load tests and the dynamic load tests conducted in Green Bay. Chapter 5 discusses the inclusion of dynamic load test data collected from driving production piling. Chapter 6 combines the results of all the tests, to investigate the ability of methods to predict capacity. The methods investigated are CAPWAP BOR, CAPWAP EOD, PDA EOD, FHWA modified Gates, and the Washington State DOT methods. Results for all the tests are presented and reviewed to develop design recommendations for estimating end bearing and side resistance for driven piles in IGMs. Chapter 7 summarizes results for the program, and Chapter 8 provides the list of references.

## 1.2 BACKGROUND AND PROBLEM STATEMENT

The Wisconsin Department of Transportation (WisDOT) has concerns with both predicting pile lengths and pile capacities for H-piles driven into Intermediate-Geo Materials (IGM). IGM materials are the transition material from soil to hard bedrock. Materials could range from very dense sand and gravels to very hard tills to weak sandstones to weathered limestone and weathered granite. Typically, the SPT N values are greater than 50, uniaxial compressive strength in the range of 10 ksf to 100 ksf as defined by O'Neill and Reese (1999).

WisDOT typically designs using the FHWA computer program DRIVEN to determine pile capacities for a given soil profile. When IGM is encountered WisDOT assumes a large cohesive value to resist the load. This assumes that the H-pile will achieve the Required Driving Resistance at the top of the IGM layer. However, with the higher Required Driving Resistance established using the Load and Resistance Design methodologies, the H-piles were found to either run longer than the design length or be damaged. In an effort to eliminate this issue, WisDOT reduced the Required Driving Resistance for H-piles and increased the resistance factor, thus reducing the driving concerns. However, there are still unknowns with both the design and construction of H-piles driven into IGM.

The goal of the research is to perform three static axial load tests at one location and 4 static load tests at another location in the Green Bay area to compare results with capacities determined with the WisDOT driving formula, and with PDA and CAPWAP. Furthermore, driving stresses will be monitored using PDA measurements and CAPWAP interpretations.

## 1.3 LITERATURE REVIEW

There is little published work that has focused on piles driven into Intermediate Geo-Materials (IGMs). Intermediate Geo-Materials are defined as ground that is stronger than what is normally considered soil, and weaker than what is normally considered as rock.

Although there has been little work performed for IGM on driven piles, there have been more studies focused on drilled shafts embedded into IGMs. O'Neill and Reese (1999) identified two types of IGMs, cohesive and cohesionless. Cohesive IGMs exhibited unconfined compression strengths between 10 and

100 ksf, while cohesionless IGMs exhibited blow counts greater than 50 blows per foot (bpf) using a Standard Penetration Test.

The literature review discusses two main topics: studies that have focused on driven piles in IGMs, and studies that provide information on soil strength, end bearing pressure, and side resistance, for IGM's.

### *1.3.1 MOKWA AND BROOKS (2008)*

The most recent completed work on piles driven into IGM's has been performed by Mokwa and Brooks (2008) and Brooks (2008). They contracted with the Montana DOT to investigate the capacity of piles driven into cohesive and cohesionless IGM's in the state of Montana. Their investigation used two pile databases. With an international database, they selected several cases in which static load tests and CAPWAP results were available and concluded that CAPWAP provided reasonable axial capacity estimates for piles driven into IGM. They also concluded that the Washington State DOT formula was the more accurate dynamic formula for determining pile capacity from simple measurements of hammer stroke, ram weight, and pile set. They used a smaller and more local database based on nine bridge sites in Montana where piles had been driven into IGM to conduct a more detailed investigation; however, no static load tests were in this database. Accordingly, they used CAPWAP results as the estimate for capacity as well as the capacities developed in end bearing and side resistance.

The results of back calculated end bearing capacity developed from driven piles in IGM's are shown in Figs. 1.1a and 1.1b. Values of end bearing pressure are from both H-piles and pipe piles. Cohesive IGMs are defined with unconfined strengths between 10-100 ksf (500-5000 kPa) and therefore, only a few of the data fall into the IGM range. Most of the back-calculated values for end bearing appear to range from 1 to 100 ksf (50 to 5000 kPa).

Fig. 1.1b identifies the back calculated end bearing pressures for both cohesive and cohesionless IGMs versus length. The figure shows the range of end bearing pressures to range from 1 – 640 ksf (50 to 32000 kPa) with most of the values below 200 ksf (10000 kPa). The back-calculated values for end bearing pressures results show considerable variation.

Results for side resistance ( $N_{s\text{layer}}$ ) of piles driven into IGMs are shown in Figs. 1.2a and 1.2b. Figure 1.2a shows values of side resistance versus unconfined compression strength for the IGM. The range of unconfined strength for IGM is between 10 and 100 ksf (500 to 5000 kPa). Figure 1.2b shows the side resistance versus length of pile in the IGM. This figure is shown to exhibit all the results from the study including both cohesive and cohesionless IGMs. The range of side resistance exhibited in Figs. 1.2a and 1.2b range from 0.2 to 27 ksf (10 to 1370 kPa) with an average side resistance around 10 ksf (500 kPa).

Results of their study pointed to the extreme variability for the IGM's and the difficulty of predicting pile driving behavior in these types of soils. Back-calculated estimates of mobilized end bearing and side resistance exhibited considerable variability. Often piles would reach refusal earlier than expected, or drive through the IGM to lengths much greater than anticipated. While they identified both cohesive and cohesionless IGM's they also identified difficulties with getting representative samples for the IGM and representative field values for penetration resistance, and noted that the difficulty for identifying the IGM and its properties is a major challenge.

### 1.3.2 STRENGTH PROPERTIES FROM STANDARD PENETRATION TESTS

A relationship between the strength of a soil and its penetration resistance is a concept that has been used extensively in geotechnical engineering. There has been extensive discussion relating strength to penetration resistance. Using penetration resistance to quantify strength requires that a standard method be used for conducting the penetration test and for interpreting the measurements. The most common penetration test in the United States is the Standard Penetration test (SPT) which has been used for several decades. Several correlations between STP values and soil properties have been proposed. Herein we focus on two correlations which are relating penetration results to soil strength, and relating penetration results to soil/pile parameters such as end bearing capacity and maximum side resistance. Interpretation of penetration results may be different for cohesive and cohesionless soil.

Penetration tests may provide some advantages for characterizing IGMs because they provide a relatively simple means to conduct an insitu measurement of penetration resistance while collecting a (disturbed) sample of the soil. Undisturbed sampling of IGMs is typically a more difficult task. Accordingly, there are several studies that have related STP resistance values to strength of stiff, hard soils and of IGMs.

The standard penetration test is conducted by lifting a 140 lb hammer and dropping it 30 inches onto a length of rod. At the end of the rod is a standard sampler. The hammer weight is lifted and dropped to penetrate the sampler into soil at the bottom of the borehole. The number of blows are recorded to penetrate the sampler from 0-6", 6-12", and from 12-18". The penetration resistance,  $N_{spt}$ , is taken as the number of blows required to penetrate the sampler from 6 to 18. Correlations made with results of the standard penetration test are affected greatly by the energy of the hammer delivered to the sampler. For the same soil profile, greater hammer energy delivered to the sampler will result in a smaller  $N_{spt}$  values. Accordingly, the  $N_{spt}$  values are standardized to an assumed energy level corresponding to 60 percent of the theoretical value. The standard value for penetration resistance  $N_{60}$  is used to reflect this standardized value.

### 1.3.3 USE OF STANDARD PENETRATION TEST FOR DETERMINING STRENGTH

There are several studies that relate the standard penetration resistance to soil strength. Peck, et. al., (1974) related soil strength to  $N_{60}$  in an approximate way (Table 1.1) for soils ranging from very soft to hard clays. The ratio of unconfined compressive strength (tsf) to  $N_{60}$  ranges from 0.125 to 0.133. Peck, et. al (1974) consider this relationship between blow count and strength to be approximate and somewhat unreliable. Accordingly, using the relationship between strength and penetration resistance provided by Peck, et. al.(1974), we can relate soil shear strength ( $s_u$ ) to  $N_{60}$  as follows:

$$s_u \text{ (ksf)} = 0.125 \text{ to } 0.133 * N_{60} \quad \text{eqn. 1.1}$$

Stroud (1974) suggested that standard penetration test results on stiff clays to soft rocks could provide a reasonable means to determine strength of the ground. Standard penetration results were compared with triaxial strengths for thick deposits of very stiff overconsolidated soils and the standard penetration test results exhibited less scatter than triaxial tests. Terzaghi, et. al. (1996) summarized Stroud's results with the relating shear strength to standard penetration test value ( $N_{60}$ ) as shown in Fig. 1.3. Values of  $s_u$  (kPa)/ $N_{60}$  vary between 4 and 6. In term of the units used in this report (ksf) the following equation is representative of Stroud (1974) and Terzaghi, et. al. (1996):

$$s_u \text{ (ksf)} = 0.08 \text{ to } 0.12 * N_{60} \quad \text{eqn. 1.2}$$

Accordingly, Stroud's (1974) results indicate similar, but a slightly smaller ratio of  $s_u / N_{60}$  than suggested by Peck, et. al. (1974).

#### *1.3.4 USE OF A MODIFIED STANDARD PENETRATION TEST FOR DETERMINING STRENGTH*

As soil strength increases from typical soil strengths to strengths representative of IGMs, the penetration resistance ( $N_{60}$ ) increases to values that are excessive and therefore, too many blows with the hammer are required to attain a penetration of 18 inches within a reasonable number of blows. Accordingly, it becomes impractical to follow the standard procedure for attaining an  $N_{60}$  value. Stark, et al. (2014) developed a modified version of the standard penetration test (MSPT) to allow the same equipment used for an SPT to be used for soft shales and weak rock.

The MSPT test is conducted by hammering the sampler in the same manner as the SPT, however, readings of sampler penetration are taken every 10 blows, and results are plotted as penetration versus number of blows as shown in Fig. 1.4. The data used in Fig. 1.4 come from a soil boring exploration program conducted in 2015 and discussed in detail in Chapter 6 of this report. The plot of penetration versus number of blows typically becomes linear, or nearly linear after 60 blows, and the slope of the linear portion of the curve is converted to an equivalent penetration resistance value in terms of blows per foot. While the units for penetration resistance are the same, the values of  $N_{spt}$  and MSPT are not the same because it is determined using a different procedure.

There are a number of practical modifications that could be made to the MSPT to achieve similar values. For example, a normal SPT test could be conducted and after 50 blows, the sample has not penetrated enough for a SPT result. The driller could stop and mark a reference point on the sampler, and then measure the sampler penetration after 50 more blows. The MSPT value could then be determined as the ratio of 50 blows divided by the sampler penetration measured in the last 50 blows.

The differences in values for  $N_{spt}$  and MSPT are illustrated for three cases: 1) when the final penetration after 100 blows is between 12 and 18 inches (Fig. 1.5), 2) when the final penetration after 100 blows is between 6 and 12 inches (Fig. 1.6), and 3) when the final penetration after 100 blows is less than 6 inches (Fig. 1.7).

When the final penetration after 100 blows is between 12 and 18 inches, the equivalent  $N_{spt}$  value was determined as the penetration resistance (in blows/ft) after 6 inches of penetration. Accordingly, the equivalent  $N_{spt}$  was determined as

$$N_{spt} = (100 - \text{\#blows for pen of 0.5ft}) / (\text{total penetration} - 0.5\text{ft}) \quad \text{eqn. 1.3}$$

and is illustrated in Fig. 1.5.

The equivalent  $N_{spt}$  value, when the total penetration after 100 blows was between 6 and 12 inches, was determined as the penetration resistance (in blows/ft) after 6 inches of penetration using the same equation as above (Eqn. 1.3) and a comparison of the penetration rates for the equivalent  $N_{spt}$  and MSPT are shown in Fig. 1.6.

When the total penetration rate is less than 6 inches for 100 blows, the equivalent N<sub>spt</sub> rate is taken as the ratio of number of blows divided by the penetration, and a comparison between N<sub>spt</sub> and M<sub>spt</sub> is shown in Fig. 1.7. The (equivalent) N<sub>spt</sub> estimate includes the initial portion of the penetration versus resistance curve, which is affected by cutting in the drill hole and seating of the sampler during penetration. Accordingly, there is a greater difference between N<sub>spt</sub> and M<sub>spt</sub> when the total penetration is less than 6 inches.

Only a very few of the M<sub>spt</sub> tests experienced less than 6 inches of penetration, therefore, the relationship between N<sub>spt</sub> and M<sub>spt</sub> was developed for M<sub>spt</sub> penetrations exceeding 6 inches. A comparison of the M<sub>spt</sub> penetration resistance with the equivalent N<sub>spt</sub> values is shown in Fig. 1.5. It can be seen that the M<sub>spt</sub> values are approximately 27 percent higher for the same soil than N<sub>spt</sub> values.

M<sub>spt</sub> and N<sub>spt</sub> values are affected by the energy being delivered to the sampler. Therefore, energy corrections for M<sub>spt</sub> values may be necessary. It is estimated (but currently unconfirmed) that the efficiency values for tests reported by Stark, et. al, are in the range of 88 percent based on results from energy measurements reported by GRL (2015) from tests conducted in Wisconsin.

Stark, et. al. (2013) conducted several M<sub>spt</sub> tests in weak shale and also collected and tested sample cores. They related strength of the soil to M<sub>spt</sub> value as follows:

$$s_u \text{ (ksf)} = 0.039 * M_{spt} \quad \text{eqn. 1.4}$$

This ratio is smaller than observed for the N<sub>spt</sub> values, which is to be expected for two reasons: 1) the M<sub>spt</sub> and N<sub>spt</sub> are not equivalent, and 2) the energy efficiency is greater than 60 percent for the M<sub>spt</sub> tests used in developing correlations strength. Correcting for the difference between M<sub>spt</sub> and N<sub>spt</sub> and for the difference in efficiency, we get the following relationship:

$$M_{spt} = 1.27 * N_{spt} \quad \text{eqn. 1.5}$$

$$N_{60} = N_{spt} * (\text{Efficiency}/60) \quad \text{eqn. 1.6}$$

Combining eqn. 1.4 with eqns 1.5 and 1.6, we get

$$\begin{aligned} s_u \text{ (ksf)} &= (0.039 * M_{spt} * (N_{spt}/M_{spt}) * (N_{60}/N_{spt})) = 0.039 * (1/1.27) * (88/60) \\ &= 0.045 * N_{60} \quad \text{eqn. 1.7} \end{aligned}$$

These corrections still show the ratio of strength to penetration resistance is about half of the ratios proposed by Peck, et. al (1974), Terzaghi, et al. (1996), and Stroud (1974).

### *1.3.5 PENETRATION RESISTANCE RELATED TO PILE END BEARING PRESSURE - COHESIVE*

Penetration resistance has also been related to end bearing pressure and side resistance for piling and drilled shafts. These relationships can be developed by directly comparing penetration resistance with measurements of end bearing capacity and side resistance, or indirectly by relating penetration resistance to soil strength and then relating soil strength to end bearing capacity to strength.

End bearing capacity for piles can be determined as  $9 * s_u$ . Therefore, using the relationship between strength and penetration resistance proposed by Terzaghi, et. al. (Eqn. 1.2) the end bearing capacity (qeb) is

$$qeb \text{ (ksf)} = 9 * (0.08 \text{ to } 0.12) * N_{60} = (0.72 \text{ to } 1.08) * N_{60} \quad \text{eqn. 1.8}$$

Stark., et. al. (2013) related end bearing to MSPT values for drilled shafts. Their suggested equation is:

$$qeb \text{ (ksf)} = 0.347 * \text{MSPT} \quad \text{eqn 1.9}$$

and converting MSPT to  $N_{60}$  as previously shown in Eqns. 1.5, 1.6, and 1.7,

$$qeb \text{ (ksf)} = 0.4 * N_{60} \quad \text{eqn. 1.10}$$

Abu-Hejleh and Attwooll also developed a relationship between penetration resistance and end bearing capacity for drilled shafts. The equation is:

$$qeb \text{ (ksf)} = 0.92 * N_{60} \quad \text{eqn. 1.11}$$

which is within the range using Terzaghi, et. al, 1996 (Eqn. 1.8).

### 1.3.6 END BEARING PRESSURE FOR PILES - COHESIONLESS

Relationships for limiting end bearing pressure for piles in granular soil have been proposed by Meyerhof (1976) as

$$qeb \text{ (ksf)} = 8 * N_{60} \quad \text{eqn. 1.12}$$

O'Neil and Reese (1999) suggest an end bearing pressure for drilled shafts equal to

$$qeb = 0.59 * [N_{60} * (\text{patm} / \sigma'_{vb})]^{0.8} * \sigma'_{vb} \quad \text{eqn 1.13}$$

where patm is atmospheric pressure, and  $\sigma'_{vb}$  is the effective stress at the elevation of the end bearing. Using units of ksf, and assuming depths of 20 ft and 80 ft, and effective unit weight of 70 pcf, Eqn. 1.13 can be simplified to the following formula

$$qeb \text{ (ksf)} = 1.10 * N_{60}^{0.8} \text{ for a depth of 20 ft} \quad \text{eqn. 1.14}$$

and

$$qeb \text{ (ksf)} = 1.45 * N_{60}^{0.8} \text{ for a depth of 80 ft} \quad \text{eqn. 1.15}$$

Olson (1990) suggested limiting values for end bearing pressure for piles in granular soils based on  $N_{60}$  values. His recommendations are as follows: 1) for  $N_{60}$  values from 30 to 50, the maximum end bearing pressure is recommended as 190 ksf, 2) for  $N_{60}$  values between 50 and 100, a maximum end bearing pressure of 200 ksf is recommended, and for  $N_{60}$  values exceeding 100, a limiting value of 520 ksf is recommended.

Coyle and Castello (1981) looked at a database for piles in sand. Although the sands were not classified as IGMs, the maximum bearing pressure they recommended for very dense sands was 300 ksf.

### 1.3.7 SIDE RESISTANCE FOR PILES - COHESIVE

There is a paucity of data identifying the side resistance for piling driven into IGMs. The observations from Mokwa and Brooks (2008) have already been presented above range from 0.2 to 27 ksf (10 to 1370 kPa) with an average side resistance around 10 ksf (500 kPa). Accordingly, it is useful to report what side resistance values have been reported by others in cohesive soils.

Tomlinson (1957) back calculated side resistance for a number of driven piles. The maximum resistance developed along the side of the pile was 0.75 ksf; however, the maximum compressive strength of the soil was 6 ksf, which is below the range of strengths (10-100 ksf) for IGMs.

Bustamante and Gianeselli (1983) developed a method, commonly referred to as the LPC method for predicting axial capacity of piles based on cone penetration results. The maximum side resistance using their recommendations is approximately 2 ksf.

Stark, et. al. (2013) back calculated side resistances from a database of drilled shafts in IGM. They found side resistances varied from 3 to 23 ksf in which the side resistance was proportional to the unconfined strength of the IGM ( $f_s = 0.3 \cdot q_u$ ). Stark, et. al. related the strength to MSPT, therefore, the value of unit side resistance can be expressed as

$$f_s \text{ (ksf)} = 0.023 \cdot \text{MSPT} \quad \text{eqn. 1.16}$$

Or in terms of  $N_{60}$ ,

$$f_s \text{ (ksf)} = 0.027 \cdot N_{60} \quad \text{eqn. 1.17}$$

### 1.3.8 SIDE RESISTANCE FOR PILES - COHESIONLESS

Similar to the case for cohesive IGMs, there is a paucity of data identifying the side resistance for piling driven into cohesionless IGMs. Observations of side resistance by Mokwa and Brooks (2008) range from 4 to 10 ksf (200 to 500 kPa), with an average side resistance of approximately 6 ksf (300 kPa). Accordingly, it is useful to report side resistance values that have been reported by others in cohesionless soils.

Meyerhof suggested that the unit side resistance ( $f_s$ ) in driven, low-displacement piles could be approximated as

$$f_s \text{ (ksf)} = N_{60}/50 \quad \text{eqn. 1.18}$$

which corresponds to unit side resistances of 1, 2, and 4 ksf for  $N_{60}$  values of 50, 100, and 200 respectively.

Olson (1990) provides recommendations for limiting side resistance based on  $N_{60}$  values as follows: a limiting value of 1.9 ksf for  $N_{60}$  between 11 and 30, 2.6 ksf for  $N_{60}$  between 31 and 50, 3.3 ksf between 51 and 100, and 3.8 ksf for  $N_{60}$  values in excess of 100.

Bustamante and Gianeselli (1983) recommend limiting the side resistance to 2.5 ksf for granular soils with penetration resistances values greater than 50.

**Table 1.1 Ratio of strength to blow count from Peck, Hanson, and Thornburn (1974)**

Consistency	Approximate Compressive Strength (tsf)	Nspt	Ratio of $q_u$ (tsf)/Nspt Or $s_u$ (ksf)/Nspt
Very Soft	Less than 0.25	0-2	0.125
Soft	0.25 - 0.5	2-4	0.125 - 0.125
Medium	0.5 - 1.0	4-8	0.125 - 0.125
Stiff	1.0 - 2.0	8-15	0.125 - 0.133
Very Stiff	2.0-4.0	15-30	0.133 - 0.133
Hard	Over 4.0	Over 30	0.133

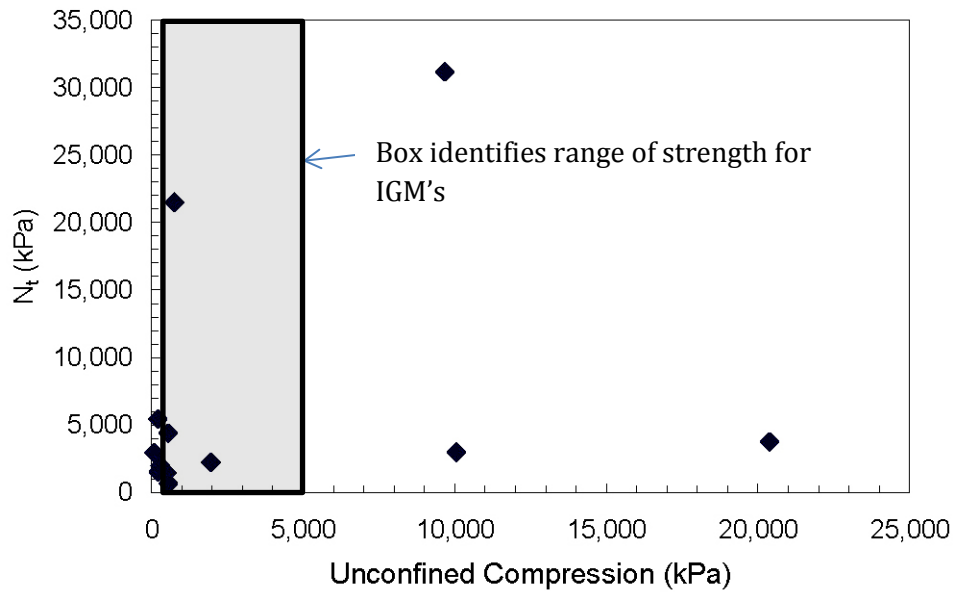
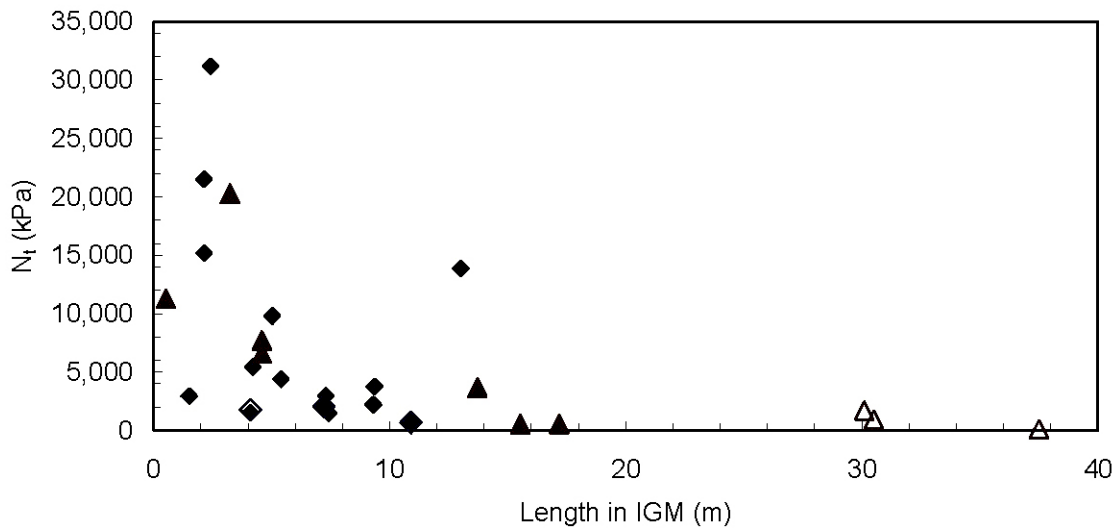


Figure 1.1a. Back-calculated end bearing pressure versus unconfined strength of IGM (Mokwa and Brooks, 2008)



◆ Cohesive IGM   ◇ Cohesive IGM Restrike   ▲ Cohesionless IGM   △ Cohesionless IGM Restrike

Figure 1.1b. Back-calculated end bearing pressure versus pile length embedded in IGM (Mokwa and Brooks, 2008)

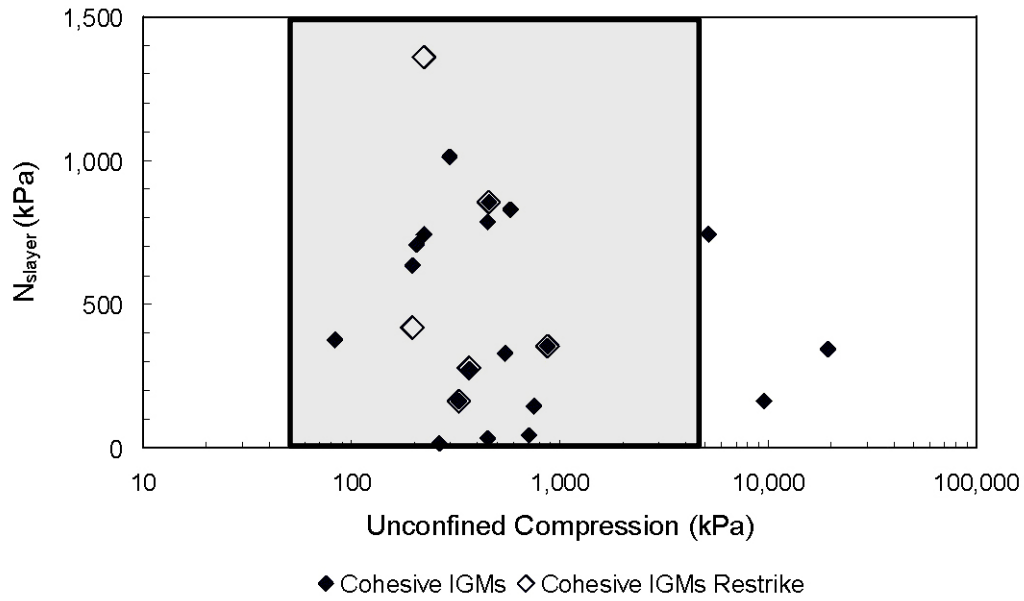


Figure 1.2a. Back-calculated side resistance versus unconfined strength of IGM (Brooks, 2008)

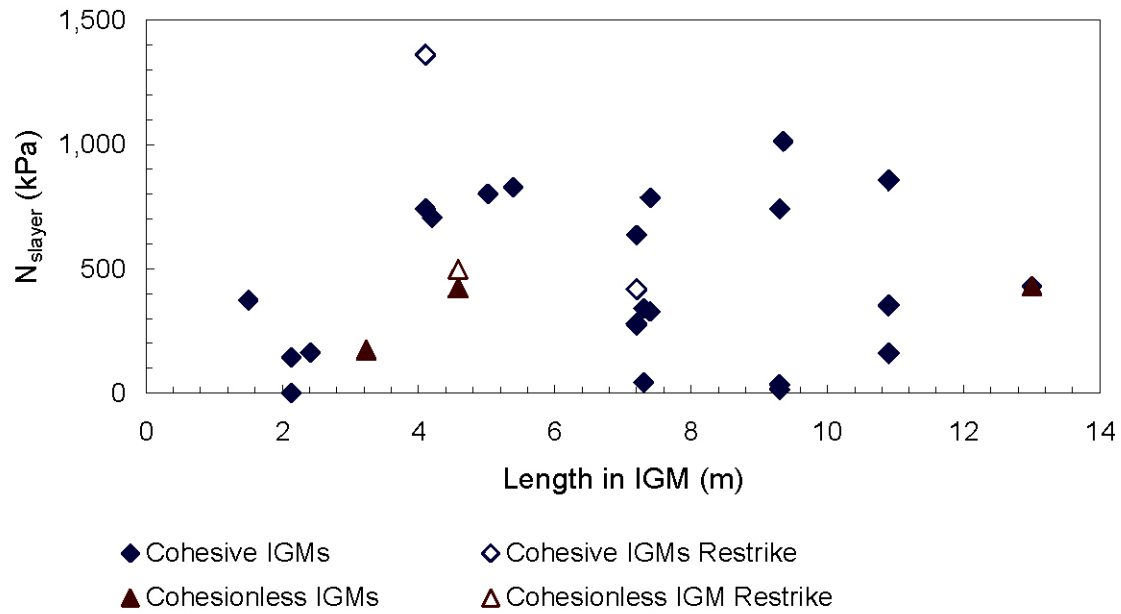


Figure 1.2b. Back-calculated side resistance versus pile length embedded in IGM (Brooks, 2008)

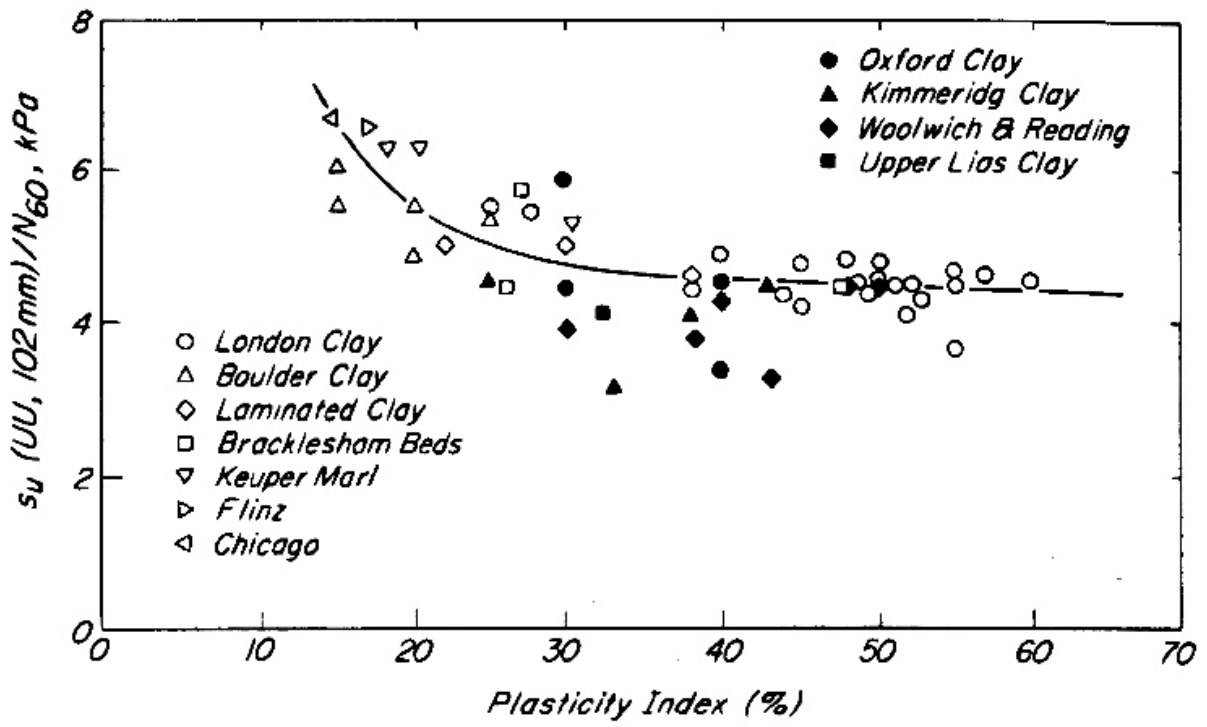


Figure 1.3 Relationship of the ratio of soil strength/ $N_{60}$  and Plasticity Index (Terzaghi, et. al, 1996).

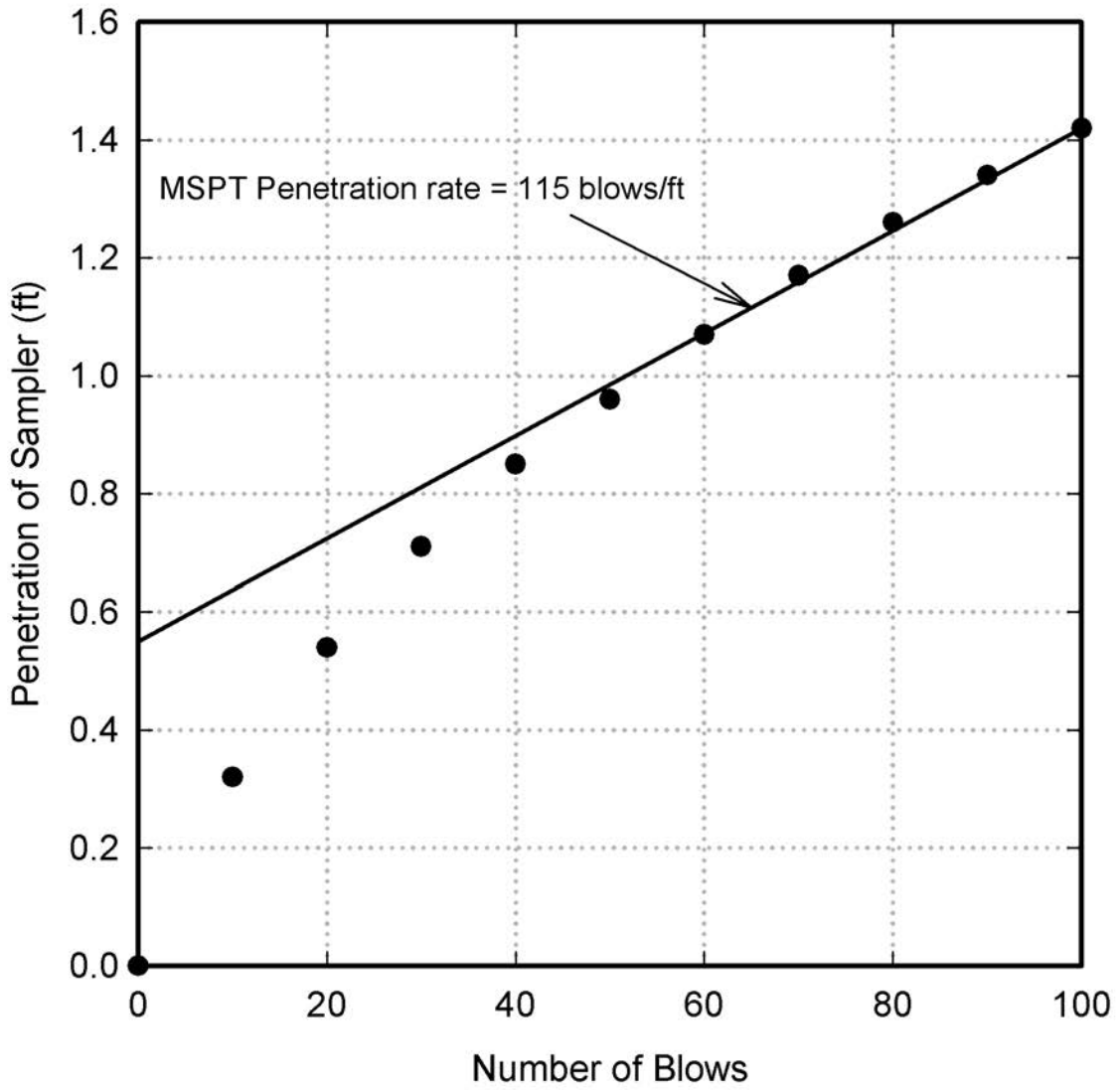


Figure 1.4. Penetration versus Blow Count for GB North, Site 1 at Elev 546.79

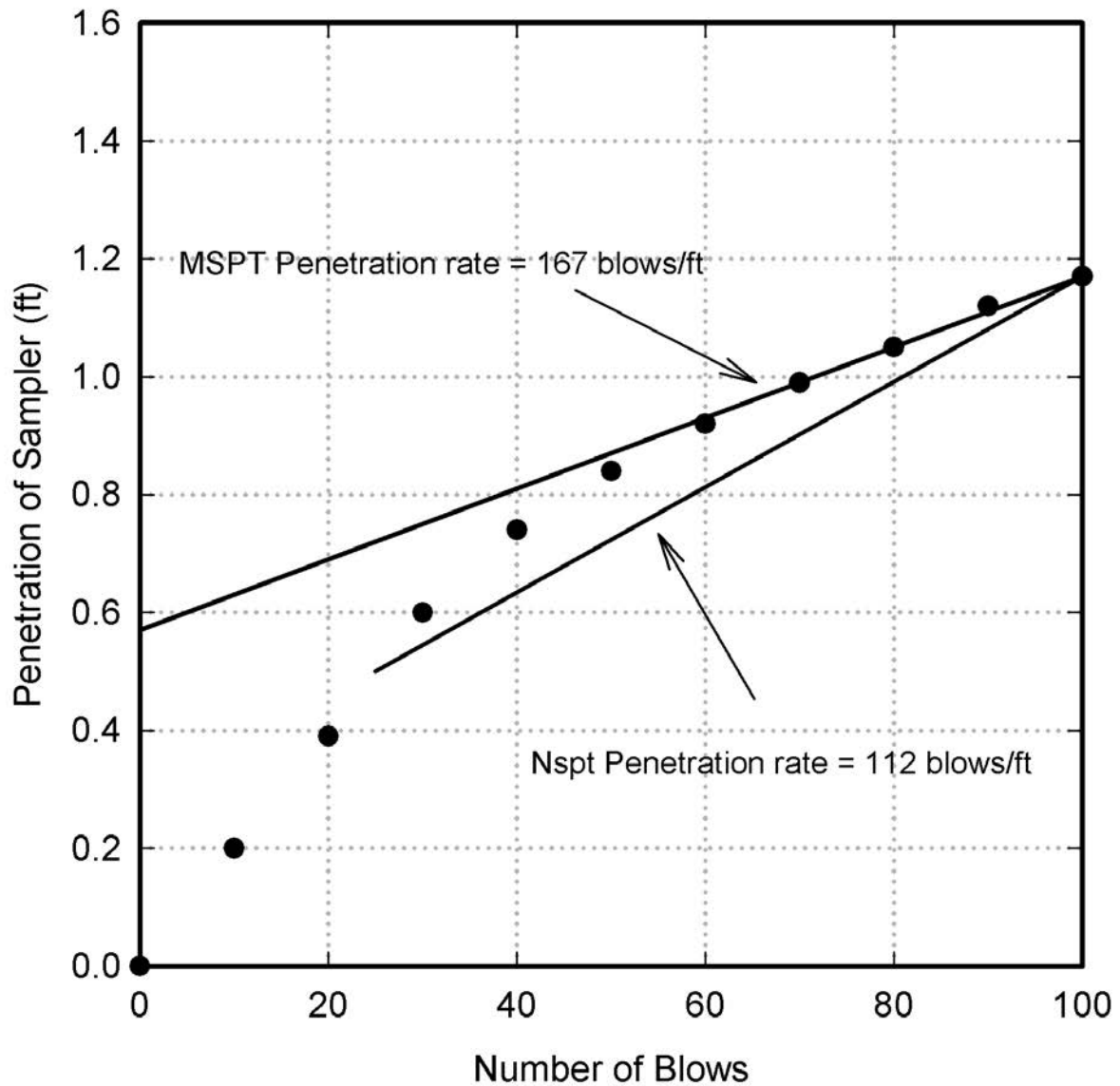


Figure 1.5. Penetration versus Blow Count when final sampler penetration is between 12 and 18 inches (B-5-658, Pier 16 depth of 72ft).

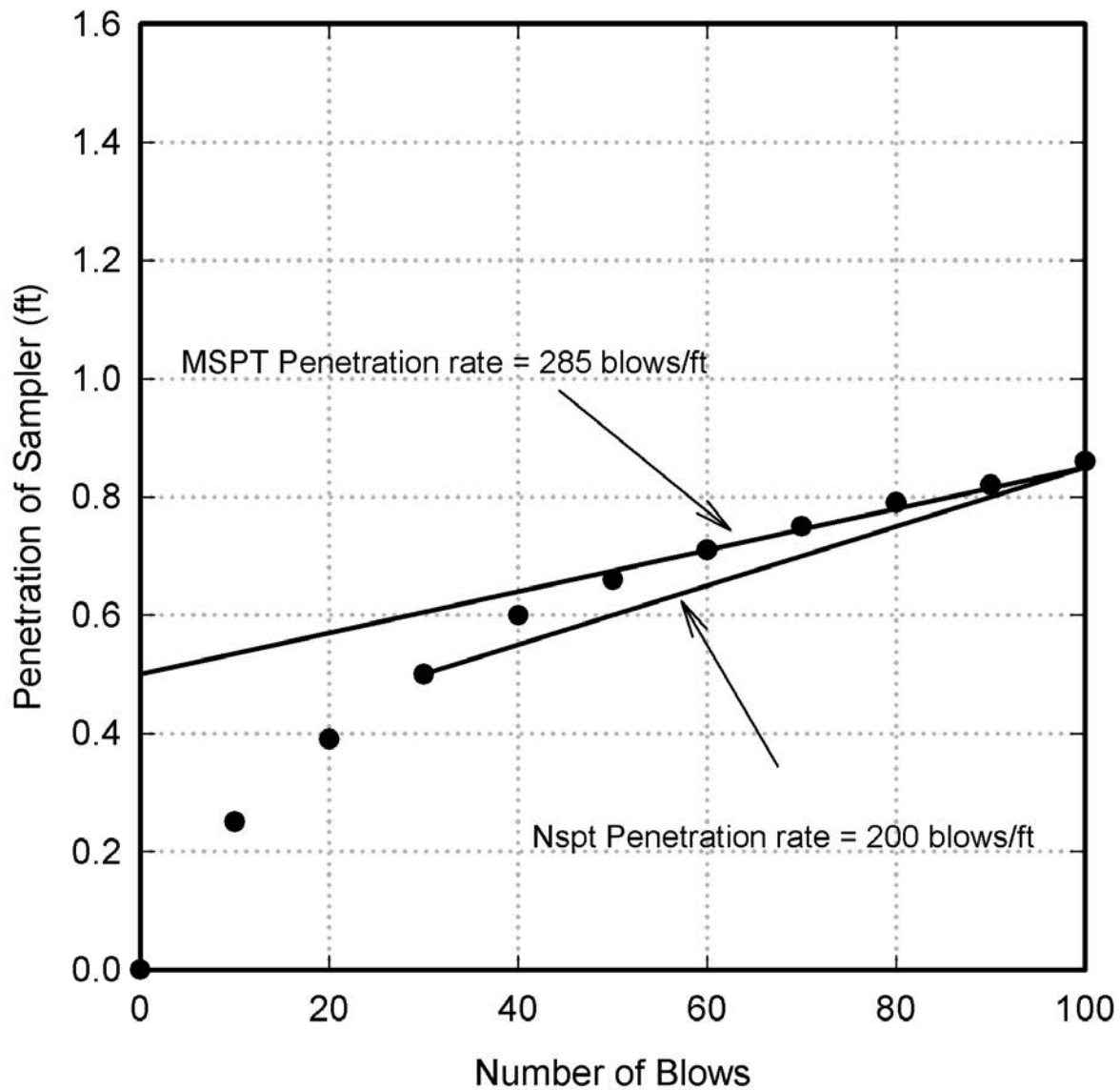


Figure 1.6. Penetration versus Blow Count when final sampler penetration is between 6 and 12 inches (B-5-658, Pier 16 depth of 70ft).

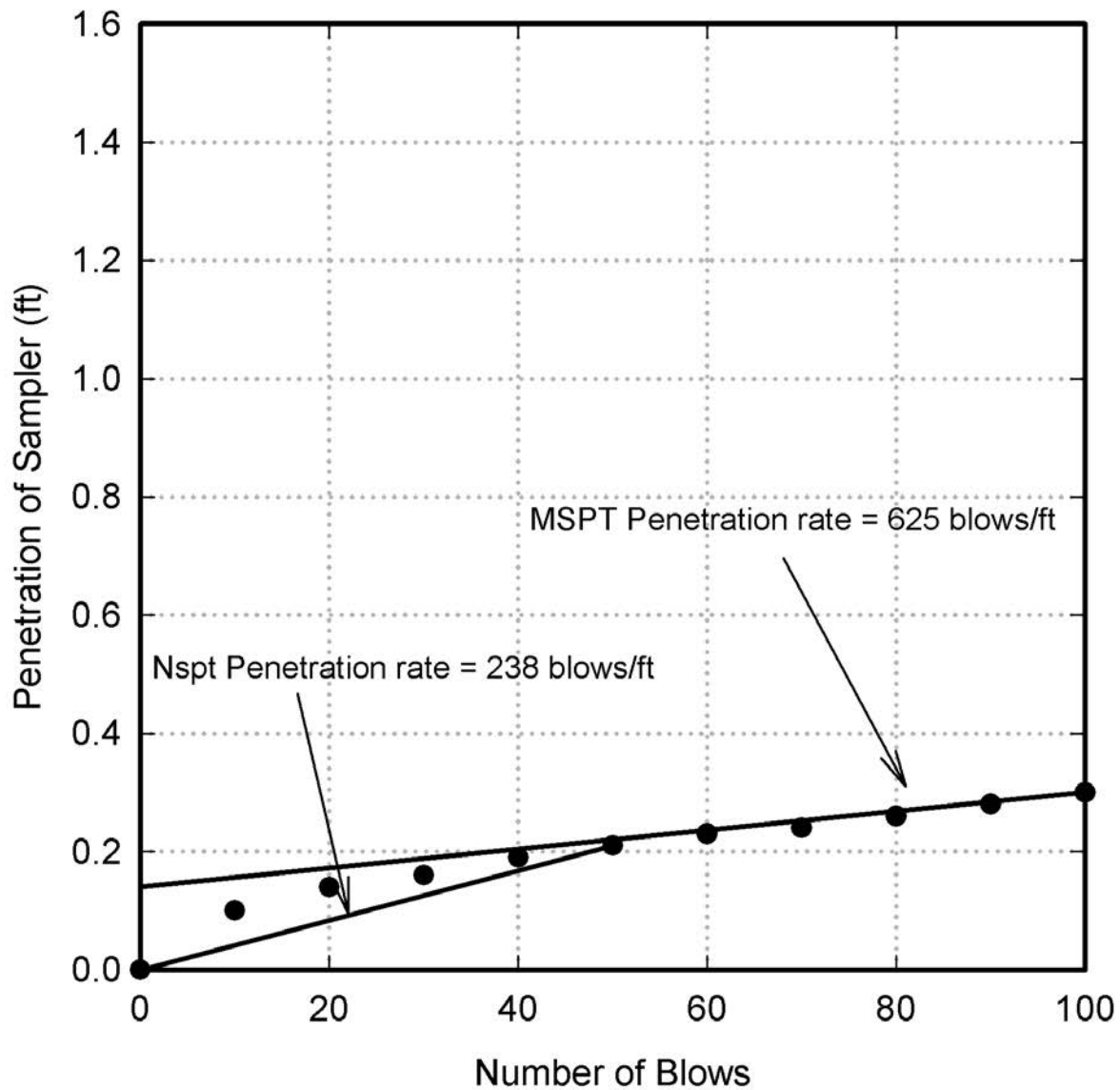


Figure 1.7. Penetration versus Blow Count when final sampler penetration is between 0 and 6 inches (B-5-678, Pier 1 depth of 81ft).

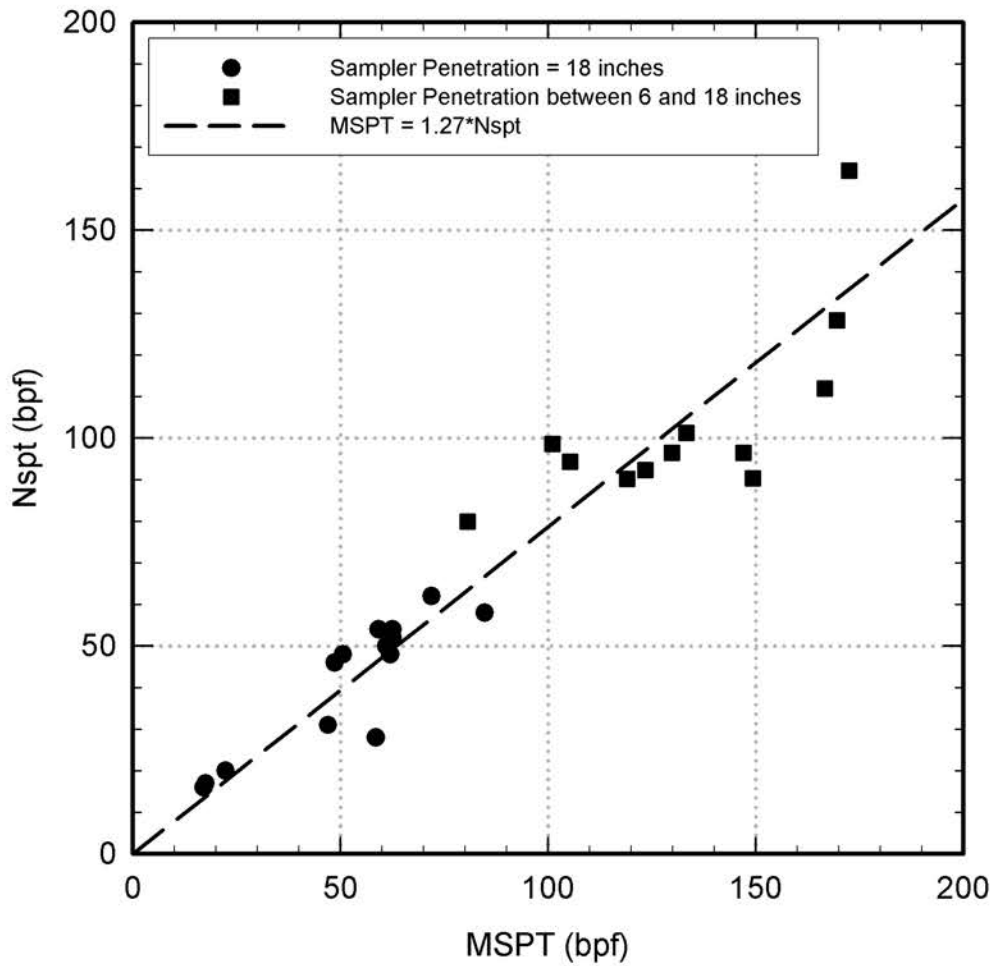


Figure 1.8. Nspt versus MSPT for cases where the sampler penetrates between 6 inches and 18 inches for 100 blows.

# CHAPTER 2 LOAD TEST PROGRAM

## 2.1 INTRODUCTION

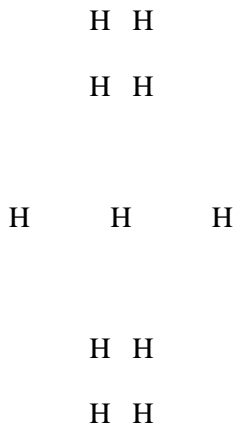
This chapter will discuss the general setup for the static load test program that are discussed in more detail in chapters 3 and 4. The load test program was designed to test piles driven into IGM's. Static load tests were planned as well as dynamic load tests. Special provisions were developed as part of the program, and are also provided in this chapter.

## 2.2 EVALUATION AND MONITORING OF STATIC PILE LOAD TESTS

Static pile load tests were conducted to comply with ASTM D1143/D1143M-07e1: Standard Test Methods for Deep Foundations Under Static Axial Compressive Load. All static load tests were conducted in Brown county with 3 static load tests conducted along the corridor of USH 41/STH 29 and 4 static load tests were conducted at the USH41/IH43 corridor. The static load was designed to either cause failure of the pile (as determined by the offset limit method as proposed by Davisson (1972)) or a minimum of three times the design load. The Quick Test Method was used to control the times between load increments. The quick test method is the appropriate method to use when interpreting the load capacity using Davisson's offset method.

All driven piles for the load test and reaction piling were monitored dynamically using a Pile Driving Analyzer and data reduced using CAPWAP. Pile driving behavior was collected and interpreted for both end of driving (EOD) and beginning of restrike (BOR).

The basic setup for the testing program was to drive 11 piles in a pattern similar to that illustrated below.



The piles form the rough shape of a cross, with the static load test pile being the center pile. The 4-pile rectangles provide reaction piling for the load transfer beam that acts as a reaction for the static load test pile. Four reaction piles are used on each end (for a total of 8 reaction piles) to provide adequate anchorage against pullout. Some of the soil profiles consisted of soft clay over an IGM. This soil

condition results in piles with large compression capacity but little pullout capacity. One static load test site came very close to pulling out the reaction piling before the static load test was completed.

As identified earlier, the static load test pile was the “H” directly in the center of the figure. The other two piles, directly to the left and right of the static load test pile were termed “dynamic load test piles.” These piles were driven in a manner similar to the static load test pile and the reaction piles, however, the piles were not disturbed to isolate them from influences such as loading from the load transfer beam, or load from the static load test. Accordingly, designations were assigned the piling as given below:

RP1 - RP8: Reaction Pile 1 through Reaction Pile 8

SLTP: Static Load Test Pile

DLTP1-DLTP2: Dynamic Load Test Pile 1 and Dynamic Load Test Pile 2

The timeline for installation and testing was proposed as:

Sequence	Pile	Comment
1	RP1-RP8	Install Piles with Dynamic Monitoring
2	DLTP1-DLTP2	Install piles with Dynamic Monitoring
3	SLTP	Install pile with Dynamic Monitoring
4	RP1, RP5, DLTP1	Conduct 24 hour restrrike
5	SLTP	Setup load test and conduct load test
6	SLTP, DTP1, DLPT2 RP1-RP8	Conduct BOR on all piles

## 2.2 SPECIAL PROVISION FOR THE STATIC LOAD TEST

Special provisions were created for the load test program. Below is the special provision.

General: This work includes designing and constructing a static pile load test reaction frame and reference frame, providing and installing all load and displacement measurement equipment, and providing and operating a hydraulic loading system. This work shall be performed at the location shown in the plans according to ASTM D 1143.

The pile load test will be directed by Dr. Jim Long or his representative from the University of Illinois at Urbana Champaign (UIUC). Reading and recording data will be performed by either UIUC or WisDOT personnel. All other work shall be performed by Contractor personnel.

Submittals: The Contractor shall submit the following information to the Engineer for approval, at least 14 days prior to driving the load test pile.

- 1) Shop drawings sealed by a Structural Engineer licensed in the State of Wisconsin detailing:
  - a) Reaction frame configuration, component sizes, dimension, connections, reaction pile locations, lengths and installation requirements, dial gage locations, as well as the reference beam sizes and locations.

- b) Load cell size, capacity and dimension as well as its arrangement with the hydraulic jack and other bearing elements between the pile and frame.
- c) Design calculations demonstrating that the structural capacity and lateral stability of the frame and frame-to-reaction pile connections satisfy AASHTO LRFD design code.
- 2) Certification and supporting data demonstrating the proposed jacking system, load cell, pressure gages, and dial indicators have been calibrated as described in ASTM D1143.
- 3) The anticipated static load test date to allow the Engineer to coordinate and schedule with Dr. Long at (217-333-2543).

Any changes to the proposed load test date or equipment shall be submitted to the Engineer to determine if they can be accommodated by Dr. Long.

Equipment: The Contractor shall obtain a hydraulic jacking system with a minimum capacity of 800 kips. The jack shall be equipped with spherical bearings and capable of being used in series with a load cell to apply the design load against the load frame and the load test pile. A calibrated gauge measuring jack pressure shall be used, along with the load cell, as a check and back-up in case of malfunctions.

Deflection near the top of the pile shall be measured with two dial gauges (with readings to 0.001 inches) placed on opposite sides of the pile to allow recording of top of pile displacement downward of up to 2.5 inches as well as the upward rebound displacement upon unloading. In addition, secondary method for recording displacement to the nearest 1/32 of an inch (such as a wire, mirror and scale) should be used. Lateral movements, pile compression, strain measurements, described in ASTM D 1143 Sections 7.3 and 7.4 are not required.

Design Requirements: The loading apparatus and reaction frame design configuration shall conform to any of the options described in ASTM D 1143 Section 6. The frame, connections, reaction piles, jacks and load cell shall be designed to safely apply an 800 kip load to the load test pile.

Reaction piles shall be located at least 8 ft. center to center from the load test pile. Some or all of the piles used as reaction piles may be production piles.

Construction and Testing: All reaction piles and dynamic test piles shall be installed prior to driving the static load test pile. The top elevation of the load test pile shall be determined immediately after driving and again just before load testing to check for heave.

The load test procedure is expected to take less than 6 hours during which time no other construction activity which could cause vibration at the load test pile, such as demolition, compaction, pile driving, etc., will be permitted. During the test, the Contractor will be responsible for jack operation (loading and unloading) while all data collection and analysis will be done by UIUC and/or WisDOT personnel. The load Test shall be according to ASTM D 1143 Procedure A: Quick Test. The load test pile shall be loaded in increments until either the cumulative loading reaches 800 kips or when 2.5 inches of pile deflection is obtained. Upon application of each load increment, the cumulative loading will be held constant a short period.

The load shall be removed in 10 approximately equal decrements, holding each load constant for a short period. Time, cumulative load, and movement shall be recorded before and after the application of each load increment or decrement. When the maximum load or deflection has been reached, readings of time, cumulative load and deflection rebound shall be recorded until all load has been removed.

After completion of the load test, the Contractor shall remove the load test frame and at the direction of WisDOT, extract the piling, or cut off the non-production reaction piles 2 ft below the existing or finished grade, whichever is lower. All frame components and pile cutoffs shall become the property of the Contractor and are to be removed from the job site.

### 2.3 SPECIAL PROVISION FOR DYNAMIC PILE MONITORING

General: This work consists of accommodating dynamic pile monitoring at locations shown in the plans. Dynamic pile monitoring will be conducted during initial driving and during re-driving piles. All pile driving operations shall follow article 512 of the standard specifications unless otherwise indicated in this special provision.

Dynamic monitoring is accomplished by attaching sensors near the top of the pile which transmit data by cable or wireless connection to a Pile Driving Analyzer (PDA) unit at the site. The sensors, PDA equipment, and the operation of the PDA will be provided by Dr. Jim Long or other PDA operator from the University of Illinois at Urbana Champaign (UIUC). The Contractor shall connect the sensor to the pile before driving and remove it following driving.

Equipment: For the HP 14x89 piles located at the static load test site, the hammer shall be capable of producing the energy required to achieve a nominal driven bearing of 500 kips with a penetration rate between 2 and 10 blows per 1 inch.

Submittals: The Contractor shall submit a completed "Pile Driving Equipment Data" Form (<http://www.dot.il.gov/Forms/BBS%20136.doc>) to the Engineer for transmittal by email to Dr. Long at [jhlong@illinois.edu](mailto:jhlong@illinois.edu) to prepare the PDA. The Contractor shall also notify the Engineer in writing of the anticipated driving and re-driving date(s) of the pile(s) to be dynamically monitored to allow the Engineer to inform Dr. Long at 217-333-2543 of the schedule. Both the completed form and driving schedule shall be provided to the Engineer and sent to Dr. Long a minimum of two weeks prior to driving the first dynamically monitored pile.

Construction: The Contractor shall inform the Engineer and Dr. Long of any changes in the proposed driving equipment or driving schedule at least 3 working days prior to initial driving and re-driving.

Dynamic monitoring will be performed during the final 20 to 50 ft of initial driving. Depending on the location of any Contractor planned pile splices and the total estimated pile length, the PDA operator will determine if all pile segments or only selected pile segments will require monitoring. Prior to lifting the section(s) of the pile to be monitored into the leads, the Contractor may elect to prepare the pile for sensor attachment as directed by the PDA operator. After the pile has been positioned in the leads, the Contractor shall attach the sensor as directed by the PDA operator

When the level of the sensors is within 1 ft of any obstruction endangering the survival of sensors and/or cables, driving shall be halted to allow the Contractor to remove the sensors and reattach them after passing the obstruction. When sensors are within 1 ft of the ground surface, driving shall be halted to allow the Contractor to remove the sensors and reattach them near the top of the next pile segment prior to lifting into place and splicing.

The initial driving will be terminated when the pile tip reaches the elevation shown in the plans or when driving criteria have been met according to Dr. Long. Upon completion of the initial driving process, the Contractor shall remove the sensors. During the subsequent waiting period, other piles in the substructure and elsewhere on the project may be driven.

After the minimum waiting period has elapsed, the Contractor must reattach the sensors to the experimental pile prior to re-driving. The Contractor shall warm up the hammer by driving another pile a minimum of an additional 20 blows and reposition the driving equipment on the experimental pile. The Contractor shall re-drive the pile until directed by Dr. Long to terminate. Following re-driving, the Contractor shall remove the sensors. After the sensors are removed following re-driving, the Contractor may cut-off the pile or extract the pile according to directions from Dr. Long or the Engineer.

Method of Measurement and Basis of Payment: This work will not be measured for payment but shall be included in the contract unit price for DRIVING PILES.

# CHAPTER 3 LOAD TEST PROGRAM AT US41 AND STH29

## 3.1 INTRODUCTION

Three axial load tests were conducted in November and December of 2011 along the interchange of US 41 – STH 29 flyovers located in Brown County, Wisconsin. Results of the static pile load tests, and results of the dynamic monitoring are provided in this report.

The overall site plans and locations for each of the load tests are shown in Fig. 3.1. Test Site 1 is located at Pier 6 of bridge structure B-05-658 and was the first site at which piles were to be driven and tested. Test Site 2 is located at Pier 2 of bridge structure B-05-660. Test site 3 is located at Pier 12 of bridge structure B-05-660. Subsurface exploration logs for each site are given in Fig. 3.2.

The typical pile configuration for all three sites was to drive eight reaction piles, one static load test pile, and 2 dynamic load test piles. The configuration for the piles is shown for sites 1, 2, and 3 in Figs. 3.3, 3.4, and 3.5, respectively. These three figures provide the pile layout at each site as well as the labeling system used for the piles, and the location of the piles with respect to the planned foundations for the bridge structure. The configuration of piles was located to maximize the piling that could also be used for production piling. Therefore, four reaction piles, and 2 dynamic load test piles were located within the footprint of the planned footing. The static load test pile and the other four reaction piles were not part of the production piling.

The installation procedure for driving piles to capacity was to drive reaction piles first, then the two dynamic load test piles, and finally the static load test pile. Sites 2 and 3 required splices. Lower portions of piling were typically driven first, and then the upper sections of piling were spliced and driven in the prescribed order of reaction piles, then dynamic test piles, and finally the static load test pile. All piles were driven with a Delmag D30-32 open ended diesel hammer.

The sequence of testing and driving was as follows:

- 1) Drive all eleven piles with dynamic monitoring.
- 2) Re-strike selected piles (usually four reaction piles and one dynamic test pile). Re-strikes were conducted after approximately 24 hours or more.
- 3) Setup load frame, and conduct a static load test no sooner than 3 days after driving the static load test pile.
- 4) Remove load test frame and restrike piles with dynamic monitoring with 24 hours.

Results for each site are given below; however, a more extensive treatment of the results is given later in this report.

### 3.1 SITE 1 - PIER 6 OF BRIDGE STRUCTURE B-05-658

The overall soil conditions at site 1 are shown in Fig. 3.2, with a more detailed plot given in Fig. 3.6. The soil profile consists of 80 ft of silty soil over limestone. The consistency of the silt between elevations 580

and 548 ft is hard with compressive strengths (using pocket penetrometer) greater than 4.5 tsf. Furthermore, very high blowcounts were reported using standard penetration tests.

Table 3.1 presents details of the pile driving, pile penetration, pile driving resistance, and results of initial driving for each pile at site 1. The last three columns of the table present pile capacities estimated using the Wisconsin DOT method (the FHWA modified Gates method), the capacity predicted with the Pile Driving Analyzer (PDA) using the RMX method with damping equal to 0.7, and the capacity based on a CAPWAP analysis of selected blows near the end of driving. Dynamic results for three piles (RP5, RP7, and RP8) are not reported because of a sensor malfunction in the equipment.

Table 3.2 presents details for 5 piles subjected to re-strike approximately 24 hours after initial driving. There is an overall slight increase in capacity predicted for both PDA and CAPWAP predictions.

Table 3.3 gives the results based on the final restrrike for all the piles. On the average, both CAPWAP and PDA predict capacities about 10-15 percent greater than predicted for the end of driving.

Details for the static load test are given in Table 3.4, and a summary plot of the load-settlement behavior is given in Fig. 3.7. Two load-settlement curves are illustrated; one curve shows load based on the hydraulic pressure used for the jack, and one curve shows the load-settlement curve using the load cell reading. The load cell reading is used as the more accurate measure of load.

The Davisson criterion was used for selecting the failure load for the pile. The Davisson line is shown as a straight line in Fig 3.7, and the failure load is identified when the load settlement curve for the pile intersects the Davisson line. A pile capacity equal to 655 kips is selected based on the Davisson method. The static load capacity from the static load test exceeds the capacity predicted using the Wisconsin DOT method (522 kips), the PDA (526 and 569 kips based on EOD and BOR, respectively), and CAPWAP (496 kips and 554 kips based on EOD and BOR, respectively).

## 3.2 SITE 2 - PIER 2 OF BRIDGE STRUCTURE B-05-660

The overall soil conditions at site 2 are shown in Fig. 3.2, with a more detailed plot given in Fig. 3.8. The soil profile consists primarily of 80-90 ft of silt and clay soil over limestone. The consistency of the soil between elevations 614 and 580 ft increases from weaker soil to hard with some unconfined compression strengths equal to and greater than 4.5 tsf (based on pocket penetrometer). Some depths exhibited high blowcounts using standard penetration tests (approximately 60 blows/ft). Below 35 ft the soil becomes weaker until elevation 540 (at a depth of about 80 ft) where the soil increases in strength and the standard penetration resistance also increases.

Table 3.5 summarizes details of the pile driving, pile penetration, pile driving resistance, and results of initial driving for each pile at site 2. The last three columns of the table present pile capacities estimated using the Wisconsin DOT method (the FHWA modified Gates method), the capacity predicted with the Pile Driving Analyzer (PDA) using the RMX method with damping equal to 0.7, and the capacity based on a CAPWAP analysis of selected blows near the end of driving.

All piles drove with minimal deviation from their target position, however, the pile designated for the static load test pile encountered a subsurface obstruction at a depth of about 30 ft. As a result, the static load test pile rotated and translated and was no longer in a position safe for testing. Accordingly, another

section of piling was driven halfway between the original position of the static load test pile, and the reaction piling (RP2 and RP4). The new static load test pile remained in a position satisfactory for conducting the static load test safely.

Table 3.6 presents details for 5 piles subjected to re-strike approximately 24 hours after initial driving and a couple of piles with a 4 day delay. There is an overall slight increase in capacity predicted for both PDA and CAPWAP predictions compared to the predictions of capacity at EOD (Table 3.5). PDA and CAPWAP results exhibit greater than a 50 percent increase in capacity between EOD and the BOR1 (1-4 days later).

Table 3.7 gives the results based on the final restrike for all the piles. On the average, both CAPWAP and PDA predict capacities about 55-70 percent greater than predicted for the end of driving, respectively.

Details for the static load test at Site 2 are given in Table 3.8, and a summary plot of the load-settlement behavior is given in Fig. 3.9. Two load-settlement curves are illustrated; one curve shows load based on the hydraulic pressure used for the jack, and one curve shows the load-settlement curve using the load cell reading. The load cell reading is taken as the more accurate measure of load.

The Davisson criterion was used for selecting the failure load for the pile. The Davisson line is shown as a straight line in Fig 3.9, and the failure load is identified when the load settlement curve for the pile intersects the Davisson line. It can be seen that the load-settlement curve for the pile did not intersect the Davisson line for loads up to 800 kips which was the limit for the load test equipment. Accordingly, the pile did not fail. Therefore the pile exhibits a capacity exceeding 800 kips.

The static load capacity from the static load test (800 kips) exceeds the capacity predicted using the Wisconsin DOT method (513 kips), the PDA (404 and 761 kips based on EOD and BOR, respectively), and CAPWAP (352 kips and 666 kips based on EOD and BOR, respectively). During the final restrike, the penetration resistance for the static load test pile was recorded as 12 blows per inch. It is not unusual for PDA and CAPWAP to underestimate pile capacity when the blow count is at 12 blows per inch.

### 3.3 SITE 3 - PIER 12 OF BRIDGE STRUCTURE B-05-660

The overall soil conditions at site 3 are shown in Fig. 3.2, with a more detailed plot given in Fig. 3.10. The soil profile consists of 65-70 ft of soft clay and silt over limestone. The upper 15 ft of soil exhibits compressive strengths between 1 and 3 tsf, however, below 15 ft, the soil is very soft with very low standard penetration resistance. The strength and resistance of the soil profile increases rapidly at a depth of about 65-70 ft until limestone is encountered.

Table 3.9 presents details of the pile driving, pile penetration, pile driving resistance, and results of initial driving for each pile at Site 3. The last three columns of the table present pile capacities estimated using the Wisconsin DOT method (the FHWA modified Gates method), the capacity predicted with the Pile Driving Analyzer (PDA) using the RMX method with damping equal to 0.7, and the capacity based on a CAPWAP analysis of selected blows near the end of driving.

Four piles (RP5, RP8, DLTP1, and DLTP2) were stopped about 1 foot short of the bearing layer so that an attempt could be made to estimate the resistance provided by the soil above the bedrock. Determining this resistance helped to assess whether we would be able to develop enough pile capacity in tension (in

the reaction piles) to provide 800 kips of downward load on the static load test pile. Accordingly, these four piles (RP5, RP6, DLTP1, and DLTP2) exhibit capacities significantly less than the seven other piles that were driven to bearing.

During initial driving of the piles, the pile driving resistance was little for most of the penetration. Pile driving resistance began to increase within the 2 ft of pile penetration. Final penetration resistance was very high. While reported values of 1.75 and 2.5 inches of penetration for the final 10 blows are accurate, most of the pile penetration occurred on the first five blows. The penetration for the last 2 or 3 blows was less than 0.1 inches based on field observations. The observation of high penetration resistance is being emphasized here, because it appeared the piles were resting on rock.

Table 3.10 presents details for 3 piles subjected to re-strike approximately 24 hours after initial driving. There is an increase in capacity between 25 and 35 percent predicted for both PDA and CAPWAP predictions. Setup is expected to occur in the soft soils at this site. Estimates of pile capacities based on PDA and CAPWAP were great enough to confirm adequate tensile pile capacity needed for conducting the load test to 800 kips.

Table 3.11 gives the results based on the final restrike for all the piles. Of significance is the resistance provided by the piles driven to bearing (piles RP1, RP2, RP3, RP4, RP6, RP7, and SLTP). These piles exhibited a decrease in capacity with time. The average ratio of final capacity / EOD capacity is 0.74 for both PDA and CAPWAP. The decrease in capacity is due to a significant reduction in tip resistance. During restrike, four piles that had met refusal for EOD, were exhibiting pile driving resistance of 2-3 blows per inch. Accordingly, this appears to be a site where relaxation is significant. Production piles driven at this location should be driven to bearing, and then subjected to restrikes to further penetrate the pile into the soil and reduce the impact of relaxation.

Finally, Table 3.12 provides results for the four piles that were driven 1-2 ft short of bearing. The capacities for these four piles are reported in the last three columns of the table. Pile capacities were estimated as EOD capacities because they were re-driven in excess of 1 ft of penetration. The three methods reported are the Wisconsin DOT method (the FHWA modified Gates method), the capacity predicted with the Pile Driving Analyzer (PDA) using the RMX method with damping equal to 0.7, and the capacity based on a CAPWAP analysis of selected blows near the end of driving.

Details for the static load test for Site 3 are given in Table 3.13, and a summary plot of the load-settlement behavior is given in Fig. 3.11. Two load-settlement curves are illustrated; one curve shows load based on the hydraulic pressure used for the jack, and one curve shows the load-settlement curve using the load cell reading. The load cell reading is used as the more accurate measure of load.

The Davisson criterion was used for selecting the failure load for the pile. The Davisson line is shown as a straight line in Fig 3.11, and the failure load is identified when the load settlement curve for the pile intersects the Davisson line. A pile capacity equal to 721 kips is selected based on the Davisson method. The static load capacity from the static load test is slightly greater than the capacity predicted using the Wisconsin DOT method (699 kips), and slightly less than the capacity estimated from PDA (814 kips) and CAPWAP (840 kips). However, using restrike behavior (BOR), PDA and CAPWAP estimates for capacity are similar (721 kips for PDA, 739 kips for CAPWAP).

### 3.4 SUMMARY

Three pile load tests were conducted for the interchange of US 41 – STH 29 flyovers located in Brown County, Wisconsin. Site 1 developed a pile capacity of 655 kips in the hard silt layers at a penetration of less than 40 ft. A small amount of setup (10-15 percent) occurred between the time of driving and the load test (7 days). Estimates for capacity using WisDOT method, PDA, and CAPWAP were less than determined with the static load test.

The test pile driven at Site 2 exhibited an axial capacity greater than 800 kips. Capacities increased between 55-70 percent between end of driving and beginning of restrike (6 days). Pile capacity estimated using WisDOT, PDA, and CAPWAP for EOD conditions underestimate the capacity. PDA and CAPWAP also underestimated capacity for BOR conditions. This could be due to the high blow count (pile penetration resistance).

The test pile driven at Site 3 exhibited an axial pile capacity of 721 kips. This site experienced significant relaxation at the tip of the pile. In spite of the side resistance increasing in capacity with time, the overall capacity of the pile decreased because of significant relaxation at the pile tip. It is recommended at this site, and at sites nearby with similar soil profiles, the production piles be driven to bearing, and then be redriven at a later time to mitigate the effects of relaxation.

Table 3.1. End of initial driving, Site 1

Pile ID	Date Driven	Total Pile Length (ft)	Pile* Penetration (ft)	Hammer Stroke (ft)	Pile Penetration for last 10 blows (in/10blows)	WisDOT Pile Driving Formula (kips)	PDA Capacity (J=0.7) (kips)	CAPWAP Capacity (kips)
RP1	11/29/2011	55.33	36.5	10	3.75	542	610	572
RP2	11/29/2011	55.33	32.5	9.5	3.50	539	571	548
RP3	11/29/2011	55.33	35.0	9.0	3.75	509	513	465
RP4	11/29/2011	55.33	37.2	9.5	3.75	526	578	540
RP5	11/29/2011	55.33	45.0	9.0	3.25	535	na	na
RP6	11/29/2011	55.33	46.0	10	2.38	631	502	394
RP7	11/29/2011	55.25	45.0	9.5	2.75	585	na	na
RP8	11/29/2011	55.33	44.5	9.5	2.75	585	na	na
DLTP1	11/29/2011	55.33	46.5	10	2.88	594	469	448
DLTP2	11/30/2011	55.33	30.8	9.5	3.25	553	558	477
SLTP	11/30/2011	55.33	38.5	9.0	3.50	522	526	496

\*note: elevation of ground surface is 602.8ft

Table 3.2. Intermediate restrike results on selected piles, Site 1

Pile ID	Date Driven	Elapsed Time Since Initial Driving (days)	PDA Capacity (J=0.7) (kips)	CAPWAP Capacity (kips)
RP1	11/30/2011	0.99	600	613
RP2	na	na	na	na
RP3	na	na	na	na
RP4	11/30/2011	0.90	587	600
RP5	11/30/2011	1.03	575	500
RP6	na	na	na	na
RP7	11/30/2011	1.06	617	447
RP8	na	na	na	na
DLTP1	11/30/2011	1.10	605	551
DLTP2	na	na	na	na
SLTP	na	na	na	na

Table 3.3. - Final restrike results on all piles, Site 1

<b>File ID</b>	<b>Date Driven</b>	<b>Elapsed Time Since Initial Driving (days)</b>	<b>PDA Capacity (J=0.7) (kips)</b>	<b>CAPWAP Capacity (kips)</b>
RP1	12/8/2011	8.86	589	568
RP2	12/8/2011	8.73	594	563
RP3	12/8/2011	8.81	521	532
RP4	12/8/2011	8.76	535	487
RP5	12/8/2011	8.88	617	521
RP6	12/8/2011	8.84	680	558
RP7	12/8/2011	8.94	755	590
RP8	12/8/2011	8.87	533	537
DLTP1	12/8/2011	8.69	593	586
DLTP2	12/8/2011	7.96	585	573
SLTP	12/8/2011	7.90	569	554

Table 3.4. Load test results for Site 1 conducted on 12/7/2011

Time	Nominal Load	Jack		Load Cell			Dial Gage			Wireline	
		Gage Pressure	Jack Load	Initial Load Cell Rdg	Final Load Cell Rdg	Load Cell Load	Dial Gage 1	Dial Gage 2	Avg Displ	Wireline Rdg	Wireline Displ
	(kips)	(psi)	(kips)	(rdg)	(rdg)	(kips)	(in)	(in)	(in)	(in)	(in)
11:15	0	0	0	-435	-435	0	2.000	2.001	0.000	1.35	0.00
11:17	25	256	25	na	na	na	1.996	1.994	0.005		
11:19	50	513	50	na	na	na	1.988	1.985	0.014		
11:20	75	769	75	na	-110	70	1.976	1.975	0.025		
11:21	100	1025	100	16	11	96	1.965	1.966	0.035	1.40	0.05
11:23	125	1281	125	na	108	117	1.956	1.958	0.044		
11:26	150	1538	150	na	255	149	1.942	1.945	0.057		
11:28	175	1794	175	na	386	177	1.930	1.933	0.069		
11:30	200	2050	200	495	489	200	1.918	1.923	0.080		
11:32	225	2306	225	654	646	233	1.900	1.905	0.098	1.46	0.11
11:35	250	2563	250	765	756	257	1.886	1.892	0.112		
11:37	275	2819	275	898	886	285	1.869	1.875	0.129		
11:39	300	3075	300	1043	1027	316	1.846	1.853	0.151	1.51	0.16
11:42	325	3331	325	1162	1159	344	1.825	1.832	0.172		
11:45	350	3588	350	1275	1269	368	1.805	1.812	0.192		
11:47	375	3844	375	1417	1392	394	1.780	1.790	0.216		
11:50	400	4100	400	1511	1526	423	1.755	1.765	0.241	1.62	0.27
11:53	425	4356	425	1635	1622	444	1.735	1.745	0.261		
11:56	450	4613	450	1763	1763	474	1.705	1.715	0.291		
11:59	475	4869	475	1883	1862	496	1.680	1.693	0.314		
12:01	500	5125	500	2012	1985	522	1.650	1.661	0.345	1.73	0.38
12:05	525	5381	525	2083	2079	542	1.615	1.627	0.380		
12:08	550	5638	550	2234	2196	567	1.573	1.586	0.421		
12:11	575	5894	575	2360	2302	590	1.527	1.540	0.467		
12:14	600	6150	600	2483	2478	628	1.438	1.450	0.557	1.92	0.57
12:17	625	6406	625	2596	2596	654	1.327	1.340	0.667		
12:21	650	6663	650	2725	2669	669	1.115	1.130	0.878	2.26	0.91
0:00	500	5100	498	2183	2183	565	1.137	1.152	0.856		
12:29	400	4100	400	1812	1812	485	1.178	1.192	0.816		
12:31	300	3075	300	na	na	na	1.232	1.244	0.763		
12:33	200	2000	195	805	805	268	1.293	1.303	0.703		
12:35	100	1000	98	172	172	131	1.358	1.364	0.640		
12:41	0	0	0	-445	-445	-2	1.439	1.440	0.561	1.90	0.55

Table 3.5. End of initial driving, Site 2

<b>Pile ID</b>	<b>Date Driven</b>	<b>Total Pile Length (ft)</b>	<b>Pile* Penetration (ft)</b>	<b>Hammer Stroke (ft)</b>	<b>Pile Penetration for last 10 blows (in/10blows)</b>	<b>WisDOT Pile Driving Formula (kips)</b>	<b>PDA Capacity (J=0.7) (kips)</b>	<b>CAPWAP Capacity (kips)</b>
RP1	12/5/2011	95.42	89.0	10.5	1.75	710	534	577
RP2	12/6/2011	95.17	85.0	10.0	3.25	570	522	459
RP3	12/5/2011	95.25	82.5	9.0	2.75	566	400	353
RP4	12/6/2011	95.33	88.8	10.0	1.75	691	617	681
RP5	12/2/2011	95.23	83.4	10.0	3.50	555	402	433
RP6	12/2/2011	95.33	82.5	10.0	4.00	529	379	389
RP7	12/2/2011	95.42	84.7	9.5	4.00	513	349	373
RP8	12/2/2011	95.17	87.5	10.0	2.50	621	730	748
DLTP1	12/5/2011	95.42	85.0	9.0	3.50	522	367	421
DLTP2	12/6/2011	95.25	87.0	9.5	3.50	539	375	418
SLTP2	12/6/2011	90.17	84.5	9.5	4.00	513	404	352

\*note: ground surface at EL 614.4 ft

Table 3.6. Intermediate restrrike results on selected piles, Site 2

<b>Pile ID</b>	<b>Date Driven</b>	<b>Elapsed Time Since Initial Driving (days)</b>	<b>PDA Capacity (J=0.7) (kips)</b>	<b>CAPWAP Capacity (kips)</b>
RP1	12/6/2011	1.11	730	779
RP2	na	na	na	na
RP3	12/6/2011	1.02	624	511
RP4	na	na	na	na
RP5	na	na	na	na
RP6	12/6/2011	4.07	812	712
RP7	12/6/2011	4.00	748	646
RP8	na	na	na	na
DLTP1	12/6/2011	0.93	680	580
DLTP2	na	na	na	na
SLTP2	na	na	na	na

Table 3.7. - Final restrike results on all piles, Site 2

<b>Pile ID</b>	<b>Date Driven</b>	<b>Elapsed Time Since Initial Driving (days)</b>	<b>PDA Capacity (J=0.7) (kips)</b>	<b>CAPWAP Capacity (kips)</b>
RP1	12/12/2011	7.03	758	829
RP2	12/12/2011	6.11	722	665
RP3	12/12/2011	6.94	671	571
RP4	12/12/2011	6.17	736	805
RP5	12/12/2011	9.93	808	743
RP6	12/12/2011	10.04	765	621
RP7	12/12/2011	9.97	749	707
RP8	12/12/2011	10.05	807	815
DLTP1	12/12/2011	6.82	796	718
DLTP2	12/12/2011	6.05	700	617
SLTP2	12/12/2011	5.94	761	666

Table 3.8. Load test results for Site 2 conducted on 12/12/2011

Time	Nominal Load	Jack		Load Cell			Dial Gage			Wireline	
		Gage Pressure	Jack Load	Initial Load Cell Rdg	Final Load Cell Rdg	Load Cell Load	Dial Gage 1	Dial Gage 2	Avg Displ	Wireline Rdg	Wireline Displ
	(kips)	(psi)	(kips)	(rdg)	(rdg)	(kips)	(in)	(in)	(in)	(in)	(in)
7:42	0	0	0	-450	-450	0	2.000	2.000	0.000	1.00	0.00
7:45	25	256	25	-346	-346	22	1.995	1.992	0.006	1.01	0.01
7:47	50	513	50	-250	-250	43	1.989	1.983	0.014		
7:48	75	769	75	-156	-156	63	1.982	1.974	0.022		
7:49	100	1025	100	-19	-23	93	1.966	1.958	0.038	1.04	0.04
7:51	125	1281	125	64	60	111	1.955	1.946	0.050		
7:53	150	1538	150	192	185	138	1.936	1.927	0.069		
7:55	175	1794	175	300	294	161	1.918	1.908	0.087		
7:57	200	2050	200	419	408	186	1.894	1.884	0.111	1.10	0.10
8:00	225	2306	225	549	533	214	1.869	1.858	0.137		
8:03	250	2563	250	660	651	239	1.844	1.834	0.161		
8:05	275	2819	275	790	776	266	1.816	1.806	0.189		
8:07	300	3075	300	896	884	289	1.790	1.780	0.215	1.21	0.21
8:10	325	3331	325	1026	1011	317	1.760	1.750	0.245		
8:12	350	3588	350	1117	1112	338	1.736	1.727	0.269		
8:15	375	3844	375	1262	1248	368	1.701	1.691	0.304		
8:17	400	4100	400	1395	1382	397	1.664	1.655	0.341	1.34	0.34
8:20	425	4356	425	1510	1498	422	1.627	1.619	0.377		
8:22	450	4613	450	1630	1607	446	1.591	1.580	0.415		
8:24	475	4869	475	1745	1721	471	1.551	1.541	0.454		
8:27	500	5125	500	1867	1867	500	1.503	1.494	0.502	1.50	0.50
8:29	525	5381	525	1970	1958	521	1.473	1.462	0.533		
8:32	550	5638	550	2115	2092	551	1.434	1.422	0.572		
8:34	575	5894	575	2220	2213	575	1.398	1.384	0.609		
8:37	600	6150	600	2345	2330	601	1.360	1.345	0.648	1.65	0.65
8:39	625	6406	625	2450	2436	624	1.321	1.307	0.686		
8:42	650	6663	650	2568	2555	649	1.282	1.268	0.725		
8:44	675	6919	675	2686	2676	675	1.236	1.224	0.770		
8:46	700	7175	700	2795	2781	698	1.194	1.180	0.813	1.81	0.81
8:49	725	7431	725	2939	2915	728	1.137	1.123	0.870		
8:52	750	7688	750	3034	3034	751	1.082	1.070	0.924		
8:55	775	7944	775	3140	3128	772	1.021	1.010	0.985		
8:58	800	8200	800	3271	3270	802	0.930	0.919	1.076	2.08	1.08
9:04	683	7000	683	2948	2948	732	0.940	0.930	1.065		
9:06	585	6000	585	2552	2552	647	0.987	0.976	1.019		
9:08	488	5000	488	2113	2123	554	1.067	1.056	0.939		
9:10	390	4000	390	1723	1732	470	1.160	1.150	0.845		
9:12	293	3000	293	1329	1340	385	1.270	1.260	0.735		
9:14	195	2000	195	852	865	282	1.406	1.395	0.600		
9:15	98	1000	98	259	261	153	1.562	1.552	0.443		
9:18	0	0	0	-451	-451	0	1.748	1.757	0.248	1.24	0.24

Table 3.9. End of initial driving, Site 3

<b>Pile ID</b>	<b>Date Driven</b>	<b>Total Pile Length (ft)</b>	<b>Pile Penetration (ft)</b>	<b>Hammer Stroke (ft)</b>	<b>Pile Penetration for last 10 blows (in/10blows)</b>	<b>WisDOT Pile Driving Formula (kips)</b>	<b>PDA Capacity (J=0.7) (kips)</b>	<b>CAPWAP Capacity (kips)</b>
RP1	12/14/2011	75.50	68.2	10.20	1.75	699	976	975
RP2	12/13/2011	75.58	68.7	10.30	1.50	733	758	756
RP3	12/13/2011	75.58	68.5	9.90	2.50	617	783	806
RP4	12/13/2011	75.50	68.5	10.75	1.75	720	829	818
RP5	12/14/2011	75.50	68.5	7.00	1.70	190	118	121
RP6	12/15/2011	77.67	69.2	9.90	1.75	687	914	873
RP7	12/14/2011	75.58	69.0	10.5	1.75	710	910	931
RP8	12/14/2011	75.50	68.5	7.00	20.0	163	176	111
DLTP1	12/14/2011	75.33	68.8	7.50	20.0	172	241	253
DLTP2	12/15/2011	75.50	67.5	7.50	20.0	172	194	166
SLTP1	12/15/2011	75.58	68.9	10.20	1.75	699	814	840

Table 3.10. Intermediate restrrike results on selected piles, Site 3

<b>Pile ID</b>	<b>Date Driven</b>	<b>Elapsed Time Since Initial Driving (days)</b>	<b>PDA Capacity (J=0.7) (kips)</b>	<b>CAPWAP Capacity (kips)</b>
RP1	na	na	na	na
RP2	na	na	na	na
RP3	na	na	na	na
RP4	na	na	na	na
RP5	12/15/2011	0.91	173	142
RP6	na	na	na	na
RP7	na	na	na	na
RP8	12/15/2011	0.87	207	172
DLTP1	12/15/2011	1.02	340	267
DLTP2	na	na	na	na
SLTP1	na	na	na	na

Table 3.11. - Final restrike results on all piles, Site 3

<b>Pile ID</b>	<b>Date Driven</b>	<b>Elapsed Time Since Initial Driving (days)</b>	<b>PDA Capacity (J=0.7) (kips)</b>	<b>CAPWAP Capacity (kips)</b>
RP1	12/19/2011	5.08	854	836
RP2	12/19/2011	5.92	436	450
RP3	12/19/2011	5.87	561	584
RP4	12/19/2011	5.98	474	465
RP5	12/19/2011	4.97	348	299
RP6	12/19/2011	4.03	749	763
RP7	12/19/2011	5.03	645	626
RP8	12/19/2011	4.95	286	274
DLTP1	12/19/2011	5.04	461	448
DLTP2	12/19/2011	4.20	329	311
SLTP1	12/19/2011	4.16	721	739

Table 3.12. - Final redrive results on selected piles, Site 3

<b>Pile ID</b>	<b>Date Driven</b>	<b>Hammer Stroke (ft)</b>	<b>Pile Penetration for last 10 blows (in/10blows)</b>	<b>WisDOT Pile Driving Formula (kips)</b>	<b>PDA Capacity (J=0.7) (kips)</b>	<b>CAPWAP Capacity (kips)</b>
RP1	na	Na	na	na	na	na
RP2	na	Na	na	na	na	na
RP3	na	Na	na	na	na	na
RP4	na	Na	na	na	na	na
RP5	12/19/2011	10	1.5	721	958	918
RP6	na	Na	na	na	na	na
RP7	na	Na	na	na	na	na
RP8	12/19/2011	10	1.500	721	924	892
DLTP1	12/19/2011	10	2.625	612	805	764
DLTP2	12/19/2011	10	1.75	691	807	798
SLTP1	na	Na	na	na	na	na

Table 3.13. Load test results for Site 3 conducted on 12/19/2011

Time	Nominal Load	Jack		Load Cell			Dial Gage			Wireline	
		Gage Pressure	Jack Load	Initial Load Cell Rdg	Final Load Cell Rdg	Load Cell Load	Dial Gage 1	Dial Gage 2	Avg Displ	Wireline Rdg	Wireline Displ
	(kips)	(psi)	(kips)	(rdg)	(rdg)	(kips)	(in)	(in)	(in)	(in)	(in)
7:43	0	0	0	-451	-451	0	2.000	2.000	0.000	1.00	0.00
7:43	25	256	25	-369	-369	18	1.990	1.989	0.011		
7:45	50	513	50	-258	-259	42	1.972	1.972	0.028		
7:46	75	769	75	-155	-155	64	1.953	1.953	0.047		
7:49	100	1025	100	-55	-58	85	1.931	1.933	0.068	1.06	0.06
7:51	125	1281	125	58	54	110	1.904	1.907	0.095		
7:53	150	1538	150	176	172	135	1.872	1.875	0.127		
7:54	175	1794	175	286	278	158	1.840	1.844	0.158		
7:56	200	2050	200	395	387	182	1.809	1.813	0.189	1.19	0.19
7:59	225	2306	225	512	504	207	1.771	1.776	0.227		
8:01	250	2563	250	621	611	230	1.742	1.744	0.257		
8:04	275	2819	275	738	729	256	1.703	1.709	0.294		
8:06	300	3075	300	842	831	278	1.670	1.677	0.327	1.32	0.32
8:08	325	3331	325	945	945	301	1.634	1.640	0.363		
8:11	350	3588	350	1056	1048	324	1.604	1.611	0.393		
8:13	375	3844	375	1175	1163	350	1.567	1.575	0.429		
8:16	400	4100	400	1300	1286	376	1.527	1.535	0.469	1.46	0.46
8:19	425	4356	425	1409	1399	400	1.490	1.499	0.506		
8:21	450	4613	450	1516	1509	424	1.455	1.464	0.541		
8:24	475	4869	475	1625	1621	448	1.418	1.427	0.578		
8:26	500	5125	500	1748	1733	473	1.379	1.388	0.617	1.62	0.62
8:29	525	5381	525	1857	1852	497	1.339	1.348	0.657		
8:31	550	5638	550	1980	1974	524	1.298	1.307	0.698		
8:34	575	5894	575	2090	2089	548	1.256	1.266	0.739		
8:36	600	6150	600	2216	2210	575	1.212	1.221	0.784	1.77	0.77
8:38	625	6406	625	2334	2323	599	1.165	1.175	0.830		
8:41	650	6663	650	2440	2432	623	1.121	1.129	0.875		
8:43	675	6919	675	2557	2547	648	1.069	1.079	0.926		
8:46	700	7175	700	2673	2657	672	1.020	1.030	0.975	1.97	0.97
8:49	725	7431	725	2790	2773	697	0.965	0.978	1.029		
8:52	750	7688	750	2905	2900	723	0.910	0.922	1.084		
8:54	775	7944	775	3035	3024	750	0.851	0.864	1.143		
8:57	800	8200	800	3155	3123	774	0.785	0.799	1.208	2.20	1.20
9:03	683	7000	683	2729	2729	686	0.851	0.868	1.141		
9:04	585	6000	585	2314	2322	597	0.949	0.959	1.046		
9:05	488	5000	488	1908	1915	510	1.054	1.063	0.942		
9:07	390	4000	390	1499	1508	422	1.168	1.174	0.829		
9:08	293	3000	293	1118	1126	340	1.282	1.288	0.715		
9:10	195	2000	195	725	736	255	1.402	1.407	0.596		
9:12	98	1000	98	239	249	150	1.525	1.527	0.474		
9:15	0	0	0	-451	-451	0	1.655	1.656	0.345	1.34	0.34





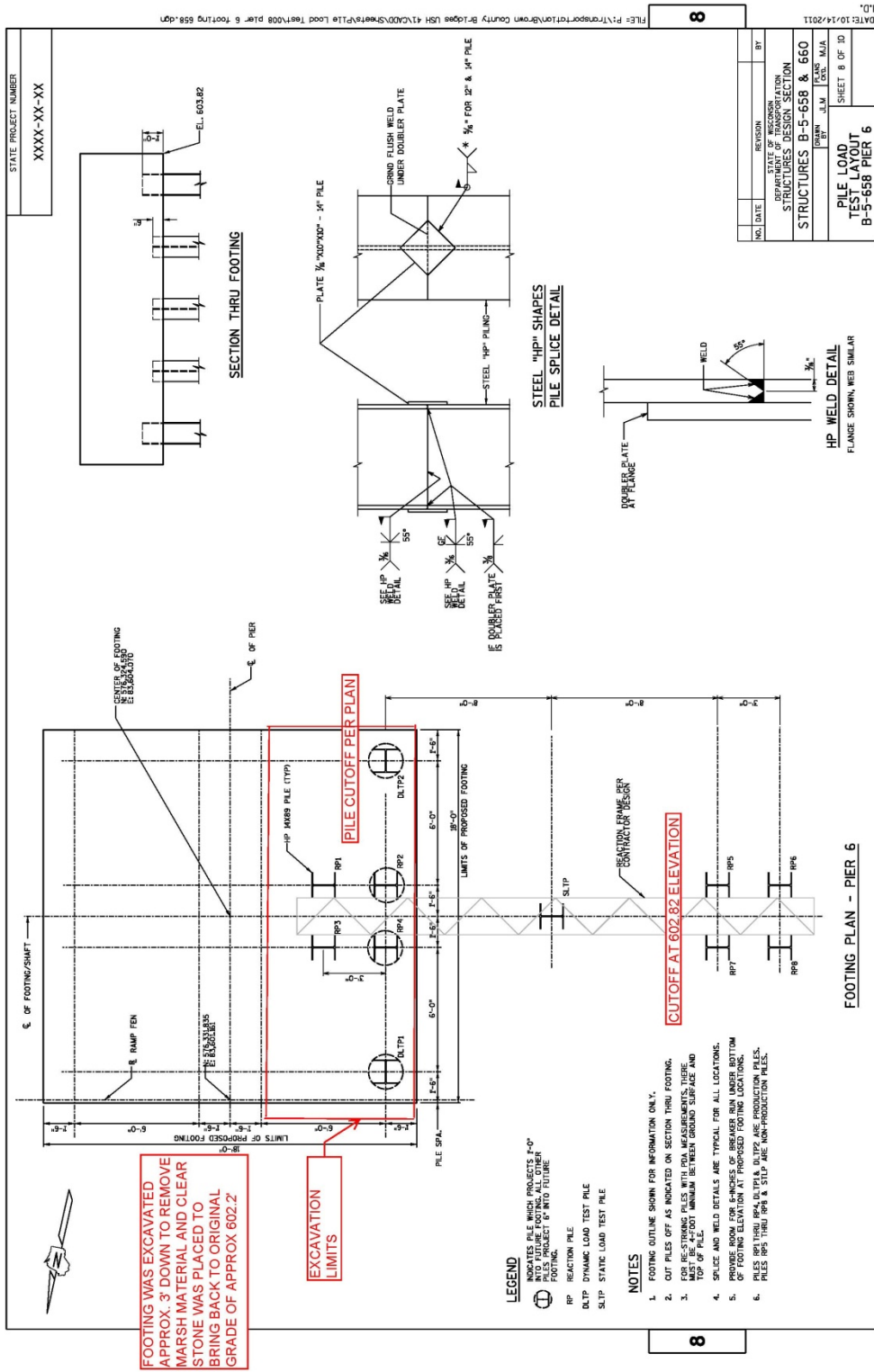


Figure 3.3. Plan View for Site 1.



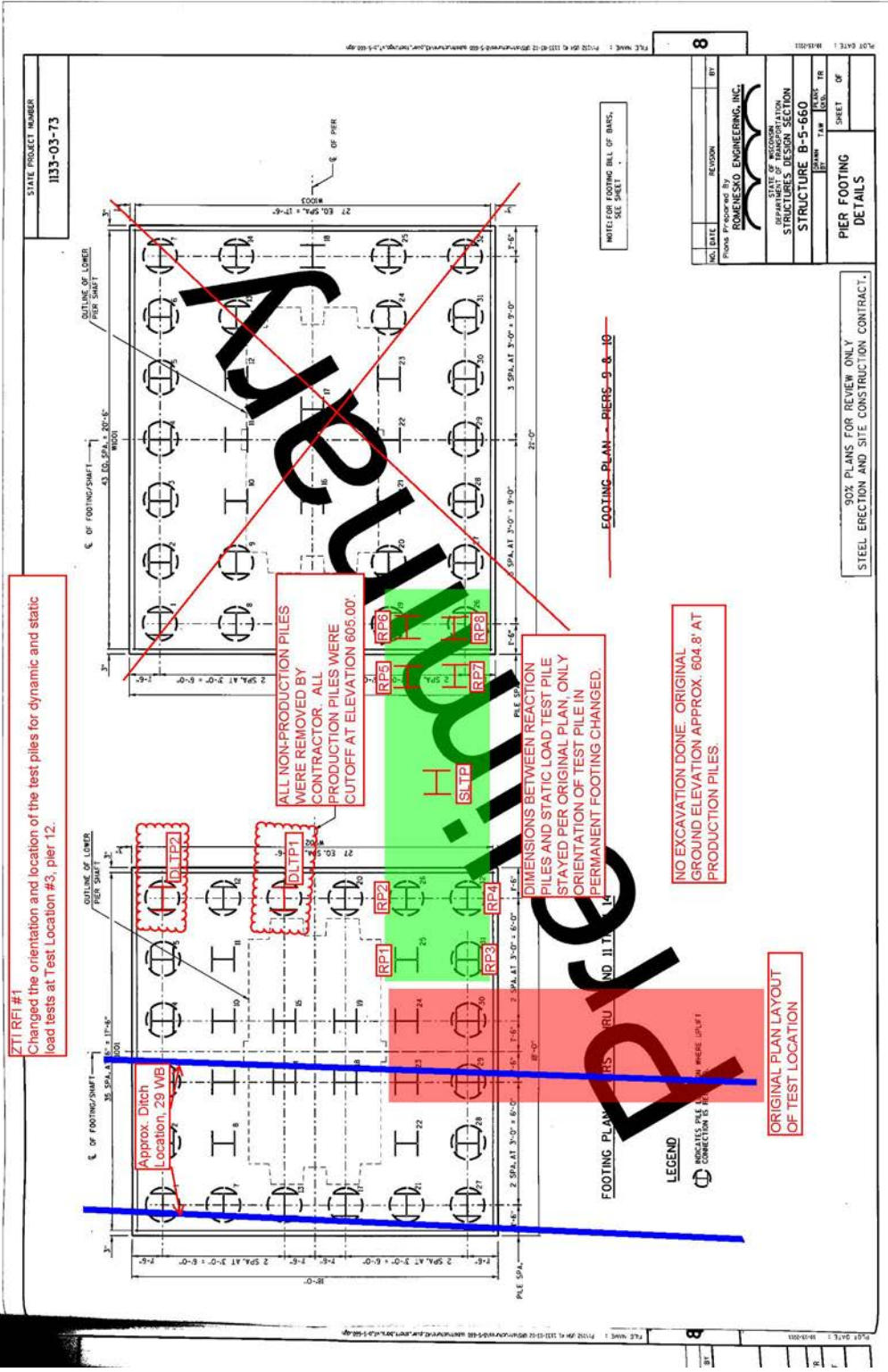


Figure 3.5. Plan View for Site 3.

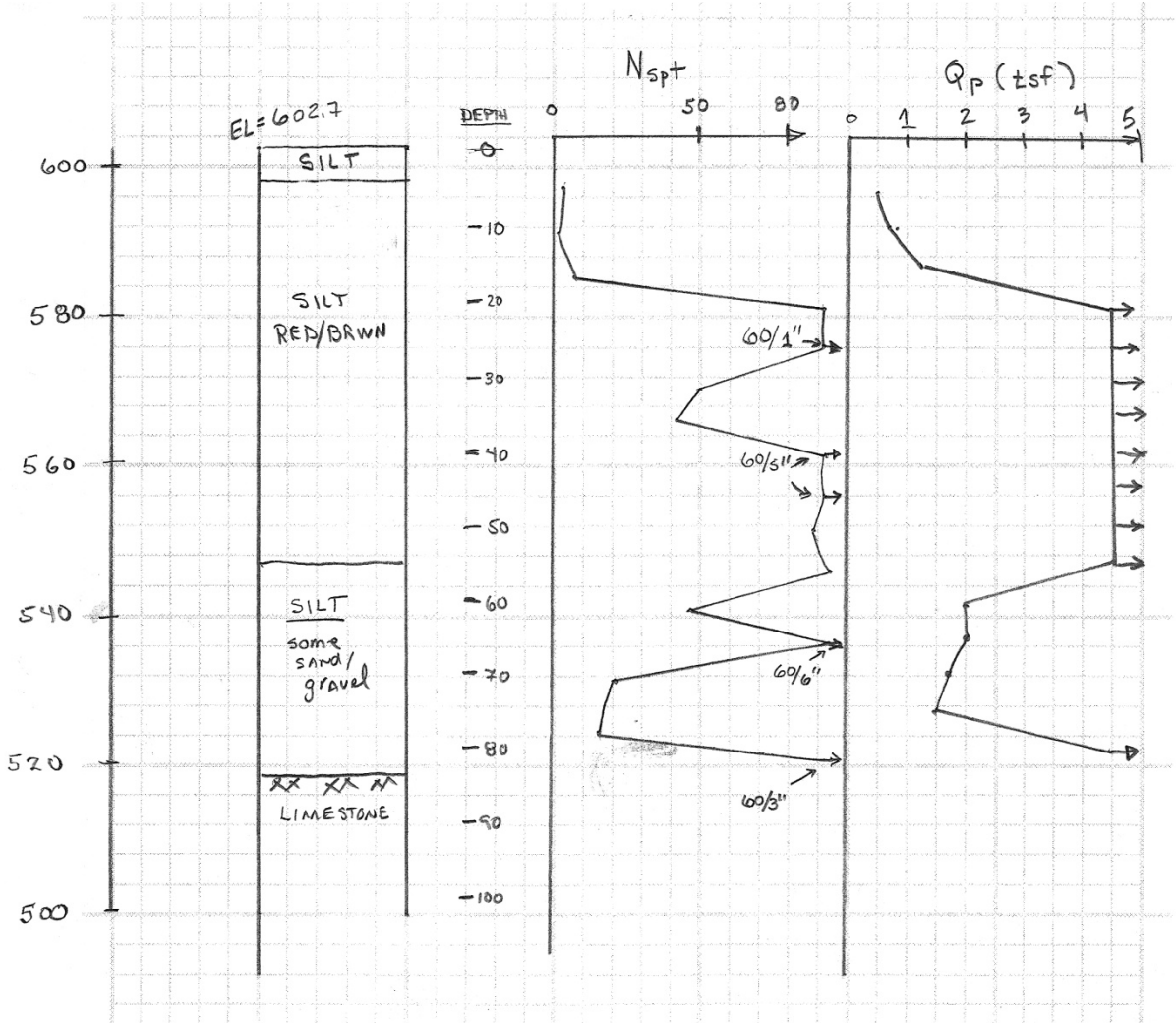


Figure 3.6. Soil profile for Load Test Site 1

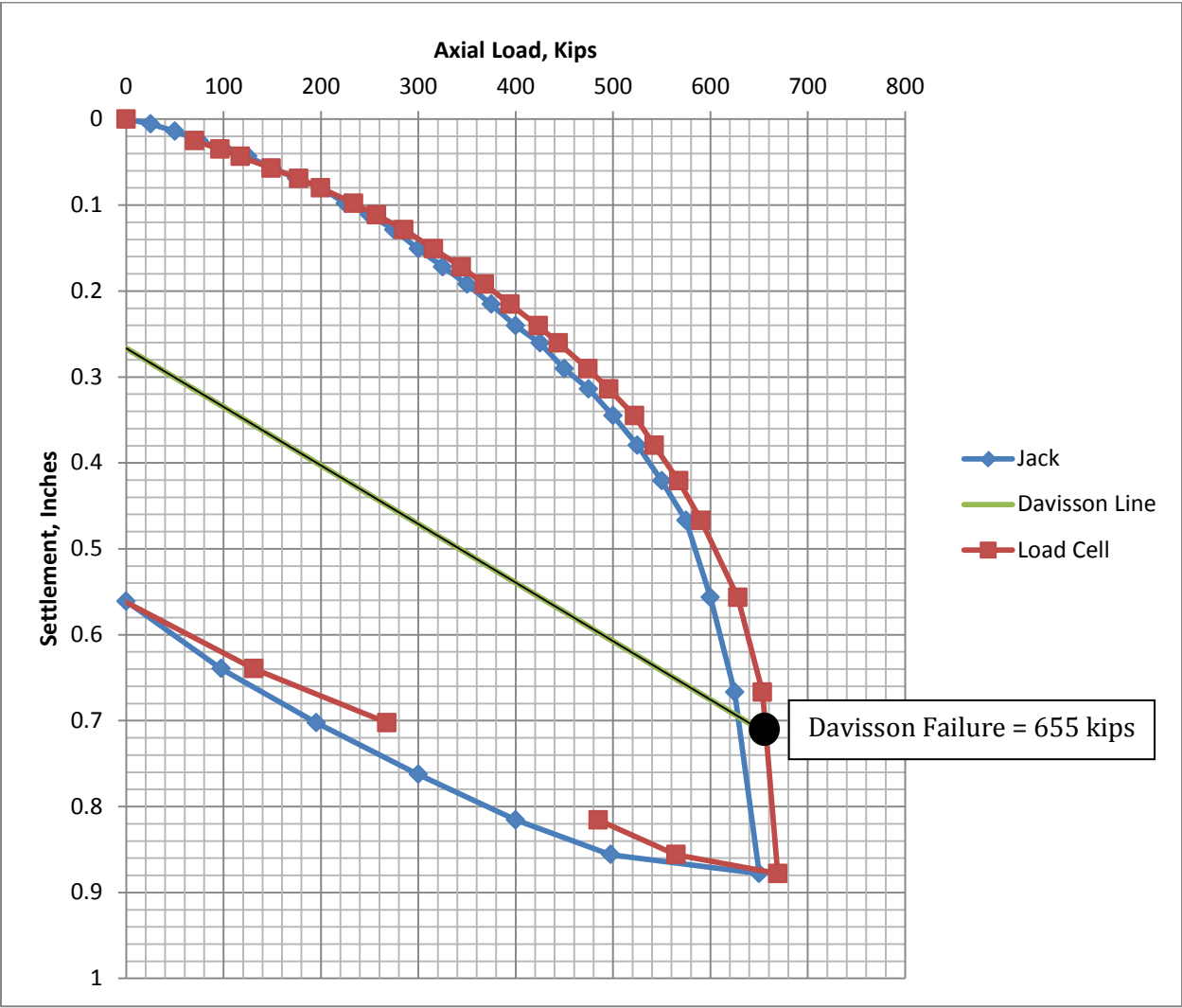


Figure 3.7. Load Settlement curve for load test at Site 1.

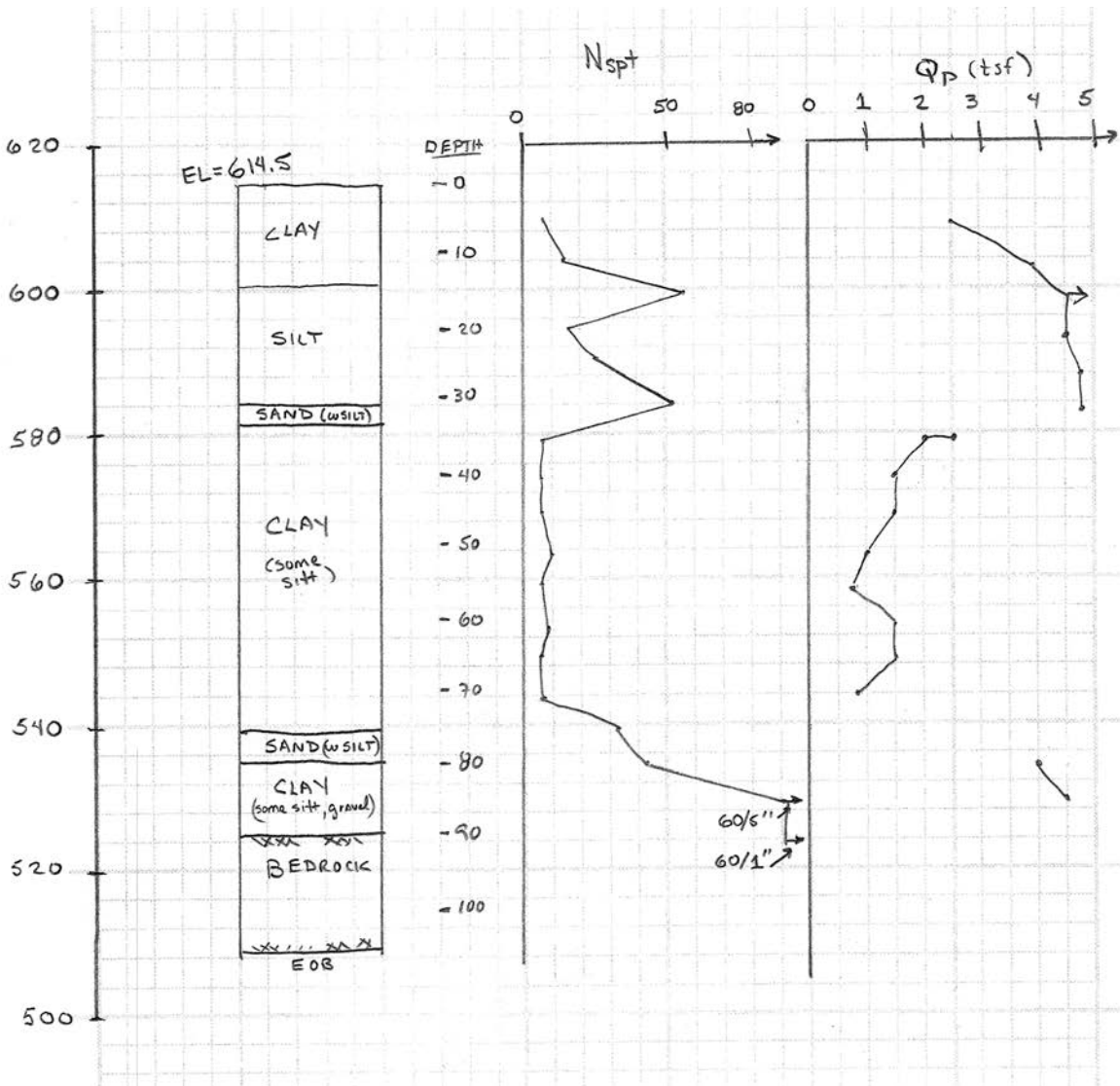


Figure 3.8. Soil profile for Load Test Site 2

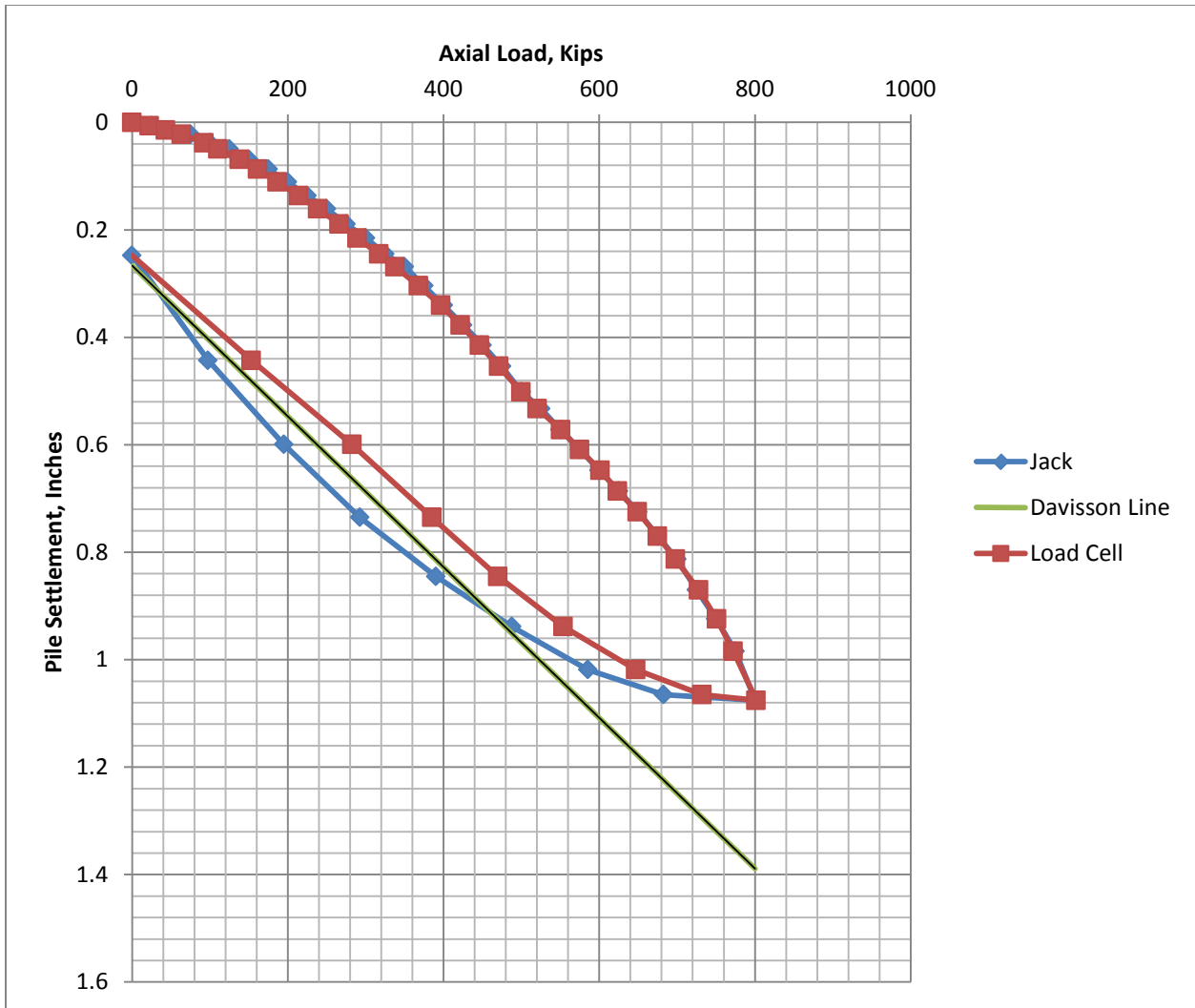


Figure 3.9. Load Settlement curve for load test at Site 2.

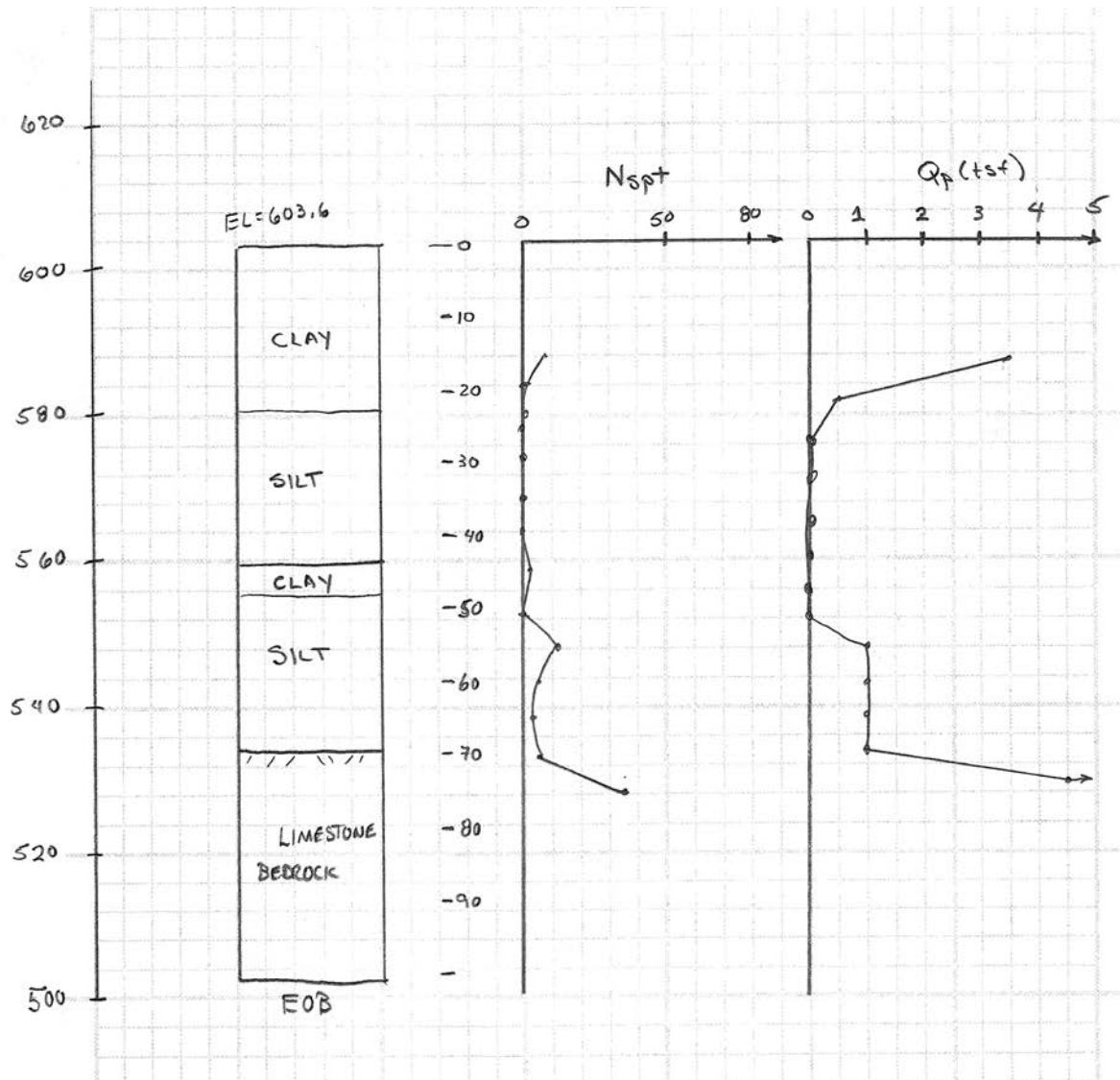


Figure 3.10. Soil profile for Load Test Site 3.

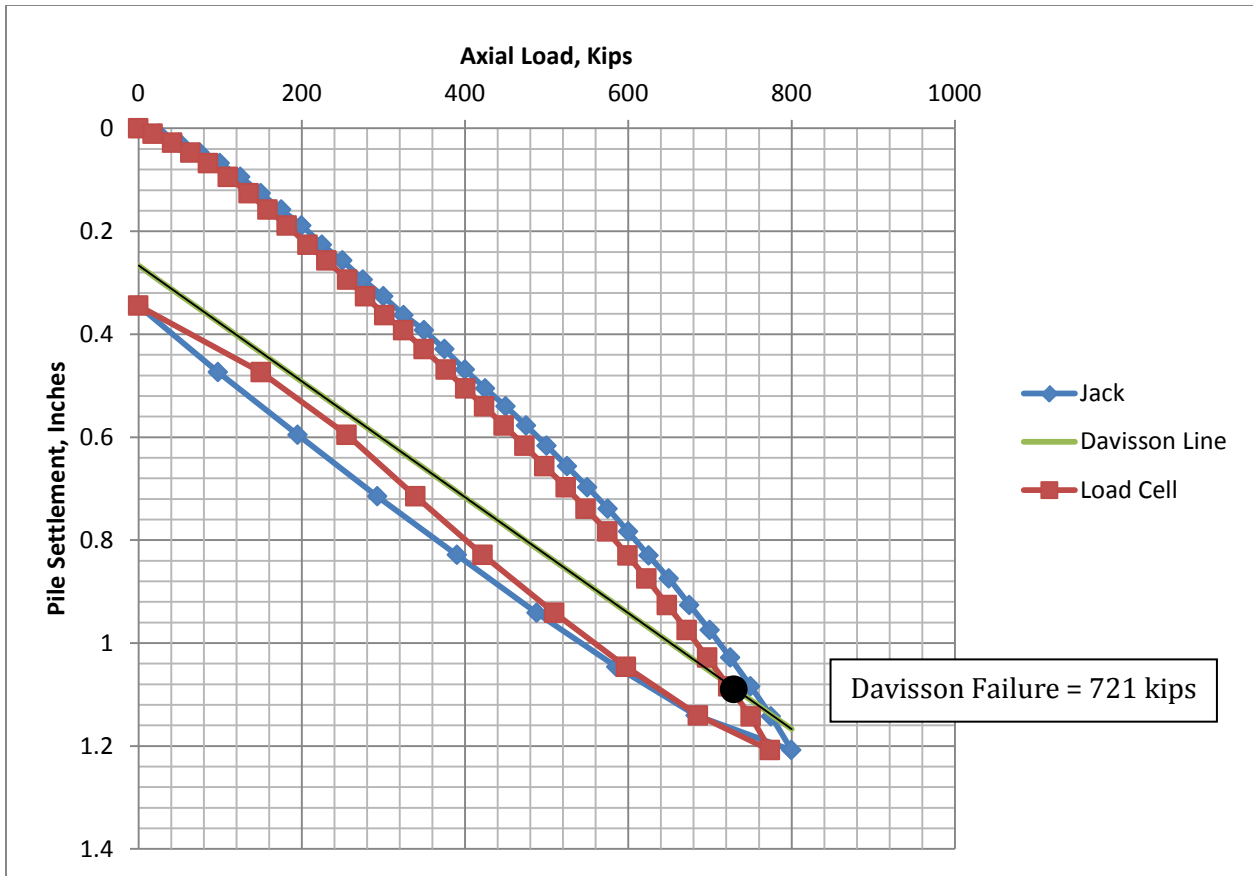


Figure 3.11. Load Settlement curve for load test at Site 3.

# CHAPTER 4 PILE LOAD TESTS - INTERSECTION OF US41 AND IH43

## 4.1 INTRODUCTION

Four static axial load tests were conducted on H14x73 piles between September and November of 2012 along the interchange of US 41 – IH43 flyovers located in Brown County, Wisconsin. Results of static pile load tests and dynamic monitoring of the piles are provided in this chapter.

The overall site plan and location for each load test is shown in Fig. 4.1. Piles were driven tested at one site before proceeding to the next site. The timing and location for each test site is given below.

<u>Test Site</u>	<u>Pier No.</u>	<u>Structure No.</u>	<u>Date Installed and Tested</u>
1	5	B-05-671	11/06/2012 – 11/14-2012
2	16	B-05-678	10/03/2012 – 10/11-2012
3	10	B-05-681	09/18/2012 – 09/27-2012
4	1	B-05-678	10/24/2012 – 11/01-2012

Test site 3 was the first site to be driven and tested, followed by Test sites 2, 4, and 1. Test site 4 was re-located from the original location to an alternate location as identified in Fig. 4.1

The pile configuration for sites 1, 2, 3, and 4 is shown in Figs. 4.2, 4.3, 4.4, and 4.5, respectively. These four figures provide the pile layout at each site as well as the labeling system used to identify the reaction piling, the dynamic load test piling, and the static load test pile. Also shown are the locations for the piles with respect to the planned foundations for the bridge structure. The piles RP1, RP2, RP3, RP4, DLTP1, and DLTP2 were located within the footing area of the planned foundation to maximize the piling that could also be used for production piling. All piles were driven with a Delmag D25-32 open ended diesel hammer. The static load test pile (SLTP) and the other four reaction piles (RP5, RP6, RP7, and RP8) were not part of the production piling.

The sequence of testing and driving was as follows:

- 1) Drive all eleven piles with dynamic monitoring.
- 2) Re-strike selected piles (usually four reaction piles and one dynamic test pile) . Re-strikes were conducted after approximately 24 hours or more.
- 3) Setup load frame, and conduct a static load test approximately 7 days after driving the static load test pile.
- 4) Remove load test frame and restrike all piles with dynamic monitoring within 24 hours.

Detailed results for each site are given below and a more extensive treatment of the results is given later in this report.

## 4.2 SITE 1 - PIER 5 OF BRIDGE STRUCTURE B-05-671 (11/06/2012 – 11/14/2012)

The location of the soil boring and the overall soil conditions at site 1 are shown in Figs. 4.6 and 4.7. The soil profile consists of about 30 ft of soft silt and clay overlying a layer of very dense silt and the clayey sand with cobbles and boulders. The transition appears to occur rapidly between the soft upper soil and the very stiff and dense layer at 30 ft. Standard Penetration Test results indicate very hard conditions ( $N_{spt} = 50$  blows for 3 inches of penetration.). The soil at greater depth alternates between clay, boulders with sand and gravel, with  $N_{spt}$  values exceeding 60 blows per foot, and often exhibiting higher resistances. Bedrock is encountered at a depth of about 70 ft.

Although no additional borings were conducted in the immediate area, pile driving records indicate the extent and character of the transition at a depth of 30 ft is variable. Piles located within the foundation area (RP1, RP2, RP3, RP4, DLTP1, and DLTP2) met capacity (based on the WisDOT dynamic formula) within six inches of penetration into the transitional layer. However, the static load test pile, located 8 ft away from the footing area, required about 1.5 ft of penetration. Reaction piles RP5, RP6, RP7, and RP8 were 16 ft away from the footing and required about 7 ft of penetration into the transitional layer before reaching capacity (using the WisDOT dynamic formula).

Table 4.1 provides the schedule for installing piles, the lengths of piling, the penetration of the piles below the ground surface, and the date and time for initial drive, restrike, and if conducted, redrive. Redriving piles was conducted for piles RP1, RP2, RP4, DLTP1, and DLTP2.

Table 4.2 presents information on estimates of pile capacity based on the response of the pile during pile driving. Capacities are reported for end of initial driving (EOID), beginning of restrike (BOR), and if conducted, end of redrive (EOD). Estimates of pile capacity are based on the Wisconsin DOT pile driving formula (WisDOT), the Pile Driving Analyzer (PDA) using the RMX method with a damping factor of 0.9, and CAPWAP. Also provided in the table is the time between EOID and restrike and the specific blow number and pile set used to determine capacity for PDA and CAPWAP. PDA and CAPWAP capacities are not provided for RP3 because dynamic measurements indicated damage to the pile (Beta value = 62) at a depth of about 34 ft below the ground surface.

Table 4.3 presents CAPWAP results for total, end and side resistance. The distribution between end bearing and side resistance should be considered approximate because a large portion of the side resistance occurs near the tip of the pile, where it is difficult to distinguish effects of side resistance and end bearing.

Measurements of load and displacement for the static load test are given in Table 4.4, and a summary plot of the load-settlement behavior is given in Fig. 4.8. The two load-settlement curves are in very close agreement. One curve shows load based on the hydraulic pressure used for the jack, and one curve shows the load-settlement curve using the load cell reading. The load cell reading is used as the more accurate measure of load.

The Davisson criterion was used for selecting the failure load for the pile. The Davisson line is shown as a straight line in Fig 4.8, and the failure load is identified when the load settlement curve for the pile intersects the Davisson line. A pile capacity equal to 570 kips is selected based on the Davisson method. The static load capacity from the static load test is slightly less than the capacity predicted using the

Wisconsin DOT method (585 kips). PDA estimates for the static load test pile are 561 kips based on EOID and 596 based on BOR. CAPWAP estimates are 467 for EOID and 536 for BOR.

A wireline and mirror setup was also used to record uplift displacements of selected reaction piles during the load test. Uplift displacements were recorded for reaction piles RP1, RP2, RP3, RP4, RP5, and RP7 and the results are given in Table 4.5. Figure 4.9 shows uplift displacements versus applied compression load. The real tension load applied to each individual reaction pile is unknown because the connection between the reaction beam and the 8 reaction piles is indeterminate. However, the average tension load on each pile is the total compressive load/number of piles subtracted by the weight of the load frame (26.4 kips) and connection hardware. Accordingly,

$$\text{Avg. Tension Load} = (\text{Applied Compression Load} - 26.4)/8 \quad \text{eqn 4.1}$$

The maximum compressive load on the static load test pile was 783 kips, therefore the average tension loads on the reaction piles is  $[(783-26.4)/8]$  94.6 kips. The estimate for average side capacity based on CAPWAP (BOR) for piles RP1-RP4, DLTP1, and DLTP2 is 117 kips, and the average CAPWAP(BOR) side capacity is 138 kips for all piles at this site.

The piles driven in the foundation area (RP1, RP2, RP3, RP4, DLTP1, and DLTP2) appear to exhibit relaxation. CAPWAP results suggest that these piles exhibited low side resistance and very high end bearing at end of initial driving, however, upon restrike, the side resistance increased, but the end bearing decreased more. Piles driven elsewhere (SLTP, RP5, RP6, RP7, and RP8) did not exhibit relaxation.

It is my opinion that the piles in the foundation area (RP1-RP4, DLTP1, and DLTP2) behave differently than piles outside the foundation area (SLTP1, RP5-RP8). The piles outside the foundation area penetrated deeper into the dense soil (at about 30 ft depth) because the very dense silt layer was either less dense or not present. The total capacity of piles outside the foundation area generally increased between EOID and BOR. However, the total capacity of the piles within the foundation area generally decreased between EOID and BOR. Accordingly, piles within the foundation area are subject to relaxation.

### 4.3 SITE 2 - PIER 16 OF BRIDGE STRUCTURE B-05-678 (10/03/2012 – 10/11/2012)

The general location of test site 2 is given in Fig. 4.1, the pile layout at site 2 is given in Fig. 4.3, and the location of the soil boring, overall soil conditions, and soil profile are shown in Fig. 4.10, with a more detailed plot of the soil profile given in Fig. 4.11. The general soil profile consists of about 53 ft of clay overlying 25 ft of granular soil, overlying limestone. The clay layer has a dense gravel layer about 2 ft thick) at a depth of 30 ft. Below the clay layer is approximately 25 ft of granular soils (gravel, cobbles, silty sand, sand) overlying limestone. Most of the piling was driven to a depth of approximately 70 to 75 ft, which corresponds to a dense sand and gravel layer above the limestone.

Table 4.6 provides the schedule for installing piles, the lengths of piling, the penetration of the piles below the ground surface, and the date and time for initial drive, restrike, and if conducted, redrive.

Table 4.7 presents information on estimates of pile capacity based on the response of the pile during pile driving. Capacities are reported for end of initial driving (EOID) and beginning of restrike (BOR). Estimates of pile capacity are based on the Wisconsin DOT pile driving formula (WisDOT), the Pile Driving Analyzer (PDA) using the RMX method with a damping factor of 0.9, and CAPWAP. Also

provided in the table is the time between EOID and restrike and the specific blow number and pile set used to determine capacity for PDA and CAPWAP. PDA and CAPWAP capacities are not provided for RP5 because dynamic measurements indicated damage to the pile (Beta value = 62) at a position of about 7 ft from the tip of the pile. PDA(BOR) and CAPWAP(BOR) capacities are not reported for RP6 because measurements for this pile were not recorded during restrike.

Table 4.8 presents CAPWAP results for total, end and side resistance. The distribution between end bearing and side resistance should be considered approximate.

Detailed results for the static load test are given in Table 4.9, and a summary plot of the load-settlement behavior is given in Fig. 4.12. The compressive load on the static load test pile is estimated using jack pressure. The readout unit for the load cell was defective and failed during the conduct of the load test. Accordingly, only one measure of load was available for this test.

The Davisson criterion was used for selecting the failure load for the pile. The Davisson line is shown as a straight line in Fig 4.12. The pile capacity using Davisson's method equals 790 kips based on the intersection of Davisson's line with the load settlement curve. The static load capacity from the static load test is significantly greater than estimates of pile capacity based on driving behavior. The WisDOT pile driving formula estimated a capacity of 580 kips. PDA estimates were 400 (EOID) and 505 (BOR) kips. Estimates for capacity based on CAPWAP were also lower than measured in the static load test: 427 kips for EOID and 546 for BOR. PDA and CAPWAP can underestimate pile capacity when the hammer delivers energy insufficient to mobilize full capacity along the sides and end of the pile. As an approximate guideline, penetration rates are recommended to be between 3 and 10 blows per inch. The penetration rate for the static load test pile at BOR was approximately 10 blows per inch; therefore it is likely that estimates for pile capacity are underpredicted.

Eight of nine piles exhibited an increase in capacity with time, therefore, pile relaxation is unlikely to occur at this site.

#### 4.4 SITE 3 - PIER 10 OF BRIDGE STRUCTURE B-05-681 (9/18/2012 – 9/27/2012)

The general location of test site 3 is given in Fig. 4.1, the pile layout is given in Fig. 4.4, and the location of the soil boring, overall soil conditions, and soil profile are shown in Fig. 4.13, with a more detailed plot of the soil profile given in Fig. 4.14. The general soil profile consists of about 33 ft of clay overlying a 24-ft thick, very hard clay with gravel. Standard Penetration Test results in this layer were consistently 50 blows for 5 inches of penetration. Below this layer is a gravel and cobble layer about 15 ft thick, followed by a 10 ft layer of clay with gravel. Fractured rock occurs at a depth of 90 ft. All Standard Penetration Test results were in excess of 50 blows per 5 inches for depths below 35 ft. Driven piling was penetrated to depths between 43 and 58 ft.

Table 4.10 provides the schedule for installing piles, the lengths of piling, the penetration of the piles below the ground surface, and the date and time for initial drive and restrike.

Table 4.11 presents estimates of pile capacity based on the response of the pile during pile driving. Capacities are reported for end of initial driving (EOID) and beginning of restrike (BOR). Estimates of pile capacity are based on the Wisconsin DOT pile driving formula (WisDOT), the Pile Driving Analyzer (PDA) using the RMX method with a damping factor of 0.9, and CAPWAP. Also provided in the table is

the time between EOID and restrrike and the specific blow number and pile set used to determine capacity for PDA and CAPWAP. PDA and CAPWAP capacities for EOID are not provided for RP5 because no PDA measurements were recorded for this pile. Piles driven before RP5 required two lengths of pile spliced together, accordingly on the second section of piling was monitored with the PDA. However, RP5 achieved capacity at a depth that only required one section of pile.

Table 4.12 presents CAPWAP results for total, end and side resistance. The distribution between end bearing and side resistance should be considered approximate.

Detailed results for the static load test are given in Table 4.13, and a summary plot of the load-settlement behavior is given in Fig. 4.15. The compressive load on the static load test pile is estimated using jack pressure and a load cell. The load cell reading is taken to be the more accurate measure of load.

The Davisson criterion was used for selecting the failure load for the pile. The Davisson line is shown as a straight line in Fig 4.15. The pile capacity using Davisson's method equals 701 kips based on the intersection of Davisson's line with the load settlement curve. The capacity from the static load test is significantly greater than the estimates of pile capacity based on driving behavior. The WisDOT pile driving formula estimated a capacity of 592 kips. PDA estimates were 450 (EOID) and 540 (BOR) kips. Estimates for capacity based on CAPWAP were also lower than measured in the static load test: 448 kips for EOID and 543 for BOR.

The average increase in capacity between EIOD and BOR (approximately 7-8 days later) for CAPWAP was 14 percent.

#### 4.5 SITE 4 - PIER 1 OF BRIDGE STRUCTURE B-05-678 (10/24/2012 – 11/01/2012)

The general location of test site 4 is given in Fig. 4.1, the pile layout at site 4 is given in Fig. 4.5, and the location of the soil boring, overall soil conditions, and soil profile are shown in Fig. 4.16, with a more detailed plot of the soil profile given in Fig. 4.17. Test Site 4 was located at the alternate site.

The general soil profile for the alternate test site 4 is about 60 ft of primarily clay. Unconfined compression strengths for the clay reach 2.5 tsf at about 10 ft below the ground surface, but a more typical strength for the clay is less than 1 tsf. Possible cobbles and boulders were encountered at a depth of 35-40 ft, resulting in high Standard Penetration Test values. A 6 ft thick layer of sand underlies the clay layer, followed by a 20 ft thick layer of clay. The unconfined strength of this clay layer is higher (approximately 3 tsf) and Standard Penetration Test Results suggest the strength of the soil increases with depth. Below 86 ft the soil transitions from clayey gravel with possible boulders to weathered bedrock at a depth of 94 ft. Piles at this site were driven to depths ranging from 74 to 81 ft.

Table 4.14 provides the schedule for installing piles, the lengths of piling, the penetration of the piles below the ground surface, and the date and time for initial drive, restrrike, and re-driving.

Table 4.15 presents information on estimates of pile capacity based on the response of the pile during pile driving. Capacities are reported for end of initial driving (EOID), beginning of restrrike (BOR) and for final re-drive. Estimates of pile capacity are based on the Wisconsin DOT pile driving formula (WisDOT), the Pile Driving Analyzer (PDA) using the RMX method with a damping factor of 0.9, and CAPWAP. Also provided in the table is the time between EOID and restrrike and the specific blow number and pile

set used to determine capacity for PDA and CAPWAP. PDA and CAPWAP capacities for EOID are not provided for RP7 and DLTP1 because PDA measurements indicated damage occurred in the pile. Pile RP7 consistently indicated a beta value of 75 located about 21 ft above the tip of the pile. Pile DLTP1 consistently indicated damage (beta value = 81) for depths of driving greater than 70 ft.

Table 4.16 presents CAPWAP results for total, end and side resistance. The distribution between end bearing and side resistance should be considered approximate.

Detailed results for the static load test are given in Table 4.17, and a summary plot of the load-settlement behavior is given in Fig. 4.18. The compressive load on the static load test pile is estimated using jack pressure and a load cell. The load cell reading is taken to be the more accurate measure of load.

The Davisson criterion was used for selecting the failure load for the pile. The Davisson line is shown as a straight line in Fig 4.18. The pile capacity using Davisson's method equals 491 kips based on the intersection of Davisson's line with the load settlement curve. The static load capacity from the static load test is significantly greater than the estimates of pile capacity based on driving behavior. The WisDOT pile driving formula estimated a capacity of 603 kips. PDA estimates were 432 (EOID) and 444 (BOR) kips. Estimates for capacity based on CAPWAP were also lower than measured in the static load test: 447 kips for EOID and 471 for BOR.

The average increase in capacity between EIOD and BOR (approximately 7-8 days later) for CAPWAP was 14 percent.

Several piles within the foundation area were re-driven after determining the 8-day BOR capacity because the capacity of the static load test pile was determined to be below 500 kips and because PDA(BOR) capacities were below 500 kips. Wisconsin DOT pile driving capacities, PDA, and CAPWAP capacities for these redrives are given in Table 4.15. Piles that were re-driven include RP1-RP3 and DLTP2. Each of these piles were driven an additional distance that exceeded 6 inches. RP4 was also re-driven, however, the location of the pile instrumentation (strain gages and accelerometers) prevented the pile from penetrating further without damaging the gages.

## 4.6 SUMMARY

Four pile load tests were conducted for the interchange of US 41 – IH43 flyovers located in Brown County, Wisconsin. Site 1 developed a pile capacity of 570 kips, however, soil conditions were different at the location of the static load test and the location of the production piles (RP1-RP4, DLTP1, and DLTP2). Piles in the foundation area exhibited relaxation due to the very dense silt layer at about 30 ft depth. Accordingly, it is recommended that driven piles be driven through the dense silt layer. This may require the pile to be driven, and then allowed to sit for some time (e.g. 1-6 hours), and then re-driven to get adequate penetration. Tension capacity for the piles appear to be in excess of 90 kips.

The static load test pile driven at Site 2 exhibited an axial capacity of 790 kips. Capacities increased approximately 15 percent between end of driving and beginning of restrike (7 days) based on CAPWAP estimates. Pile capacity estimated using WisDOT, PDA, and CAPWAP for EOD conditions underestimate the capacity by over 200 kips. BOR estimates using PDA and CAPWAP also underestimated capacity.

The test pile driven at Site 3 exhibited an axial pile capacity of 701 kips. Capacities were underpredicted by the WisDOT pile driving formula (592 kips). PDA estimated capacities of 450 (EOD) and 540 (BOR) kips, and CAPWAP estimated a capacity of 543 (BOR) kips.

The static load test pile at site 4 exhibited an axial capacity of 491 kips, which is significantly less than estimated using the dynamic formula (604 kips). PDA and CAPWAP underestimated the static load test capacity. PDA(EOD) estimated 430 kips for EOD and 444 kips for BOR. CAPWAP estimated a capacity of 447 kips for EOD and 471 kips for BOR. Capacities for piles within the foundation footprint were re-driven after BOR to additional penetration to improve their axial capacity.

PDA measurements indicated damage for 4 of the 44 piles driven. Test site 1 had 1 damaged pile (RP3). Test site 2 had one damaged pile (RP5) and test site 4 had 2 damaged piles (RP7 and DLTP1). Of these 4 piles, only RP3 and DLTP1 are within the footprints of the bridge foundations.

Table 4.1. Details of Initial Driving, Restrike, and Redrive, Site 1

Pile	Drive Detail	Total Pile Length (ft)	Lpen * (ft)	Date	Time
RP1	Pile	50.3	38.3	11/07/12	7:41
	7day Restrike (BOR)		38.3	11/14/12	13:44
	7day Redrive (EOD)		38.8	11/14/12	13:44
RP2	Pile	50.3	35.8	11/06/12	14:07
	24hr Restrike (BOR)		35.8	11/08/12	7:16
	7day Restrike (BOR)		35.8	11/14/12	13:35
	7day Redrive (EOD)		36.2	11/14/12	13:35
RP3	Pile	50.3	35.6	11/07/12	7:10
	7day Restrike (BOR)			11/14/12	13:51
RP4	Pile	50.3	36.4	11/06/12	13:30
	24hr Restrike (BOR)		36.4	11/08/12	7:26
	7day Restrike (BOR)		36.4	11/14/12	13:25
	7day Redrive (EOD)		36.9	11/14/12	13:25
RP5	Pile	50.3	43	11/07/12	9:03
	24hr Restrike (BOR)		43	11/08/12	7:08
	7day Restrike (BOR)		43	11/14/12	13:05
RP6	Pile	50.3	43.9	11/07/12	8:40
	7day Restrike (BOR)		43.9	11/14/12	12:53
RP7	Pile	50.3	43.9	11/07/12	10:12
	24hr Restrike (BOR)		43.9	11/08/12	7:02
	7day Restrike (BOR)		43.9	11/14/12	13:09
RP8	Pile	50.3	44.1	11/07/12	9:50
	7day Restrike (BOR)		44.1	11/14/12	12:43
DLTP1	Pile	50.3	35	11/06/12	12:35
	24hr Restrike (BOR)		35	11/08/12	7:35
	7day Restrike (BOR)		35	11/14/12	14:07
	7day Redrive (EOD)		35.5	11/14/12	14:07
DLTP2	Pile	50.3	38.3	11/07/12	9:15
	7day Restrike (BOR)		38.3	11/14/12	13:58
	7day Redrive (EOD)		38.8	11/14/12	13:58
SLTP	Pile	50.3	38	11/07/12	10:43
	7day Restrike (BOR)		38	11/14/12	13:18

\*note: Lpen is depth of pile penetration, elevation of ground surface is 585.57ft

Table 4.2. Pile Capacity Based on WisDOT Pile Formula, PDA, and CAPWAP, Site 1

Pile	Drive Detail	Time After EOID (days)	WisDOT Pile Driving Formula			Blow Number BN	Pile Set (in)	PDA-RMX Capacity (J=0.9) (kips)	CAPWAP Capacity (kips)
			Hammer Stroke (ft)	Pile Pen In 10 blows (in)	Pile Capacity (kips)				
RP1	Pile (EOID)	0.00	9.5	2	580	211	0.2	529	462
	7day Restrike (BOR)	7.25				6	0.366	426	434
	7day Redrive (EOD)	7.25	8.4	2.2	524	20	0.333	433	380
RP2	Pile (EOID)	0.00	9.5	1.75	604	103	0.175	610	524
	24hr Restrike (BOR)	1.71				4	0.267	438	404
	7day Restrike (BOR)	7.98				7	0.25	453	450
	7day Redrive (EOD)	7.98	8.8	1.5	603	16	0.2	478	459
RP3	Pile (EOID)	0.00	10	2	598	na*	na	na	na
	7day Restrike (BOR)	7.28				na	na	na	na
RP4	Pile (EOID)	0.00	9.5	2	580	141	0.2	594	517
	24hr Restrike (BOR)	1.75				3	0.333	392	391
	7day Restrike (BOR)	8.00				7	0.283	387	361
	7day Redrive (EOD)	8.00	8.7	1.5	599	25	0.3	457	455
RP5	Pile (EOID)	0.00	9.5	2	580	254	0.2	431	410
	24hr Restrike (BOR)	0.92				4	0.217	426	397
	7day Restrike (BOR)	7.17				4	0.25	418	400
RP6	Pile (EOID)	0.00	9	1.75	585	313	0.175	408	409
	7day Restrike (BOR)	7.18				6	0.133	442	462
RP7	Pile (EOID)	0.00	9.5	2	580	297	0.2	433	414
	24hr Restrike (BOR)	0.87				3	0.267	432	414
	7day Restrike (BOR)	7.12				4	0.25	460	480
RP8	Pile (EOID)	0.00	9	1.75	585	252	0.175	423	410
	7day Restrike (BOR)	7.12				7	0.15	480	524
DLTP1	Pile (EOID)	0.00	9.5	2	580	16	0.2	529	471
	24hr Restrike (BOR)	1.79				5	0.333	444	416
	7day Restrike (BOR)	8.06				3	0.283	424	381
	7day Redrive (EOD)	8.06	8.1	1.6	564	23	0.2	462	445
DLTP2	Pile (EOID)	0.00	9.5	2	580	150	0.2	533	462
	7day Restrike (BOR)	7.20				5	0.333	378	369
	7day Redrive (EOD)	7.20	8.7	1.8	569	18	0.2	487	460
SLTP	Pile (EOID)	0.00	9	1.75	585	148	0.175	561	467
	7day Restrike (BOR)	7.11				4	0.2	596	536

\*Note: RP3 is damaged

Table 4.3. CAPWAP results for all piles, Site 1

Pile	Drive Detail	Time After EOID (days)	CAPWAP CAPACITY			Match Quality MQ
			Total (kips)	Side (kips)	E.B. (kips)	
RP1	Pile (EOID)	0.00	462	47	415	3.87
	7day Restrike (BOR)	7.25	434	178	256	2
	7day Redrive (EOD)	7.25	380	92	288	1.68
RP2	Pile (EOID)	0.00	524	35	489	4.65
	24hr Restrike (BOR)	1.71	404	75	329	1.7
	7day Restrike (BOR)	7.98	450	110	340	1.3
	7day Redrive (EOD)	7.98	459	100	359	1.16
RP3	Pile (EOID)	0.00	na*	na	na	na
	7day Restrike (BOR)	7.28	na	na	na	na
RP4	Pile (EOID)	0.00	517	64	453	4.51
	24hr Restrike (BOR)	1.75	391	138	253	1.59
	7day Restrike (BOR)	8.00	361	108	253	1.08
	7day Redrive (EOD)	8.00	455	93	362	1.66
RP5	Pile (EOID)	0.00	410	48	362	2.46
	24hr Restrike (BOR)	0.92	397	270	127	1.82
	7day Restrike (BOR)	7.17	400	126	274	2.06
RP6	Pile (EOID)	0.00	409	45	364	2.43
	7day Restrike (BOR)	7.18	462	153	309	1.19
RP7	Pile (EOID)	0.00	414	79	335	1.91
	24hr Restrike (BOR)	0.87	414	198	216	1.37
	7day Restrike (BOR)	7.12	480	237	243	1.11
RP8	Pile (EOID)	0.00	410	64	346	2.33
	7day Restrike (BOR)	7.12	524	175	349	1.45
DLTP1	Pile (EOID)	0.00	471	49	422	4.14
	24hr Restrike (BOR)	1.79	416	87	329	2.14
	7day Restrike (BOR)	8.06	381	55	326	1.96
	7day Redrive (EOD)	8.06	445	73	372	2.42
DLTP2	Pile (EOID)	0.00	462	54	408	3.8
	7day Restrike (BOR)	7.20	369	137	232	1.58
	7day Redrive (EOD)	7.20	460	89	371	2.38
SLTP	Pile (EOID)	0.00	467	52	415	3.37
	7day Restrike (BOR)	7.11	536	99	437	2.23

\*Note: Pile RP3 is damaged

Table 4.4. Static Load Test (Compression) results for Site 1 conducted on 11/14/2012

Time	Jack		Load Cell			Dial Gage			Wireline & Mirror	
	Gage Pressure	Jack Load	Initial Load Cell Rdg	Final Load Cell Rdg	Load Cell Load	Dial Gage 1	Dial Gage 2	Avg Displ	Wireline Rdg	Wireline Displ
	(psi)	(kips)	(rdg)	(rdg)	(kips)	(in)	(in)	(in)	(in)	(in)
7:00	0	0	-397	-397	0	3.000	3.000	0.000	1.02	0.00
7:09	0	0	-397	-397	0	3.000	3.000	0.000	1.02	0.00
7:27	250	23	-234	-237	34	2.989	2.986	0.013	1.03	0.02
7:34	500	47	-113	-113	59	2.971	2.971	0.029	1.05	0.03
7:34	750	70	-3	-1	83	2.955	2.952	0.047	1.08	0.06
7:44	1000	94	112	109	106	2.937	2.931	0.066	1.09	0.08
7:50	1250	118	235	225	131	2.915	2.907	0.089	1.13	0.11
7:57	1500	141	350	340	156	2.890	2.880	0.115	1.16	0.14
8:02	1750	165	455	452	179	2.863	2.854	0.142	1.17	0.16
8:07	2000	189	565	556	201	2.832	2.826	0.171	1.20	0.19
8:13	2250	213	672	665	224	2.805	2.798	0.199	1.22	0.20
8:18	2500	237	780	772	247	2.771	2.771	0.229	1.27	0.25
8:24	2750	261	886	855	267	2.744	2.738	0.259	1.28	0.27
8:29	3000	285	975	964	288	2.712	2.704	0.292	1.31	0.30
8:34	3250	309	1065	1065	309	2.683	2.675	0.321	1.36	0.34
8:39	3500	334	1180	1171	332	2.650	2.642	0.354	1.38	0.36
8:45	3750	358	1280	1272	354	2.621	2.612	0.384	1.41	0.40
8:50	4000	382	1383	1373	376	2.591	2.582	0.414	1.45	0.43
8:56	4250	407	1495	1470	398	2.566	2.558	0.438	1.47	0.45
9:01	4500	431	1625	1644	431	2.522	2.516	0.481	1.52	0.50
9:08	4750	456	1755	1756	457	2.491	2.482	0.514	1.55	0.53
9:13	5000	480	1868	1863	481	2.455	2.446	0.550	1.59	0.58
9:20	5250	505	1983	1976	505	2.415	2.408	0.589	1.63	0.61
9:28	5500	530	2096	2094	531	2.370	2.362	0.634	1.67	0.66
9:34	5750	555	2220	2215	557	2.328	2.319	0.677	1.72	0.70
9:39	6000	580	2322	2327	580	2.272	2.262	0.733	1.73	0.72
9:46	6250	605	2435	2429	604	2.223	2.212	0.783	1.81	0.80
9:53	6500	630	2538	2510	624	2.170	2.158	0.836	1.88	0.86
9:59	6750	655	2665	2660	654	2.090	2.077	0.917	1.95	0.94
10:05	7000	680	2775	2773	679	2.015	2.002	0.992	2.02	1.00
10:12	7250	705	2886	2869	701	1.940	1.928	1.066	2.09	1.08
10:18	7500	730	2990	2981	725	1.860	1.847	1.147	2.17	1.16
10:23	7750	756	3126	3109	754	1.746	1.732	1.261	2.28	1.27
10:28	8000	781	3247	3245	783	1.624	1.608	1.384	2.41	1.39
10:37	7000	680	2909	2906	708	1.650	1.640	1.355	2.38	1.36
10:42	6000	580	2481	2490	616	1.718	1.702	1.290	2.31	1.30
10:47	5000	480	2042	2055	520	1.794	1.781	1.213	2.23	1.22
10:51	4000	382	1600	1616	425	1.879	1.867	1.127	2.14	1.13
10:55	3000	285	1140	1153	326	1.972	1.966	1.031	2.03	1.02
10:59	2000	189	775	792	249	2.047	2.043	0.955	1.97	0.95
11:04	1000	94	260	282	140	2.150	2.150	0.850	1.86	0.84
11:08	0	0	-396	-399	0	2.296	2.298	0.703	1.70	0.69
11:23	0	0	-399	-398	0	2.309	2.310	0.691	1.69	0.67

Table 4.5. Uplift measurements for RP1, RP2, RP3, RP4, RP5, and RP7, Site 1

Load on Compression Pile (kips)	Uplift Displacement based on Wireline Measurements					
	RP1 (in)	RP2 (in)	RP3 (in)	RP4 (in)	RP5 (in)	RP7 (in)
0	0.00	0.00	0.00	0.00	0.00	0.00
0	0.00	0.00	0.00	0.00	0.00	0.00
34	0.00	0.00	0.01	0.00	0.01	0.00
59	0.00	0.02	0.00	0.02	0.02	0.00
83	0.00	0.02	0.00	0.02	0.02	0.00
106	0.00	0.02	0.01	0.02	0.02	0.01
131	0.00	0.02	0.01	0.02	0.02	0.01
156	0.00	0.02	0.01	0.02	0.02	0.01
179	0.00	0.03	0.02	0.02	0.02	0.02
224	0.00	0.03	0.02	0.03	0.02	0.02
267	0.00	0.05	0.03	0.03	0.03	0.02
309	0.02	0.05	0.03	0.03	0.03	0.03
354	0.02	0.05	0.05	0.05	0.04	0.03
398	0.02	0.06	0.05	0.05	0.05	0.05
457	0.03	0.06	0.06	0.05	0.05	0.05
505	0.03	0.08	0.08	0.06	0.05	0.06
557	0.04	0.09	0.09	0.06	0.06	0.06
604	0.05	0.10	0.12	0.08	0.06	0.08
654	0.05	0.12	0.13	0.09	0.07	0.08
701	0.06	0.13	0.17	0.11	0.08	0.09
725	0.06	0.14	0.19	0.11	0.08	0.09
754	0.07	0.16	0.20	0.13	0.09	0.10
783	0.08	0.16	0.23	0.14	0.09	0.11
708	0.08	0.16	0.23	0.14	0.09	0.11
616	0.06	0.15	0.21	0.13	0.08	0.09
520	0.06	0.15	0.21	0.13	0.08	0.09
425	0.05	0.13	0.19	0.11	0.06	0.06
249	0.03	0.11	0.15	0.09	0.05	0.05
0	0.00	0.08	0.11	0.06	0.02	0.02
0	0.00	0.08	0.11	0.06	0.02	0.02

Table 4.6. Details of Initial Driving, Restrike, and Redrive, Site 2

Pile	Drive Detail	Total Pile Length (ft)	Lpen* (ft)	Date	Time
RP1	Bottom	45.3	40.9	10/03/12	8:38
	Top (EOID)	90.5	69	10/04/12	8:15
	7day Restrike (BOR)		69	10/11/12	8:34
	7day Redrive (EOD)		69.5	10/11/12	8:34
RP2	Bottom	45.3	40.9	10/03/12	10:50
	Top(EOID)	90.6	75.4	10/03/12	11:30
	24hrRestrike(BOR)	90.6	75.4	10/04/12	13:10
	8-Day Restrike		75.4	10/11/12	8:10
RP3	Bottom	45.3	41.4	10/03/12	8:52
	Top(EOID)	90.5	74.7	10/04/12	7:29
	8-Day Restrike		74.7	10/11/12	8:25
RP4	Bottom	45.3	40.9	10/03/12	9:10
	Top(EOID)	90.6	71.3	10/03/12	10:20
	24hrRestrike(BOR)	90.6	71.3	10/04/12	13:17
	8-Day Restrike		71.3	10/11/12	8:18
RP5	Bottom	45.3	41	10/03/12	13:18
	Top(EOID)	90.6	68.2	10/03/12	14:16
	24hrRestrike(BOR)	90.6	68.2	10/04/12	12:54
	8-Day Restrike		68.2	10/11/12	7:33
RP6	Bottom	45.3	41	10/03/12	12:53
	Top(EOID)	90.6	68.4	10/04/12	11:49
	8-Day Restrike		68.4	10/11/12	8:39
RP7	Bottom	45.3	41	10/03/12	14:23
	Top(EOID)	90.7	70.2	10/03/12	14:55
	24hrRestrike(BOR)	90.7	70.2	10/04/12	13:05
	8-Day Restrike		70.2	10/11/12	8:54
RP8	Bottom	45.3	41	10/03/12	12:38
	Top(EOID)	90.6	70.9	10/04/12	11:08
	8-Day Restrike		70.9	10/11/12	8:47
DLTP1	Bottom	45.2	42	10/03/12	7:28
	Top(EOID)	90.4	71	10/03/12	8:14
	6hrRestrike(BOR)	90.4	71	10/03/12	16:40
	24hrRestrike(BOR)	90.4	71	10/04/12	13:27
	8-Day Restrike		71	10/11/12	7:55
DLTP2	Bottom	45.2	41	10/04/12	8:44
	Top(EOID)	90.4	75.6	10/04/12	9:31
	8-Day Restrike		75.6	10/11/12	8:05
SLTP	Bottom	45.2	41	10/03/12	15:35
	Top(EOID)	90.4	74	10/03/12	16:10
	8-Day Restrike		74	10/11/12	7:45

\*note: elevation of ground surface is 582.25

Table 4.7. Pile Capacity Based on WisDOT Pile Formula, PDA, and CAPWAP, Site 2

Pile	Drive Detail	Delta Time From EOD (days)	Wisconsin DOT Pile Driving Formula			Blow BN	Pile Set (in)	PDA-RMX Capacity (J=0.9) (kips)	CAPWAP Capacity (kips)
			Hammer Stroke (ft)	Pile Pen In 10 blows (in)	Pile Cap (kips)				
RP1	Pile(EOID)	0.00	9.5	1.875	592	578	0.19	481	477
	8-Day Restrike (BOR)	7.01				8	0.26	397	446
	8-Day Restrike (EOD)	7.01				25	0.23	480	500
RP2	Pile(EOID)	0.00	9.5	1.875	592	847	0.19	452	460
	24hrRestrike(BOR)	0.93				4	0.13	503	469
	8-Day Restrike	7.72				3	0.1	517	539
RP3	Pile(EOID)	0.00	9	1.75	585	787	0.18	370	405
	8-Day Restrike	7.04				3	0.08	475	522
RP4	Pile(EOID)	0.00	9.5	1.75	604	808	0.18	425	466
	24hrRestrike(BOR)	1.12				6	0.17	415	441
	8-Day Restrike	7.92				10	0.19	436	477
RP5	Pile(damaged)	0.00	9	2.5	524	644	0.25	na*	na
	24hrRestrike(BOR)	0.94				6	0.17	na	na
	8-Day Restrike	7.72						na	na
RP6	Pile(EOID)	0.00	8.5	2	544	726	0.2	266	294
	8-Day Restrike	6.87						na**	na
RP7	Pile(EOID)	0.00	9.5	2.25	560	536	0.22	449	465
	24hrRestrike(BOR)	0.92				2	0.11	464	481
	8-Day Restrike	7.75				9	0.09	494	560
RP8	Pile(EOID)	0.00	8.5	2	544	607	0.20	416	440
	8-Day Restrike	6.90				8	0.11	508	529
DLTP1	Pile(EOID)	0.00	9.5	2	580	615	0.20	381	395
	6hrRestrike(BOR)	0.35				5	0.22	405	436
	24hrRestrike(BOR)	1.22				4	0.18	448	469
	8-Day Restrike	7.99				3	0.20	437	470
DLTP2	Pile(EOID)	0.00	9.5	2	580	859	0.20	401	432
	8-Day Restrike	6.94				3	0.20	461	476
SLTP	Pile(EOID)	0.00	9.5	2	580	766	0.20	400	427
	8-Day Restrike	7.65				4	0.13	505	546

\*Note: RP5 is damaged

\*\*Note: No readings available for RP6 restrike

Table 4.8. – CAPWAP results for all piles, Site 2

Pile	Drive Detail	Delta Time From EOD (days)	CAPWAP			
			Capacity Total (kips)	Side (kips)	E.B. (kips)	MQ
RP1	Pile(EOID)	0.00	477	92	385	1.8
	8-Day Restrike (BOR)	7.01	446	208	238	1.83
	8-Day Restrike (EOD)	7.01	500	91	409	1.8
RP2	Pile(EOID)	0.00	460	154	306	2
	24hrRestrike(BOR)	0.93	469	219	250	1.71
	8-Day Restrike	7.72	539	339	200	1.91
RP3	Pile(EOID)	0.00	405	127	278	1.44
	8-Day Restrike	7.04	522	181	341	1.82
RP4	Pile(EOID)	0.00	466	161	305	2.66
	24hrRestrike(BOR)	1.12	441	178	263	1.31
	8-Day Restrike	7.92	477	175	302	1.55
RP5	Pile(EOID)	0.00	na*	na	na	na
	24hrRestrike(BOR)	0.94	na	na	na	na
	8-Day Restrike	7.72	na	na	na	na
RP6	Pile(EOID)	0.00	294	84	210	2.02
	8-Day Restrike	6.87	na**	na	na	na
RP7	Pile(EOID)	0.00	465	119	346	1.6
	24hrRestrike(BOR)	0.92	481	220	261	1.36
	8-Day Restrike	7.75	560	194	366	1.52
RP8	Pile(EOID)	0.00	440	150	290	1.62
	8-Day Restrike	6.90	529	144	385	1.17
DLTP1	Pile(EOID)	0.00	395	113	282	1.66
	6hrRestrike(BOR)	0.35	436	157	279	1.85
	24hrRestrike(BOR)	1.22	469	176	293	1.7
	8-Day Restrike	7.99	470	123	347	1.42
DLTP2	Pile(EOID)	0.00	432	155	277	1.68
	8-Day Restrike	6.94	476	146	330	1.49
SLTP	Pile(EOID)	0.00	427	124	303	1.57
	8-Day Restrike	7.65	546	198	348	1.36

\*Note: RP5 is damaged

\*\*Note: No readings available for RP6 restrike

Table 4.9. Static Load Test (Compression) results for Site 2 conducted on 10/10/2012

Time	Jack		Dial Indicators			Wireline	
	Gage Press (psi)	Load (kips)	Rdg 1 (in)	Rdg 2 (in)	Avg Displ (in)	Wireline Rdg (in)	Wireline Displ (in)
8:15	0	0	3.000	3.000	0.000	1.27	0.00
8:19	250	23	2.982	2.981	0.019	1.28	0.01
8:23	500	47	2.967	2.959	0.037	1.31	0.04
8:26	750	70	2.945	2.936	0.060	1.33	0.05
8:30	1000	94	2.920	2.910	0.085	1.36	0.09
8:34	1250	118	2.898	2.882	0.110	1.39	0.12
8:38	1500	141	2.871	2.854	0.138	1.42	0.15
8:42	1750	165	2.843	2.824	0.167	1.45	0.18
8:46	2000	189	2.812	2.790	0.199	1.48	0.21
8:50	2250	213	2.776	2.755	0.235	1.52	0.25
8:54	2500	237	2.741	2.718	0.271	1.56	0.29
8:54	2750	261	2.700	2.679	0.311	1.59	0.32
8:58	3000	285	2.661	2.643	0.348	1.64	0.37
9:02	3250	309	2.621	2.605	0.387	1.67	0.40
9:06	3500	334	2.582	2.562	0.428	1.72	0.45
9:10	3750	358	2.541	2.523	0.468	1.75	0.48
9:16	4000	382	2.499	2.480	0.511	1.80	0.52
9:22	4250	407	2.455	2.435	0.555	1.84	0.57
9:34	4500	431	2.415	2.394	0.596	1.88	0.60
9:40	4750	456	2.373	2.352	0.638	1.92	0.65
9:44	5000	480	2.334	2.314	0.676	1.97	0.70
9:48	5250	505	2.289	2.270	0.721	2.02	0.74
9:52	5500	530	2.243	2.226	0.766	2.06	0.79
9:56	5750	555	2.189	2.172	0.820	2.11	0.84
10:01	6000	580	2.145	2.131	0.862	2.16	0.88
10:05	6250	605	2.099	2.085	0.908	2.20	0.93
10:09	6500	630	2.040	2.028	0.966	2.27	0.99
10:14	6750	655	1.981	1.969	1.025	2.32	1.05
10:18	7000	680	1.926	1.914	1.080	2.38	1.10
10:22	7250	705	1.851	1.841	1.154	2.45	1.18
10:27	7500	730	1.772	1.764	1.232	2.53	1.26
10:33	7750	756	1.679	1.671	1.325	2.63	1.35
10:39	8000	781	1.611	1.602	1.394	2.69	1.41
10:44	8250	806	1.509	1.506	1.493	2.80	1.52
10:50	7000	680	1.559	1.559	1.441	2.73	1.46
10:55	6000	580	1.658	1.659	1.342	2.64	1.37
11:00	5000	480	1.779	1.782	1.220	2.52	1.24
11:04	4000	382	1.909	1.909	1.091	2.38	1.10
11:09	3000	285	2.050	2.050	0.950	2.23	0.96
11:13	2000	189	2.194	2.180	0.813	2.09	0.82
11:17	1000	94	2.343	2.330	0.664	1.94	0.66
11:42	0	0	2.530	2.510	0.480	1.75	0.48

Table 4.10. Details of Initial Driving, Restrike, and Redrive, Site 3

Pile	Drive Detail	Total Pile Length (ft)	Lpen* (ft)	Date	Time
RP1	Bottom	50.3	45.00	09/18/12	10:35
	Top(EOID)	70.5	53.80	09/19/12	12:45
	8-Day Restrike		53.60	09/27/12	9:55
RP2	Bottom	50.3	45.00	09/18/12	11:20
	Top	70.3	54.25	09/19/12	10:30
	8-Day Restrike		54.50	09/27/12	9:36
RP3	Bottom	50.3	45.00	09/18/12	9:00
	Top(EOID)	90.5	57.25	09/18/12	10:10
	6hr Restrike (BOR)	90.5	57.25	09/18/12	15:01
	6hr Restrike (EOD)	90.5	57.25	09/18/12	15:01
	24hr Restrike (BOR)	90.5	57.25	09/20/12	7:30
	8-Day Restrike		57.00	09/27/12	9:16
RP4	Bottom	50.3	45.00	09/18/12	11:00
	Top(EOID)	70.5	54.70	09/19/12	11:25
	8-Day Restrike		54.60	09/27/12	9:26
RP5	Top(EOID)	50.3	44.00	09/18/12	12:30
	8-Day Restrike		44.00	09/27/12	8:15
RP6	Bottom	50.3	43.30	09/18/12	14:25
	24hrRestrike(BOR)	50.3	43.30	09/20/12	7:17
	24hrRestrike(EOD)	50.3	43.30	09/20/12	7:17
	8-Day Restrike		43.30	09/27/12	8:25
RP7	Bottom	50.3	44.00	09/18/12	12:10
	Top(EOID)	70.3	52.30	09/19/12	15:20
	24hrRestrike(BOR)	70.3	52.30	09/20/12	7:00
	24hrRestrike(EOD)	70.3	52.30	09/20/12	7:00
	8-Day Restrike		52.80	09/27/12	8:45
RP8	Top(EOID)	50.3	45.00	09/18/12	13:40
	8-Day Restrike		45.25	09/27/12	8:34
DLTP1	Bottom	50.3	45.00	09/19/12	7:30
	Top(EOID)	70.3	53.80	09/19/12	9:10
	24hrRestrike(BOR)	70.3	53.80	09/20/12	7:44
	8-day Restrike		53.80	09/27/12	9:45
DLTP2	Bottom	50.3	45.00	09/19/12	7:15
	Top(EOID)	70.3	55.00	09/19/12	13:38
	8-Day Restrike		55.00	09/27/12	9:06
SLTP	Bottom	50.3	45.00	09/18/12	11:50
	Top(EOID)	70.5	54.50	09/19/12	14:30
	8-Day Restrike		54.60	09/27/12	8:55

\*Note Elevation of ground surface is 579.35ft.

Table 4.11. Pile Capacity Based on WisDOT Pile Formula, PDA, and CAPWAP, Site 3

Pile	Drive Detail	Delta Time From EOD (days)	Wisconsin DOT Pile Driving Formula			Blow Number BN	Pile Set (in)	PDA-RMX Capacity (J=0.9) (kips)	CAPWAP Capacity (kips)
			Hammer Stroke (ft)	Pile Penetration In 10 blows (in)	Pile Capacity (kips)				
RP1	Pile(EOID)	0.00	9.5	2	580	271	0.200	451	450
	8-Day Restrike	7.88				5	0.200	530	531
RP2	Pile(EOID)	0.00	9.5	1.5	630	338	0.150	490	488
	8-Day Restrike	7.96				5	0.170	565	554
RP3	Pile(EOID)	0.00	9.5	2	580	375	0.200	487	451
	6hr Restrike (BOR)	0.20				4	0.167	542	561
	6hr Restrike (EOD)	0.20				19	0.167	493	490
	24hr Restrike (BOR)	1.89				6	0.150	567	577
	8-Day Restrike	8.96				4	0.130	569	587
RP4	Pile(EOID)	0.00	9.5	2	580	303	0.200	524	490
	8-Day Restrike	7.92				6	0.153	548	570
RP5	Pile(EOID)	0.00	9.5	2	580	na*	na	na	na
	8-Day Restrike	8.82				9	0.150	515	522
RP6	Pile(EOID)	0.00	9.5	2.5	542	207	0.250	469	418
	24hrRestrike(BOR)	1.70				7	0.233	486	441
	24hrRestrike(EOD)	1.70				17	0.267	491	428
	8-Day Restrike	8.75				4	0.260	499	477
RP7	Pile(EOID)	0.00	9.5	2	580	278	0.200	496	520
	24hrRestrike(BOR)	0.65				5	0.200	542	579
	24hrRestrike(EOD)	0.65				29	0.300	469	491
	8-Day Restrike	7.73				6	0.230	546	563
RP8	Pile(EOID)	0.00	9.5	2	580	301	0.200	502	452
	8-Day Restrike	8.79				8	0.340	491	461
DLTP 1	Pile(EOID)	0.00	9.5	2	580	273	0.200	486	474
	24hrRestrike(BOR)	0.94				5	0.200	546	514
	8-day Restrike	8.02				5	0.187	549	551
DLTP 2	Pile(EOID)	0.00	9.5	1.75	604	296	0.175	478	461
	8-Day Restrike	7.81				4	0.210	513	488
SLTP	Pile(EOID)	0.00	9.5	1.875	592	364	0.188	450	448
	8-Day Restrike	7.77				4	0.233	540	543

\*Note: No PDA measurements were recorded for RP5 during initial driving

Table 4.12. – CAPWAP results for all piles, Site 3

Pile	Drive Detail	Delta Time From EOD (days)	CAPWAP Capacity			
			Total (kips)	Side (kips)	E.B. (kips)	MQ
RP1	Pile(EOID)	0.00	450	124	326	1.59
	8-Day Restrike	7.88	531	242	289	1.88
RP2	Pile(EOID)	0.00	488	69	419	2.05
	8-Day Restrike	7.96	554	195	359	1.87
RP3	Pile(EOID)	0.00	451	112	339	2.04
	6hr Restrike (BOR)	0.20	561	165	396	1.62
	6hr Restrike (EOD)	0.20	490	165	325	1.91
	24hr Restrike (BOR)	1.89	577	198	379	1.44
	8-Day Restrike	8.96	587	357	230	1.08
RP4	Pile(EOID)	0.00	490	125	365	2.56
	8-Day Restrike	7.92	570	319	251	2.04
RP5	Pile(EOID)	0.00	na*	na	na	na
	8-Day Restrike	8.82	522	164	358	1.75
RP6	Pile(EOID)	0.00	418	88	330	2.71
	24hrRestrike(BOR)	1.70	441	64	377	1.62
	24hrRestrike(EOD)	1.70	428	80	348	2.2
	8-Day Restrike	8.75	477	124	353	1.68
RP7	Pile(EOID)	0.00	520	114	406	1.67
	24hrRestrike(BOR)	0.65	579	252	327	2.25
	24hrRestrike(EOD)	0.65	491	170	321	1.75
	8-Day Restrike	7.73	563	242	321	1.68
RP8	Pile(EOID)	0.00	452	93	359	2.7
	8-Day Restrike	8.79	461	153	308	1.96
DLTP1	Pile(EOID)	0.00	474	131	343	2.62
	24hrRestrike(BOR)	0.94	514	173	341	2.08
	8-day Restrike	8.02	551	169	382	1.76
DLTP2	Pile(EOID)	0.00	461	108	353	2.88
	8-Day Restrike	7.81	488	157	331	2.32
SLTP	Pile(EOID)	0.00	448	122	326	1.4
	8-Day Restrike	7.77	543	282	261	2.06

\*Note: No PDA measurements were recorded for RP5 during initial driving.

Table 4.13. Static Load Test (Compression) results for Site 3 conducted on 9/26/2012

Time	Jack		Load Cell			Dial Indicators			Wireline & Mirror	
	Gage Press (psi)	Load (kips)	Rdg (initial)	Rdg (final)	Load (kips)	Rdg 1 (in)	Rdg 2 (in)	Avg Displ (in)	Wireline Rdg (in)	Wireline Displ (in)
10:16	0	0	-398	-398	0	3.000	3.000	0.000	0.96	0.00
10:21	250	23				2.975	2.980	0.023	0.98	0.02
10:24	500	47	-116	-116	59	2.959	2.958	0.041	1.00	0.04
10:27	750	70	22	19	88	2.933	2.934	0.067	1.02	0.05
10:31	1000	94	147	139	113	2.909	2.909	0.091	1.05	0.09
10:34	1250	118	279	271	141	2.879	2.881	0.120	1.08	0.12
10:37	1500	141	396	383	165	2.851	2.855	0.147	1.11	0.15
10:40	1750	165	519	507	191	2.820	2.826	0.177	1.13	0.16
10:46	2000	189	627	615	214	2.787	2.794	0.210	1.16	0.20
10:51	2250	213	742	736	239	2.759	2.768	0.237	1.19	0.23
10:55	2500	237	859	851	264	2.725	2.733	0.271	1.23	0.27
10:55	2750	261	960	966	287	2.693	2.703	0.302	1.25	0.29
10:59	3000	285	1067	1070	310	2.659	2.669	0.336	1.30	0.34
11:03	3250	309	1186	1182	334	2.623	2.633	0.372	1.33	0.37
11:07	3500	334	1305	1309	361	2.581	2.592	0.414	1.38	0.41
11:11	3750	358	1412	1421	384	2.548	2.559	0.447	1.41	0.45
11:15	4000	382	1531	1527	408	2.511	2.522	0.484	1.44	0.48
11:19	4250	407	1641	1646	433	2.471	2.484	0.523	1.47	0.51
11:23	4500	431	1767	1775	461	2.428	2.440	0.566	1.52	0.55
11:27	4750	456	1871	1877	483	2.388	2.402	0.605	1.56	0.60
11:31	5000	480	1981	1982	506	2.353	2.367	0.640	1.59	0.63
11:35	5250	505	2101	2104	532	2.307	2.321	0.686	1.64	0.68
11:39	5500	530	2213	2216	557	2.257	2.271	0.736	1.69	0.73
11:43	5750	555	2334	2342	584	2.208	2.225	0.784	1.74	0.78
11:47	6000	580	2433	2447	606	2.159	2.177	0.832	1.78	0.82
11:51	6250	605	2561	2570	633	2.109	2.128	0.882		
11:55	6500	630	2677	2683	658	2.052	2.074	0.937	1.89	0.93
11:59	6750	655	2790	2797	683	1.996	2.019	0.993	1.94	0.98
12:03	7000	680	2906	2906	708	1.936	1.961	1.052	2.00	1.04
12:08	7250	705	3018	3022	733	1.874	1.900	1.113	2.06	1.10
12:12	7500	730	3127	3127	757	1.803	1.833	1.182	2.14	1.18
12:19	6500	630	2814	2814	688	1.845	1.870	1.143	2.09	1.13
12:23	5750	555	2474	2477	614	1.909	1.931	1.080	2.03	1.07
12:27	5000	480	2128	2139	539	1.982	2.006	1.006	1.97	1.01
12:31	4000	382	1696	1707	446	2.090	2.110	0.900	1.84	0.88
12:35	3000	285	1275	1283	355	2.199	2.220	0.791	1.75	0.79
12:40	2000	189	847	854	263	2.311	2.332	0.679	1.63	0.66
12:45	1000	94	296	305	147	2.431	2.451	0.559	1.50	0.54
12:49	0	0	-400	-400	0	2.581	2.597	0.411		
13:15	0	0	-399	-399	0	2.591	2.602	0.404		

Table 4.14. Details of Initial Driving, Restrike, and Redrive, Site 4

Pile	Drive Detail	Total Pile Length (ft)	Lpen (ft)*	Date	Time
RP1	Bottom	40.2	36	10/24/12	10:17
	Top (EOID)	80.5	77.5	10/25/12	8:21
	8-Day Restrike (BOR)		77.5	11/01/12	8:54
	8-Day Restrike (EOD)		79	11/01/12	8:54
RP2	Bottom	40.3	36	10/24/12	10:30
	Top (EOID)	80.5	77	10/24/12	11:06
	Extra Add On	100.5	77	10/24/12	12:05
	24hr Restrike (BOR)	100.5	77	10/25/12	13:25
	8-Day Restrike (BOR)		77	11/01/12	8:35
	8-Day Restrike (EOD)		77.5	11/01/12	8:35
RP3	Bottom	40.2	36	10/24/12	10:05
	Top (EOID)	80.5	77.5	10/25/12	9:11
	8-Day Restrike (BOR)		77.5	11/01/12	9:10
	8-Day Restrike (EOD)		80.5	11/01/12	9:10
RP4	Bottom	40.3	36	10/24/12	12:49
	Top	80.6	75	10/24/12	13:40
	Extra Add On (EOID)	90.6	77.3	10/24/12	14:18
	24hr Restrike (BOR)		77.3	10/25/12	13:15
	8-Day Restrike (BOR)		77.3	11/01/12	8:25
RP5	Bottom	40.2	36	10/24/12	16:05
	Top (EOID)	80.4	76.5	10/24/12	16:36
	24hr Restrike		76.5	10/25/12	12:59
	8-Day Restrike (BOR)		76.5	11/01/12	8:05
RP6	Bottom	40.2	36	10/24/12	14:33
	Top (EOID)	80.5	77	10/25/12	12:08
	8-Day Restrike (BOR)		77	11/01/12	8:25
RP7 Damaged	Bottom	40.2	36	10/24/12	14:58
	Top (EOID)	80.4	74.5	10/24/12	15:30
	24hr Restrike (BOR)		74.6	10/25/12	12:50
	8-Day Restrike (BOR)		74.6	11/01/12	7:56
RP8	Bottom	40.2	36	10/24/12	14:45
	Top (EOID)	80.5	77.1	10/25/12	11:20
	8-Day Restrike		77.1	11/01/12	7:40
DLTP1 Damaged	Bottom	40.2	36	10/24/12	8:21
	Top (EOID)	80.4	76	10/24/12	9:08
	6hr Restrike (BOR)	80.4	76	10/24/12	18:10
	24hr Restrike (BOR)	80.4	76	10/25/12	13:06
	8-Day Restrike (BOR)		76	11/01/12	9:31
DLTP2	Bottom	40.2	36	10/25/12	10:05
	Top (EOID)	80.5	77	10/25/12	10:35
	8-Day Restrike (BOR)		77	11/01/12	9:46
	8-Day Restrike (EOD)		81.5	11/01/12	9:46
SLTP	Bottom	40.3	36	10/24/12	17:05
	Top (EOID)	80.6	74.8	10/24/12	17:47
	8-Day Restrike		74.8	11/01/12	8:15

\*Note Elevation of ground surface is 580.32ft.

Table 4.15. Pile Capacity Based on WisDOT Pile Formula, PDA, and CAPWAP, Site 4

Pile	Drive Detail	Delta Time From EOD (days)	Wisconsin DOT Pile Driving Formula			Blow Number BN	Pile Set (in)	PDA-RMX Capacity (J=0.9) (kips)	CAPWAP Capacity (kips)
			Hammer Stroke (ft)	Pile Penetration In 10 blows (in)	Pile Capacity (kips)				
RP1	Pile (EOID)	0.00	8.5	1.5	591	815	0.15	332	378
	8-Day Restrike	7.02				6	0.18	360	368
	8-Day Redrive	7.02	8.25	1.15	624	141	0.13	395	402
RP2	Pile (EOID)	0.00	9	1.5	611	24	0.15	348	376
	24hr Restrike	1.06				6	0.15	340	312
	8-Day Restrike	7.85				6	0.18	389	525
	8-Day Redrive	7.85	8.7	1.0	670	52	0.10	381	382
RP3	Pile (EOID)	0.00	9	1.75	585	862	0.18	263	303
	8-Day Restrike	7.00				3	0.15	396	396
	8-Day Redrive	7.00	8.4	1.2	623	248	0.12	346	362
RP4	Pile (EOID)	0.00	9	1	680	55	0.10	336	380
	24hr Restrike	0.96				5	0.17	422	388
	8-Day Restrike	7.75	9.4	.83	729	6	0.13	456	476
RP5	Pile (EOID)	0.00	8.5	2.375	515	796	0.24	243	315
	24hr Restrike	0.85				5	0.33	194	200
	8-Day Restrike	7.65				4	0.28	349	280
RP6	Pile (EOID)	0.00	9	2.875	501	973	0.28	205	243
	8-Day Restrike	6.85				6	0.27	379	357
RP7	Pile (EOID)	0.00	9	1.625	597	860	0.16	na*	na
	24hr Restrike(BOR)	0.89				2	0.20	na	na
	8-Day Restrike	7.68				na	na	na	na
RP8	Pile (EOID)	0.00	8.5	2	544	951	0.20	232	262
	8-Day Restrike	6.85				5	0.23	391	330
DLTP1	Pile (EOID)	0.00	9	1.75	585	775	0.18	na*	na
	6hr Restrike(BOR)	0.38				4	0.17	na	na
	24hr Restrike(BOR)	1.17				4	0.17	na	na
	8-Day Restrike	8.02						na	na
DLTP2	Pile (EOID)	0.00	9	2	562	682	0.20	292	318
	8-Day Restrike	6.97				4	0.17	325	488
	8-Day Redrive	6.97	9.5	1.5	630	282	0.15	304	374
SLTP	Pile (EOID)	0.00	9.5	1.75	604	611	0.18	432	447
	8-Day Restrike	7.60				5	0.11	444	471

\*Note: Pile Damage for piles RP7 and DLTP1

Table 4.16. – CAPWAP results for all piles, Site 4

Pile	Drive Detail	Delta Time From EOD (days)	CAPWAP			
			Capacity Total (kips)	Side (kips)	E.B. (kips)	MQ
RP1	Pile(EOID)	0.00	378	149	229	1.48
	8-Day Restrike (BOR)	7.02	368	306	62	1.28
	8-Day Redrive (EOD)	7.02	402	262	140	1.18
RP2	Pile(EOID)	0.00	376	157	219	1.37
	24hr Restrike (BOR)	1.06	312	200	112	1.08
	8-Day Restrike (BOR)	7.85	525	275	250	1.57
	8-Day Redrive (EOD)	7.85	382	266	116	1.69
RP3	Pile(EOID)	0.00	303	132	171	2.14
	8-Day Restrike (BOR)	7.00	396	187	209	1.26
	8-Day Redrive (EOD)	7.00	362	171	191	1.4
RP4	Pile(EOID)	0.00	380	169	211	1.6
	24hr Restrike (BOR)	0.96	388	269	119	1.25
	8-Day Restrike (BOR)	7.75	476	285	191	1.39
RP5	Pile(EOID)	0.00	315	146	169	2.7
	24hr Restrike	0.85	200	173	27	1.63
	8-Day Restrike (BOR)	7.65	280	243	37	1.52
RP6	Pile(EOID)	0.00	243	179	64	2.5
	8-Day Restrike (BOR)	6.85	357	262	95	1.5
RP7	Pile(EOID)	0.00	na*	na	na	na
	24hr Restrike (BOR)	0.89	na	na	na	na
	8-Day Restrike (BOR)	7.68	na	na	na	na
RP8	Pile(EOID)	0.00	262	184	78	2.69
	8-Day Restrike	6.85	330	278	52	1.99
DLTP1	Pile(EOID)	0.00	na*	na	na	na
	6hr Restrike (BOR)	0.38	na	na	na	na
	24hr Restrike (BOR)	1.17	na	na	na	na
	8-Day Restrike (BOR)	8.02	na	na	na	na
DLTP2	Pile(EOID)	0.00	318	179	139	2.1
	8-Day Restrike (BOR)	6.97	488	157	331	2.32
	8-Day Redrive (EOD)	6.97	374	148	226	1.12
SLTP	Pile(EOID)	0.00	447	112	335	1.69
	8-Day Restrike	7.60	471	248	223	1.61

\*Note: Pile Damage for piles RP7 and DLTP1

Table 4.17. Static Load Test (Compression) results for Site 4 conducted on 10/31/2012

Time	Jack		Load Cell			Dial Indicators			Wireline	
	Gage Press (psi)	Load (kips)	Rdg (initial)	Rdg (final)	Load Cell Load (kips)	Rdg 1 (in)	Rdg 2 (in)	Avg Displ (in)	Wireline Rdg (in)	Wireline Displ (in)
7:53	0	0	-397	-397	0	3.000	3.000	0.000	1.02	0.00
7:56	250	23	-217	-221	37	2.976	2.981	0.022	1.03	0.02
8:00	500	47	-110	-115	59	2.961	2.962	0.039	1.03	0.02
8:03	750	70	26	24	88	2.938	2.932	0.065	1.06	0.05
8:07	1000	94	134	129	111	2.913	2.909	0.089	1.09	0.08
8:11	1250	118	256	250	136	2.885	2.878	0.119	1.11	0.09
8:15	1500	141	363	370	160	2.856	2.850	0.147	1.14	0.13
8:19	1750	165	477	454	181	2.823	2.818	0.180	1.17	0.16
8:23	2000	189	574	568	204	2.779	2.774	0.224	1.22	0.20
8:27	2250	213	697	685	229	2.728	2.725	0.274	1.27	0.25
8:31	2500	237	810	801	253	2.661	2.661	0.339	1.33	0.31
8:31	2750	261	910	908	275	2.604	2.603	0.397	1.39	0.38
8:34	3000	285	1019	1020	299	2.538	2.535	0.464	1.47	0.45
8:39	3250	309	1128	1125	322	2.472	2.472	0.528	1.53	0.52
8:43	3500	334	1246	1236	346	2.398	2.401	0.601	1.59	0.58
8:47	3750	358	1350	1346	369	2.335	2.339	0.663	1.66	0.64
8:51	4000	382	1460	1459	393	2.268	2.275	0.729	1.72	0.70
8:55	4250	407	1572	1569	417	2.207	2.218	0.788	1.80	0.78
8:59	4500	431	1692	1689	443	2.129	2.143	0.864	1.88	0.86
9:03	4750	456	1781	1793	464	2.070	2.083	0.924	1.92	0.91
9:07	5000	480	1905	1900	489	2.008	2.018	0.987	1.98	0.97
9:11	5250	505	2013	2022	514	1.935	1.945	1.060	2.06	1.05
9:15	5500	530	2145	2145	541	1.855	1.865	1.140	2.14	1.13
9:19	5750	555	2260	2258	566	1.775	1.785	1.220	2.20	1.19
9:23	6000	580	2373	2370	591	1.692	1.702	1.303	2.30	1.28
9:27	6250	605	2475	2469	613	1.610	1.617	1.387		1.36
9:31	6500	630	2590	2596	639	1.508	1.515	1.489	2.47	1.45
9:35	6000	580	2423	2420	602	1.523	1.529	1.474	2.45	1.44
9:39	5000	480	2052	2039	520	1.593	1.600	1.404	2.38	1.36
9:43	4000	382	1609	1622	427	1.704	1.712	1.292	2.28	1.27
9:47	3000	285	1194	1209	338	1.830	1.838	1.166	2.14	1.13
9:51	2000	189	722	743	238	1.976	1.985	1.020	2.00	0.98
9:55	1000	94	279	299	144	2.113	2.123	0.882	1.86	0.84
9:59	0	0	-395	-396	0	2.315	2.335	0.675	1.67	0.66
10:15	0	0	-398	-398	0	2.325	2.348	0.664	1.66	0.64

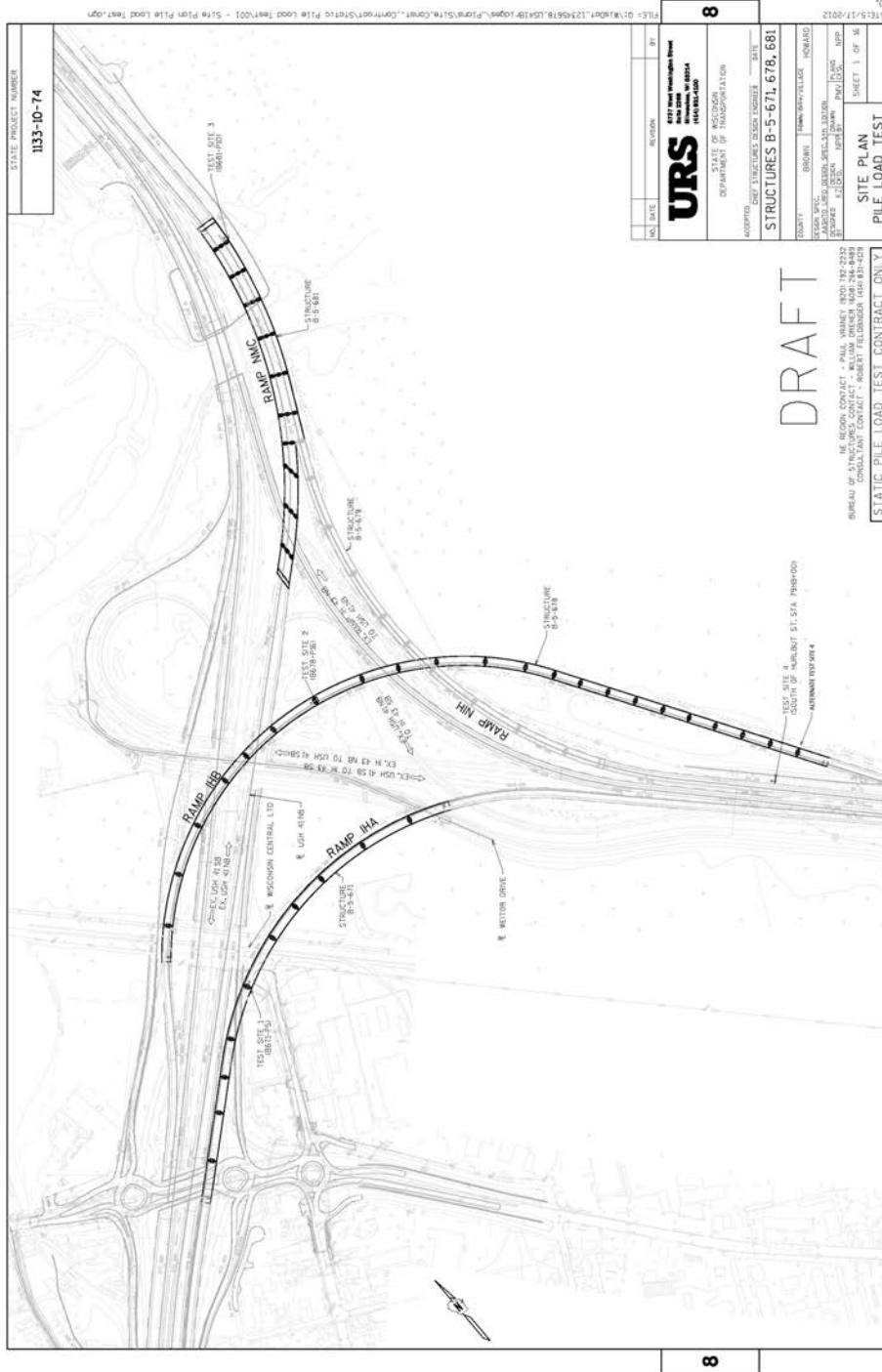


Figure 4.1. Site Plan.





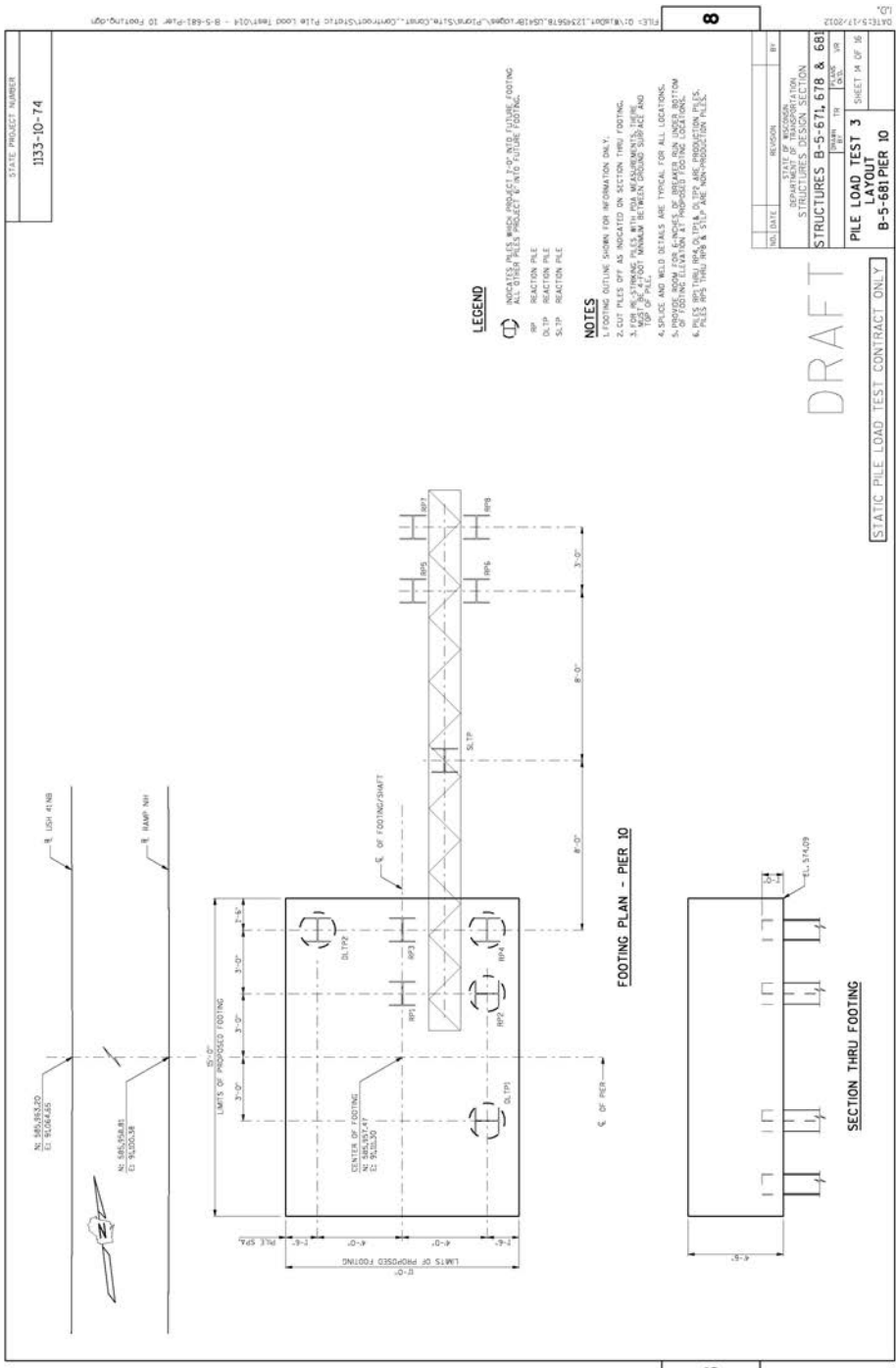


Figure 4.4. Plan View for Site 3.



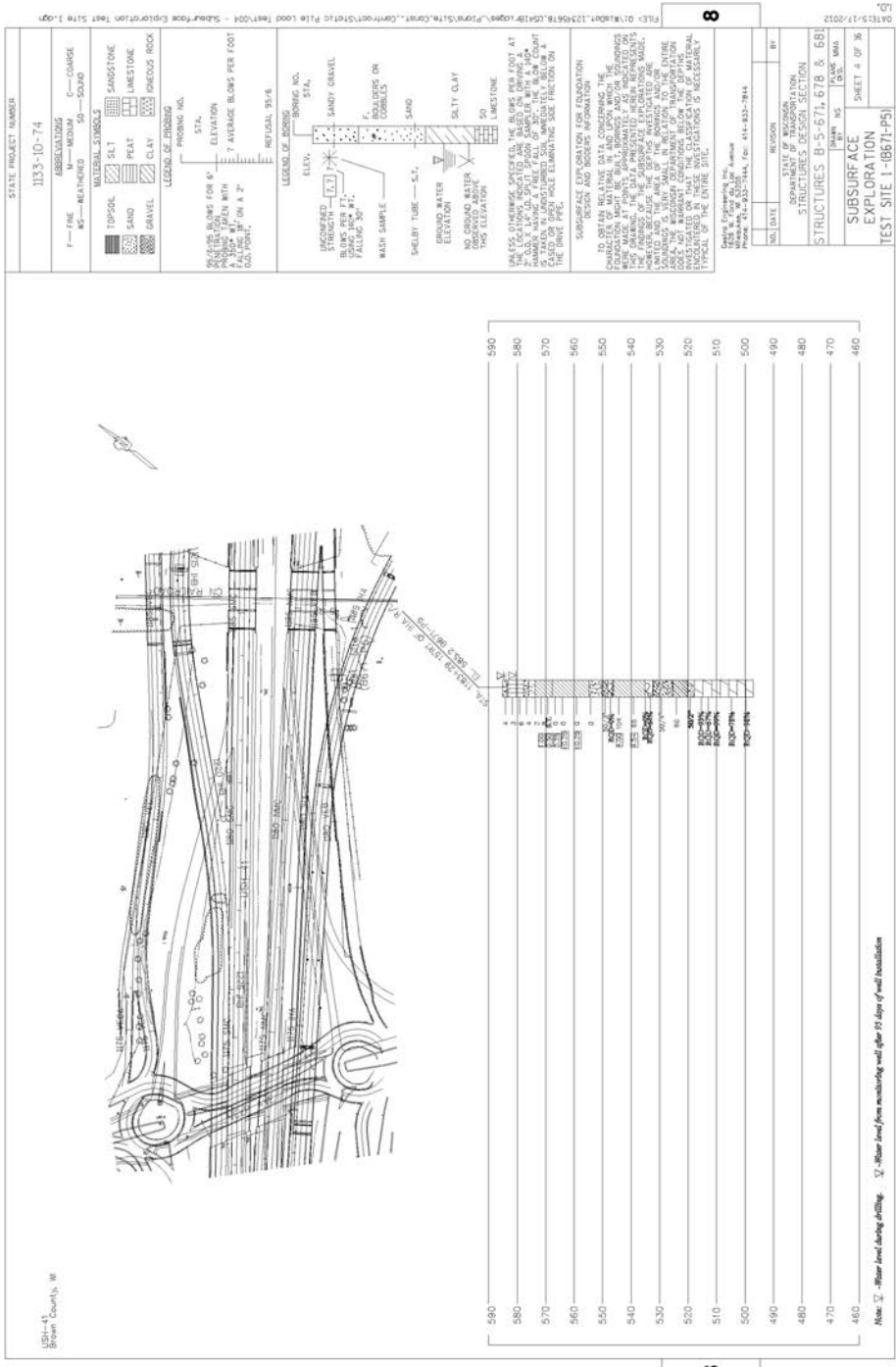
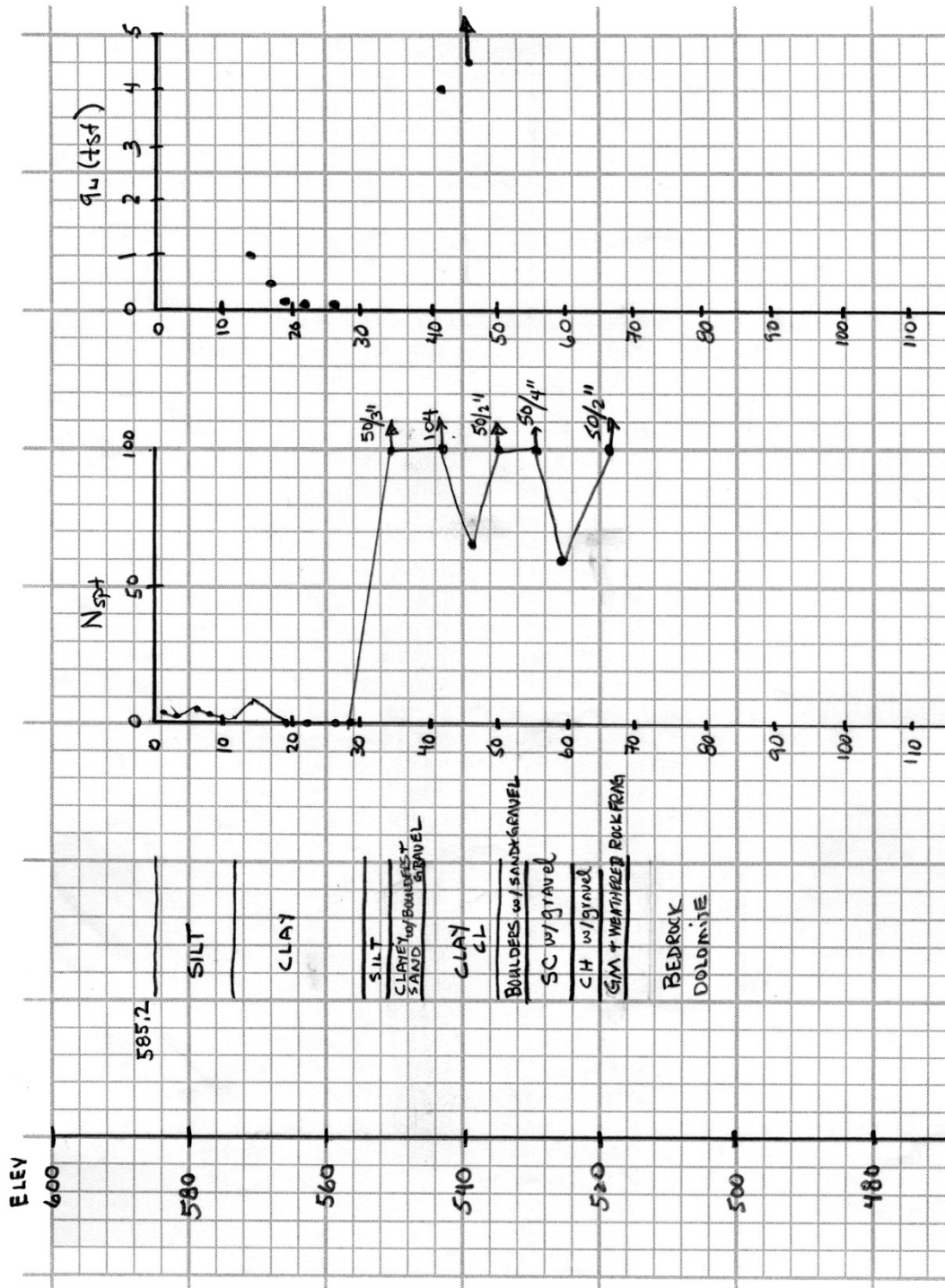


Figure 4.6. Plan View of Site 1, Boring location and Soil Profile.



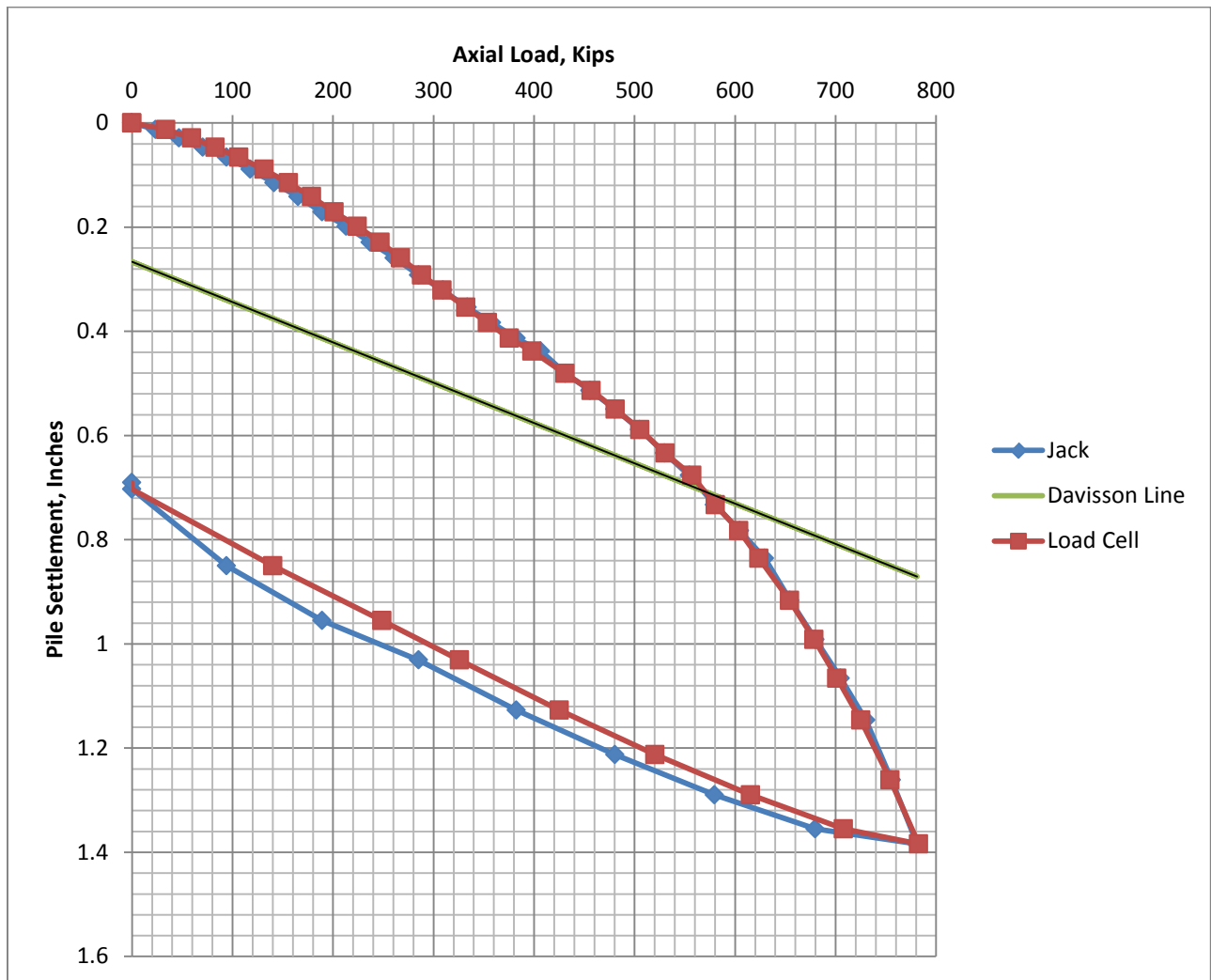


Figure 4.8. Load Settlement curve for load test at Site 1.

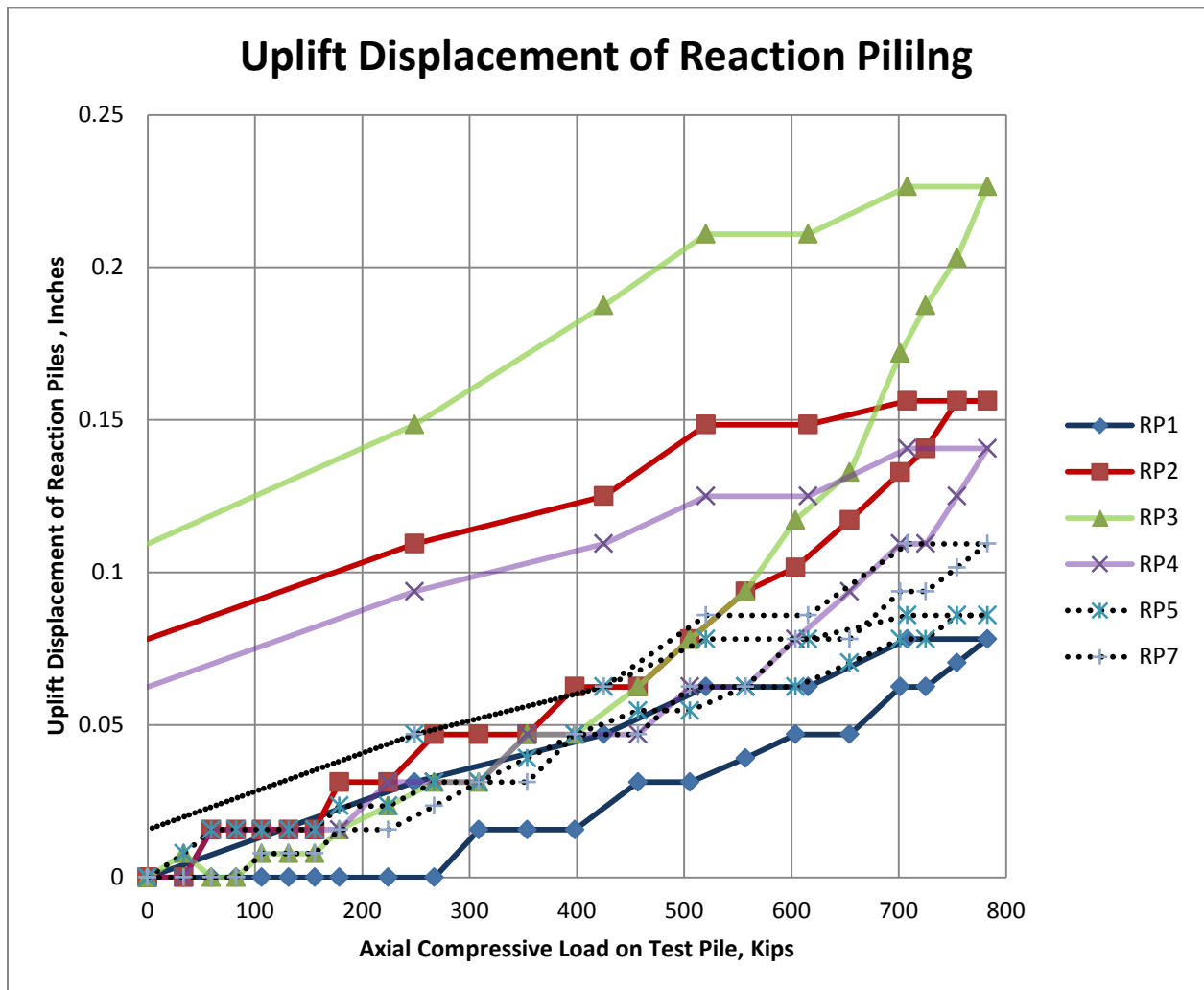


Figure 4.9. Uplift displacement versus compressive load curve for load test at Site 1.



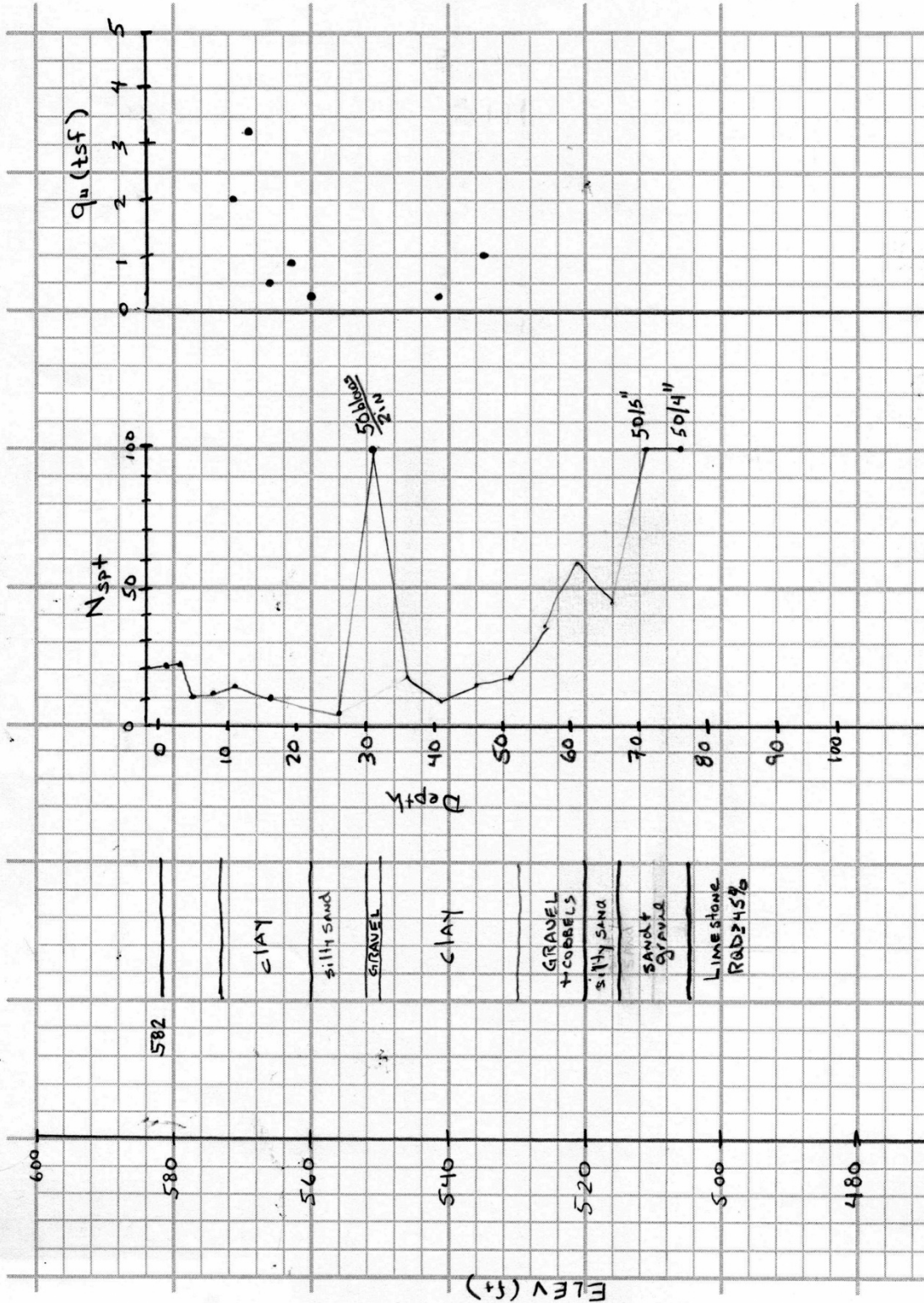


Figure 4.11. Soil Profile for Site 2.

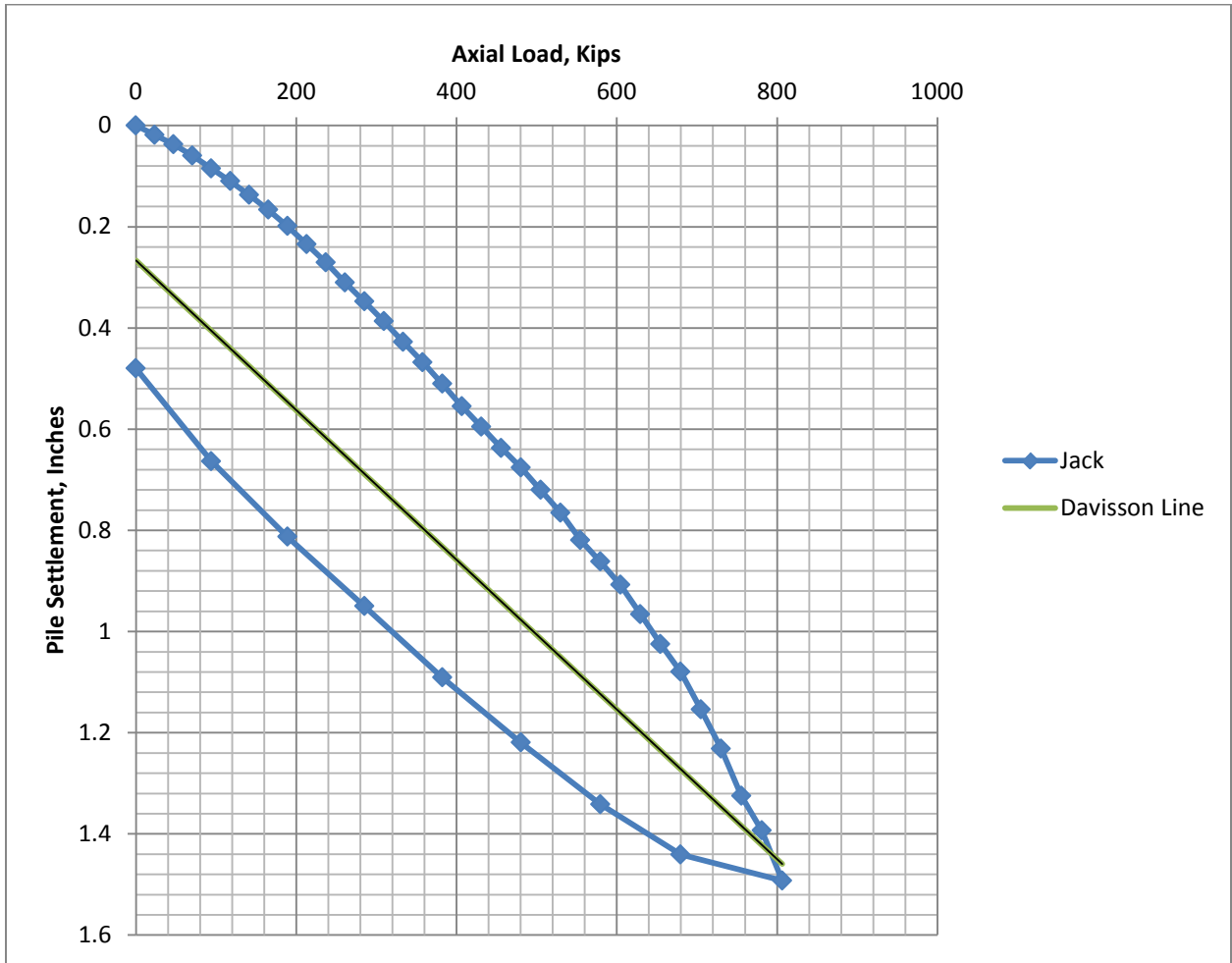


Figure 4.12. Load Settlement curve for load test at Site 2.



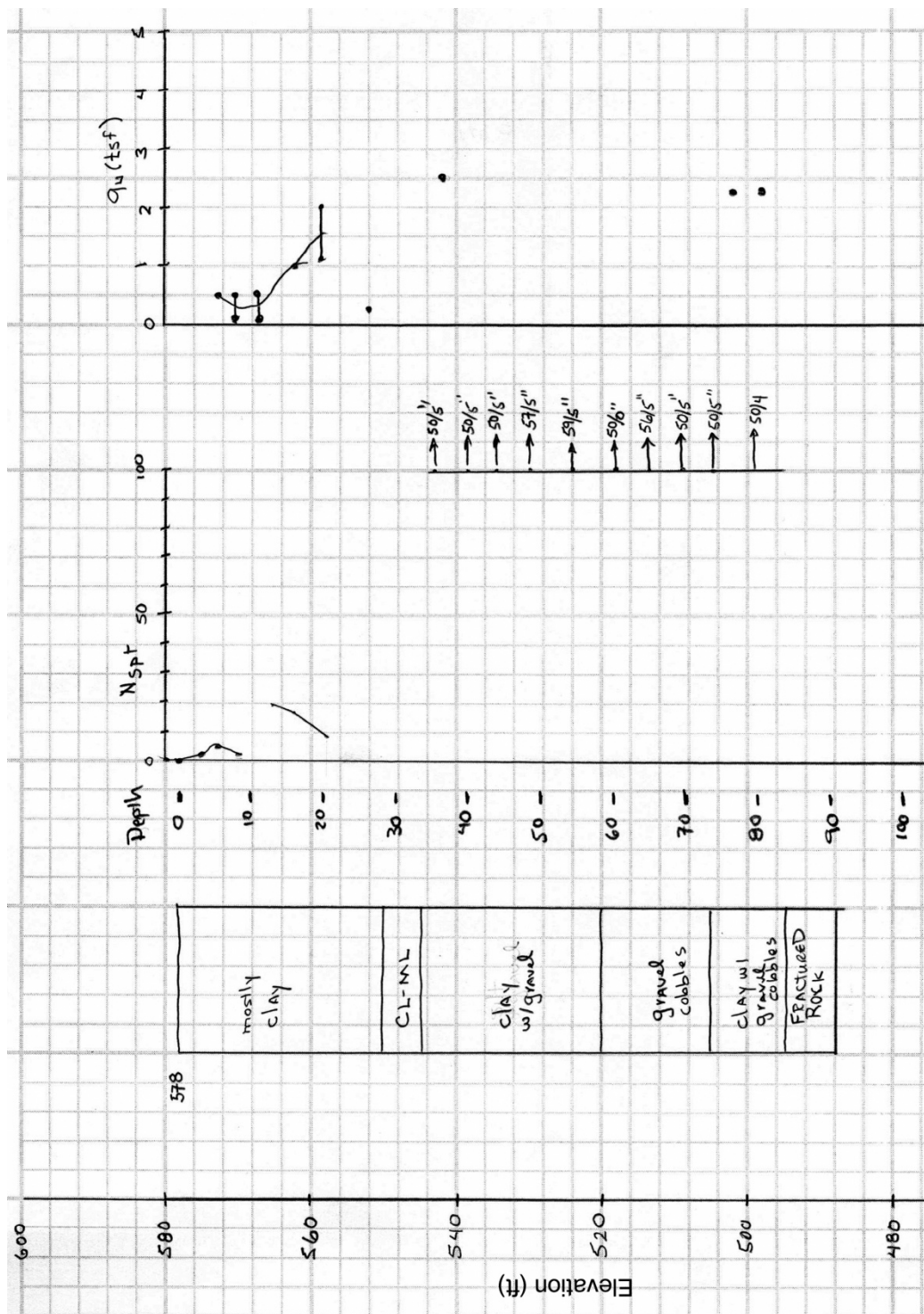


Figure 4.14. Soil profile for Load Test Site 3.

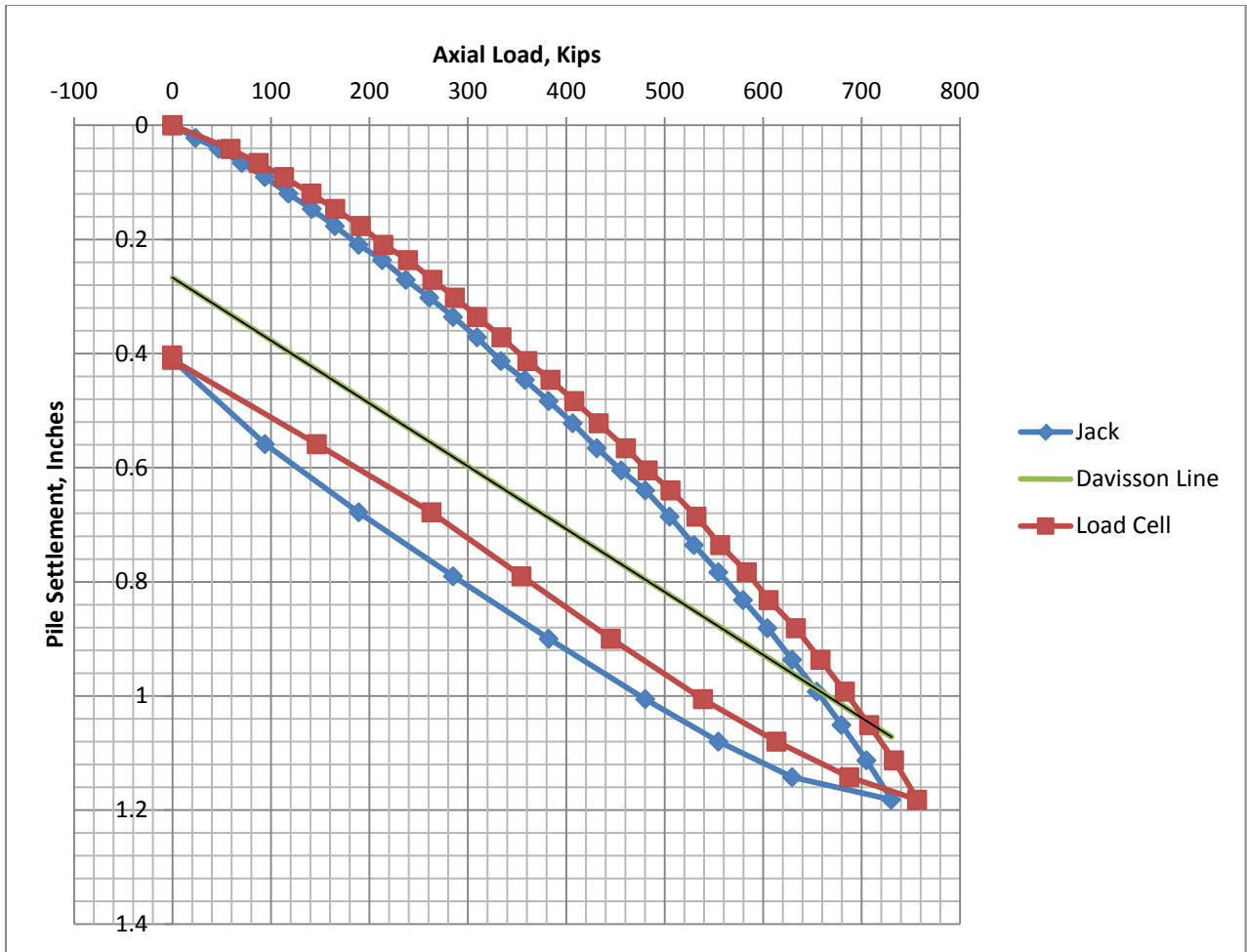


Figure 4.15. Load Settlement curve for load test at Site 3.

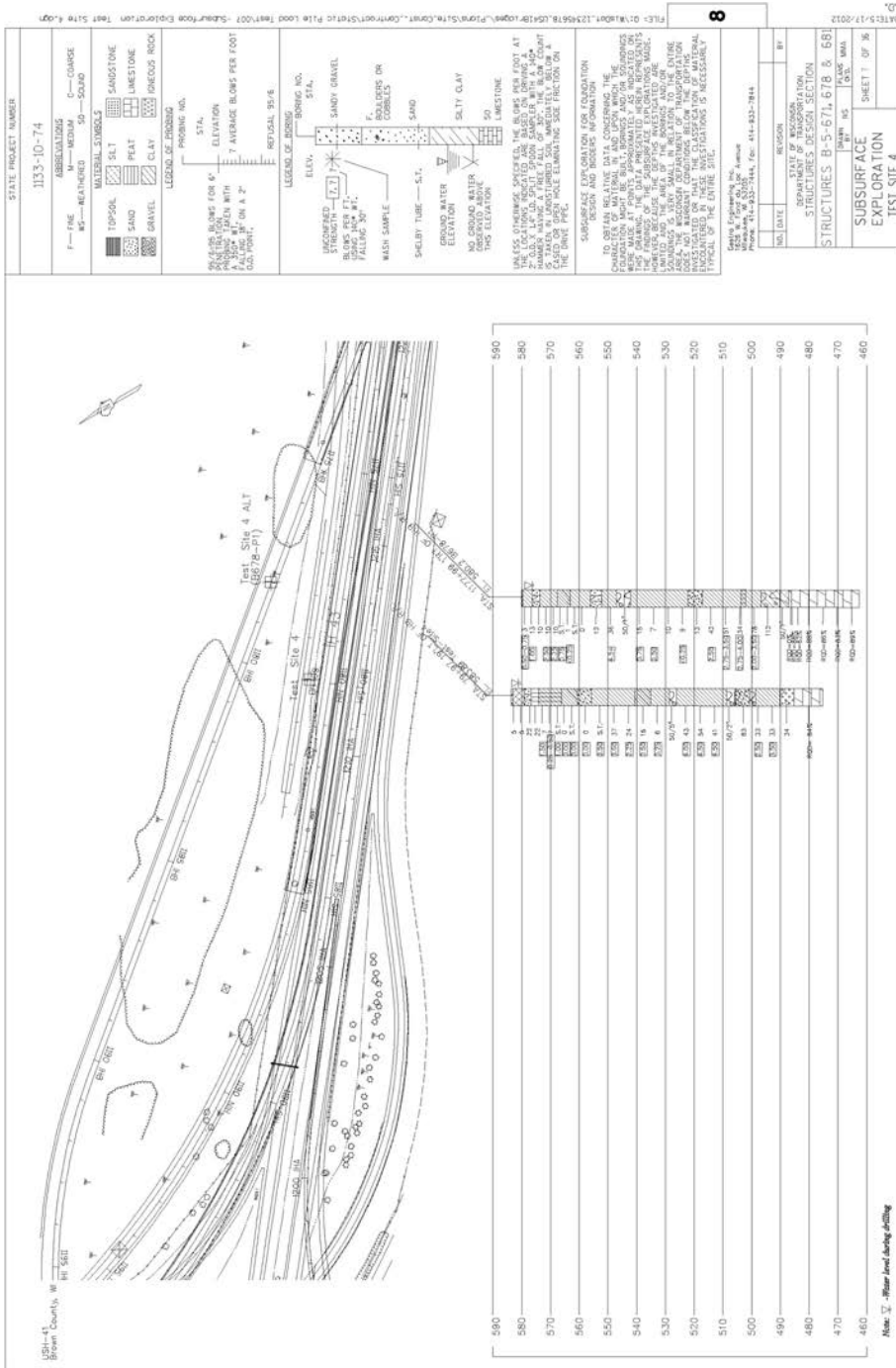


Figure 4.16. Soil Plan View of Site 4, Boring location and Soil Profile.

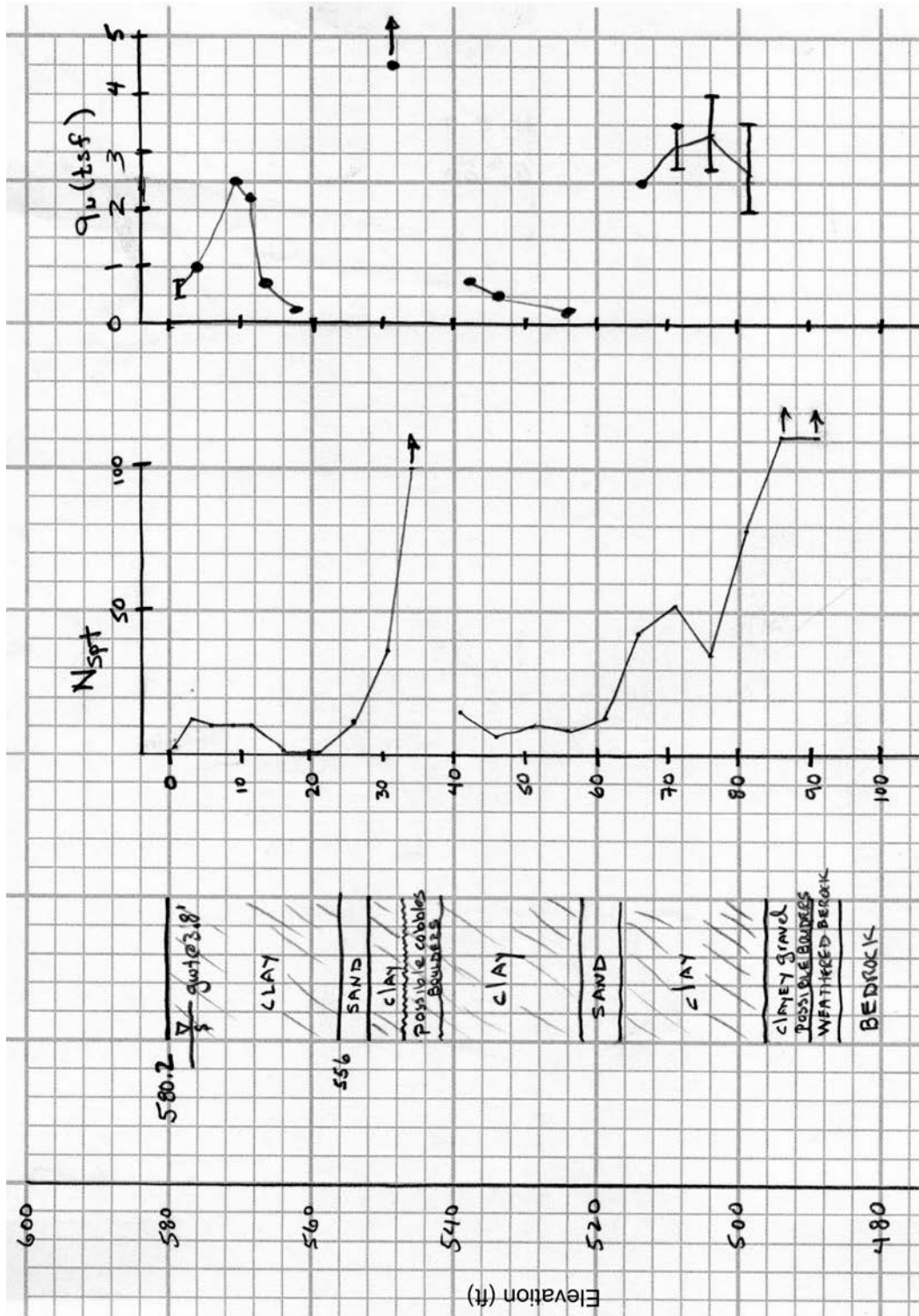


Figure 4.17. Soil profile for Load Test Site 4.

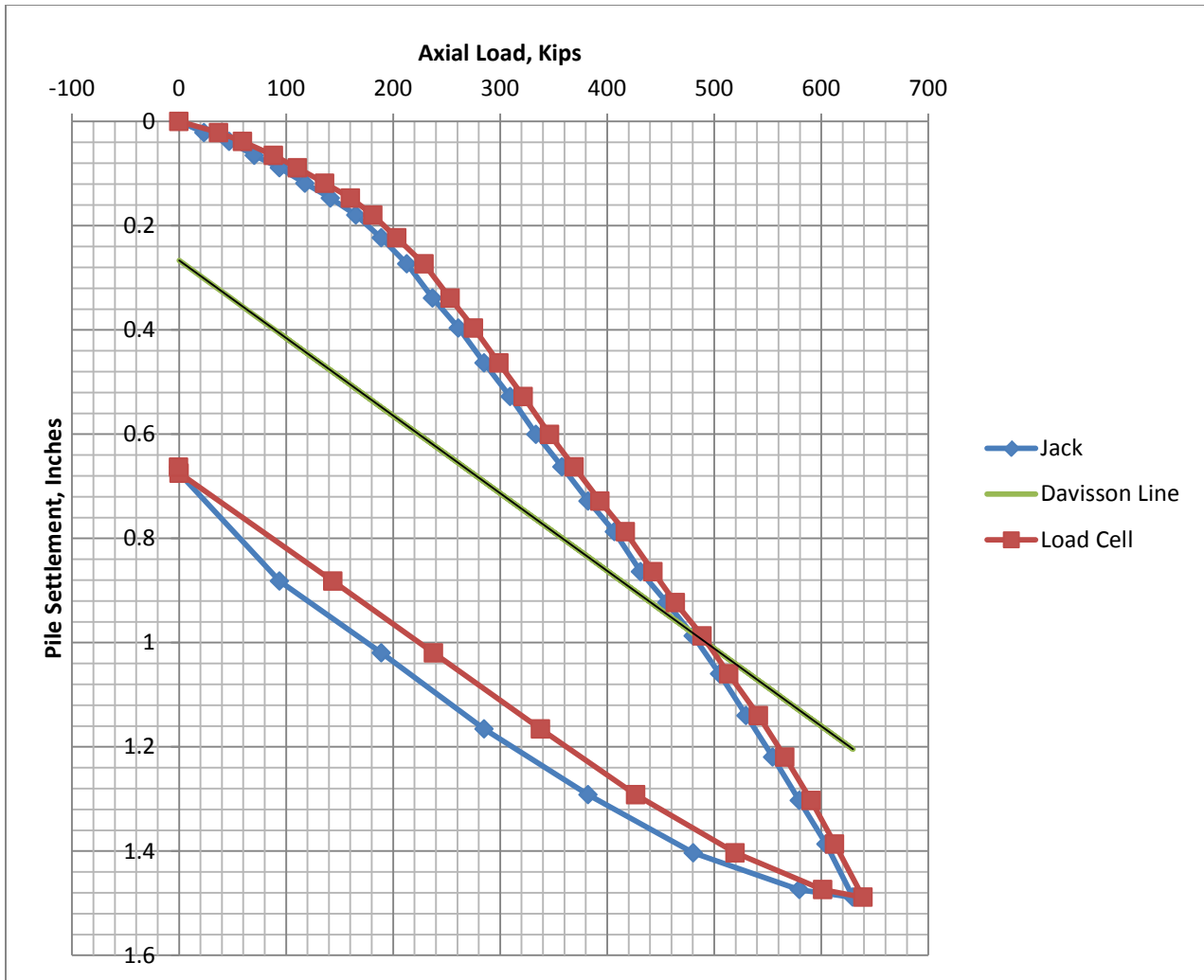


Figure 4.18. Load Settlement curve for load test at Site 4.

# CHAPTER 5 DYNAMIC TESTING OF PRODUCTION PILING

## 5.1 INTRODUCTION

Four additional programs for testing the production piling was implemented by the Wisconsin DOT for the same corridor of construction as reported in the previous two chapters. Each of the four programs monitored piles driven for the foundations of four bridge structures, B-5-671, B-5-678, B-5-679, and B-5-681. The program included dynamic monitoring of the piles with strain gages and accelerometers and interpretation of the results with PDA and CAPWAP. The primary pile driven was an HP 14x73, but some HP 12x53 piles were also driven. Some sites experience damage to the piles during driving and therefore pile shoes were attached to some of the piles being monitored. Three different pile driving hammers were used to drive the production piling: APE D30-32/42, APE D25-32, and a Delmag D30-32.

## 5.2 BRIDGE STRUCTURE B-5-671

The data used from the dynamic pile testing program conducted at bridge structure B-5-671 was collected from a report issued by GRL entitled: "Dynamic Pile Testing Summary Report GRL Job No. 137064, Structure B-5-671, USH 41 NB to IH 43 SB, "Ramp IHA", Brown County, Wisconsin.

A total of 50 piles were tested between September 30, 2013 and January 20, 2014. A summary of select data from the testing program is given in Tables 5.1 and 5.2, and summary figures showing the soil cross-section for each of the bridge pier locations is given in Figs. 5.1 and 5.2.

## 5.3 BRIDGE STRUCTURE B-5-678

The data used from the dynamic pile testing program conducted at bridge structure B-5-678 was collected from a report issued by GRL entitled: "Dynamic Pile Testing Summary Report GRL Job No. 137064, Structure B-5-678, IH 43 NB to USH 41 SB, "Ramp IHB," Brown County, Wisconsin.

A total of 114 piles were tested between October 10, 2013 and February 24, 2014. A summary of select data from the testing program is given in Tables 5.1 and 5.2, and summary figures showing the soil cross-section for each of the bridge pier locations is given in Figs. 5.3 through 5.6.

## 5.4 BRIDGE STRUCTURE B-5-679

The data used from the dynamic pile testing program conducted at bridge structure B-5-679 was collected from a report issued by GRL entitled: "Dynamic Pile Testing Summary Report GRL Job No. 137064, Structure B-5-679, IH 43 NB to USH 41 NB, "Ramp NIH," Brown County, Wisconsin.

A total of 44 piles were tested between November 14, 2013 and January 16, 2014. A summary of select data from the testing program is given in Tables 5.1 and 5.2, and summary figures showing the soil cross-section for each of the bridge pier locations is given in Figs. 5.7 and 5.9.

## 5.5 BRIDGE STRUCTURE B-5-681

The data used from the dynamic pile testing program conducted at bridge structure B-5-681 was collected from a report issued by GRL entitled: "Dynamic Pile Testing Summary Report GRL Job No. 137064, Structure B-5-681, USH 41 NB over Duck Creek, Brown County, Wisconsin.

A total of 49 piles were tested between November 25, 2013 and July 8, 2014. A summary of select data from the testing program is given in Tables 5.1 and 5.2, and summary figures showing the soil cross-section for each of the bridge pier locations is given in Figs. 5.10 and 5.11.

## 5.6 DISCUSSION OF TABLES AND SELECTION OF PILE TESTS

Tables 5.1 and 5.2 include data that were developed for this study. All of the dynamic tests performed on production piles are not included in Tables 5.1 and 5.2 because this study is focused on piles embedded in IGM. Accordingly, piles driven to rock are not included in these tables. Also eliminated are damaged piles and piles that did not have a CAPWAP(BOR) analyses conducted to determine the capacity for beginning of restrike conditions.

The seventh column in Table 5.1 is entitled “Tip Condition in Soil.” This title refers to the location of the tip of the pile relative to the surrounding ground. The tip condition is referred to as “In Soil” (IS) if the pile tip is embedded in soil/IGM and the rock interface is several feet below the tip of the pile. The condition is labelled as “Rock within 2 ft” (R2F) if the rock surface is within 2 ft of the tip of the pile.

The eighth column of Table 5.1 is entitled “Soil Type at Pile Tip” and is identified with symbols representing the mix soil soil at the location of the pile tip. The symbols follow standard conventions, B for boulders, G for gravel, S represents sand, M for silt, and C for clay. Symbols are combined to identify the soil in the ground, with the primary constituent listed first.

The ninth column in Table 5.1 is entitled “Equivalent Nspt at Pile Tip.” This column identifies the resistance recorded with a standard penetration test at the elevation of the pile tip. The value is reported in units of blows per foot (bpf). Several of the Nspt values were reported as a number of blows for a penetration less than the 18 inches normally used to determine Nspt. For example, some reports identified penetration results as fifty blows for 6 inches of penetration. This result was converted to 100 bpf and then entered as the Nspt in this column.

The tenth column identifies the pile type. There are a few cases that used a HP 12x53, but the primary pile was the HP 14x73 section. Some piles were driven with shoes and these are labeled as 14x73(shoe).

Table 5.2 documents additional pile driving details and estimates of total pile capacity as well as end bearing and side capacity for each case. Columns 2 through 5 identify the hammer used, the weight of the ram, and the stroke height, and the permanent set per blow at the end of initial driving. The remaining columns report estimates of capacity. Column 6 identifies the estimate of capacity using dynamic measurements with a pile driving analyzer. Estimates in column 6 are based on end of initial driving data and use the interpretation method identified as Case method with damping factor equal to 0.9. Column 7 is the total pile capacity based on a CAPWAP analysis of the end of driving data. CAPWAP analyses are considered to be more accurate than the Case method for determining pile capacity at the time of driving. The last two columns are also based on end of initial driving data; however, they use simple formulas and simple measurements from columns 3, 4, and 5. Columns 8 and 9 give estimates for side and end bearing capacity for the pile based on CAPWAP analyses and using beginning of restrike behavior.

Table 5.1 Select Pile Information for Production Piling

Pile Ref. No.	Bridge Structure No.	Location	Pile No.	Approx. Pile Tip Elev.	Approx. Pile Pen.	Tip Condition in Soil	Soil Type at Pile Tip	Equiv. Nspt at Pile Tip	Pile Type Size
				(ft)	(ft)			(bpf)	(in)
3	B-5-671	South Abut	7	523.4	64.8	R2F	GSC	400	14x73
7	B-5-671	Pier 1	1	524.2	61.9	R2F	GSM	600	14x73
11	B-5-671	Pier 1	6R2	524.6	61.5	R2F	GSM	600	14x73
20	B-5-671	Pier 2	6	521.5	71.5	IS	GSM	200	14x73
24	B-5-671	Pier 2	32	520.3	72.7	IS	GSM	200	14x73
26	B-5-671	Pier 3	1	533	64.7	IS	M	100	14x73
28	B-5-671	Pier 3	5	530.9	66.8	IS	M	150	14x73
30	B-5-671	Pier 3	16	539.7	58	IS	GSM	46	14x73
32	B-5-671	Pier 3	20	533.7	64	IS	M	70	14x73
34	B-5-671	Pier 4	1	541.9	56.3	IS	GSM	120	14x73
38	B-5-671	Pier 4	32	543.3	54.9	IS	GSM	120	14x73
40	B-5-671	Pier 4	38	541.2	57	IS	GSM	200	14x73
42	B-5-671	Pier 5	1	546.7	45.1	IS	C	104	14x73
44	B-5-671	Pier 5	8	538.3	53.5	IS	BG	200	14x73
46	B-5-671	Pier 5	43	543.8	48	IS	C	104	14x73
48	B-5-671	Pier 5	50	537.8	54	IS	BG	200	14x73
50	B-5-671	Pier 6	1	518.1	59	R2F	BG	600	14x73
57	B-5-671	Pier 6	38	515.7	61.3	R2F	BG	600	14x73
60	B-5-671	Pier 7	1R	510.6	64.8	R2F	SG	146	14x73
64	B-5-671	Pier 7	27	511.7	63.8	R2F	SG	146	14x73
68	B-5-671	Pier 8	1	522.8	53	IS	SM	200	14x73(shoe)
70	B-5-671	Pier 8	6	511.3	64.5	R2F	SM	93	14x73(shoe)
72	B-5-671	Pier 8	27	522.8	53	IS	SM	200	14x73(shoe)
74	B-5-671	Pier 8	32	521.8	54	IS	SM	200	14x73(shoe)
76	B-5-671	Pier 9	1	519.6	56.1	IS	GSC	200	14x73
78	B-5-671	Pier 9	6	520.7	55	IS	GSC	200	14x73
80	B-5-671	Pier 9	27	522.7	53	IS	GSC	200	14x73
82	B-5-671	Pier 9	32	521.2	54.5	IS	GSC	200	14x73
84	B-5-671	Pier 10	1	520.4	55.6	IS	GSC	300	14x73
86	B-5-671	Pier 10	6	519.1	56.9	IS	GSC	300	14x73
92	B-5-671	East Abut	1	513.4	68	IS	SM	75	14x73
96	B-5-671	East Abut	14	513.4	68	IS	SM	75	14x73

Table 5.1 continued. Select Pile Information for Production Piling

Pile Ref. No.	Bridge Structure No.	Location	Pile No.	Approx. Pile Tip Elev.	Approx. Pile Pen.	Tip Condition in Soil	Soil Type at Pile Tip	Equiv. Nspt at Pile Tip	Pile Type Size
				(ft)	(ft)				(bpf)
115	B-5-678	Pier 2	5	516.4	57.7	IS	GSC	62	14x73
117	B-5-678	Pier 2	17	521.7	52.4	IS	GSC	106	14x73
127	B-5-678	Pier 3	15	497.1	77.8	IS	GSC	74	14x73
132	B-5-678	Pier 4	1	501.3	74.5	IS	SM	120	14x73
135	B-5-678	Pier 4	16	498.8	77.0	IS	SM	120	14x73
137	B-5-678	Pier 4	20	498.2	77.6	IS	SM	120	14x73
140	B-5-678	Pier 5	1R	493.3	81.7	IS	GSC	180	14x73
142	B-5-678	Pier 5	5	495.5	79.5	IS	GSC	180	14x73
144	B-5-678	Pier 5	16	501	74.0	IS	GSC	180	14x73
147	B-5-678	Pier 5	20R	497	78.0	IS	GSC	180	14x73
152	B-5-678	Pier 6	5	501.7	72.8	IS	GSC	120	14x73
161	B-5-678	Pier 7	5	511.4	62.1	IS	GSC	120	14x73
163	B-5-678	Pier 7	21	513.3	60.2	IS	GSC	108	14x73
166	B-5-678	Pier 7	25	504.3	69.2	IS	GSC	108	14x73
168	B-5-678	Pier 8	1	515.4	58.0	IS	BG	300	14x73
174	B-5-678	Pier 8	20	515.9	57.5	IS	BG	300	14x73
176	B-5-678	Pier 9	1	515.8	57.5	IS	GSC	120	14x73
178	B-5-678	Pier 9	5	514.8	58.5	IS	GSC	120	14x73
180	B-5-678	Pier 9	16	515.7	57.6	IS	GSC	120	14x73
182	B-5-678	Pier 9	20	513.6	59.7	IS	GSC	120	14x73
184	B-5-678	Pier 10	1	510.6	63.2	IS	GM	120	14x73
186	B-5-678	Pier 10	6	511.8	62.0	IS	GM	120	14x73
188	B-5-678	Pier 10	23	512.9	60.9	IS	GM	120	14x73
190	B-5-678	Pier 10	28	512.6	61.2	IS	GM	120	14x73
196	B-5-678	Pier 11	26	506.9	67.0	IS	GSC	110	14x73(shoe)
203	B-5-678	Pier 12	1R3	510.3	63.2	IS	GM	106	14x73
205	B-5-678	Pier 12	5	511.5	62.0	IS	GM	106	14x73
207	B-5-678	Pier 12	26	512.5	61.0	IS	GM	106	14x73
211	B-5-678	Pier 12	30R2	509.5	64.0	IS	GM	106	14x73(shoe)
213	B-5-678	Pier 13	1	504.7	70.2	R2F	G	150	14x73
216	B-5-678	Pier 13	5R	506.2	68.7	R2F	G	150	14x73
220	B-5-678	Pier 13	26	504.3	70.6	R2F	G	150	14x73
222	B-5-678	Pier 13	30	506.2	68.7	R2F	G	150	14x73

Table 5.1 continued. Select Pile Information for Production Piling

Pile Ref. No.	Bridge Structure No.	Location	Pile No.	Approx. Pile Tip Elev.	Approx. Pile Pen.	Tip Condition in Soil	Soil Type at Pile Tip	Equiv. Nspt at Pile Tip	Pile Type Size
				(ft)	(ft)			(bpf)	(in)
224	B-5-678	Pier 14	1	511.4	61.4	IS	GSC	104	14x73
226	B-5-678	Pier 14	7	512.5	60.3	IS	GSC	104	14x73
228	B-5-678	Pier 14	43	505.3	67.5	R2F	B	1000	14x73
230	B-5-678	Pier 14	49	507.8	65.0	R2F	B	1000	14x73
232	B-5-678	Pier 15	1	512.4	65.8	R2F	BG	600	14x73
234	B-5-678	Pier 15	6	512.2	66.0	R2F	BG	600	14x73
236	B-5-678	Pier 15	24	509	69.2	R2F	BG	600	14x73
238	B-5-678	Pier 15	25	509.6	68.6	R2F	BG	600	14x73
240	B-5-678	Pier 16	2	506.9	69.2	R2F	SG	150	14x73
244	B-5-678	Pier 16	5R2	507.3	68.8	R2F	SG	150	14x73
246	B-5-678	Pier 16	31	505.4	70.7	R2F	SG	150	14x73
249	B-5-678	Pier 16	36R	507.9	68.2	R2F	SG	150	14x73
252	B-5-678	Pier 17	1R	512.3	78.3	IS	SG	120	14x73(shoe)
254	B-5-678	Pier 17	7	510	80.5	R2F	GS	600	14x73
258	B-5-678	Pier 17	49	508.9	81.6	R2F	GS	600	14x73(shoe)
262	B-5-678	Pier 18	8	525.8	50.0	IS	SM	100	14x73
266	B-5-678	Pier 18	39	520.7	55.1	IS	BG	200	14x73
270	B-5-678	Pier 19	31	523.3	65.0	IS	GSM	110	14x73
272	B-5-678	Pier 19	36	521.3	67.0	IS	GSM	110	14x73
274	B-5-678	Pier 20	1	525.4	63.2	IS	SM	85	14x73
278	B-5-678	Pier 20	31	528.6	60.0	IS	SM	75	14x73
282	B-5-678	Pier 21	1	536.3	40.0	IS	GSC	60	14x73
284	B-5-678	Pier 21	6	523.2	53.1	IS	SM	85	14x73
290	B-5-678	Pier 21	36R	523.9	52.4	IS	SM	85	14x73
292	B-5-678	Pier 22	1	525.1	51.6	IS	G	80	14x73
294	B-5-678	Pier 22	6	524.2	52.5	IS	G	80	14x73
296	B-5-678	Pier 22	31	526.6	50.1	IS	G	80	14x73
298	B-5-678	Pier 22	36	525.5	51.2	IS	G	80	14x73
302	B-5-678	West Abut	9	524.7	81.0	IS	SG	250	14x73
304	B-5-678	West Abut	18	523.6	82.2	IS	SG	250	14x73
306	B-5-679	South Abut	2	499.1	92.8	R2F	G	116	14x73
310	B-5-679	South Abut	7	499	92.9	R2F	G	116	14x73
315	B-5-679	Pier 1	6	505.8	69.1	IS	SM	135	14x73(shoe)
317	B-5-679	Pier 1	27	501.9	73.0	R2F	SM	150	14x73(shoe)

Table 5.1 continued. Select Pile Information for Production Piling

Pile Ref. No.	Bridge Structure No.	Location	Pile No.	Approx. Pile Tip Elev.	Approx. Pile Pen.	Tip Condition in Soil	Soil Type at Pile Tip	Equiv. Nspt at Pile Tip	Pile Type Size
				(ft)	(ft)				
319	B-5-679	Pier 1	32	505.9	69.0	IS	SM	135	14x73(shoe)
321	B-5-679	Pier 2	1	515.9	58.7	IS	B	300	14x73(shoe)
323	B-5-679	Pier 2	6	516.3	58.3	IS	B	300	14x73(shoe)
325	B-5-679	Pier 2	27	516.1	58.5	IS	B	300	14x73(shoe)
327	B-5-679	Pier 2	32	516.3	58.3	IS	B	300	14x73(shoe)
329	B-5-679	Pier 3	1	512.9	62.0	IS	GSC	600	14x73
331	B-5-679	Pier 3	6	513.9	61.0	IS	GSC	600	14x73
333	B-5-679	Pier 3	27	513.9	61.0	IS	GSC	600	14x73
335	B-5-679	Pier 3	32	513.9	61.0	IS	GSC	600	14x73
337	B-5-679	Pier 4	1	508.9	65.8	IS	M	150	14x73(shoe)
339	B-5-679	Pier 4	6	506.1	68.6	IS	M	150	14x73(shoe)
341	B-5-679	Pier 4	27	509.7	65.0	IS	M	150	14x73(shoe)
344	B-5-679	Pier 4	32R	514.7	60.0	IS	M	150	14x73(shoe)
346	B-5-679	Pier 5	1	510.2	65.1	IS	G	124	14x73
348	B-5-679	Pier 5	6	515.8	59.5	IS	SM	200	14x73
350	B-5-679	Pier 5	27	511.3	64.0	IS	G	124	14x73
352	B-5-679	Pier 5	32	517.2	58.1	IS	SM	120	14x73
355	B-5-679	Pier 6	1R	519	59.0	IS	GS	300	14x73(shoe)
357	B-5-679	Pier 6	6	519.9	58.1	IS	GS	300	14x73(shoe)
360	B-5-679	Pier 6	27	508	70.0	IS	GS	600	14x73(shoe)
362	B-5-679	Pier 6	32	508	70.0	IS	GS	600	
365	B-5-679	Pier 7	1	510	67.6	IS	GC	112	14x73(shoe)
369	B-5-679	Pier 7	27	511.5	66.1	IS	GC	112	14x73
371	B-5-679	Pier 7	32	530.6	47.0	IS	GC	150	14x73
373	B-5-679	Pier 8	1	518	57.9	IS	GC	100	14x73
375	B-5-679	Pier 8	6	526.4	49.5	IS	GC	120	14x73
397	B-5-681	South Abut	14	537.4	81.3	IS	GSC	99	14x73
403	B-5-681	Pier 1	Footing3#9	510.4	76.0	R2F	GSC	600	14x73
407	B-5-681	Pier 2	Footing1#1	508.8	77.0	IS	SM	125	14x73
409	B-5-681	Pier 2	Footing1#9	508.8	77.0	IS	SM	125	14x73
412	B-5-681	Pier 2	Footing3#4	512.7	73.1	IS	SM	125	14x73
415	B-5-681	Pier 2	Footing3#12	511.8	74.0	IS	SM	125	14x73

Table 5.1 continued. Select Pile Information for Production Piling

Pile Ref. No.	Bridge Structure No.	Location	Pile No.	Approx. Pile Tip Elev.	Approx. Pile Pen.	Tip Condition in Soil	Soil Type at Pile Tip	Equiv. Nspt at Pile Tip	Pile Type Size
				(ft)	(ft)			(bpf)	(in)
417	B-5-681	Pier 3	Footing1#1	512.8	67.1	IS	SM	140	14x73
419	B-5-681	Pier 3	Footing1#9	513.9	66.0	IS	SC	150	14x73
421	B-5-681	Pier 3	Footing3#4	509.7	70.2	IS	SM	140	14x73
424	B-5-681	Pier 3	Footing3#12R	511.9	68.0	IS	SM	140	14x73
426	B-5-681	Pier 4	Footing1#1	497.2	79.3	R2F	SM	300	14x73(shoe)
428	B-5-681	Pier 4	Footing1#7	499.9	76.6	R2F	SM	300	14x73(shoe)
430	B-5-681	Pier 5	Footing1#1	498.8	77.9	R2F	SM	106	14x73(shoe)
433	B-5-681	Pier 5	Footing1#13R	499.7	77.0	R2F	SM	106	14x73(shoe)
439	B-5-681	Pier 6	Footing1#1	497.5	79.6	R2F	GSC	130	14x73(shoe)
456	B-5-681	Pier 8	Footing1#5	517.1	58.3	IS	GS	200	14x73
458	B-5-681	Pier 8	Footing1#9	516.6	58.8	IS	GS	200	14x73
460	B-5-681	Pier 8	Footing3#8	509.4	66.0	IS	GS	114	14x73
464	B-5-681	Pier 9	Footing1#1	522.8	49.0	IS	G	600	14x73
466	B-5-681	Pier 9	Footing1#9	523.4	48.4	IS	G	600	14x73
470	B-5-681	Pier 9	Footing3#12	515.2	55.9	IS	G	600	14x73
473	B-5-681	Pier 10	Footing1#10R	505.7	65.6	IS	GSC	120	14x73
475	B-5-681	Pier 10	Footing2#1	509.5	61.3	IS	GSC	120	14x73
479	B-5-681	North Abut	2	531.3	55.3	IS	GSC	118	12x53
481	B-5-681	North Abut	9	538.1	48.5	IS	GSC	106	12x53
483	B-5-681	North Abut	14	523.3	63.3	IS	SG	150	12x53

Table 5.2. Select Pile Information for Production Piling

Pile Ref. No.	Pile Hammer	Weight of Ram	Approx. Stroke Ht. at EOD	Pile Set at EOD	Average Total Case Cap. RX9	CW EOD Total Cap	CW BOR Toe Cap	CW BOR Total Cap	FHWA Modified Gates Cap	Washington DOT Cap
		(kips)	(ft)	(in)	(kips)	(kips)	(kips)	(kips)	(kips)	(kips)
3	APE D30-32	6.615	9.1	0.125	585	617	510	702	717	818
7	Delmag D30-32	6.615	9.1	0.160	529	597	360	649	671	772
11	Delmag D30-32	6.615	9.6	0.025	764	718	550	724	1048	1180
20	APE D30-42	6.615	10.0	0.050	685	664	510	719	936	1087
24	APE D30-42	6.615	10.1	0.088	684	698	444	723	831	982
26	APE D30-42	6.615	9.8	0.088	526	546	415	571	817	953
28	APE D30-42	6.615	9.8	0.088	596	626	515	664	817	953
30	APE D30-42	6.615	9.4	0.188	549	556	430	612	654	767
32	APE D30-42	6.615	9.8	0.088	527	539	398	579	817	953
34	APE D25-32	5.512	8.5	0.095	534	542	415	533	666	676
38	APE D25-32	5.512	8.4	0.085	524	493	390	516	679	685
40	APE D25-32	5.512	8.4	0.075	482	495	365	510	700	703
42	APE D30-32	6.615	8.9	0.279	642	575	340	593	560	654
44	APE D30-32	6.615	9.0	0.171	577	582	350	594	654	751
46	APE D30-32	6.615	9.0	0.182	622	610	402	635	643	740
48	APE D30-42	6.615	8.5	0.194	599	581	370	682	611	688
50	APE D30-32	6.615	8.9	0.056	525	476	225	532	855	946
57	APE D30-32	6.615	9.1	0.119	542	530	318	546	727	828
60	APE D30-32	6.615	8.2	0.075	689	707	590	706	766	823
64	APE D30-32	6.615	7.6	0.125	594	626	455	641	647	683
68	APE D30-32	6.615	8.8	0.100	579	598	380	583	744	832
70	APE D30-32	6.615	9.7	0.025	681	714	475	690	1053	1193
72	APE D30-32	6.615	8.8	0.100	555	568	370	540	744	832
74	APE D30-32	6.615	8.8	0.150	523	541	350	524	670	758
76	APE D30-32	6.615	8.3	0.100	520	542	430	582	720	784
78	APE D30-32	6.615	8.1	0.112	532	526	390	569	690	746
80	APE D30-32	6.615	7.9	0.174	540	526	435	549	604	657
82	APE D30-32	6.615	8.2	0.112	555	567	400	586	695	756
84	APE D30-32	6.615	8.3	0.100	599	626	435	644	720	784
86	APE D30-32	6.615	7.6	0.125	579	584	395	597	647	683

Table 5.2 continued. Select Pile Information for Production Piling

<b>Pile Ref. No.</b>	<b>Pile Hammer</b>	<b>Weight of Ram</b>	<b>Approx. Stroke Ht. at EOD</b>	<b>Pile Set at EOD</b>	<b>Average Total Case Cap. RX9</b>	<b>CW EOD Total Cap</b>	<b>CW BOR Toe Cap</b>	<b>CW BOR Total Cap</b>	<b>FHWA Modified Gates Cap</b>	<b>Washington DOT Cap</b>
		<b>(kips)</b>	<b>(ft)</b>	<b>(in)</b>	<b>(kips)</b>	<b>(kips)</b>	<b>(kips)</b>	<b>(kips)</b>	<b>(kips)</b>	<b>(kips)</b>
92	APE D30-32	6.615	8.9	0.150	577	600	450	684	674	767
96	APE D30-32	6.615	7.8	0.063	547	573	340	566	776	812
115	APE D30-32	6.615	9.4	0.279	545	538	225	624	578	690
117	APE D30-32	6.615	8.9	0.197	551	510	255	571	624	717
127	APE D30-32	6.615	8.8	0.088	554		315	582	769	855
132	APE D30-32	6.615	9.6	0.100	511	527	250	549	782	907
135	APE D30-32	6.615	9.4	0.075	513	528	285	558	827	944
137	APE D30-32	6.615	9.7	0.100	512	572	342	632	787	917
140	APE D30-32	6.615	8.9	0.174	483	506	335	563	647	740
142	APE D30-32	6.615	8.5	0.097	417	482	320	576	736	809
144	APE D30-32	6.615	9.4	0.150	546	525	355	602	696	810
147	APE D30-32	6.615	9.3	0.088	483	517	262	567	793	904
152	APE D30-32	6.615	9.8	0.075	538	582	435	591	847	984
161	APE D30-32	6.615	9.5	0.130	621	578	380	593	727	846
163	APE D30-32	6.615	9.4	0.112	655	632	410	561	751	866
166	APE D30-32	6.615	8.9	0.162	541		325	543	660	753
168	APE D30-32	6.615	10.1	0.100	701	691	540	702	805	954
174	APE D30-32	6.615	9.9	0.100	704	728	495	701	796	936
176	APE D30-32	6.615	8.3	0.100	606	613	502	671	720	784
178	APE D30-32	6.615	8.5	0.100	594	594	531	668	730	803
180	APE D30-32	6.615	8.4	0.100	607	609	508	663	725	794
182	APE D30-32	6.615	8.8	0.088	567	561	450	609	769	855
184	APE D30-32	6.615	8.2	0.088	488		420	565	739	797
186	APE D30-32	6.615	8.5	0.050	545	549	450	667	855	924
188	APE D30-32	6.615	9.0	0.050	615	616	510	669	883	978
190	APE D30-32	6.615	8.5	0.100	617	631	500	763	730	803
196	APE D30-32	6.615	8.6	0.050	526	524	270	579	860	935
203	APE D30-32	6.615	8.5	0.088	563	586	405	592	754	826
205	APE D30-32	6.615	9.2	0.100	594	609	333	647	763	869
207	APE D30-32	6.615	9.3	0.174	567	591	298	578	664	773

Table 5.2 continued. Select Pile Information for Production Piling

<b>Pile Ref. No.</b>	<b>Pile Hammer</b>	<b>Weight of Ram</b>	<b>Approx. Stroke Ht. at EOD</b>	<b>Pile Set at EOD</b>	<b>Average Total Case Cap. RX9</b>	<b>CW EOD Total Cap</b>	<b>CW BOR Toe Cap</b>	<b>CW BOR Total Cap</b>	<b>FHWA Modified Gates Cap</b>	<b>Washington DOT Cap</b>
		<b>(kips)</b>	<b>(ft)</b>	<b>(in)</b>	<b>(kips)</b>	<b>(kips)</b>	<b>(kips)</b>	<b>(kips)</b>	<b>(kips)</b>	<b>(kips)</b>
211	APE D30-32	6.615	8.9	0.162	617	573	327	689	660	753
213	APE D30-32	6.615	8.1	0.112	612	565	390	532	690	746
216	APE D30-32	6.615	7.2	0.000	537	529	375	520	2192	2041
220	APE D30-32	6.615	7.8	0.025	570	574	386	526	934	959
222	APE D30-32	6.615	7.3	0.038	548	508	410	537	833	837
224	APE D30-32	6.615	8.8	0.333	536	550	440	559	524	614
226	APE D30-32	6.615	9.5	0.200	602	620	470	613	645	763
228	APE D30-32	6.615	9.5	0.250	621	612	455	681	603	719
230	APE D30-32	6.615	10.1	0.150	759	748	560	724	725	870
232	APE D30-32	6.615	9.8	0.250	620	650	395	564	614	742
234	APE D30-32	6.615	10.9	0.050	696	695	460	629	981	1185
236	APE D30-32	6.615	10.9	0.112	710	724	400	615	816	1004
238	APE D30-32	6.615	10.3	0.235	604	600	380	514	644	792
240	Delmag D30-32	6.615	8.1	0.080	516	587	388	591	749	803
244	Delmag D30-32	6.615	8.2	0.100	519	549	425	543	715	775
246	Delmag D30-32	6.615	8.8	0.075	541	571	334	518	797	884
249	Delmag D30-32	6.615	8.2	0.088	565	570	440	572	739	797
252	APE D30-32	6.615	9.4	0.444	561		350	538	490	601
254	DELMAG D30-32	6.615	9.4	0.353	575	523	355	567	534	645
258	DELMAG D30-32	6.615	8.9	0.444	525	423	305	452	474	569
262	APE D30-32	6.615	8.9	0.226	680	697	500	698	599	692
266	APE D30-42	6.615	8.9	0.353	613	611	400	683	517	611
270	APE D30-32	6.615	9.8	0.200	601	592	475	638	657	787
272	APE D30-32	6.615	9.4	0.324	517	531	428	599	550	661
274	APE D30-32	6.615	8.8	0.138	520	526	460	571	685	774
278	APE D30-32	6.615	8.3	0.174	517	521	390	518	622	690
282	APE D30-32	6.615	8.4	0.174	539	543	470	536	626	698
284	APE D30-32	6.615	8.5	0.162	555	578	385	567	643	719
290	APE D30-32	6.615	8.5	0.188	512	518	390	567	617	694
292	DELMAG D30-32	6.615	9.8	0.112	626	601	540	627	769	903

Table 5.2 continued. Select Pile Information for Production Piling

Pile Ref. No.	Pile Hammer	Weight of Ram	Approx. Stroke Ht. at EOD	Pile Set at EOD	Average Total Case Cap. RX9	CW EOD Total Cap	CW BOR Toe Cap	CW BOR Total Cap	FHWA Modified Gates Cap	Washington DOT Cap
		(kips)	(ft)	(in)	(kips)	(kips)	(kips)	(kips)	(kips)	(kips)
294	DELMAG D30-32	6.615	10.8	0.112	746	743	650	730	812	995
296	DELMAG D30-32	6.615	10.8	0.063	774	736	690	782	931	1125
298	DELMAG D30-32	6.615	10.6	0.112	704	706	550	652	804	977
302	DELMAG D30-32	6.615	7.7	0.025	596	543	360	549	928	947
304	DELMAG D30-32	6.615	9.1	0.038	615	601	365	506	942	1043
306	APE D30-42	6.615	8.2	0.025	534	560	406	552	961	1008
310	APE D30-42	6.615	8.3	0.075	466	511	387	531	771	833
315	APE D30-32	6.615	8.1	0.025	522	557	450	610	954	996
317	APE D30-32	6.615	8.5	0.063	540	566	400	599	815	885
319	APE D30-32	6.615	8.5	0.100	517	543	395	544	730	803
321	APE D30-42	6.615	8.4	0.100	630	584	457	605	725	794
323	APE D30-42	6.615	8.7	0.125	608	550	405	574	699	782
325	APE D30-42	6.615	8.7	0.075	674	617	478	650	792	873
327	APE D30-42	6.615	8.4	0.100	628	594	430	604	725	794
329	APE D30-42	6.615	8.5	0.188	555	551	480	606	617	694
331	APE D30-42	6.615	8.5	0.138	574	575	486	617	672	747
333	APE D30-42	6.615	8.6	0.150	565	564	480	612	661	741
335	APE D30-42	6.615	9.0	0.112	620	632	490	616	733	829
337	APE D30-42	6.615	9.0	0.125	639	664	447	579	713	809
339	APE D30-42	6.615	8.4	0.112	518	531	390	519	704	774
341	APE D30-42	6.615	9.2	0.138	510	533	319	473	703	809
344	APE D30-42	6.615	9.1	0.100	582	501	390	530	759	860
346	APE D30-32	6.615	7.6	0.162	551	547	420	584	602	643
348	APE D30-32	6.615	8.3	0.174	587	551	380	522	622	690
350	APE D30-32	6.615	7.9	0.174	561	565	399	566	604	657
352	APE D30-32	6.615	7.9	0.125	596	596	412	583	661	710
355	APE D30-32	6.615	8.9	0.174	550	527	410	593	647	740
357	APE D30-32	6.615	9.9	0.125	625	603	550	655	752	890
360	APE D30-32	6.615	9.2	0.174	633	587	475	586	660	765
362	APE D30-32	6.615	9.6	0.125	636	675	620	699	739	863

Table 5.2 continued. Select Pile Information for Production Piling

Pile Ref. No.	Pile Hammer	Weight of Ram	Approx. Stroke Ht. at EOD	Pile Set at EOD	Average Total Case Cap. RX9	CW EOD Total Cap	CW BOR Toe Cap	CW BOR Total Cap	FHWA Modified Gates Cap	Washington DOT Cap
		(kips)	(ft)	(in)	(kips)	(kips)	(kips)	(kips)	(kips)	(kips)
365	APE D30-32	6.615	10.0	0.025	614	676	465	716	1071	1229
369	APE D30-32	6.615	9.1	0.013	480	531	425	582	1146	1248
371	APE D30-32	6.615	9.6	0.063	610	641	540	664	872	1000
373	APE D30-32	6.615	10.2	0.088	599	606	530	658	835	992
375	APE D30-32	6.615	9.3	0.125	558	590	480	605	726	836
397	APE D30-32	6.615	6.0	0.387	230	273	130	388	392	400
403	APE D30-32	6.615	9.8	0.088	605	640	470	678	817	953
407	APE D30-32	6.615	8.6	0.174	553	570	330	560	634	715
409	APE D30-32	6.615	8.2	0.150	530	561	420	539	643	707
412	APE D30-32	6.615	8.4	0.088	557	601	420	580	749	817
415	APE D30-32	6.615	9.2	0.150	570	598	326	579	687	793
417	APE D30-32	6.615	9.0	0.214	556	518	500	579	613	710
419	APE D30-32	6.615	9.0	0.200	590	581	468	571	625	722
421	APE D30-32	6.615	8.9	0.226	533	538	460	596	599	692
424	APE D30-32	6.615	9.4	0.200	631	631	545	660	641	755
426	APE D30-32	6.615	9.1	0.273	713	718	640	747	572	673
428	APE D30-32	6.615	10.5	0.250	814	801	700	838	639	795
430	APE D30-32	6.615	9.4	0.300	614	592	555	648	565	676
433	APE D30-32	6.615	9.3	0.250	698	662	600	683	595	704
439	APE D30-32	6.615	9.8	0.250	646	632	570	654	614	742
456	APE D30-42	6.615	9.3	0.316	550	568	430	555	551	659
458	APE D30-42	6.615	9.0	0.324	518	538	400	541	536	633
460	APE D30-42	6.615	9.0	0.273	574	559	450	578	568	665
464	APE D30-42	6.615	9.8	0.200	684	670	550	654	657	787
466	APE D30-42	6.615	9.4	0.214	613	584	517	661	628	741
470	APE D30-42	6.615	9.3	0.250	581	554	413	558	595	704
473	APE D30-42	6.615	9.1	0.353	665	662	570	648	524	624
475	APE D30-42	6.615	8.9	0.400	524	577	480	557	494	588
479	APE D30-42	6.615	6.3	0.226	389	377	283	369	488	490
481	APE D30-42	6.615	6.4	0.300	421	410	350	420	448	461
483	APE D30-42	6.615	6.2	0.400	356	364	245	311	395	410



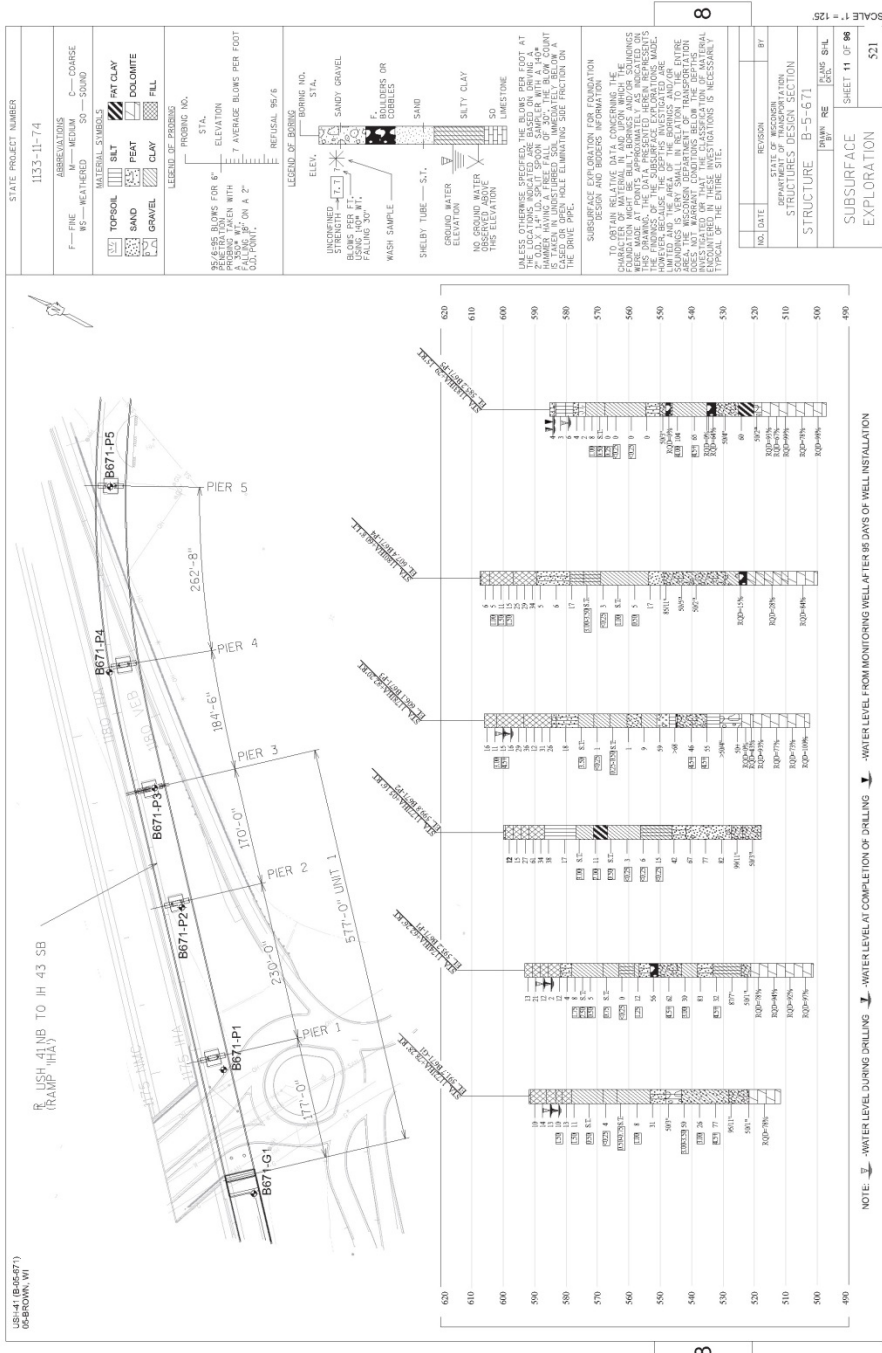


Figure 5.2 Soil profile for Bridge Structure Number B-5-671.

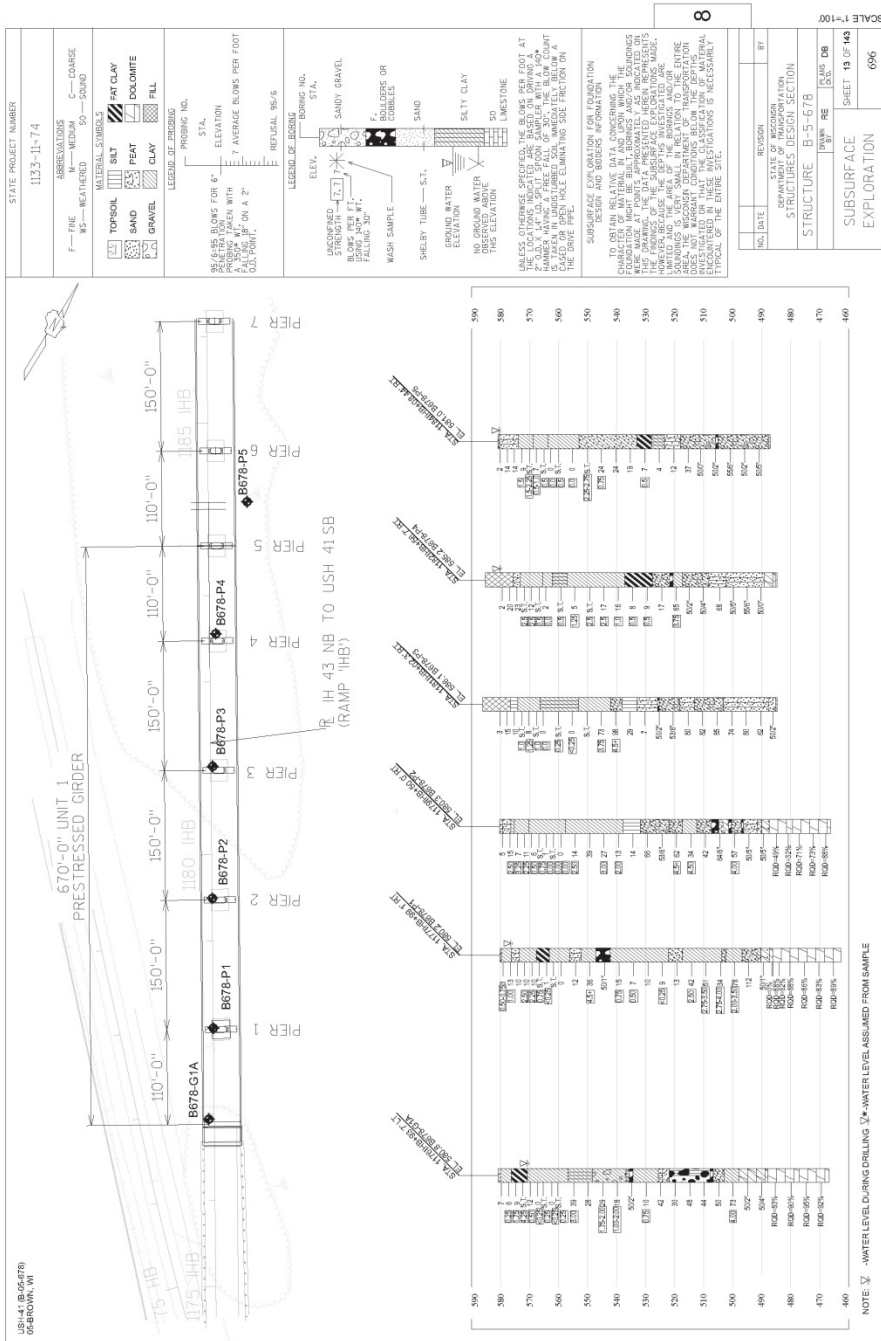


Figure 5.3 Soil profile for Bridge Structure Number B-5-678.





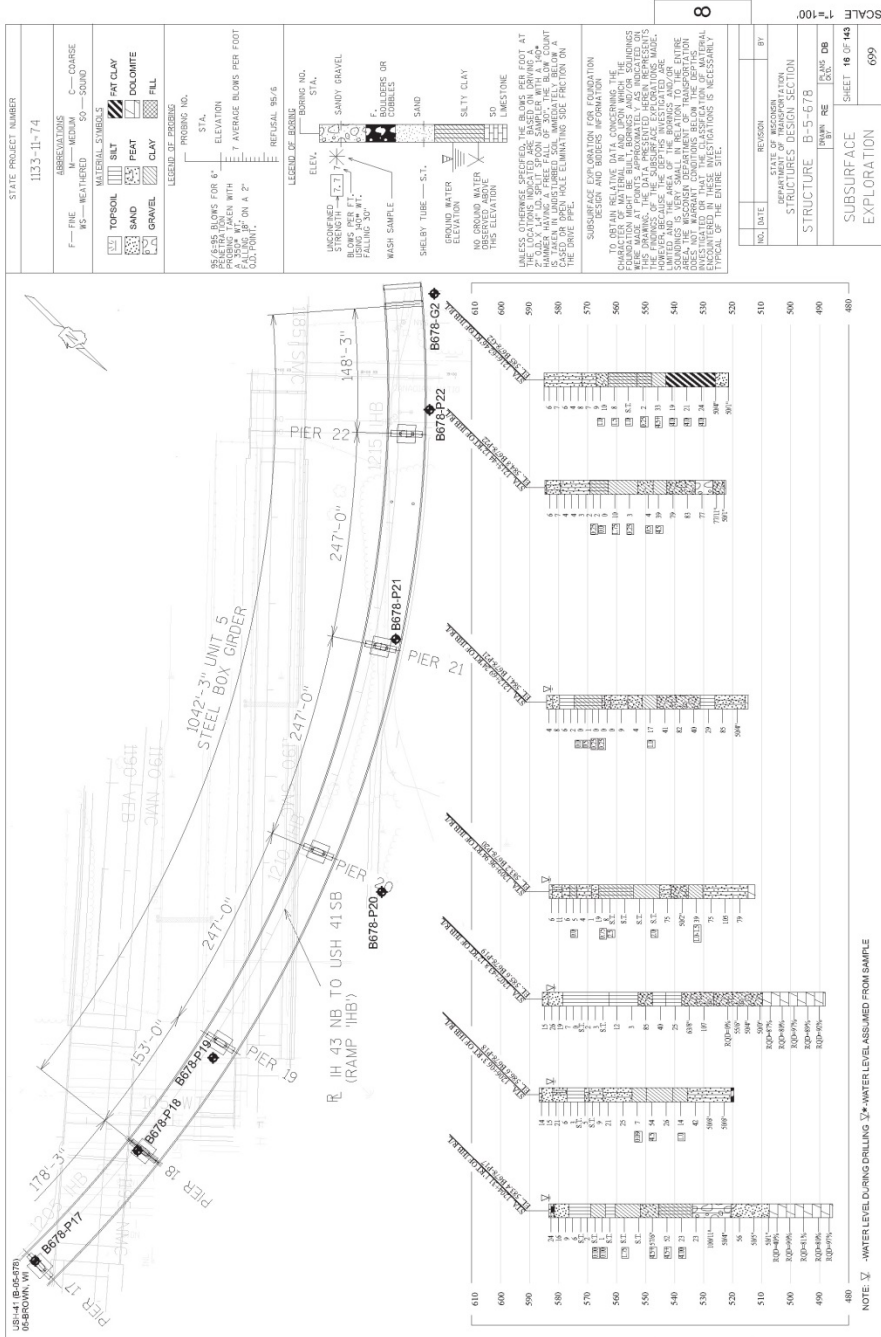


Figure 5.6 Soil profile for Bridge Structure Number B-5-678.



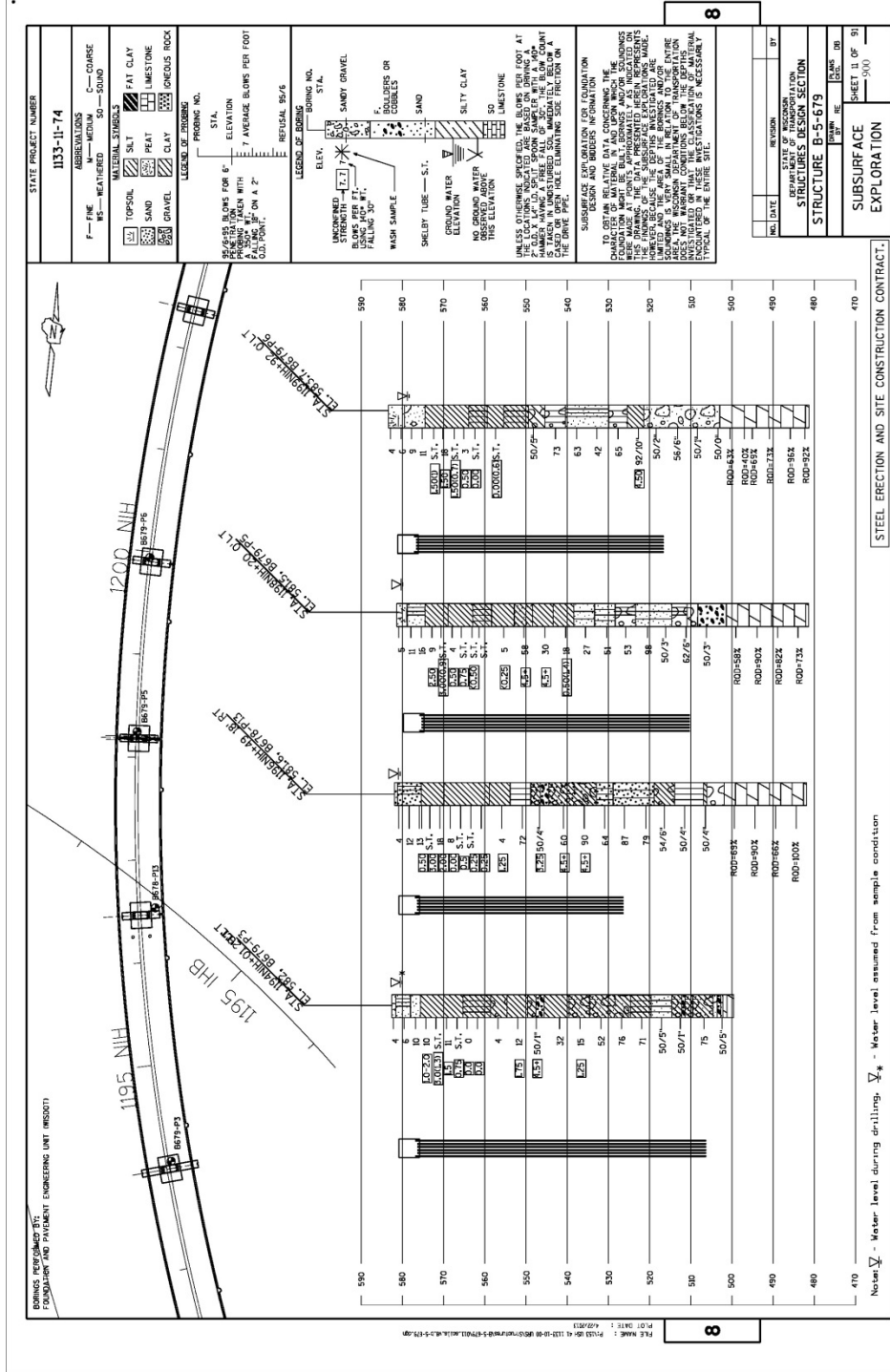


Figure 5.8 Soil profile for Bridge Structure Number B-5-679.



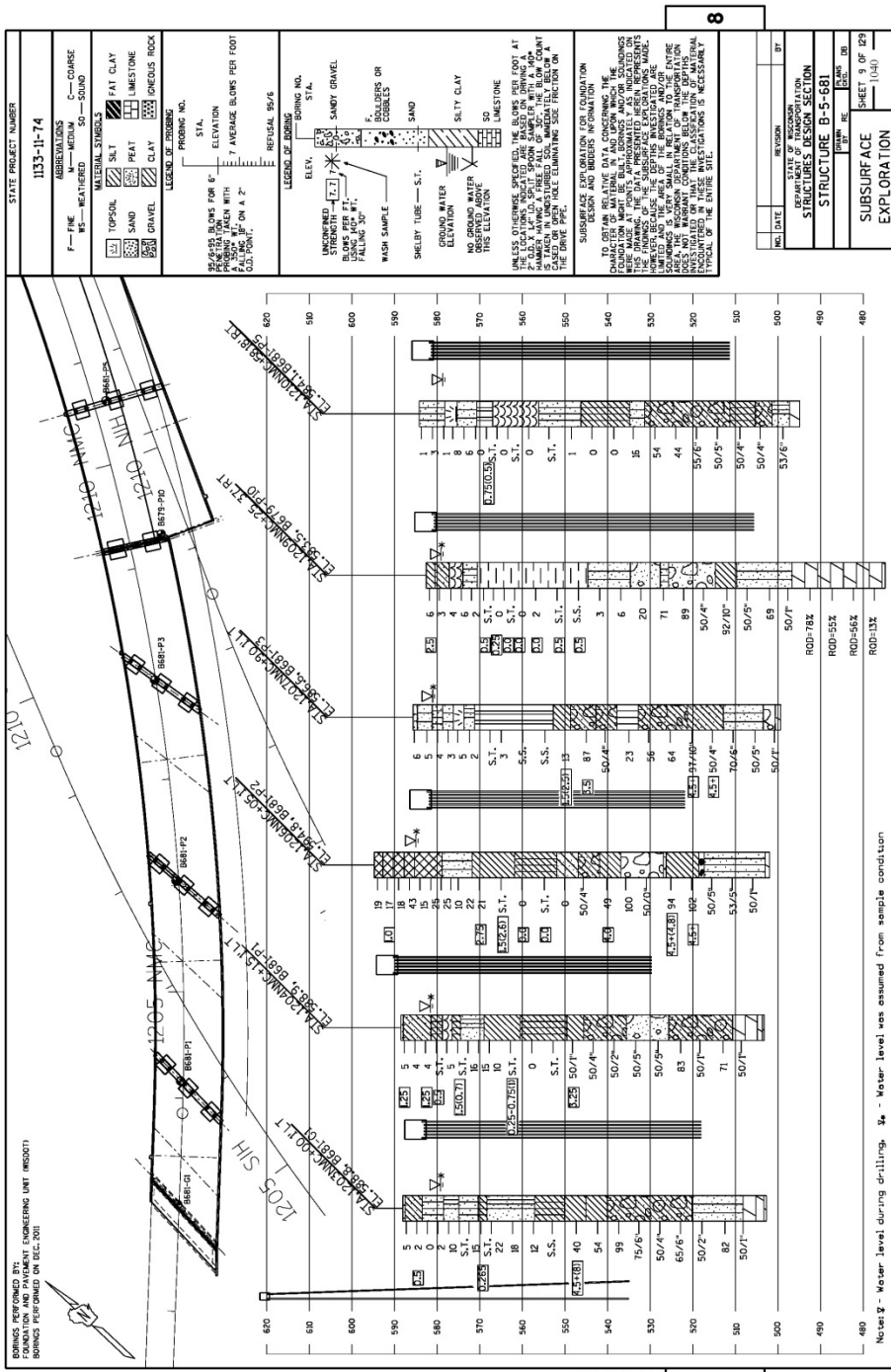


Figure 5.10 Soil profile for Bridge Structure Number B-5-681.



# CHAPTER 6 RESULTS OF STATIC AND DYNAMIC TESTING

## 6.1 INTRODUCTION

Results of 6 static load tests on piles were collected and interpreted to assess the ability of predictive methods to estimate pile capacity. The results of static load tests are presented first. Capacities measured are compared with predictions made by CAPWAP at both beginning of restrike (BOR) and at end of driving (EOD). Other predictive methods investigated include PDA-EOD (RX9) method, and 2 dynamic formulas, the FHWA modified Gates, and the Washington State DOT methods. Statistics are reported for each predictive method to allow quantitative assessment of the agreement between predicted and measured.

Results of 208 dynamic tests were collected and interpreted to assess the ability of predictive methods to estimate pile capacity. The results of static load tests were not available for these 208 tests, so estimates of capacity are based on CAPWAP(BOR). Capacities of CAPWAP (BOR) are compared with predictions made with CAPWAP(EOD), PDA-EOD(RX9), FHWA-modified Gates, and Washington State DOT.

## 6.1 STATISTICS USED TO QUANTIFY AGREEMENT BETWEEN PREDICTED AND MEASURED

Plots of predicted capacity versus measured capacity can provide a good sense of agreement between predicted and measured. However, a more quantitative approach is useful when comparing different predictive methods. Accordingly, some simple statistical parameters are described and used herein.

The predicted capacity ( $Q_p$ ) divided by the measured capacity ( $Q_m$ ) is the value used to assess the agreement between predicted and measure capacity. A value of 1 represents perfect agreement between predicted and measured. A value of 2 means the predicted capacity is twice the measured capacity. If the capacity is overpredicted, the value will be above 1 and mathematically, there is no restriction on how large the ratio can be. On the other hand, if the predictive method estimates a capacity less than measured, the ratio will be less than zero. The ratio can be between 0 and 1 if the predictive method underestimates capacity. Accordingly, the distribution of the ratio  $Q_p/Q_m$  is not a normal distribution, and it has been shown that the distribution is log-normal. Mathematically, we can make the distribution normal if we use the natural log of  $Q_p/Q_m$  instead of the original ratio. Accordingly, all operations for developing statistics will be based on  $\ln(Q_p/Q_m)$ . We define the mean of the  $\ln(Q_p/Q_m)$  as  $\mu_{ln}$  and determine its value as follows:

$$\mu_{ln} = \frac{\sum_{i=1}^n \ln\left(\frac{Q_p}{Q_m}\right)}{n} \quad \text{eqn 6.1}$$

Because  $\mu_{ln}$  is based on log values, a negative value indicates underprediction and a positive value represents a method that overpredicts. A convenient way to put  $\mu_{ln}$  in perspective is to convert the number back into an arithmetic perspective. Statistically, the median of the distribution,  $\mu_{50}$  can be determined as follows:

$$\mu_{50} = e^{\mu_{ln}} \quad \text{eqn 6.2}$$

Accordingly, half of the distribution of data will be below  $\mu_{50}$  and half will be above. The value of  $\mu_{50}$  allows assessment of whether the method tends to overpredict or underpredict capacity.

The standard deviation is used to assess the scatter in the method. Greater values for standard deviation indicate greater variability, and therefore a less reliable predictive method. The standard deviation is determined using the  $\ln(Q_p/Q_m)$  values, therefore it is referred to as  $\sigma_{ln}$  and is determined as follows:

$$\sigma_{ln} = \sqrt{\frac{1}{n} \sum_{i=1}^n \left( \ln \left( \frac{Q_p}{Q_m} \right)_i - \mu_{ln} \right)^2} \quad \text{eqn 6.3}$$

## 6.2 RESULTS FOR STATIC LOAD TESTS

Results of six static load tests were used as a basis to compare pile capacity based on driving behavior with measured pile capacity. Estimates of capacity based on CAPWAP for Beginning of Restrike conditions are given in Fig. 6.1 where capacities from the static load test are plotted on the horizontal axis and capacities for CAPWAP(BOR) are plotted on the vertical axis. A line of perfect agreement is drawn as a 45 degree line on the figure. Predicted capacities plot below the line of perfect agreement as shown in Fig. 6.1 and therefore, underpredict capacity. Table 6.1 provides statistics for the 6 static load tests for each predictive method. The value of  $\mu_{50}$  is 0.84 which indicates a tendency for the method to underpredict capacity. The standard deviation,  $\sigma_{ln}$  is 0.122 which is significantly less scatter than with all the other methods.

Figures 6.2 through 6.5 show predicted versus measured relationships for CAPWAP EOD, PDA EOD, FHWA modified Gates, and Washington State DOT. Table 6.1 provides statistical values for each of the methods. CAPWAP BOR exhibits the least amount of scatter. All three methods that require dynamic measurements (CAPWAP BOR, CAPWAP EOD, and PDA EOD) consistently underestimate capacity.

## 6.3 RESULTS FOR DYNAMIC LOAD TESTS

Results of 208 dynamic load tests were used to assess the ability of methods to predict capacity. Static load test results were not available for these tests, therefore estimates using CAPWAP BOR were taken as the static capacity of the pile. It is demonstrated above that the CAPWAP BOR might indicated capacity lower than the real static capacity. Other studies have shown that CAPWAP BOR predicts about 90 percent of the static load capacity. The results of this program indicate about 84 percent. Regardless, the result of using CAPWAP BOR as the measure of capacity instead of a static load test will increase the ratios of  $Q_p/Q_m$  by about 10 to 15 percent.

Figure 6.6 shows the agreement between CAPWAP EOD and pile capacity (as determined with CAPWAP BOR). The agreement appears good with only a small amount of scatter. Table 6.2 provides a detailed summary of statistics for all the predictive methods. Table 6.2 reports a median value ( $\mu_{50}$ ) of 0.93 for all tests, and also for each of the different sites that make up the 208 piles. Of particular note is that the site GB(South) exhibits the smallest value of ( $\mu_{50}$ ). In fact, both GB(south)

and GB(north) exhibit values in the lower range of ( $\mu_{50}$ ) for CAPWAP EOD versus CAPWAP BOR. One reason for this could be that the duration between EOD and BOR for GB(South) and GB(North) was typically greater than 4 days, and often 7 days or more, whereas the time between EOD and BOR for the production piling (B-5-671, B-5-678, B-5-679, and B-5-681) was typically 24 hours.

The agreement between PDA EOD and CAPWAP BOR is shown in Fig. 6.7 with a slightly greater scatter than observed in the case directly above (Fig. 6.6). Table 6.2 reports a median value ( $\mu_{50}$ ) of 0.93 which is similar to the overall agreement between CAPWAP EOD and CAPWAP BOR. However, the scatter is slightly greater with a value of  $\sigma_{in}$  equal to 0.16.

Figure 6.8 shows the agreement between FHWA modified Gates and CAPWAP BOR. Considerably more scatter is exhibited and the majority of the data plot above the line of perfect agreement. Accordingly, the value of  $\mu_{in}$  is 1.17 and the measure of scatter,  $\sigma_{in}$  is reported as 0.21. Both these values are greater than reported values for the methods, CAPWAP(EOD) and PDA EOD.

Likewise, the Washington State DOT method overpredicts capacity and exhibits more scatter than CAPWAP EOD and PDA EOD as shown in Fig. 6.9. The value of  $\mu_{in}$  is highest of all the methods with 1.32 and the measure of scatter,  $\sigma_{in}$  is 0.18 which is slightly less than for the FHWA modified Gates.

The results show that PDA and CAPWAP EOD provide estimates with the least degree of scatter, however they also underpredict capacity because they do not include effects of increase in pile capacity with time. The degree of underprediction is important, because the methods are under predicting capacity for CAPWAP BOR, which was shown to underpredict capacity for the piles in which static load tests were conducted.

The dynamic formulas overestimate capacity because they implicitly include setup in their calibration, and because the measure of capacity, CAPWAP BOR is slightly less than would be expected for capacity from a static load test.

Some piles in the database were driven with pile shoes to minimize pile damage. The effect of driving with shoes was investigated by determining the statistics separately for piles driven with shoes compared with results from all pile. Table 6.3 shows there is little difference in values for the median and for the standard deviation, accordingly, the methods appear to be affected minimally by the use of shoes.

#### 6.4 END BEARING LOAD AS AFFECTED BY SOIL TYPE AND NSPT

End bearing of the piles into soils with very high Nspt values should result in high toe capacities for the pile. Accordingly, CAPWAP BOR results were used to determine tip capacities and compare with the types of soil conditions and Nspt resistances reported in the soil broings. Figure 6.10 shows the end bearing load developed by the pile during restrrike as affected by Nspt, soil type, and whether the pile had shoes. While the scatter is significant, there does appear to be a trend of increasing pile tip capacity with increasing Nspt.

Piles driven into boulders and other granular soils tend to exhibit higher capacity, although there is significant scatter in the results. Piles with toes in gravel seemed to exhibit the greatest degree of

scatter and the greatest range of  $N_{spt}$  values. Some of the highest toe capacities were reported for piles driven into sand. Clays exhibited the least tip capacities and were generally in the low range of  $N_{spt}$ . Piles with shoes tended to have slightly higher tip capacities than piles without shoes. Some of the scatter in this plot is due to uncertainty in establishing a correct representation of  $N_{spt}$ .

Three sources that contribute to the scatter in Fig. 6.10 are the 1) the determination of the value for toe capacity, 2) identifying a representative value for  $N_{spt}$  for the IGM, and 3) special variation of the soil profile.

Values for end bearing are estimates based on restriking the pile while recording dynamic measurements and then conducting CAPWAP analyses on the restrikes. Separation of total capacity into end bearing and side resistance require interpretation of dynamic measurements collected with 2 accelerometers and 2 strain gages. The procedure using CAPWAP is iterative with the user controlling and changing pile and soil parameters to achieve a reasonable match between predicted and measured change in force with time. Accordingly, the interpretation of these results and performing signal-matching operations with CAPWAP results in solutions that are not unique. While results from CAPWAP usually provide a good estimation of overall capacity when using BOR results, the ability to accurately separate total capacity into estimates for side resistance and end bearing is less reliable, particularly for piles which are driven through softer soils and then penetrate into stiff soils.

$N_{spt}$  values are also subject to error due to different energy being delivered to the sampler and due to IGMs providing a significant resistance to penetration, requiring the SPT to terminate early (before a penetration of 18 inches). MSPT tests were conducted to attain more reproducible measurement of penetration resistance for characterizing IGMs.

Soil layering, soil type, soil strength, and soil density are controlled by the geological processes that deposited the soil and can result in significant special variation in soil properties and soil type. Glacial depositional processes can result in highly variable soil profiles. Accordingly, the soil profile at the borehole location may be slightly different for each pile driven within a pile group. This difference is often reflected by different penetration depths for piles within the same group.

Accordingly, additional efforts were conducted to identify the penetration resistance of the IGM soils more reliably than with  $N_{spt}$  measurements.

## 6.5 USE OF MSPT TO IDENTIFY PENETRATION RESISTANCE OF IGMs AT SIX SITES

### 6.5.1 MSPT PROCEDURE

Intermediate Geo-Materials (IGMs) can exhibit significant resistance to penetration from a sampler used during a standard penetration test (SPT). Accordingly, the procedure for quantifying penetration resistance in an IGM using standard procedures (the number of blows required to drive the sampler from 6 inches to 18 inches of penetration) can be inefficient or impossible to conduct. Others have modified the SPT to better quantify penetration resistance for IGMs. Stark, et. al. (2013) have proposed a Modified Standard Penetration Test (MSPT) which is described in detail in Section 1.2.4 of this report. Briefly, the MSPT test is conducted in the same manner as the SPT,

except the sampler penetration is recorded after every ten blows from 10 to 100 impacts from the hammer. The plot of penetration resistance becomes linear, or nearly linear between 60 and 100 blows and the slope is reported as penetration resistance in blows per foot. Although the MSPT provides a penetration resistance with units of blows per foot, just like the  $N_{spt}$ , the two values are not equal.

While the MSPT procedure measures the penetration every 10 blows from 0-100 blows, there are alternative readings that would yield similar results. For example, in most cases, the user would get exactly the same results measuring penetration at every 20 blows, rather than every 10. The modification would decrease the number of readings and appears to be just as accurate. Another option would be to measure penetration at 60 and 100 blows, thus only 2 reading are required. While this option would yield acceptable results the majority of the time, there were cases where the sampler struck a hard object during penetration, and accordingly, the penetration rate changed. It is unlikely that option 2 would have identified the change in penetration. Option 1 would most likely detect the change in penetration rate, but with less resolution than the original procedure.

### *6.5.2 RESULTS OF MSPT CONDUCTED AT PILE LOAD TEST SITES IN GREEN BAY, WIS*

Modified Standard Penetration Tests were conducted at six sites in the Green Bay area. MSPT tests were conducted at sites 1, 2 and 3 for the Green Bay south tests (Chapter 3) and sites 1, 2, and 4 at Green Bay North (Chapter 4). MSPT tests were conducted in the soils at depths where the tips of the piles were driven. Several MSPTs were conducted at each site, usually at intervals of two feet. Table 6.4 provides the MSPT results for all the sites and depths, as well as the soil description and soil strength.

Energy measurements were also conducted at the site on each of the two drill rigs used for the MSPTs. The average measured energy delivered to the sampler was determined to be 85-90 percent with an average around 88 percent. Accordingly, all MSPT values correspond to a hammer efficiency of 88 percent.

### 6.6 END BEARING LOAD AS AFFECTED BY SOIL TYPE AND MSPT

End bearing load for the piles at the six Green Bay sites compared with MSPT values are shown in Fig. 6.11. Most of the IGM is fine grained, and accordingly, smaller end bearing loads are exhibited when compared with Fig. 6.10. End bearing load for all of the data from production piling combined with the Green Bay test sites are plotted in Fig. 6.12. MSPTs were not conducted for the sites where production piling was driven, so values of  $N_{spt}$  were converted to MSPT using the following relationship developed in Section 1.2.4.

$$MSPT = 1.27 * N_{spt} \qquad \text{eqn. 6.4}$$

There is considerable scatter exhibited in Fig. 6.12 which means that while it is possible that the scatter was reduced by replotting the results with MSPT, scatter still remains due to uncertainties in estimating end bearing load from CAPWAP analyses and special variations in soil profile across the site where piles were driven. Nevertheless, some general observations can be drawn.

There appears to be a tendency for piles with shoes to have a greater tip resistance than piles without shoes. Piles driven into coarse grained IGM tend to exhibit greater end bearing than piles driven into fine grained IGM. Accordingly, the data were split into two separate categories: 1) piles driven into fine grained IGMs and 2) piles driven into coarse grained IGMs.

The relationship between end bearing and MSPT for fine grained IGMs is shown for all pile data in Fig. 6.13. While the scatter is significant, the trend shows that less end bearing is developed for fine grained soil. There is a trend of increasing end bearing with increasing MSPT, however, there are some data that show a wide variation in end bearing for very high MSPT values (900). This variation of end bearing at the very high MSPT values may due to inaccuracies and limitations with estimating tip load with CAPWAP. In very hard driving, permanent set per blow may be small and therefore unable to mobilize the full capacity at the pile tip. Accordingly, the tip capacity is reported as less than the real tip capacity. Piles with shoes appear to exhibit a greater end bearing load than piles without shoes, and silts may tend to have a slightly greater average end bearing load than for the clay.

End bearing as influenced by MSPT and soil type for coarse grained IGMs is shown for all pile data in Fig. 6.14. The scatter is significant but there is a trend of increasing end bearing with increasing MSPT values, and the end bearing values tend to be greater than observed for fine grained IGMs. There does not appear to be a clear differentiation for the effect of grain size. Boulders, gravel and sand all show about the same degree of scatter and about the same average end bearing. Piles with shoes do show a slight tendency toward greater end bearing load.

Assessing trends in the data was accomplished by relying on previous relationships for strength and bearing capacity that have been proposed for piles and drilled shafts in soil and IGMs. The data are separated into two categories: 1) fine grained IGMs and 2) coarse grained IGMs. Different design methods for estimating strength, end bearing, and side resistance for piles driven into soil and IGM were reviewed and used to compare predicted and measured end bearing values. Comparisons were also conducted for methods developed for drilled shafts in IGMs.

### *6.6.1 END BEARING LOAD FOR FINE GRAINED IGMs*

A comparison of end bearing load for piles in IGM with different predictive methods is show in Fig. 6.15 for fine grained IGMs. All the predictive methods show estimates of end bearing load to increase with MSPT value. The relationship between MSPT and end bearing for all the predictive methods is linear. The concave shape exhibited in the figure is a result of plotting MSPT on a log scale. Each predictive method is discussed below.

The predictive method, Terzaghi, et. al. (1996) uses very traditional relationships found in soil mechanics. The predictive method is based on using penetration resistance to determine soil strength, and the end bearing is determined from traditional bearing capacity equations. Terzaghi, et. al. (1996) reports studies conducted by Stroud (1974) in which the soil strength is related to the  $N_{60}$  value by the following equation:

$$s_u = (4 \text{ to } 6) * N_{60} \quad \text{eqn. 6.5}$$

The unit end bearing capacity for a pile embedded in a fine grained soil is determined as

$$q_{eb} \text{ (ksf)} = 9 * s_u \quad \text{eqn. 6.6}$$

and combining Eqns. 6.5 and 6.6, we get

$$q_{eb} \text{ (ksf)} = 0.02 * (4 \text{ to } 6) * 9 * N_{60} = 0.02 * (36 \text{ to } 54) * N_{60} \quad \text{eqn. 6.7}$$

and end bearing load, QEB, is the tip area (A<sub>eb</sub>) multiplied by the unit end bearing capacity (q<sub>eb</sub>),

$$QEB \text{ (kips)} = 0.02 * (36 \text{ to } 54) * N_{60} * A_{eb} \quad \text{eqn. 6.8}$$

Converting N<sub>60</sub> values to MSPT values requires two relationships to be quantified. The first is the relationship between N<sub>spt</sub> and MSPT. This has been discussed previously in Chapter 1, and can be summarized as follows:

$$MSPT = 1.27 * N_{spt} \quad \text{eqn. 6.9}$$

Also, the N<sub>spt</sub> value will be influenced by the efficiency with which the SPT hammer applies energy during a penetration test. Results for energy efficiency are discussed in Chapter 1 and range between 85-90 percent for the tests conducted in Green Bay, accordingly, and average value of 88 percent efficiency is used herein, and the relationship between N<sub>60</sub> and N<sub>spt</sub> (with 88 percent efficiency) is as follows:

$$N_{60} = N_{spt} (88/60) \quad \text{eqn 6.10}$$

Combining Eqns 6.9 and 6.10, we get

$$MSPT = N_{60} * (N_{spt}/N_{60}) * (MSPT/N_{spt}) = N_{60} * (60/88) * (1.27) = 0.866 * N_{60} \quad \text{eqn 6.11}$$

Or inversely,

$$N_{60} = 1.16 * MSPT \quad \text{eqn. 6.12}$$

Combining Eqns 6.8 and 6.12, we get the following equation for end bearing load for a pile

$$QEB = (0.832 \text{ to } 1.25) * MSPT * A_{eb} \quad \text{eqn. 6.13}$$

The prediction of end bearing load versus MSPT value for the Terzaghi, et. al. (1996) method is shown in Fig. 6.15 to follow the trend of the data with the upper-bound line closer to the overall fit.

The other two methods show similar trends. The method by Abu-Hejleh and Attwooll (2005) is also based on penetration results, and therefore only differs from the Terzagi, et. al. (1996) method by a constant. The equation used by Abu-Hejleh and Attwooll (2005) is

$$QEB = 1.07 * MSPT * A_{eb} \quad \text{eqn 6.14}$$

The predictive method identified as Stark, et. al. (2013) was developed for drilled shafts in weak shales that exhibit strengths consistent with IGMs. The equation for end bearing is

$$QEB = 0.346 * MSPT * Aeb \quad \text{eqn. 6.15}$$

Predictions of end bearing load using the method by Stark. et. al (2013) are well below the trend of the data and the trend of the other predictive methods because the method was developed for drilled shafts in IGMs rather than driven piling. Drilled shafts have larger diameter than driven piling, therefore, more displacement is needed to mobilize full end bearing capacity. Other reasons that drilled shafts would develop less end bearing load than piles include the facts that shafts are drilled and stress is relieved at the bottom of the hole whereas driven piling penetrates into the soil without drilling and relaxing the soil at the tip. Furthermore, incomplete cleanout at the bottom of the drilled shaft hole can reduce the end bearing load for drilled shafts. Accordingly, it is expected that end bearing estimates developed with drilled shaft load test data would predict less capacity than would be developed in a driven pile.

### 6.6.2 END BEARING LOAD FOR COARSE GRAINED IGMs

Figure 6.16 shows the agreement between all the pile test results in coarse grained IGMs and 4 different predictive methods. Meyerhof (1976) developed a simple relationship between  $N_{60}$  and end bearing pressure

$$qeb \text{ (ksf)} = 8 * N_{60} \quad \text{eqn. 6.16}$$

Converting  $N_{60}$  to MSPT and end bearing pressure (qeb) to end bearing load (QEB), we get

$$QEB = 9.2 * MSPT * Aeb \quad \text{eqn 6.17}$$

The Meyerhof method greatly overestimates the results of the pile load tests.

O'Neill and Reese (1999) proposed a bearing capacity equation for drilled shafts in coarse grained IGMs for the FHWA. The unit end bearing capacity is

$$qeb = 0.59 * (N_{60} * patm / \sigma'_{vb})^{0.8} * \sigma'_{vb} \quad \text{eqn. 6.18}$$

where  $\sigma'_{vb}$  is the vertical effective stress at the tip of the shaft,  $patm$  is the value of 1 atmospheric of pressure in the same units as  $\sigma'_{vb}$ . Estimates for end bearing load were made for end bearing depths of 20 ft and 80 ft below the ground surface and are shown as dotted lines in Fig. 6.16. The method predicts significantly less end bearing load than demonstrated with the test piles. The other predictive method for drilled shafts developed by Stark, et. al. (2013) has already been discussed (eqn. 6.15) and it too, predicts values smaller than exhibited by the test piles. The method predicts results similar to the O'Neill and Reese method. Therefore, both methods developed for drilled shafts in IGM's underpredict bearing load in the driven piles.

The curves identified as Olson's (1990) method are limits of end bearing for piles that are based on pile load tests and standard penetration test values. There are two curves, one for gravel and one for sand. The curve for sand appears to provide an upper bound value, in which all the pile end bearing values fall below, while the curve for gravel seems to predict, on the average, slightly lower end bearing loads. Furthermore, Olson's recommendations do not follow the observed trend of increasing end bearing load with MSPT values for penetration values greater than 100. Accordingly,

none of these methods exhibit good agreement with the data and therefore, it will be necessary to develop an empirical relationship for better agreement with the results.

An option for determining end bearing in coarse grained IGM is to estimate end bearing load based on the rectangular area enclosed by the flanges of the H-pile, or the cross-sectional area of the steel in the H-pile. To investigate the effect of area on the predictions, the same equations used for piles in coarse grained IGM were used with a smaller area (the cross-sectional area of steel). The results are shown in Fig. 6.17. Meyerhof's method produces a curve that underpredicts measured values, but overall, fits the trend of the data. Accordingly, Meyerhofs method should only use the structural cross-sectional area for estimating total end bearing load. The other methods predict loads much less than measured; therefore, using the tip area enclosed by the pile flanges produces more reasonable agreement.

## 6.7 UNIT SIDE RESISTANCE

The unit side resistance along the piles in the IGM is a difficult value to identify when interpreting CAPWAP results and in IGMs. Interpretations for end bearing developed in CAPWAP influence the results in side resistance. Soil profiles are quite variable along the length of the pile in IGMs. Furthermore, the resistance along the length of the pile can change with time depending on the soil type, and the time between initial driving and re-strike. Other attempts to determine side resistance with CAPWAP results exhibited significant scatter (Brooks, 2008) without showing any intelligible trends. Accordingly, unit side resistance for IGMs will be based on a rational review of several methods developed for driven piles and drilled shafts.

Some unit side resistance values for fine grained IGMs are shown in Fig. 6.18. On the right hand side of the graph is a vertical line identifying the range of back-calculated unit side resistance values for piles driven into IGMs as reported by Brooks(2008). The range varies from almost 0 to about 27 ksf, and the average was about 10 ksf. These values are quite high for side resistance in driven piling and could be a result of CAPWAP analyses interpreting a low end bearing load so a higher side resistance was specified to compensate.

The two data points come from design methods. The square symbol comes from Tomlinson's 1957 paper and represents the highest unit side resistance (0.75 ksf) he reported for a pile in stiff clay (not an IGM). The circular data point comes from Bustamante and Ganeselli (1983) in which they used a database of piles and drilled shafts to develop relationships between cone penetration test results and unit side resistance for piles. Their design curves suggest a limiting value of 2 ksf for piles driven into very stiff and hard clays and silts, some with strengths in the range of IGMs.

Stark, et. al. (2013) developed a relationship between MSPT and unit side resistance for drilled shafts. The equation is as follows:

$$f_s(\text{ksf}) = 0.0231 * \text{MSPT} \quad \text{eqn 6.19}$$

This is shown as the dotted line in Fig. 6.18. The relationship falls near the point identified for Bustamante and Ganeselli (1983) and continues to increase with MSPT. Stark et. al (2013) collected a database of drilled shafts in IGM, some exhibiting unit side resistances up to 20 ksf.

Extending results from drilled shaft to driven piling is problematic because the difference in installation procedure and the final geometry of the foundation influences differently the mobilization of side resistance. Drilled shafts usually develop a rough interface along the sidewalls of the drilled shaft hole. Furthermore, the hole is filled with concrete to bring soil and foundation into contact. Driven piling results in a smooth steel/IGM interface along the sides and therefore, may not be able to develop as much side resistance as a drilled shaft.

Different methods for predicting unit side resistance for coarse grained IGMs are given in Fig. 6.19. On the right hand side of the graph is a vertical line identifying the range of unit side resistances back-calculated by Brooks (2008). The range observed was 3.5 to 10 ksf with an average of the 4 piles at approximately 6 ksf.

Meyerhof (1976) recommended that the unit side resistance for a low-displacement pile is related to  $N_{60}$  in the following manner

$$f_s \text{ (ksf)} = N_{60}/50 = .0232 * \text{MSPT} \quad \text{eqn. 6.20}$$

and the results are shown on Fig. 6.19 as a dotted line.

Unit side resistances recommended by Bustamante and Ganeselli (1983) are shown as a dashed line. The relationship is based on a pile database in which they relate unit side resistance to cone penetration resistance. The trend is to increase in unit side resistance, gradually reaching a limiting value of about 2.6 ksf.

Olson(1990) made recommendations of limiting unit side resistance for several ranges of  $N_{60}$  and the results are plotted as a solid line in Fig. 6.19. The trend predicts unit side resistance values slightly greater but similar to that proposed by Bustamante and Ganeselli.

## 6.8 DESIGN RECOMMENDATIONS FOR PILES DRIVEN INTO IGMs

Recommendations are provided herein for estimating unit end bearing and unit side resistance for driven piles into IGMs. There are four separate conditions: 1) unit end bearing for piles in fine grained IGM, 2) unit end bearing for piles in coarse grained IGM, 3) unit side resistance for piles in fine grained IGM and 4) unit side resistance for pile driven into coarse grained IGMs. Design curves for each of the conditions has an equation that relates MSPT to the unit end bearing or side resistance, and each method also has a limit pressure that cannot be exceeded. Recommendations are based on reasonable representation of the trends observed in the data. Trends and limits proposed by predictive method discussed in this chapter also influence the recommendations.

### 6.8.1 UNIT END BEARING IN FINE GRAINED IGM

The unit end bearing for piles driven into fine grained IGMs is specified as a function of the MSPT value as follows:

$$Q_{eb}(\text{ksf}) = 0.935 * \text{MSPT} \quad (\text{not to exceed } 200 \text{ ksf}) \quad \text{eqn. 6.21}$$

The design recommendation, along with the pile data collected for this research project is shown in Fig. 6.20. The design equation is very close to the classical bearing capacity factor for undrained deep foundation.

### 6.8.2 UNIT END BEARING IN COARSE GRAINED IGM

The unit end bearing ( $q_{eb}$ ) for piles driven into coarse grained IGMs is specified as a function of the MSPT value as follows:

$$q_{eb}(\text{ksf}) = 65 * \text{MSPT}^{0.3} \quad (\text{not to exceed } 300 \text{ ksf}) \quad \text{eqn. 6.22}$$

The design recommendation, along with the pile data collected for this research project is shown in Fig. 6.21. The design equation is empirically based to best model the trend exhibited by the data. A limit of 300 ksf is based on an average end bearing values of the data.

### 6.8.3 UNIT SIDE RESISTANCE

The unit side resistance ( $f_s$ ) for piles driven into fine grained IGMs is specified as a function of the MSPT value as follows:

$$f_s(\text{ksf}) = 0.021 * \text{MSPT} \quad (\text{not to exceed } 2 \text{ ksf}) \quad \text{eqn. 6.23}$$

This design recommendation is shown in Fig. 6.22. The design equation closely represents the strength of the soil using Terzaghi, et. al. (1996) and using a ratio of unit side resistance to undrained strength of 0.2. Limiting the unit side resistance to 2 ksf is based on the work of Bustamante and Ganeselli (1983).

The unit side resistance for piles driven into coarse grained IGMs is shown in Fig. 6.22. The side resistance is specified as a function of the MSPT value as follows:

$$f_s(\text{ksf}) = 0.9 * \text{MSPT}^{0.25} \quad (\text{not to exceed } 3 \text{ ksf}) \quad \text{eqn. 6.24}$$

The design recommendation for this relationship is an empirical relationship similar to the trends proposed by Olson (1990) and Bustamante and Ganeselli (1983) for sands.

Table 6.1. Statics for Predicted/Measured for Static Load Test Results

<b>Method of Prediction</b>	<b>n</b>	<b><math>\mu_{ln}</math></b>	<b><math>\sigma_{ln}</math></b>	<b><math>\mu_{50}</math></b>
CW(BOR)/SLT	6	-0.180	0.122	0.835
CW(EOD)/SLT	6	-0.409	0.274	0.664
PDA(EOD)/SLT	6	-0.362	0.285	0.696
Mgates/SLT	6	-0.154	0.232	0.857
WashDOT/SLT	6	-0.038	0.198	0.963

Table 6.2. Statics for Predicted/Measured using Dynamic Measurements and Observations

Method of Prediction	Site	n	$\mu_{in}$	$\sigma_{in}$	$\mu_{50}$
CW(EOD)/CW(BOR)	GB(South)	16	-0.314	0.234	0.731
	GB(North)	38	-0.105	0.170	0.900
	GB(All)	54	-0.167	0.212	0.846
	B-5-671	32	-0.042	0.051	0.959
	B-5-678	59	-0.030	0.090	0.970
	B-5-679	31	-0.022	0.069	0.979
	B-5-681	26	-0.026	0.089	0.974
	All B-5 tests	147	-0.032	0.076	0.969
	All Data	201	-0.068	0.141	0.934
PDA(EOD)/CW(BOR)	GB(South)	16	-0.267	0.285	0.766
	GB(North)	38	-0.111	0.234	0.895
	GB(All)	54	-0.157	0.258	0.855
	B-5-671	32	-0.051	0.065	0.950
	B-5-678	63	-0.033	0.103	0.968
	B-5-679	31	-0.024	0.091	0.976
	B-5-681	26	-0.035	0.113	0.966
	All B-5 tests	151	-0.037	0.094	0.964
	All Data	205	-0.068	0.163	0.934
Mgates/CW(BOR)	GB(South)	19	-0.082	0.137	0.921
	GB(North)	38	0.2183	0.159	1.244
	GB(All)	57	0.118	0.208	1.125
	B-5-671	32	0.181	0.147	1.199
	B-5-678	63	0.196	0.238	1.217
	B-5-679	31	0.244	0.170	1.276
	B-5-681	26	0.016	0.152	1.016
	All B-5 tests	151	0.169	0.204	1.184
	All Data	208	0.155	0.206	1.168
WashDOT/CW(BOR)	GB(South)	19	0.109	0.133	1.116
	GB(North)	38	0.297	0.155	1.346
	GB(All)	57	0.234	0.172	1.264
	B-5-671	32	0.287	0.148	1.333
	B-5-678	63	0.325	0.207	1.384
	B-5-679	31	0.353	0.163	1.423
	B-5-681	26	0.153	0.122	1.165
	All B-5 tests	151	0.290	0.183	1.337
	All Data	208	0.275	0.181	1.317

Table 6.3. Statics for Predicted/Measured, Dynamic Measurements, Piles with Shoes

<b>Method of Prediction</b>	<b>Condition</b>	<b>n</b>	$\mu_{in}$	$\sigma_{in}$	$\mu_{50}$
CW(EOD)/CW(BOR)	Shoes	27	-0.028	0.069	0.972
	All B-5 Data	147	-0.032	0.076	0.969
PDA(EOD)/CW(BOR)	Shoes	28	-0.005	0.073	0.995
	All B-5 Data	151	-0.037	0.094	0.964
Mgates/CW(BOR)	Shoes	28	0.148	0.205	1.159
	All B-5 Data	151	0.169	0.204	1.184
WashDOT/CW(BOR)	Shoes	28	0.280	0.174	1.323
	All B-5 Data	151	0.290	0.183	1.337

Table 6.4 MSPT Results for Green Bay

Site	Elev (ft)	MSPT (bpf)	qu (tsf)	Soil Description
GBSouth Site 1, Bridge B-5-658, Pier 6	569.36	61	2.75/2.75	Clay, some silt, trace of F-sand and gravel, brown
	567.36	85	na	Clay, some silt, trace of F-sand and gravel, brown
	565.36	62	4.5+/4.5+	Clay, some silt, trace of F-sand and gravel, brown
	563.36	72	4.5+/4.5+	Silt, Some clay, F-M gravel, brown
	561.36	169		fine Sand, trace of F-M gravel, brown
South Site #2, Bridge B-5-660, Pier 2	536.62	81	4.5+	Sandy Silt and Silty Sand, Gray
	534.62	63	4.5+	Silty Clay, trace of gravel, Brown
	532.62	49	4.5+	Silty Clay, Brown w/ gray silt seams
	530.62	20	2.5	Clay over Limestone Boulder
	527.62	172	4.5+	Silt with F-M sandy, Gray
South Site #3, Bridge B-5-660, Pier 12	540.37	22	4.5+/4.5+	clayey Silt, Some Gravel, gray
	538.37	47	4.5+/3.25	Silty Clay, brown, a little gravel
	536.37	30	4.5+/4.5+	Silt, F-M sandy then a limestone boulder
	532.37	909	4.5+/4.5+	Silt, F-M sandy, lt gravel, gray
North Site #1, Bridge B-5-671, Pier 5	552.79	244	4.5+/4.5+	Silt, some clay, little F-M sand and gravel, brown
	550.79	123	4.5+/4.5+	Silt, some clay, little F-M sand and gravel, brown
	548.79	105	4.5+/4.5+	Silt, some clay, little F-M sand and gravel, brown
	546.79	119	3.75/3.75	Clay, some silt, trace F-M sand and gravel, brown
	544.79	147	4.5+/4.5+	Silt, some clay, little F-M sand and gravel, brown
	542.79	130	4.5+/4.5+	Silt, some clay, little F-M sand and gravel, brown
	540.79	133	4.5+/4.5+	Silt, some clay, little F-M sand and gravel, brown
	538.79	59	4.5+/4.5+	Silt with clay seams
	536.79	63	4.5+/4.5+	Silt with clay seams
North Site #2, Bridge B-5-678, Pier 16	514.5	286		Sand, trace of gravel, gray
	512.5	167	4.5+/4.5+	Silt, trace of gravel, trace of fine sand, gray
	510.5	149	4.5+/4.5+	Silt, trace of gravel, trace of fine sand, gray
	508.5	101	4.5+/4.5+	Silt, trace of gravel, trace of fine sand, gray
	506.5	156		F-M Sand, F-C gravel, gray
North Site #4, Bridge B-5-678, Pier 1	510.65	51	4.5+/4.5+	Silt w/ clay seams, brown
	508.65	18	1.75/1.5	Clay w/ silt seams, brown
	506.65	17	1.5/2.5	Clay w/ silt seams, brown
	504.65	58	2.0/2.5	Clay w/ silt seams, brown
	502.65	625	4.5+	Silt, some clay, little F-M sand and gravel, brown

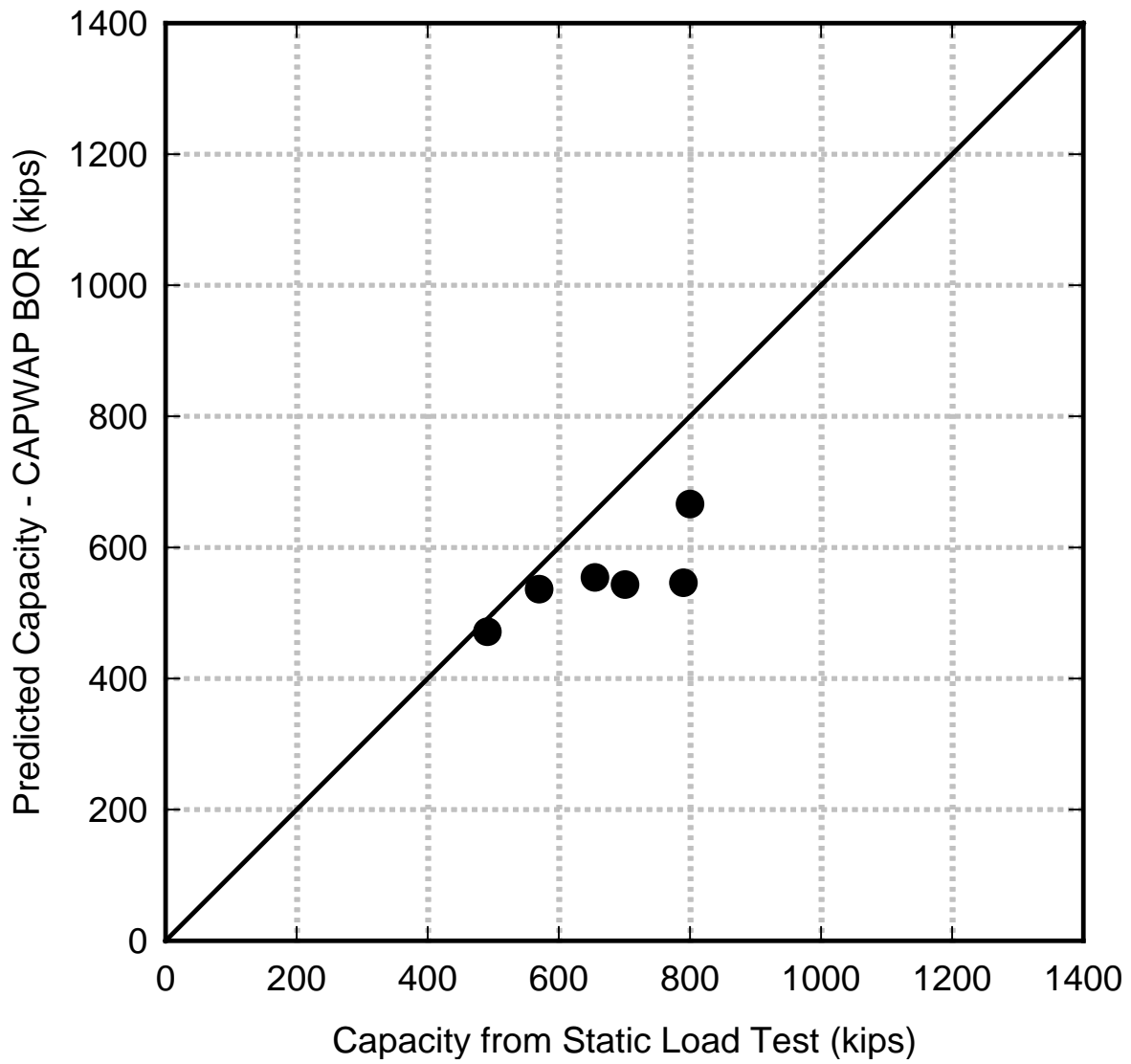


Figure 6.1 Comparison of CAPWAP BOR capacity with results of static load test.

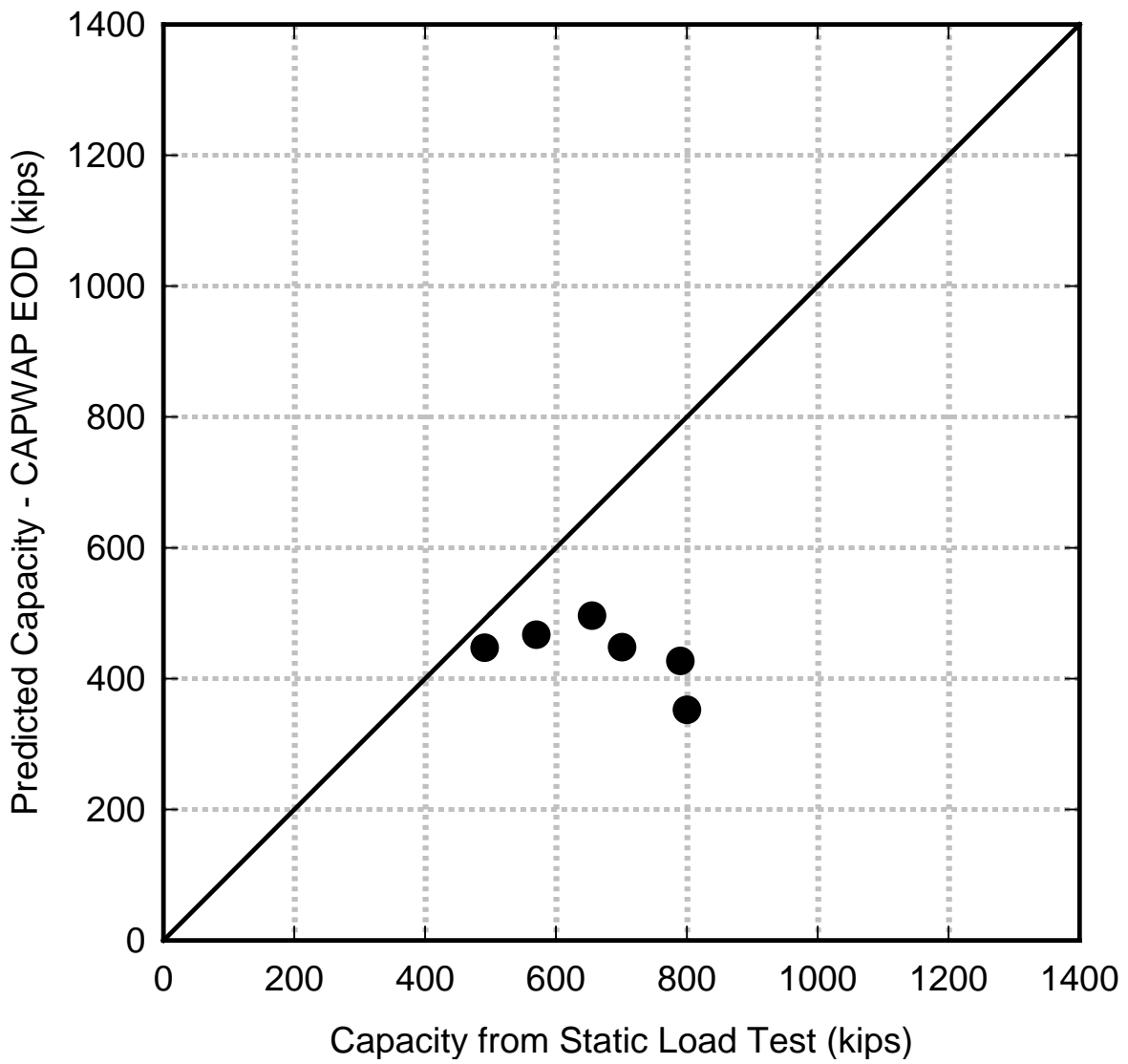


Figure 6.2 Comparison of CAPWAP EOD capacity with results of static load test.

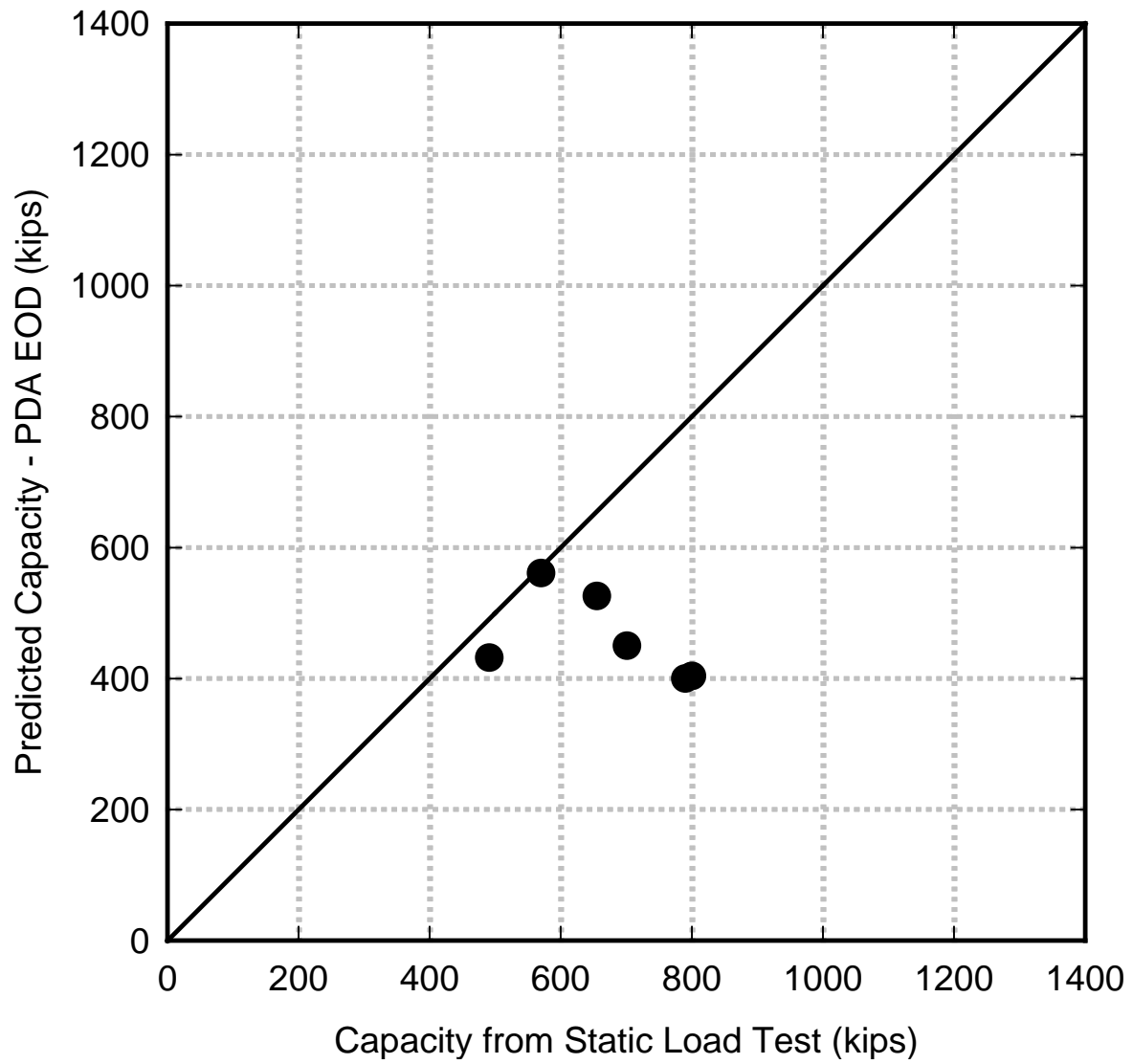


Figure 6.3 Comparison of PDA EOD capacity with results of static load test.

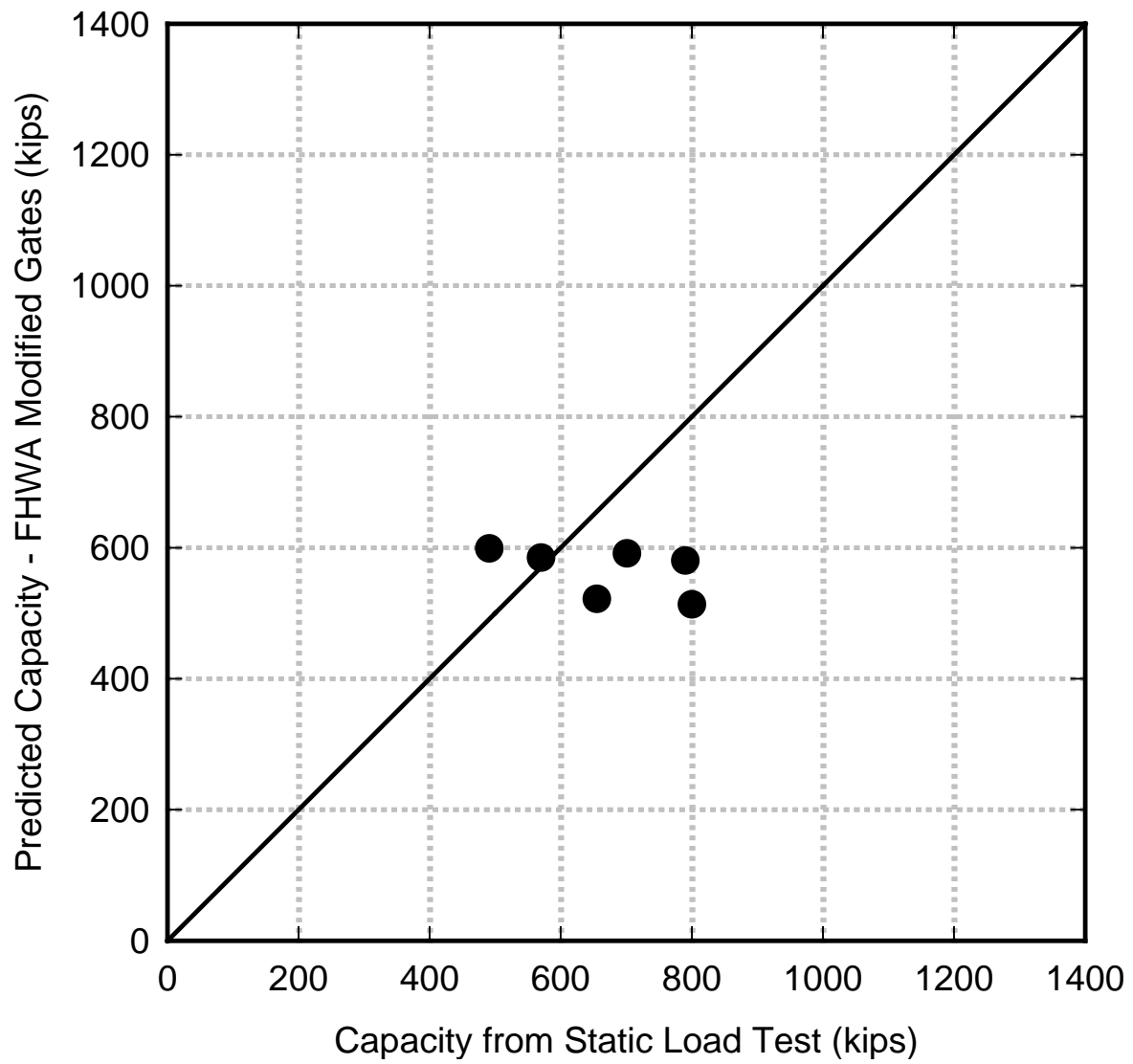


Figure 6.4 Comparison of FHWA modified Gates capacity with results of static load test.

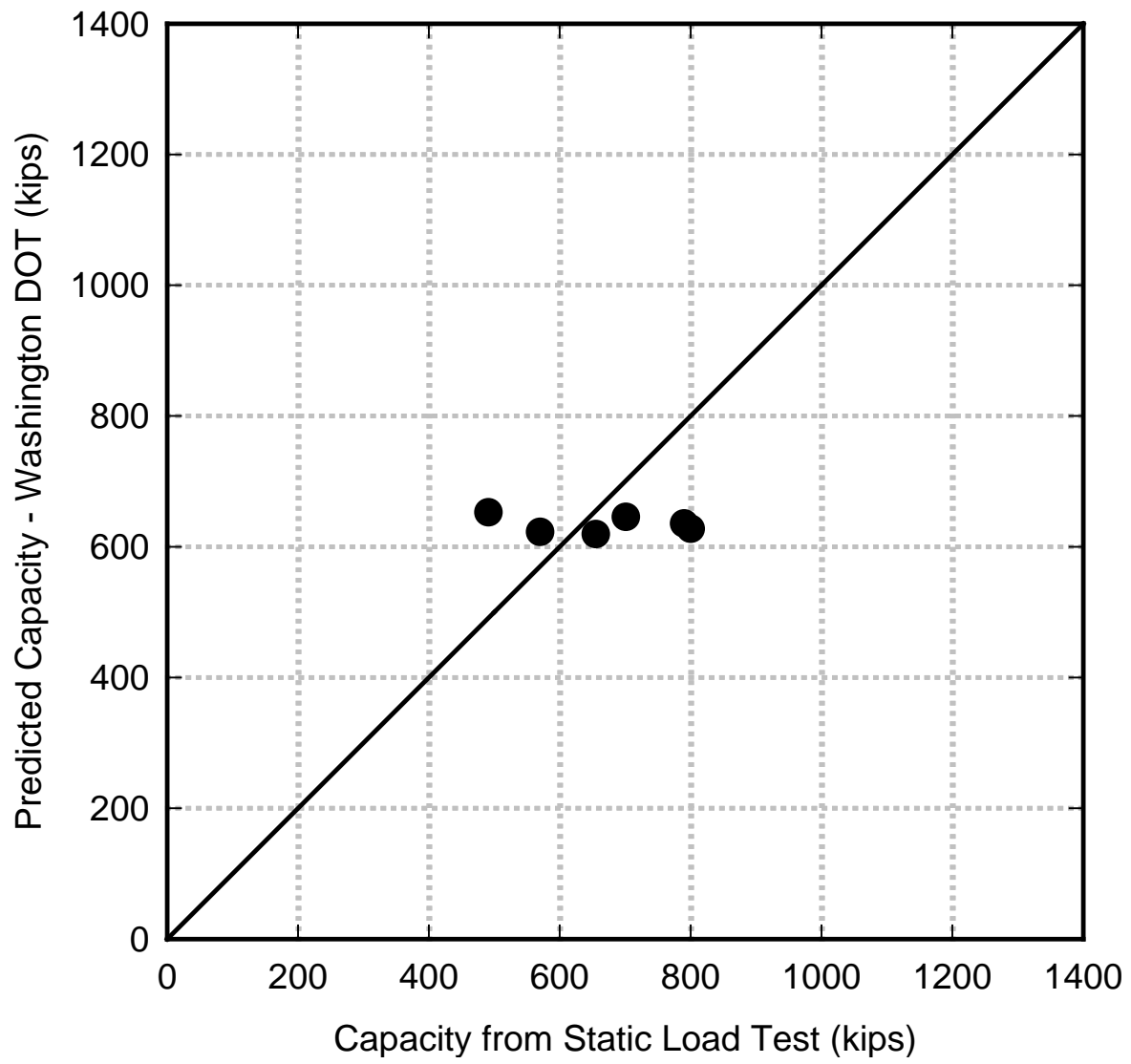


Figure 6.5 Comparison of Washington State DOT capacity with results of static load test.

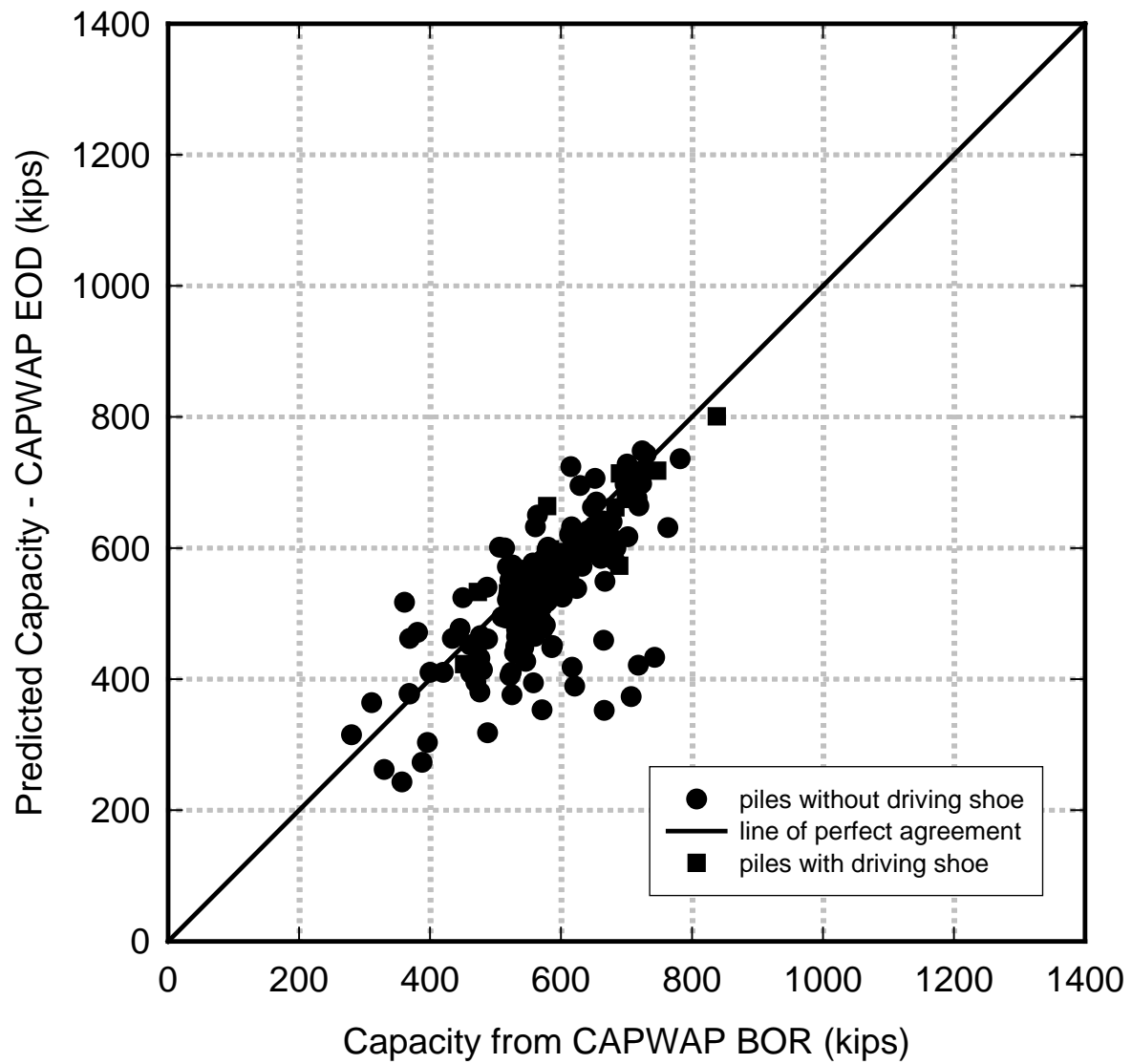


Figure 6.6 Comparison of CAPWAP EOD capacity with CAPWAP BOR using results of all piles with dynamic test results.

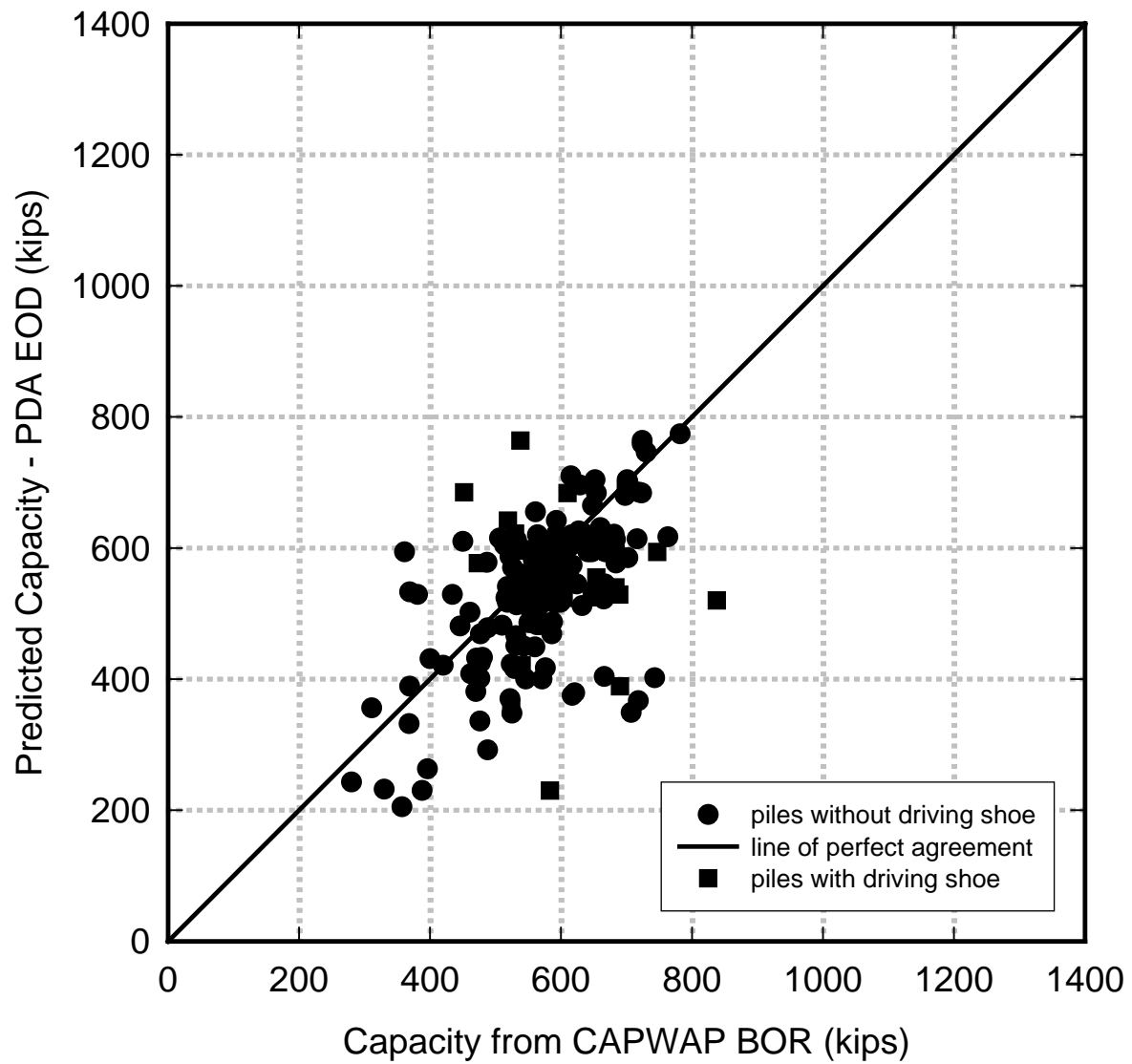


Figure 6.7 Comparison of PDA EOD capacity with CAPWAP BOR using results of all piles with dynamic test results.

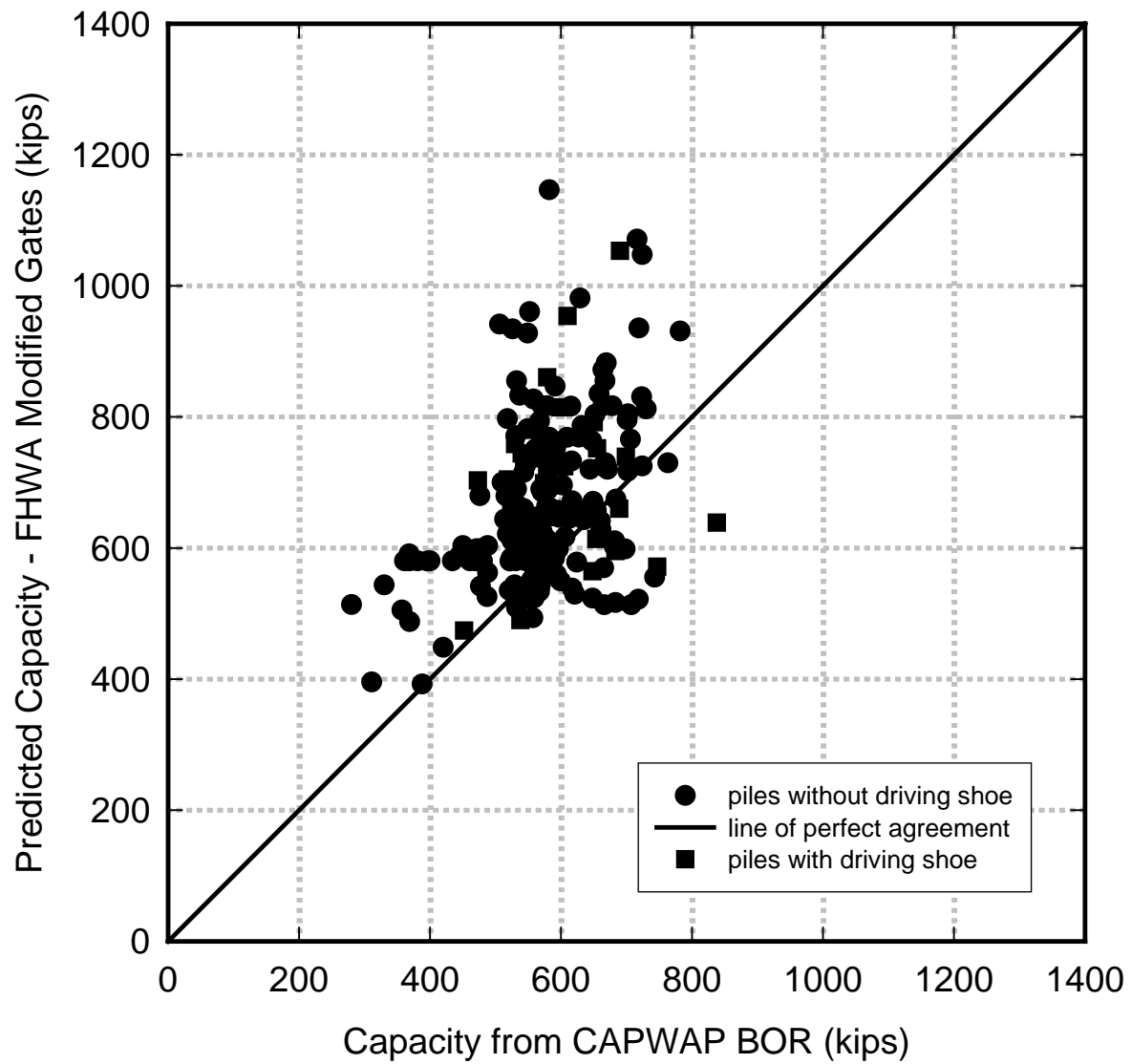


Figure 6.8 Comparison of FHWA modified Gates capacity with CAPWAP BOR using results of all piles with dynamic test results.

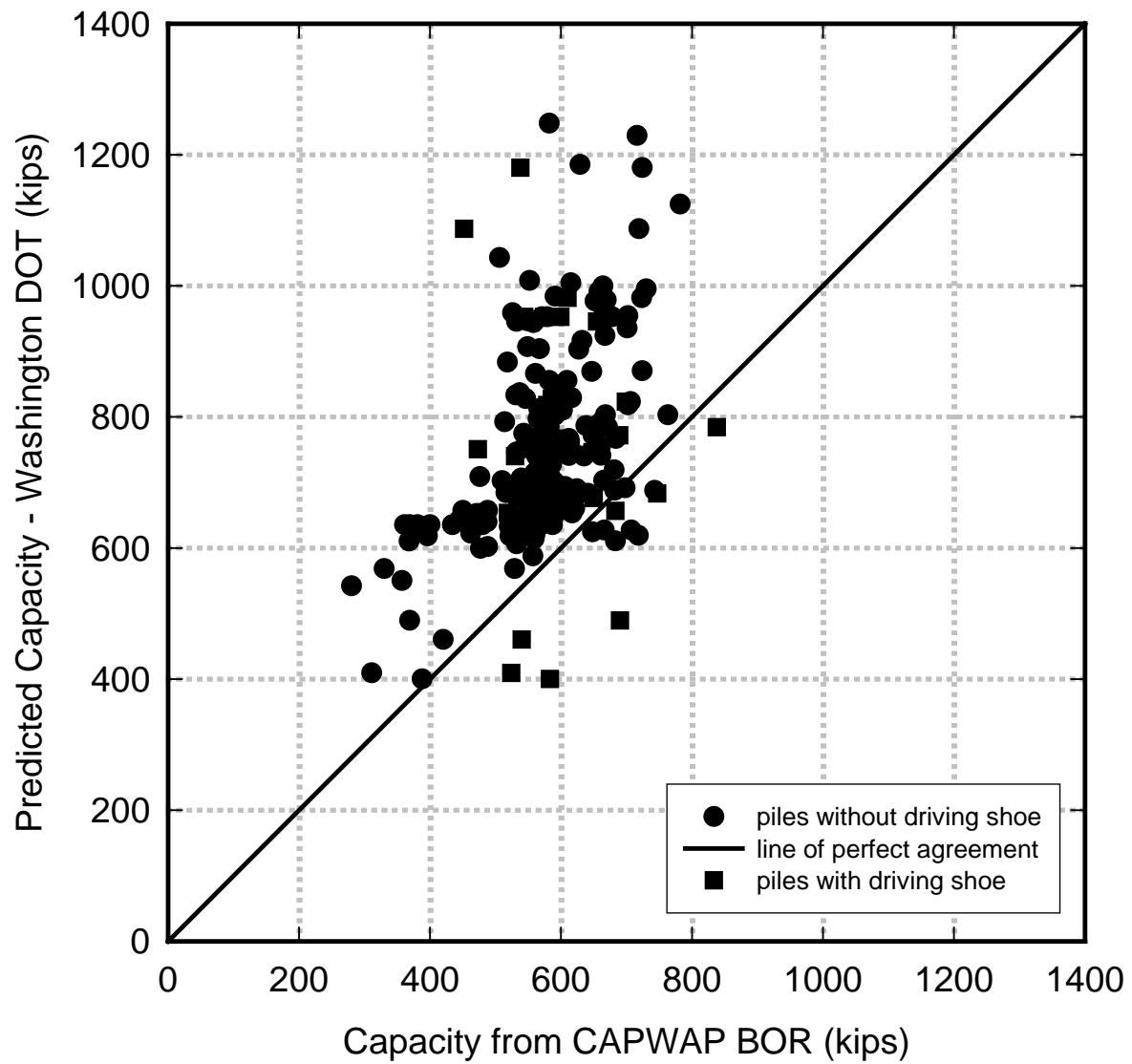


Figure 6.9 Comparison of Washington State DOT capacity with CAPWAP BOR using results of all piles with dynamic test results.

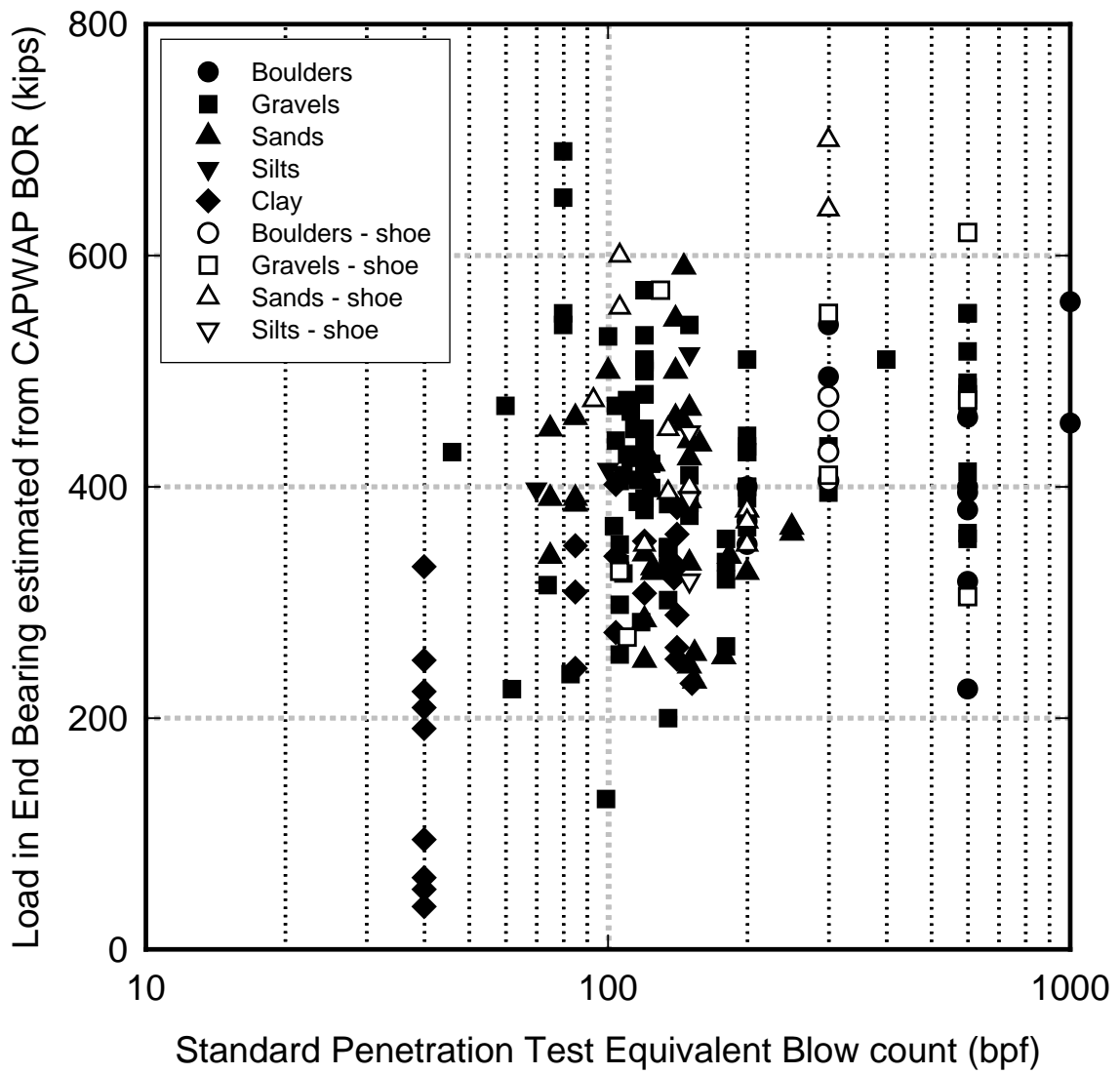


Figure 6.10 Tip capacity as affected by  $N_{spt}$ , soil type, and presence of pile shoe.



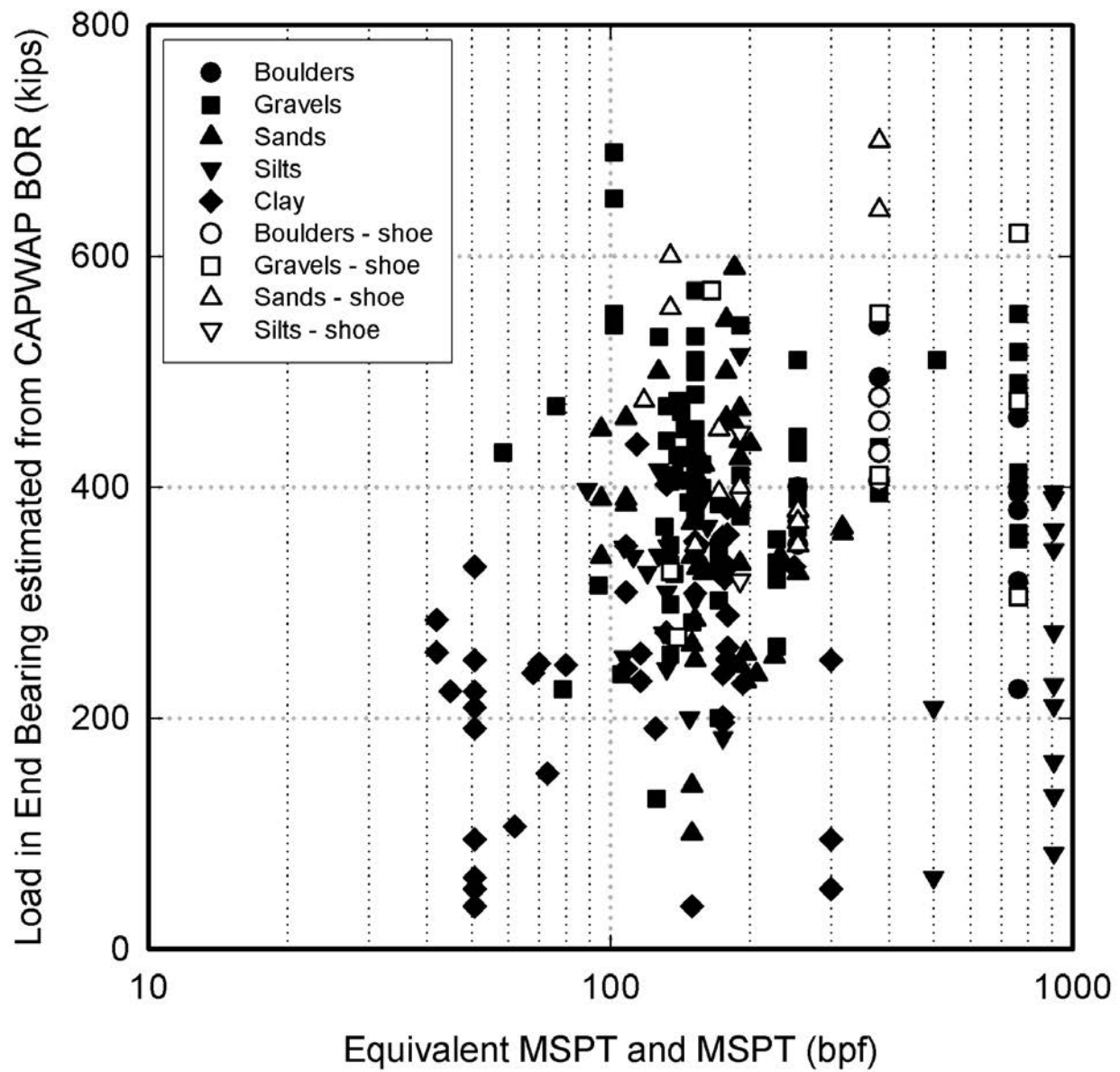


Figure 6.12. End Bearing (CAPWAP BOR) versus MSPT for all soil types and shoes and all data.

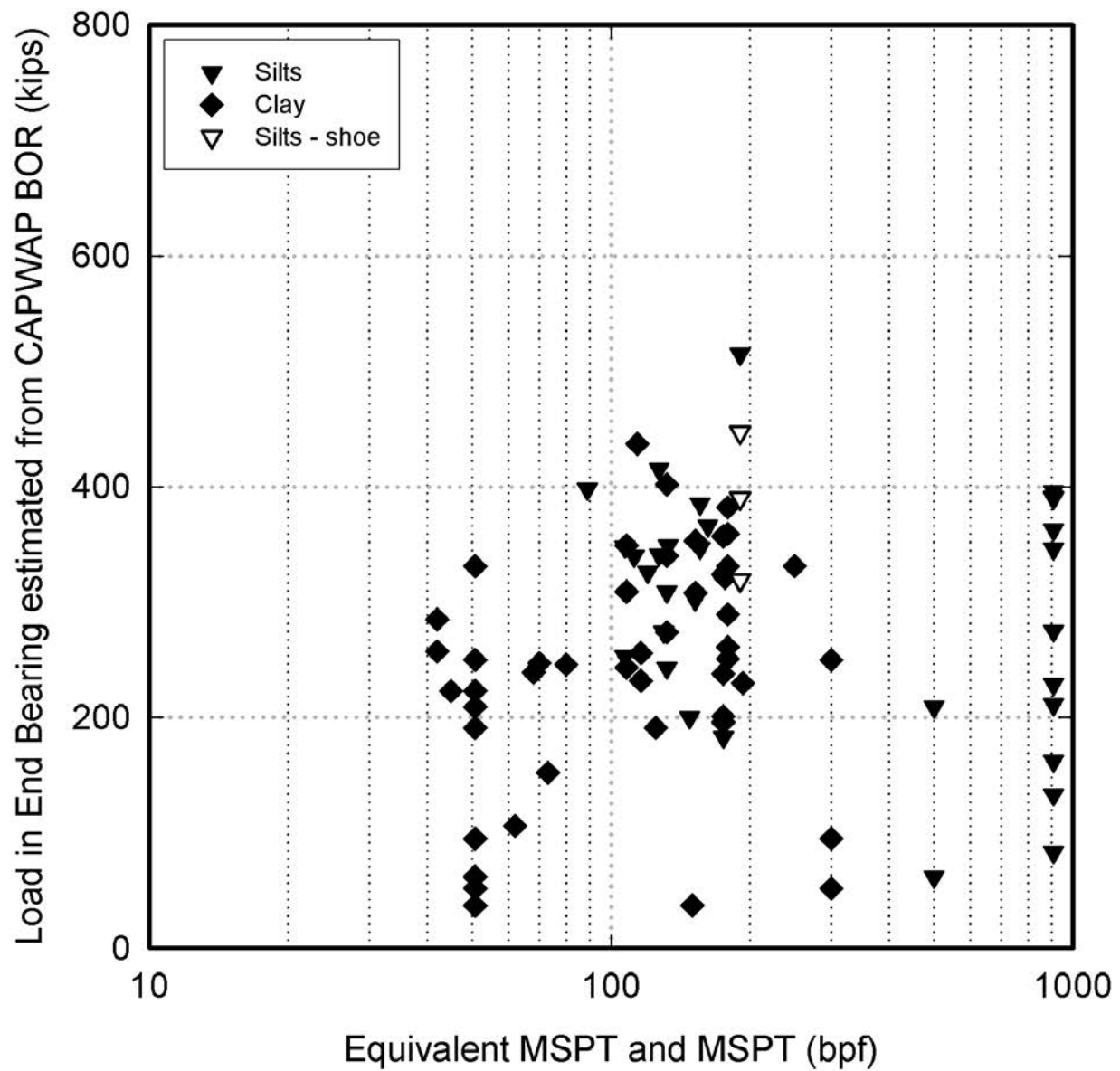


Figure 6.13. End Bearing (CAPWAP BOR) versus MSPT for all data with fine grained soil.

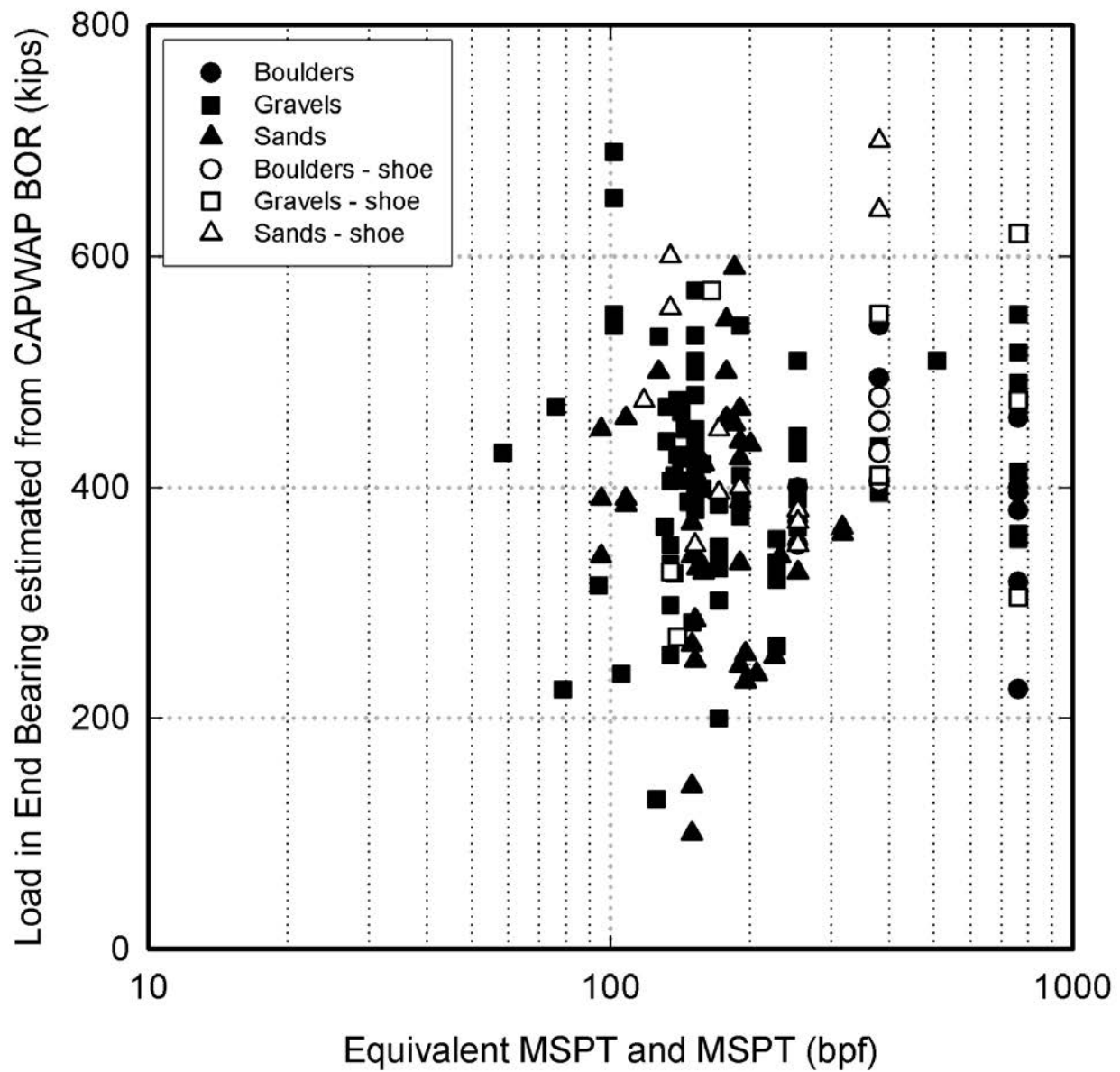


Figure 6.14. End Bearing (CAPWAP) versus MSPT for all data with coarse grained soil.

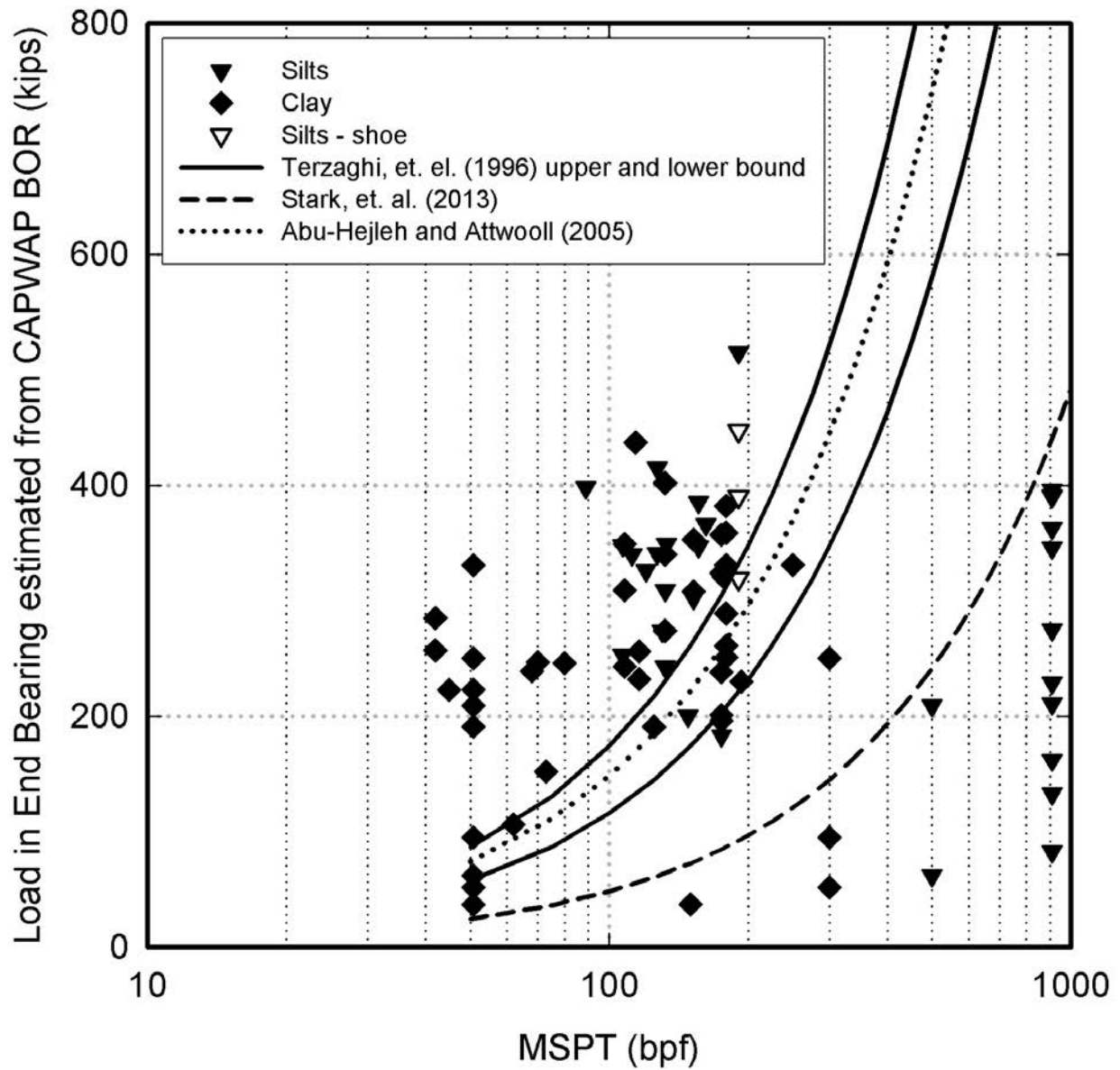


Figure 6.15. Predictions for End Bearing Load versus MSPT using different predictive methods - fine grained IGM.

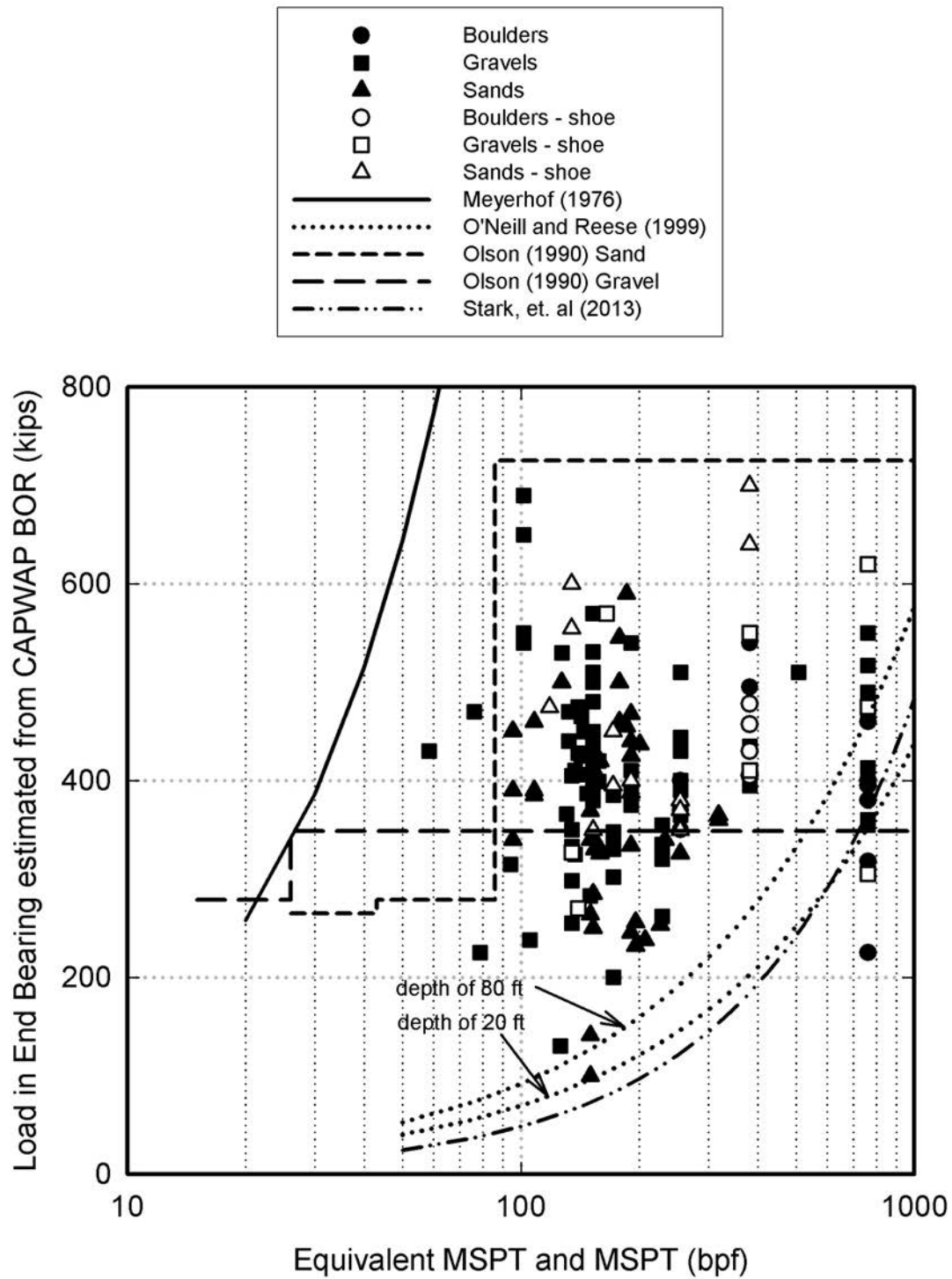


Figure 6.16. Prediction for end bearing load versus MSPT using different predictive methods - coarse grained IGM and whole area at pile tip

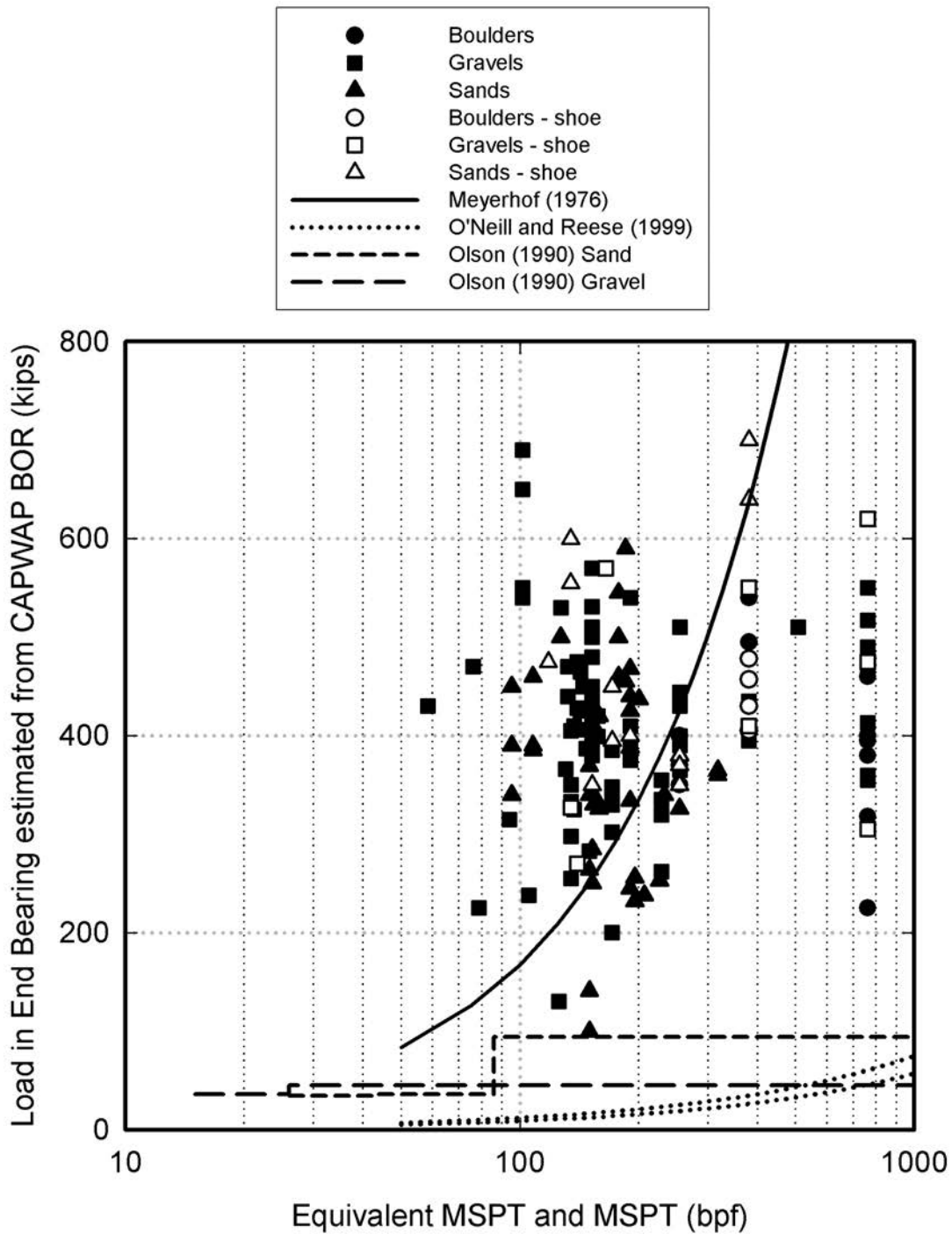


Figure 6.17. Prediction for end bearing load versus MSPT using different predictive methods - Coarse grained IGM and use crosssectional area of steel.

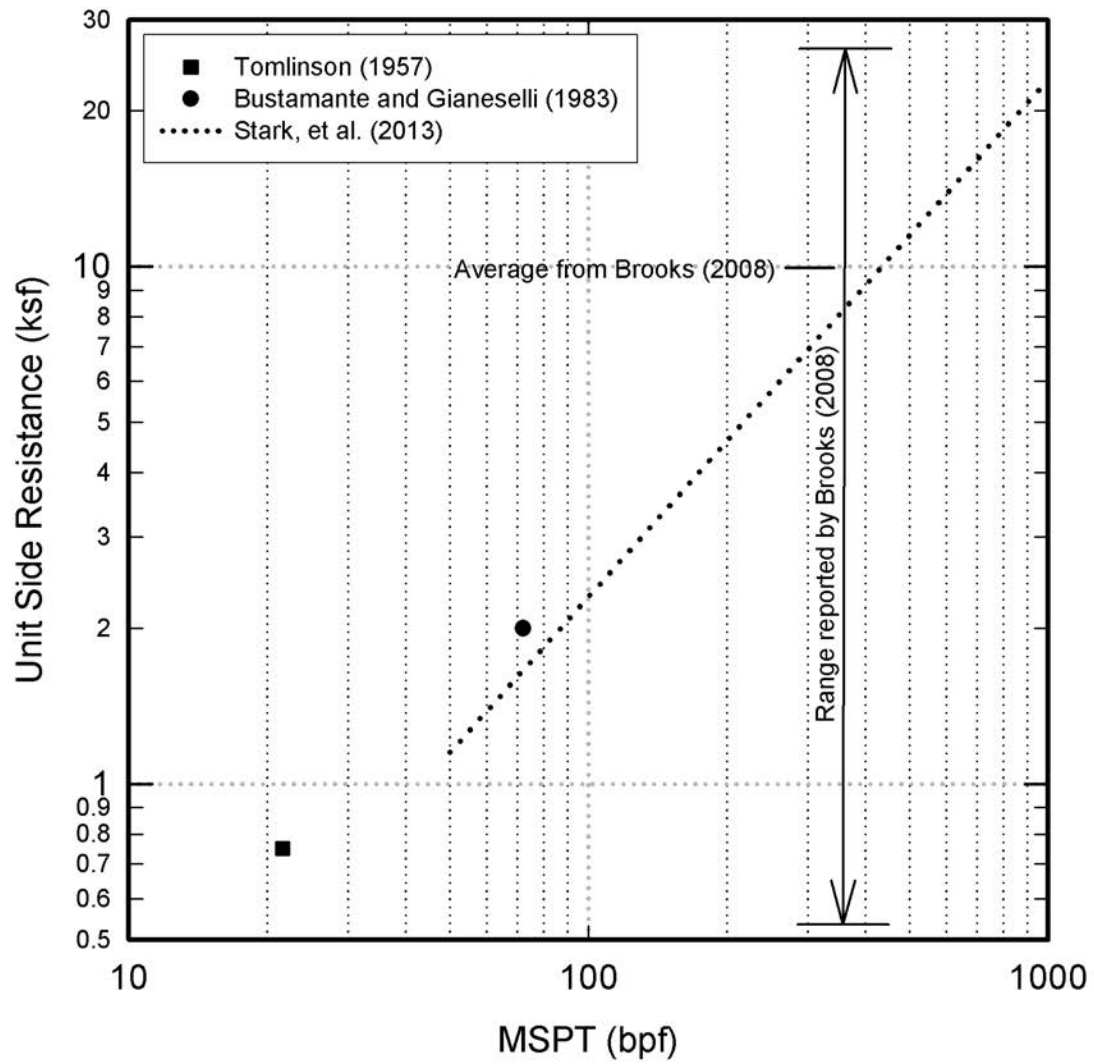


Figure 6.18. Unit Side Resistance versus MSPT using different predictive methods - fine grained IGM.

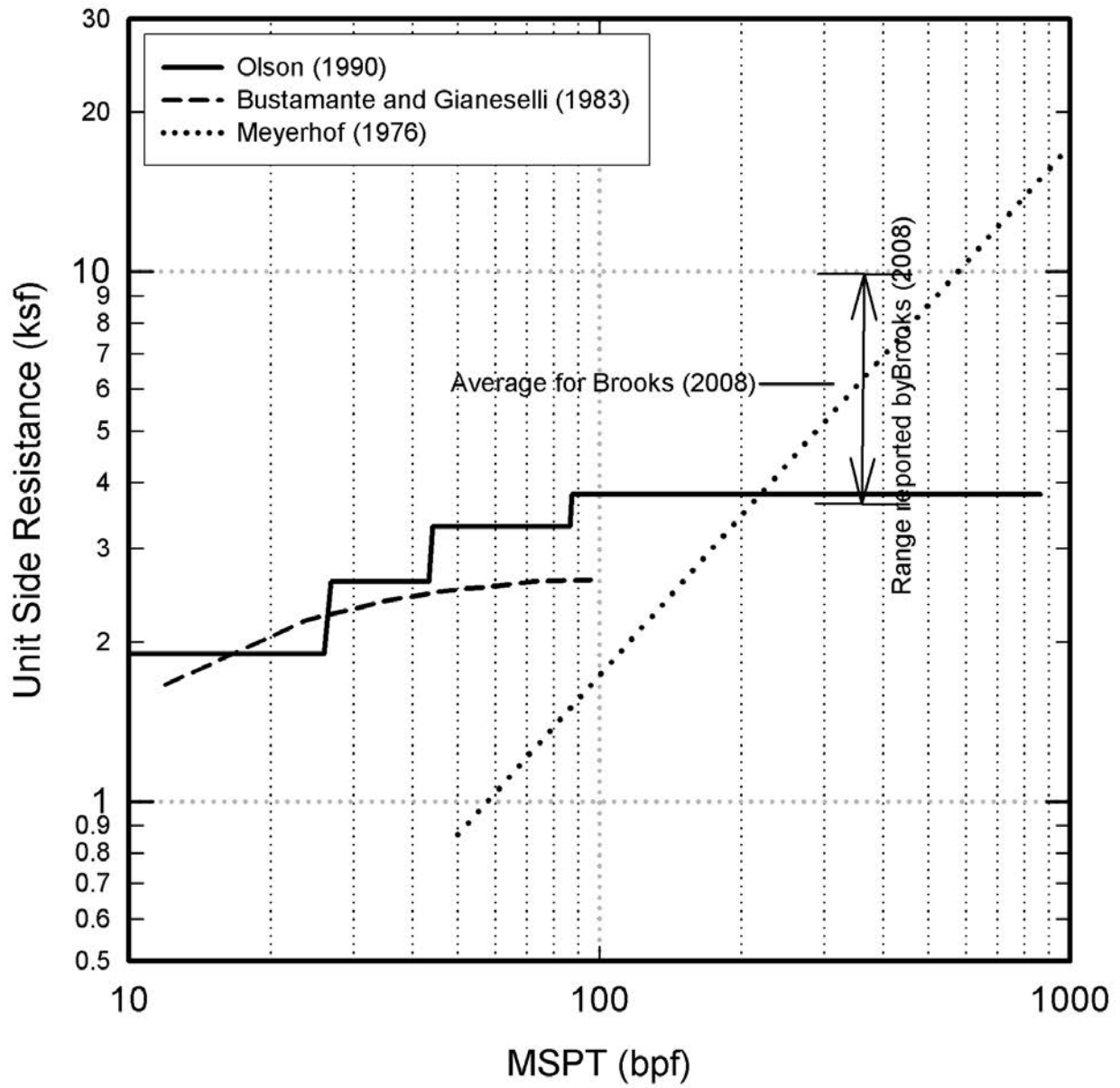


Figure 6.19. Unit Side Resistance versus MSPT using different predictive methods-coarse grained IGM.

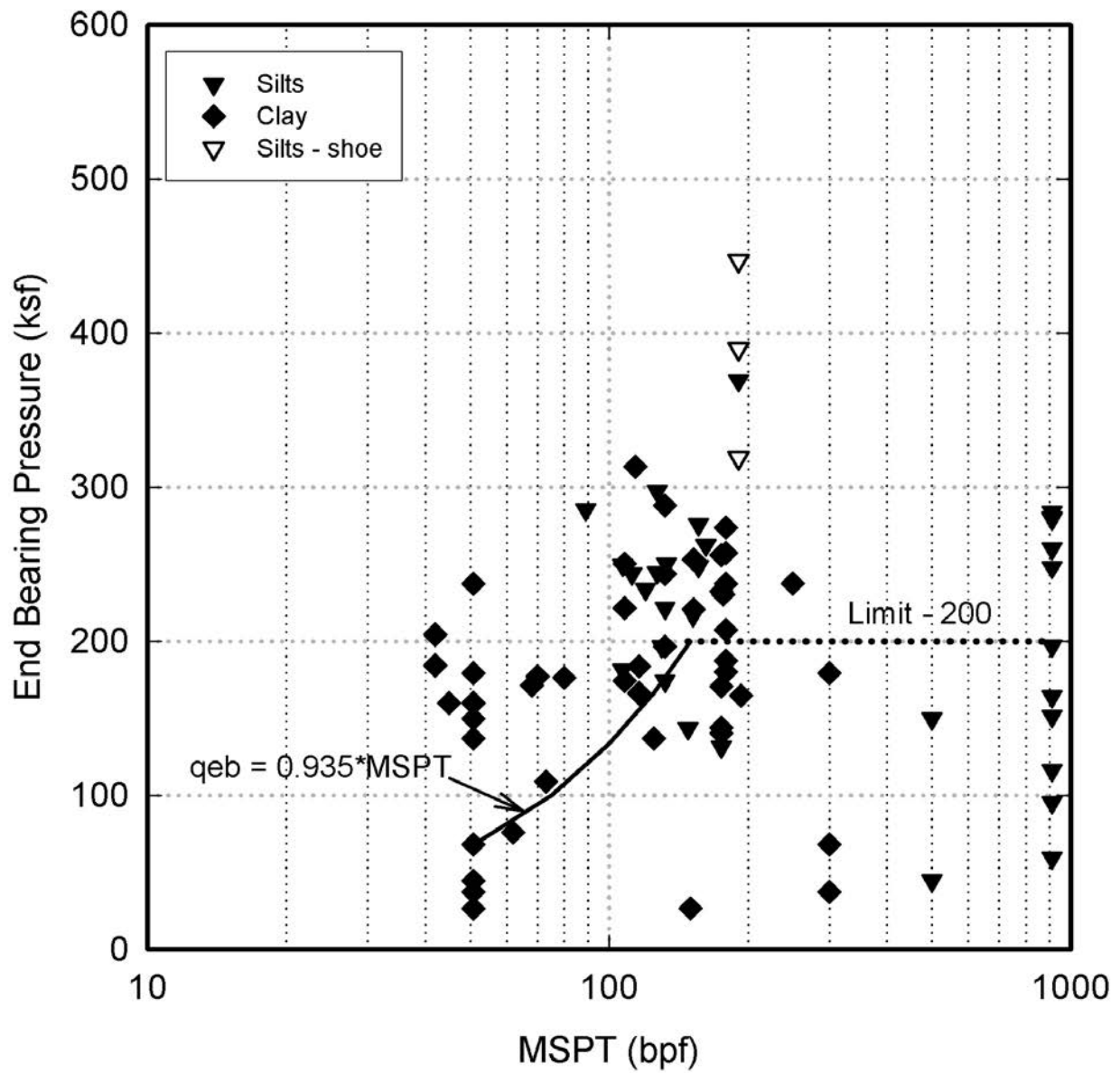


Figure 6.20. Design recommendations for end bearing pressure versus MSPT- fine grained IGM.

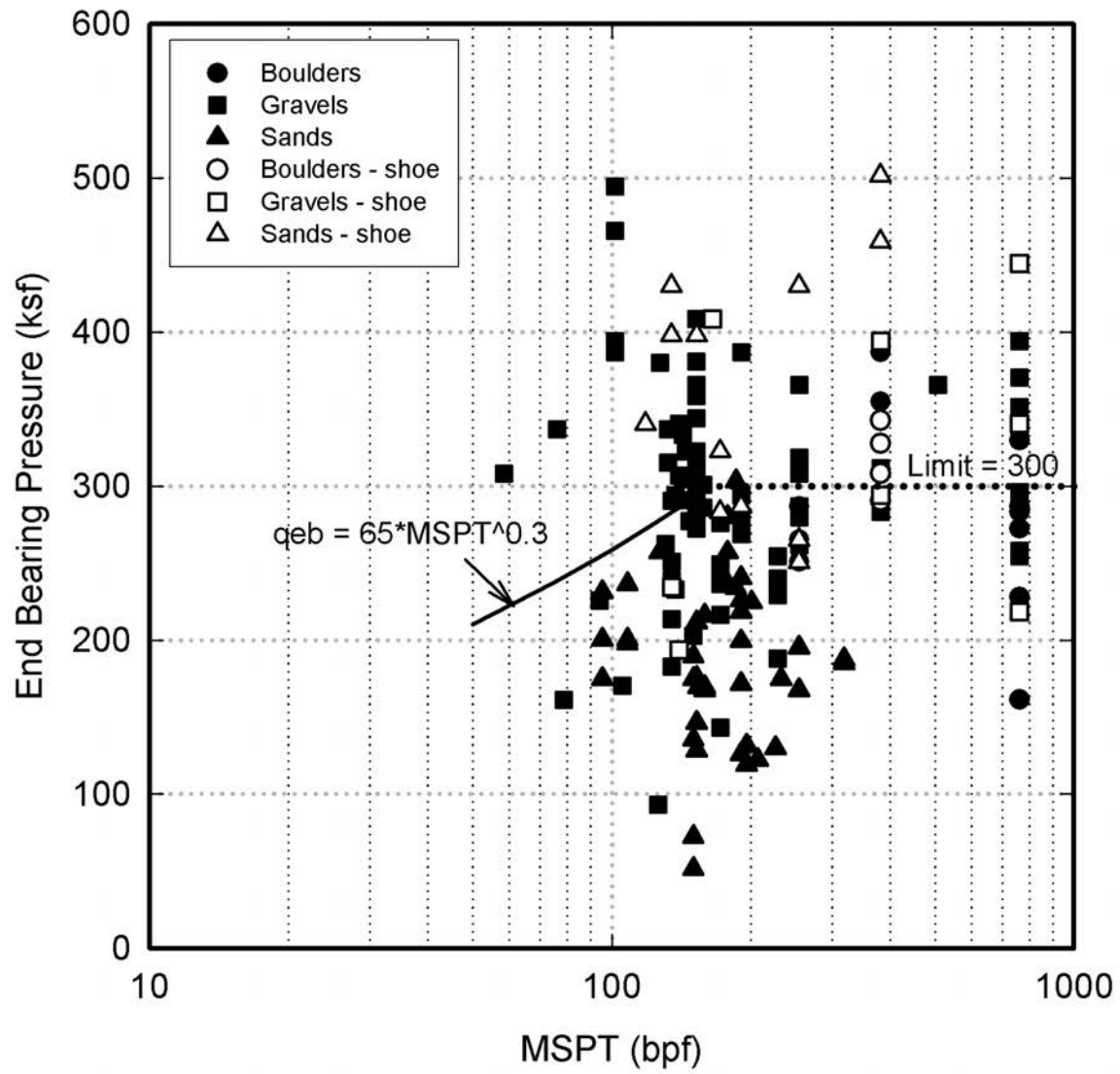


Figure 6.21. Design recommendations for end bearing pressure versus MSPT - coarse grained IGM.

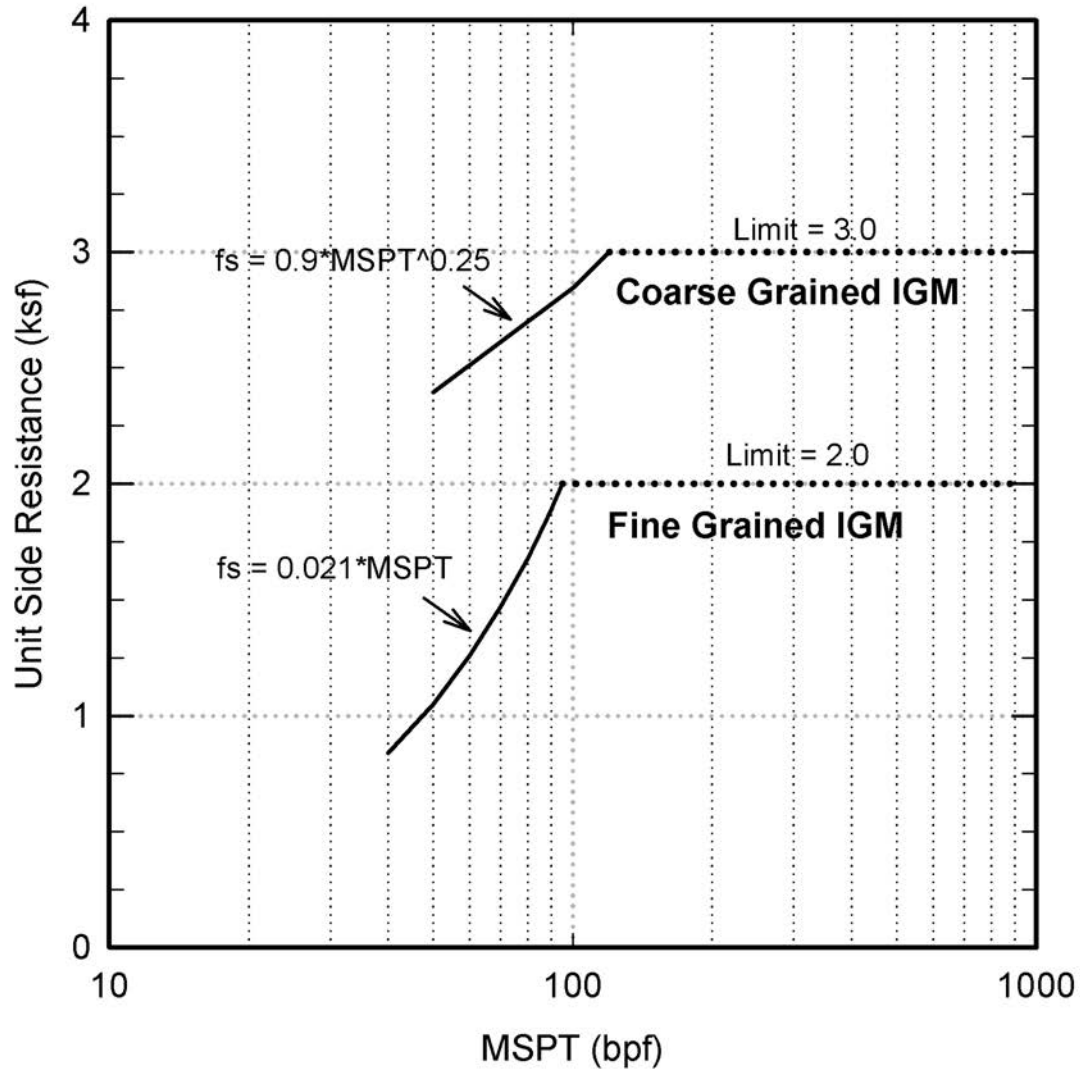


Figure 6.22. Design Recommendations for unit side resistance versus MSPT.

## CHAPTER 7 SUMMARY AND CONCLUSIONS

It is a challenge to determine the driving behavior of piles driven into Intermediate GeoMaterials (IGM). IGM's can exhibit significant variability and it is challenging to identify, sample, and quantify engineering parameters representative of the IGM material.

Modified Standard Penetration Tests were performed at several sites in the Green Bay area. The MSPT requires application of 100 blows. The relationship between blow count and sampler penetration usually becomes linear for blow counts greater than 50 to 60, accordingly, a site investigation conducting standard penetration tests could transition easily to conducting MSPT's. There are a number of practical modifications that could be made to the MSPT to achieve similar values. For example, a normal SPT test could be conducted and after 50 blows, the sample has not penetrated enough for a SPT result. The driller could stop and mark a reference point on the sampler, and then measure the sampler penetration after 50 more blows. The MSPT value could then be determined as the ratio of 50 blows divided by the sampler penetration measured in the last 50 blows.

As part of this research program, three sets of load test data were collected and interpreted. The first set of data was collected from results of 3 static load tests and dynamic load tests on 33 piles for piles driven at the US41/STH29 corridor. The second set of data was collected from the results of 4 static load tests and 44 piles with dynamic load tests. These tests were located along the US41/IH43 corridor. All dynamic load tests included monitoring at the end of driving (EOD) and at the beginning of restrike (BOR). Typical times between EOD and BOR were between 3 -7 days.

The third set of data was collected from 208 production piles subjected to dynamic testing along the same corridors, but no static load tests were conducted. All dynamic load tests included monitoring at the end of driving (EOD) and at the beginning of restrike (BOR). Typical times between EOD and BOR were 24 hours for the production piles.

Pile capacities as determined from static load tests for piles along the US41/STH29 corridor and the US41/IH43 corridor were compared with predictive methods. The CAPWAP BOR predicted capacities less than measured during the static load test. Median values of Predicted Capacity ( $Q_p$ ) to Measured Capacity ( $Q_m$ ) ( $Q_p/Q_m$ ) were around 85 percent, meaning that CAPWAP (BOR) predicted about 85 percent of the capacity as determined from a static load test. Other studies have identified that 90 – 92 percent is typical, so these findings are slightly less than other studies. However, there were only 6 static load tests in this study, and the median value may change as more data becomes available.

The CAPWAP EOD and PDA EOD methods underestimated static pile capacity because the pile capacities increased with time. Typical delays of 3-7 days were used between EOD and BOR. However, the scatter for the two methods was low.

The dynamic formulas from FHWA modified Gates and Washington State DOT also under predicted capacities for the static load test, but not as much as CAPWAP EOD and PDA EOD; and there was less scatter associated with the predictions.

Capacities were compared for dynamic tests conducted on the piling from all three datasets. These results do not have static load test results, so the pile capacity is taken as the prediction made with CAPWAP BOR. Furthermore, most of the dynamic load tests used a 24-hour restrrike to determine BOR, therefore, it is likely that the capacity for CAPWAP BOR for the dynamic test data is less than the true static piles capacity. The result is that ratios of  $Q_p/Q_m$  for the 208 pile database are higher than they would be if static pile capacity was used as the measure of  $Q_m$ .

The methods that exhibited the least scatter are the CAPWAP EOD and PDA EOD. This result is reasonable since the methods are based on measurements of energy delivered by the hammer and measured response of the pile. Values of  $\mu_{50}$  for CAPWAP EOD and PDA EOD were approximately 0.93, meaning that these two methods predicted, on the average, about 93 percent of the capacity of the pile as determined by CAPWAP BOR. The scatter associated with FHWA modified Gates and Washington State DOT were greater, and values of  $\mu_{50}$  were also greater: 1.16 and 1.31 for Gates and Washington, respectively. Although these ratios appear high, the ratios are based on CAPWAP BOR. If CAPWAP BOR predicts 85 percent of the static capacity (as determined from the static load tests), then the corrected ratios of  $Q_p/Q_m$  are  $1.16 \cdot 0.85 = 0.98$  and  $1.31 \cdot 0.85 = 1.11$ . These ratios indicate more reasonable estimates. The presence of driving shoes did not appear to influence the ability of predictive methods to estimate capacity.

Tip capacity developed in IGMs was investigated by noting the soil type, the penetration resistance in the soil ( $N_{spt}$ ), and whether the pile had shoes. A plot of tip capacity versus  $N_{spt}$  for different soil types showed that there is significant scatter. However, a general trend can be noted of increasing tip resistance with increasing  $N_{spt}$ . Piles with shoes developed slightly more tip capacity than piles without shoes. Tip capacities in the range of 300 to 500 kips were common. Tip capacities increased for  $N_{spt}$  values between 10 and 200; however, above 200 there is no discernable trend.

Design recommendations are developed to predict the capacity for piles driven into IGMs. Separate recommendations are given for IGMs that are primarily fine grained, and IGMs that are primarily coarse grained. Recommendations for end bearing pressure and side resistance are made for each IGM based on the penetration resistance exhibited by the layer using a Modified Standard Penetration Test (MSPT).

Design recommendations for unit end bearing and unit side resistance are given below:

The unit end bearing ( $q_{eb}$ ) for piles driven into fine grained IGMs is specified as

$$q_{eb}(\text{ksf}) = 0.935 \cdot \text{MSPT} \quad (\text{not to exceed } 200 \text{ ksf})$$

and for piles driven into coarse grained IGMs

$$q_{eb}(\text{ksf}) = 65 \cdot \text{MSPT}^{0.3} \quad (\text{not to exceed } 300 \text{ ksf})$$

The unit side resistance ( $f_s$ ) for piles driven into fine grained IGMs is specified as a function of the MSPT value as follows:

$$f_s(\text{ksf}) = 0.021 \cdot \text{MSPT} \quad (\text{not to exceed } 2 \text{ ksf})$$

and the unit side resistance for piles driven into coarse grained IGMs is

$$f_s(\text{ksf}) = 0.9 * \text{MSPT}^{0.25} \text{ (not to exceed 3 ksf)}$$

## CHAPTER 8 REFERENCES

Abu-Hejleh, N., and W. J. Attwooll (2005), Colorado's Axial Load Tests on Drilled Shafts Socketed in Weak Rocks: Synthesis and Future Needs, Final Contract Report No. CDOT-DTD-R-2005-4, Colorado Department of Transportation, Denver, CO, September, 178 p.

Bustamante, M. and Gianceselli, L (1983), "Prevision de la capacite portante des pieux par la methode penetrometrique," Compte Rendu de Recherche F.A.E.R., 1.05.02.2, Laboratoire Central des Ponts et Chaussees (in French).

Brooks, H.M (2008), "Axial Capacity of Piles Supported on Intermediate Geomaterials," thesis submitted in partial fulfillment for the degree of MS in CE, Montana State University, July, 108p.

Coyle H. M. and Castello, R. R., 1981. New design correlations for piles in sand. American Society of Civil Engineers, ASCE, Journal of the Geotechnical Engineering Division, Vol. 107, GT7, pp. 965 - 986.

Davisson, M.T. (1972) "High capacity piles" Proceedings, Lecture Series, Innovations in Foundation Construction, ASCE, Illinois Section, 52 pp.

GRL Report (2015), SPT Energy Measurement Summary Report, GRL Job No. 157082, Green Bay, Wisconsin, December.

GRL Report," Dynamic Pile Testing Summary Report GRL Job No. 137064, Structure B-5-671, USH 41 NB to IH 43 SB, "Ramp IHA", Brown County, Wisconsin.

GRL Report," Dynamic Pile Testing Summary Report GRL Job No. 137064, Structure B-5-678, IH 43 NB to USH 41 SB, "Ramp IHB," Brown County, Wisconsin.

GRL Report, " Dynamic Pile Testing Summary Report GRL Job No. 137064, Structure B-5-679, IH 43 NB to USH 41 NB, "Ramp NIH," Brown County, Wisconsin.

GRL Report," Dynamic Pile Testing Summary Report GRL Job No. 137064, Structure B-5-681, USH 41 NB over Duck Creek, Brown County, Wisconsin.

Mokwa, R. and H. Brooks (2008), "Axial Capacity of Piles Supported on Intermediate Geomaterials, FHWA/MT-08-008/8117-32, 79p.

Olson, R. E. (1990), "Axial Load Capacity of Steel Pipe Piles in Sand," Proc. Of the Offshore Technology Conference, Houston, Tx, pp. 17-24.

O'Neill, M. and L.C. Reese (1999), "Drilled Shafts: Construction Procedures and Design Methods, FHWA Report #FHWA-IF-99-025, 537p.

Peck, R.B, W. E. Hanson, and T.H. Thornburn (1974), Foundation Engineering, John Wiley and Sons, New York, 514p.

Stark, T. D., J.H. Long, and P. Assem (2013), "Improvement for Determining the Axial Capacity of Drilled Shafts in Shale in Illinois," Research Report No. FHWA-ICT-13-017, Illinois Center for Transportation, University of Illinois, May, 68p.

Stroud, M. A. (1974), The Standard Penetration Test in Insensitive Clays and Soft Rocks, "Proc. Of the European Symposium on Penetration Testing, Stockholm, 2.2, pp. 367-375.

Terzaghi, K., R. B. Peck, and G. Mesri (1996), Soil Mechanics in Engineering Practice, John Wiley and Sons, New York, 549p.

Tomlinson, M.J. (1957), "The Adhesion of Piles Driven in Clay Soils," Proc. Of the 4<sup>th</sup> Intl. Conf. On Soil Mechanics and Fnd. Engineering, Vol. 2, pp. 66-71.

